NASA-CR-159056
19830008126

NASA Contractor Report 159056

Repair Techniques for Graphite/Epoxy Structures for Commercial Transport Applications

R.H. Stone
Lockheed-California Company
Burbank, California

Contract NAS 1-15269
January 1983

NASA
National Aeronautics and
Space Administration

Langley Research Center
Hampton, Virginia 23665

NASA Contractor Report 159056

Repair Techniques for Graphite/Epoxy Structures for Commercial Transport Applications

R.H. Stone
Lockheed-California Company
Burbank, California

Contract NAS 1-15269
January 1983

National Aeronautics and
Space Administration

Langley Research Center
Hampton, Virginia 23665

TABLE OF CONTENTS

TABLE OF CONTENTS (Continued)

TABLE OF CONTENTS (Continued)

LIST OF FIGURES

LIST OF FIGURES (Continued)

LIST OF FIGURES (Continued)

LIST OF FIGURES (Continued)

LIST OF TABLES

FOREWORD

This is the final report for the program "Repair Techniques for Graphite/Epoxy Structures for Commercial Transport Applications". This program was administered by the Langley Research Center, National Aeronautics and Space Administration with J. W. Deaton, the Technical Monitor. The contract number is NAS1-15269.

The program has been performed by the Lockheed-California Company with R. H. Stone, the Program Manager. Northrop Corporation has been a major subcontractor to this program, and J. D. Labor was the Northrop Program Manager.

Lockheed-California Company activities included the Phase 1 airline survey, fabrication of parent laminates and external patch repairs for the Phase 2 specimens, design of the Phase 3 subelement repairs, and all Phase 4 activities on large-area repair. Northrop activities included the Phase 1 damage tolerance survey and defect categorization matrix, fabrication of flush repairs and testing of the Phase 2 specimens, and repair and testing of the Phase 3 subelement specimens. Lockheed-Georgia Company also participated in the program by fabrication of the stiffened wing cover specimen used in the Phase 3 tests.

Lockheed-California Company personnel who contributed to the program include F. H. Strunk who assisted in the airline survey; R. C. Young who fabricated parent laminates, external repairs, and the large area repair; A. C. Jackson who designed the subelement repairs and the large-area repair; and F. Dorward who was responsible for fatigue cycling and static testing of the large-area repair. At Lockheed-Georgia Company, R. H. Kilpatrick was responsible for fabrication of the wing cover component.

Northrop personnel contributing to the program include N. M. Bhatia who assisted in the damage tolerance survey and defect categorization; A. Hall and T. Ishimine who were responsible for specimen fabrication and testing respectively; and J. F. Knauss who assisted the Northrop Program Manager in the Phase 2 tests and directed the Phase 3 subelement repair activities.

Use of commercial products or names of manufacturers in this report does not constitute official endorsement of such products or manufacturers, either expressed or implied, by the National Aeronautics and Space Administration.

REPAIR TECHNIQUES FOR GRAPHITE/EPOXY STRUCTURES FOR COMMERCIAL TRANSPORT APPLICATIONS

Robert H. Stone

Lockheed-California Company
Burbank, California

SUMMARY

This program was performed in four phases. Phase 1 consisted of three separate tasks: Task A- survey of theoretical and experimental work on composite defect sensitivity; Task B- survey of airline damage experience and airline repair and maintenance procedures; and Task C- preparation of a matrix defining and categorizing flaws and damage. Task A was performed by Northrop Corporation Aircraft Group, which is a major participant in this program with Lockheed. Task B was performed by Lockheed, while Task C was performed primarily by Northrop using Lockheed inputs from the Task B survey.

In the Task A survey, documents and reports on composite defect studies were obtained through a literature search and industry contacts. These documents were reviewed for analytical and experimental data showing the effects of various defects on composite laminate properties. The data primarily were based on idealized flaws, such as holes and slots, and included both analytical treatments of the defects and experimental data which were correlated in some cases with analytical techniques. Some data were found relating to realistic flaws resulting from impact damage.

The available experimental test data were then organized to show strength reduction as a function of flaw size for various defect types including holes, slots, and impact damage. The data were compared with predicted strength curves obtained from the analytical techniques, and are presented in this manner.

In the Task B survey, a questionnaire was prepared and submitted to eleven participating airlines. The airlines were asked to provide a listing of typical defect types and sizes encountered in service on various categories of parts. These parts included fiberglass and advanced composite parts, as well as metal parts considered likely candidates for composites usage. Responses were, as expected, based primarily on experience with metal components which comprise most current aircraft structure.

Another part of the questionnaire dealt with airline maintenance and repair procedures, and airline facilities and equipment available for repair operations. The airlines were asked about defect detection and NDI procedures; the types of equipment available at line stations and the major maintenance bases, as well as the percentage of repairs performed at each type of facility; airline background and experience with the structural bonded repairs considered optimum for composite repairs; maintenance down

times and inspection intervals; and the policy on flush aerodynamic repairs as opposed to external patches. These are all factors determining the type of repair procedures which need to be developed for airline maintenance of composite structures.

Submittal of the questionnaire was followed by visits to the airline maintenance bases by a Lockheed survey team. Discussions were held with airline engineering and maintenance personnel and the questionnaire responses were reviewed.

In Task C, a matrix table was prepared defining and categorizing defects by part category, size, and origin using the airline damage experience data which had been organized by defect type within each part category. This compilation of damage types, based primarily on metallic components, was used for estimations of damage size for comparable composite components. Estimates were also made on composite strength reduction, flaw growth potential, and the type of maintenance action required for the composite parts. These data were organized into the table presented herein. This was done for impact damage only. It was assumed no comparable damage to corrosion effects would occur in composites, and for fatigue damage it was assumed (based on considerable available data) that the type of crack growth occurring in metals would not occur in composites.

Phase 2 of this program consisted of a single task identified as Task D, "Development and Verification of Repair Methods". The objective of this task was to provide a comparative evaluation of various composite repair techniques suitable for use in airline maintenance operations. This task involved fabrication and testing of coupon type specimens incorporating the various repair techniques and processes selected for evaluation.

The repairs evaluated in Phase 2 were selected based on results of the Phase 1 surveys on defect sensitivity of composites and on airline damage experience and maintenance/repair capabilities. The results of these surveys indicated a need for a wide range of repair procedures suitable for both maintenance base (depot level) and line station (field level) operations, and providing a wide choice of simplicity and ease of processing versus structural efficiency. The results indicated the need for both flush, aerodynamic and external patch repairs, and the need for structural bonded, cold bonded, and bolted repairs.

These repairs were accomplished using parent laminates fabricated with the Narmco 5208/T300 graphite/epoxy system currently used in the NASA ACEE programs. These laminates included 50 ply lay-ups representative of a highly loaded structure such as a wing cover and 16 ply lay-ups representative of a lightly loaded structure such as a stabilizer or control surface. Most of the tests were performed using sandwich beam specimens incorporating the repaired laminates on one face of the sandwich. A few tabbed laminate coupon specimens were included for comparison. All repairs were performed after moisture conditioning of the parent laminates to simulate the typical in-service condition of composite parts.

The repair specimens were tested for static tension and compression at room temperature, -54°C (-67°F) and 82°C (180°F). Some fatigue tests were also run on both the 16 ply and 50 ply specimens using fatigue spectra representative of a vertical stabilizer and wing cover respectively.

The test results indicated that flush, aerodynamic graphite repairs with tapered bond lines and incorporating structural grade adhesives and pre-pregs, provided the greatest structural efficiency and strength recovery; and restored design strength for both lightly loaded and highly loaded structures. These repairs are the most complex and expensive and are limited to use by properly equipped maintenance base operations. External graphite patch repairs incorporating structural grade systems are less complex and expensive, and provide an adequate restoration of design strength for lightly loaded components. Cold-bonded and wet lay-up repairs and bolted repairs with blind fasteners are well adapted to the limitations of line station operations, but provide limited strength recovery. This limited recovery is adequate, however, for many lightly loaded components.

Phase 3 of this program, "Small Area Repair," consisted of a single task identified as Task E, "Demonstration of Repairability and Repair Quality on Structural Component Subelements." This activity involved simulated damage and repair of three subelement specimens: 1) an L-1011 composite vertical fin cover segment (Type I) representative of a lightly loaded hat-stiffened skin cover, 2) a stiffened cover segment taken from a composite wing design concept (Type II) representative of a highly loaded hat-stiffened skin cover, and 3) an L-1011 vertical fin spar segment (Type III) representative of a substructure for a lightly loaded component. These subelement specimens consisted of a single stiffener element in the instance of the two hat-stiffened covers and a cap and partial web section in the case of the spar segment.

The damage consisted of a complete cut through the stiffener element and adjacent skin for Type I and II and through the cap and web segment for Type III. These cuts simulated small area damage extending across a single stiffener or structural element. The damage was then repaired using the following concepts developed and evaluated in the Phase 2 coupon tests:

- Type I, fin cover - An external cure-in-place graphite patch skin repair and a precured bonded graphite hat splice
- Type II, wing cover - A flush cure-in-place graphite patch skin repair and a precured bonded graphite hat splice
- Type III, fin spar - A bolted repair with aluminum splice plates mechanically attached to the cap and web sections.

The two repaired skin segments were tested to failure in compression along with undamaged control specimens. The repaired spar segment was tested to failure in tension, also with an undamaged control specimen. The control and

repaired specimens were conditioned to one percent moisture content prior to repair, and the bonded repairs were moisture conditioned prior to test.

The test results on the control specimens correlated with predicted unflawed strengths, and the three repaired specimens achieved from 79 percent to 92 percent of unflawed strength, which in all cases was well above design strength levels.

Phase 4 of this program, "Large Area Repair" consisted of a single Task identified as Task F, "Repairability and Repair Quality of Large-Area Repairs on Structural Components." This Task utilized the full-scale ground test article (GTA) of the L-1011 advanced composite vertical fin (ACVF) developed under Contract NAS1-14000.

Large area damage, representative of lightning strike damage, was inflicted on the ACVF cover and adjacent hat stiffeners following two lifetimes of fatigue cycling. A bonded external precured graphite patch was applied to the skin, followed by mechanical attachment of the disbonded stiffeners to the repaired skin. After repair, the fin GTA was subjected to one additional lifetime of fatigue cycling, followed by loading to ultimate strength and failure.

The fin GTA failed at 120% of design ultimate load. The repair patch remained intact and unaffected by the fatigue cycling and testing to failure. Strain measurements indicated no effect of the patch on far-field strains in the fin component.

The ACVF program under Contract NAS1-14000 covered application of damage, repair design and fabrication, and testing to ultimate strength and failure. Phase 4 of this program supplemented the ACVF ground test program by providing for the post-repair fatigue cycling for one lifetime.

INTRODUCTION

Background

The introduction of graphite/epoxy structural components into commercial aircraft service will require development of structural repair procedures adapted to the needs and requirements of commercial airlines, while still meeting the structural requirements of the components. All repairs on commercial aircraft structures must be permanent repairs approved by the FAA. These repairs must restore the capability of the component to carry design ultimate loads, and must not adversely affect fail-safe characteristics of the part. It is also desirable to restore the fatigue life of the component to the remaining useful service life on the aircraft.

The maximum tensile design strength for a critical composite structure is typically about 50 percent of unnotched material strength to account for holes and stress concentrators. Repairs for this type of composite part must

restore the design strength at least and preferably should demonstrate by test an ultimate strength greater than 50 percent of unnotched strength. Composite components designed for stiffness, sonic fatigue, or other factors may have a design strength requirement less than 50 percent of unnotched strength. The repairs on these parts may therefore be less critical, and a less complex and costly repair approach may be possible. In addition to restoring strength and fatigue life, repairs must not adversely affect such factors as environmental durability, damage propagation rate, damage tolerance, and part function; and must not introduce unacceptable stress concentrations in the patch area.

Components which are critical in compression also have an ultimate design strength approximately 50% of unnotched strength to allow for fastener holes, etc. However, compression loading appears to be more critical than tension loadings. Available data indicate damage growth is more likely to occur under compression dominated fatigue than in tensile loading conditions. This damage growth is most often dominated by disbonding along inherent planes of interlaminar weakness which under compressive loading can result in buckling instability. Repairs of compression loaded parts must take this factor into consideration.

Current structural repairs used by the airlines on conventional metal structure consist primarily of mechanically fastened metal patches. Adhesive bonded repairs are used to a lesser degree on bonded structures and fiberglass components, and these are often nonstructural cold bonded repairs. The conventional mechanically fastened patches may be adequate in some cases for composite parts, and for many repair situations such as line station repairs performed away from the maintenance base, this may be the only repair technique which can be accomplished within equipment, personnel, and down-time limitations. The inherent nature of composites, however, indicates that a structural bonded repair is more efficient, can more readily restore full load carrying capability, and in some cases may be mandatory to effect an adequate repair.

Other factors determining the type of repair include part removability, accessability of the repair site, aerodynamic requirements at the damage location, special environmental requirements, and complexity of the surrounding structure. Repairs must often be performed under adverse conditions, and the baseline laminate may be in a condition which adversely affects repair integrity, for example having surface contamination or high moisture content.

The types of damage encountered in service on commercial transports result from such factors as manufacturing defects, fatigue wearout, stress, corrosion, ground handling damage, in-flight foreign object damage from hail or bird strikes, tire tread impact during takeoff and landings, etc. The susceptability of composite structures to these causes of damage is different than metallic parts. Composites obviously will not suffer corrosion damage, and there is evidence that composites have excellent fatigue life and resistance to damage propagation particularly for tensile loading conditions.

Graphite/epoxy composites appear to have fairly good impact resistance, but impact may tend to produce nonvisible delamination and matrix damage in composites which may not be visually detectable. This could increase the frequency and level of effort required for nondestructive inspection of compressive strength critical composite parts compared to that now required for metal components.

Objectives

The objective of the overall program was to develop and validate repair procedures for composite structures, adapted to commercial airline maintenance operations and meeting the basic criteria of restoring design strength and service life capability to the components.

The objectives of Phase 1 were to determine the effects of various types and sizes of flaws and damage on the structural properties of the composite; the typical types and sizes of flaws and damage encountered by airlines in commercial transport service; and definition and categorization of the flaws and damage types by size, origin, part category, and type of repair required. These data along with information from the airlines on their maintenance procedures, facilities, and equipment, and the compatibility of various composite repair techniques with these operations, provide a basis for development of composite repair techniques for commercial transport applications.

The objectives of Phase 2 were to screen and evaluate various types of composite repairs, selected on the basis of the Phase 1 survey results to meet both the structural requirements for composite repairs and airline requirements and capabilities.

The objectives of Phases 3 and 4 were to evaluate respectively small-area and large-area repairs which incorporate the repair concepts determined most suitable based on the Phase 2 screening test results.

Approach

This program was divided into four phases as follows:

Phase 1 - Assessment of repair capabilities

- Task A - Survey of theoretical and experimental work on composite defect sensitivity
- Task B - Survey of airline damage experience, repair and maintenance procedures
- Task C - Definition and categorization of flaws

Phase 2, Task D - Development Repair and Verification of Repair Methods

Phase 3, Task E - Repair of Composite Subelement Specimens

Phase 4, Task F - Repair of Full Size Composite Structure

The four Phases of this program were performed sequentially, and the results of each Phase were used to develop the detail test plans and repair designs for the next Phase. Phase 1 provided information on composite defect sensitivity, and also provided information on airline damage experience, requirements and capabilities.

This information from the Phase 1 surveys was used to select the repair concepts for screening in Phase 2. These repair concepts are also based on procedures developed by a number of military agency funded programs (refs. 1, 2, 3, and 4), and also by Lockheed-California Co. programs (refs. 5 and 6). The Navy and Air Force programs referenced above were based on military needs and requirements and emphasized the more complex depot level repairs. In this program, an emphasis was placed on simpler external patch repairs, and cold-bonded and metal patch repairs were included to reflect the limitations and concerns of airline operations.

The results of the Phase 2 screening tests indicated the effectiveness of vacuum bonded graphite repairs, and this approach was used for repair of two types of hat-stiffened cover sub-element specimens in Phase 3. Bolted patches were evaluated for repair of a third sub-element specimen, a spar cap and web segment.

The Phase 3 results further verified the effectiveness of graphite external repairs bonded with vacuum pressure, and also indicated the effectiveness of properly designed bolted repairs. A bonded graphite repair was therefore used for the large-area repair of a full-size component in Phase 4. The component selected for use in the Phase 4 activities was the L-1011 composite vertical fin ground test article (GTA). The GTA is a full-size production component, and is a complete box structure approximately 25 by 9 feet in area with hat-stiffened covers and composite spars and ribs. The Phase 4 activities were conducted in conjunction with ground tests performed as part of the vertical fin program.

PHASE 1 - ASSESSMENT OF REPAIR CAPABILITIES

Phase 1 consisted of three Tasks: Task A - survey of theoretical and experimental work on composite defect sensitivity; Task B - survey of airline

damage experience and airline repair and maintenance procedures; and Task C - preparation of a matrix defining and categorizing flaws and damage.

Task A - Survey Of Theoretical And Experimental Work On Composite Defect Sensitivity And Fracture

The initial activity in the program was a survey of existing theoretical and experimental data on the effects of flaws on the static strength, stability, and fatigue life of composites.

Durability and safety-of-flight requirements for commercial aircraft structures must be satisfied for areas of the aircraft that are susceptible to the presence of flaws introduced during manufacturing and/or service environment. Typical flaws that can occur are cracks initiating from fastener holes, surface scratches, improper cure, edge delaminations and impact damage. Since strength degradation occurs in the presence of flaws, the objective of this survey was to review data supported by work on the residual strength capability of composite structures in the presence of flaws and subjected to service loads and environmental exposure. This information can be used to establish B-allowable static strength values that will satisfy life assurance requirements. This assessment will also allow repairability judgments to be made regarding specific flaws or damage to specific aircraft components relative to repair or replacement.

The documents listed in Table I were assembled through a library search and industry contacts. All documents which dealt with the effects of defects in advanced composite structures were reviewed to determine the type of information contained. The total activity consisted of assembling and screening of over 40 documents dealing with experimental or analytical effect of defects on advanced composite materials.

Many of the documents dealt primarily with analytical treatments of idealized defects such as through holes and slots, using fracture mechanics theory, point and average stress failure criteria, and wearout models. In some documents, the analytical treatments were substantiated with various types of test data.

Several of the documents reported empirical data which in some cases were correlated with one or more analytical techniques. Much of the test data are based on idealized flaws such as holes and slots, although some data are available on realistic flaws such as delaminations, scratches, low velocity impact damage, higher velocity foreign object damage (FOD), and very high velocity ballistic damage. The test data include both static and fatigue data, and although more data are available for tensile loading, some compressive data are also reported. The majority of data deal with small specimens such as coupons, although limited data are available on larger specimens more representative of real aircraft structure. A variety of material systems and laminate orientations are represented.

The test data are presented in a variety of formats, i.e., tabular values and curves plotted showing the effect of various parameters such as defect size, energy level, strength loss, life under cyclic loading and damage growth. The information contained in the documents which were screened is summarized in Table I.

Experimental data. - The documents (references 7-47) summarized in Table I were reviewed and all available experimental data on strength reduction as a function of flaw size were plotted. Very few of the documents contained original experimental data. Furthermore, most of the data were for tension loading conditions. Very limited amounts of data were found for the compression loading conditions. Data were available for several material systems including graphite/epoxy, boron/epoxy, and glass/epoxy systems. For the present review, only the graphite/epoxy laminate data were considered. Furthermore, the graphite/epoxy laminate orientations of specialized applications to fan blades and filament wound pressure vessels were not considered because they are not typical of the airframe structures being considered under the present study.

The experimental data on static tensile strength of various laminates as a function of flaw size for holes and slots are presented in Figures 1 and 2, respectively. Also presented in these Figures are the limited amount of data available for laminates with countersunk holes and half-through holes and slots. Most of the data were generated for specimens that were relatively wise as compared to the hole size so that the finite-width correction factor was nearly unity. The only exception was in the case of the test data obtained from reference 10 that had been previously adjusted by multiplying the failure stress by the finite-width correction factor to obtain the equivalent infinite width panel failure stress. The results show that, even for relatively wide panels with negligible finite-width effect, strength is reduced as the flaw size is increased. For both holes and slots, approximately 50 percent strength loss is indicated for the laminate with the 1.0 cm flaw. For larger size flaws, further strength reduction at a more gradual rate is indicated. The test data for laminates with countersunk holes, tested with fasteners in place, show greater strength loss than with non-countersink holes of the same size. This is due to the presence of the countersink which results in increased effective hole size. The laminates with half-through holes and slots show considerably higher strength than those with through flaws of comparable size. The effect of tension dominated fatigue loading was evaluated in references 7 and 11, and it was determined that the spectrum and the cyclic fatigue loads did not induce additional degradation of laminates with holes and slots. However, compression dominated fatigue loading does degrade strength of laminates containing holes and slots as shown in references 7 and 46. Other data indicate that for low velocity impact causing interlaminar damage and limited fiber fracture, the damage does not propagate under either tensile or compression dominated fatigue loading. The predicted strength curves based on the average stress criterion and the fracture mechanics approach (described later in this section) are also presented in Figures 1 and 2 for comparison.

For laminates with holes, the correlation is reasonably good. However, for laminates with through-slots, test data of reference 10 did not agree with the data from references 7 and 11, and the predicted curves showed fair correlation with data from references 7 and 11. The lack of correlation between data from various sources does not appear to be due to variations in the slot shapes because the data of references 10 and 11 which show poor correlation, had identical slot shapes, whereas data of references 7 and 11 showed good correlation even with different slot shapes.

The residual tensile strength data for impact damaged laminates, as a function of the measured surface crack and C-scan detected width of the damaged area, are presented in Figure 3. Results indicate that C-scan observations show a larger area of damage than the size of the surface cracks. This occurs because C-scan inspection detects internal delaminations which typically cover a larger area than the visible fiber failures. To compare strength reduction caused by impact damage and through slots, the analytical curves based on the average stress criterion and the fracture mechanics approach for laminates with through slots are also presented in Figure 3. The same curves showed reasonable correlation with slot data presented in Figure 2. Comparison of impact damage and slot data shows that the measured surface cracks provide a better indication of strength loss than the size of the C-scan observed damage. The effect of tension dominated spectrum fatigue exposure was evaluated in reference 20 and it was shown that fatigue loading did not cause additional tensile strength degradation. C-scan inspection also showed that impact damage size did not grow due to fatigue loading. The same residual tensile strength data for impact damaged laminates are given in Figure 4, plotted against impact energy.

The strength degradation caused by other types of flaws including surface scratches, edge delaminations, and low pressure cure, were evaluated in reference 7 and the results are presented in Table II in the form of residual strength of AS/3501-5 graphite/epoxy laminates with flaws as percentages of unflawed strength. As shown in the table, residual strength values vary considerably with the types and sizes of flaws.

The tension and compression strength retention data from Table II are plotted as functions of flaw size in Figures 5 and 6, respectively. The tension data presented in Figure 5 for 5.1 cm (2-in.) wide specimens show that through slots and fastener holes cause the maximum strength reduction in graphite/epoxy laminates. As compared to through flaws, scratches are somewhat less severe and low pressure cure and edge delaminations are the least severe. For laminates with design ultimate tension strength under 45 percent of unflawed strength, which is a typical design condition for current composite applications, crack growth and catastrophic failure is not expected to occur due to maximum service loads for all of the flaw types shown except for through slots longer than 0.939 cm (0.370 in.). The compression data presented in Figure 5 for 7.6 cm (3-in.) wide specimens show that low pressure 206.8 KPa (30psi) cure causes the most strength reduction and edge scratches (20 percent of laminate thickness) cause the least strength reduction. For laminates with design ultimate compression strength less than

62 percent of unflawed strength, crack growth and catastrophic failure are not expected to occur due to maximum service loads for all the flaw types shown.

The data presented here are not intended to be universal nor complete as they only pertain to a specific material, to specific specimen/flaw sizes, and to specific fatigue exposures. The data are, however, an indication of the susceptibility to flaws one may expect to encounter with conventional graphite/epoxy tape material such as AS/3501-5 or T300/5208. The significantly greater retention of compressive strength of laminates containing scratches is a result of compressive loads causing the cracks to close up resulting in improved load transfer. This effect does not occur in tensile loading. There is a similar effect in laminates containing fastener holes tested with fasteners in place, and compressive strength retentions for these laminates is much higher than tensile strength retentions.

Analytical methods. - Several analytical approaches have been described in the literature for predicting strength of laminates with various types of flaws. For laminates with holes and slots, the use of the linear elastic fracture mechanics approach and a characteristic flaw length was proposed in reference 45. Using this approach, the residual strength of a laminated composite panel with a through-slot of length 2c is expressed as

$$\sigma_R = \frac{K_Q}{\sqrt{\pi (c + a)}} \qquad (1)$$

where K_Q is the fracture toughness of the material and a is the characteristic dimension of the intense energy region that is assumed to exist at the end of the slot. These two parameters are determined from the test data for failure strength of a control specimen with no slot and a specimen with a central slot. This approach can also be used for other shapes of cutouts for which stress-intensity factors are available in the literature.

Another approach proposed in the literature is the average stress failure criterion described in reference 10. Under this criterion, failure is assumed to occur when the average value of the stress over some fixed distance from the edge of the hole or slot first reaches the unnotched tensile strength of the material. For simple configurations such as a through hole, closed form solutions can be used for obtaining the stress distribution adjacent to the hole. For more complex flaws such as countersunk holes or irregular shapes, a finite element analysis can be used. Failure is predicted when the average stress, $\overline{\sigma}$, is equal to the failing strength of the unflawed material. The average stress is given by:

$$\sigma = \frac{1}{a_o} \int_{c}^{c + a_o} \sigma_y \, dx \qquad (2)$$

in which a_o is the characteristic distance over which the stress σy is averaged. An advantage of this method is that the laminate strength can be predicted directly from the calculated stress distribution for any shape of flaw under any biaxial or shearing load conditions. The characteristic length a_o must be known, and is assumed constant for a material.

A model to predict the fatigue failure mode and strength of notched composite laminates under uniaxial tensile loading, including interlaminar effects, is presented in reference 13. The model divides the notched laminate into: 1) a central core region that is the projection of the notch in the loading direction; 2) an adjacent over-stressed region of average stress concentration; and 3) an average stress region. The interlaminar effects are included by discretizing the core region further to the lamina level. Consequently the following failure modes can be predicted by the model: 1) an axial inplane crack in any lamina between the core and the stress concentration regions; 2) an interlaminar delamination between any two laminae in the core region; and 3) a transverse crack, through the thickness, across the laminate. A large number of inplane and interlaminar damages could occur before the entire laminate fails, depending on the material behavior. An elastic-perfectly plastic and an elastic, secant modulus approximation of the nonlinear shear behavior were made in reference 13. The numerical complexity associated with monitoring a large number of defects restricts the capability of the model to predicting the growth of a limited number (three) of defects.

An approach to predicting the uniaxial strength of laminates containing a planar surface scratch normal to the load direction has been presented in reference 47. In this strength of materials approach, the assumption is made that the normal stress on the plane normal to the load direction and through the scratch varies linearly in the thickness direction. This allows the maximum stress on the scratched surface to be found from equilibrium. Failure is predicted to occur when this maximum stress reaches the ultimate tensile strength of the unnotched, unflawed laminate. Since the matrix material of a laminate is so much weaker than the fibers, a scratch that initially terminates at or within a 90 degree ply is considered to extend completely through that ply for the purpose of strength prediction.

In this approach, no overt recognition is given to the localized stress concentration that would be expected to occur along the crack periphery. Rather, a stress concentration occurs across the entire width of the specimen at the scratched surface. Nor is any change in the bending moment on the normal plane containing the scratch due to possible bending displacements assumed to occur. In spite of the simplicity of the assumptions involved in this approach, good comparisons to the test results given in Table II were reported in reference 47 for both circular arc surface scratches in a

$(0/\pm 45/0)_{3s}$ laminate and for rectangular surface scratches in various laminates.

Numerous analytical approaches have been described in the literature for predicting residual strength of impact-damaged laminates. In references 33 and 37, use of linear elastic fracture mechanics for predicting residual tensile strength was considered using an idealized through-crack simulating the impact damaged area. In reference 33, this approach was used to develop an analytical model for predicting residual strength as a function of impact energy represented by the following equation.

$$\frac{\sigma_R}{\sigma_o} = \sqrt{\frac{W_s - K\bar{W}_{ke}}{W_s}} \qquad (3)$$

where,

σ_R is the residual strength

σ_o is the unflawed laminate strength

W_s is the strain energy required to break the unflawed laminate under static load ($= \sigma_o^2/2E_L$ for linear stress-strain response), expressed in Newton-meters (N·m)

$\bar{W}_{ke}$ is impact energy per unit laminate thickness imparted to the specimen expressed in Newton-meters (N·m)

K is effective damage constant determined by fitting the test data to the theory at one value of impact energy.

To evaluate the accuracy of this approach, analytical predictions were compared with residual strength impact test results obtained for 12 ply (0, 90) symmetric laminated composite specimens impacted with 0.45 cm (0.177 in.) and 0.635 cm (0.25 in.) diameter steel projectiles at several velocities. Good correlation was shown between predicted and test results for residual strength as a function of impact energy (see Figure 4). However, the model was found to be accurate only for relatively low impact energies that caused much less than through-penetration damage.

In reference 37, to predict the length of the crack, it was assumed that a certain percentage of the impact energy was consumed in creating the fracture surface in the laminate and a linear relationship between damage size and impact energy per laminate thickness was proposed. The laminate residual strength was then predicted by using a modified form of equation (1).

A finite element analysis method was employed in reference 34 to determine the impact response to multilayer, generally orthotropic solids and multilayer orthotropic cylinders subjected to impact by an impacter in the

form of a body of revolution. The quasi-dynamic approach employed in studying the impact response of generally orthotropic plates involved: 1) determination of the time-dependent surface pressure in the composite target material caused by the impacter; 2) determination of the internal triaxial stresses due to the surface pressure; 3) determination of failure modes due to these stresses; and 4) determination of coupling between impact velocity, properties of target and failure modes. To compare analytical predictions with experimental data, a test program was conducted with all graphite and hybrid graphite-glass and graphite-Kevlar laminates. Composite plates of three different laminate thicknesses - 0.168 cm (0.066 in.), 0.353 cm (0.139 in.), and 0.660 cm (0.260 in.) were considered. The important results of this analysis and test program were: 1) impact damage resistance of composite materials increases as the strain to failure of the fibers and matrix increases; 2) bidirectional (0/90), layups are more efficient in resisting impact damage than tridirectional (0/$\pm$60) and unidirectional layups; 3) uniform dispersion of layers (having different fiber orientations) through the thickness provided better impact damage resistance than nonuniformly dispersed layers; 4) effects of hybridization on impact damage were inconclusive because of poor quality test specimens; and 5) theoretical predictions of impact damage in composites showed fair correlation with test results; however, further refinement of the theory appears desirable.

Task B - Survey Of Airline Damage Experience

Survey activities. - A survey was made of domestic airline operators to determine the types and extent of damage most frequently encountered in service. This survey covered damage experiences on fiberglass components, current advanced composite components, and metal components considered likely candidates for future composites use. The survey also covered the subjects of airline repair facilities and maintenance practices, the effects on airline maintenance operations of widespread composites usage on commercial aircraft, and the types of composite repair procedures most compatible with airline maintenance operations.

Letters were written to sixteen domestic airlines requesting their participation in the survey, and eleven airlines agreed to participate. They were American Airlines, Braniff International, Continental Airlines, Delta Air Lines, Eastern Air Lines, Flying Tiger Line, Pan American World Airways, Piedmont Airlines, Southern Airways, Trans International Airlines, and Trans World Airlines.

The survey consisted of the following activities: 1) preparation of a questionnaire covering the survey subjects and submittal of the questionnaire to airline engineering and maintenance personnel; 2) on-site discussions at the airlines' major maintenance bases between a Lockheed engineering survey team and airline engineering and maintenance personnel; 3) preparation of a summary of the airline damage experience data organized by part category and by defect type within each part category, and preparation of a summary of airline responses to questions on their maintenance operations.

The questionnaire was submitted to the participating airlines several weeks before the on-site discussions, and the airlines were requested to complete the questionnaire prior to the Lockheed visit so that the airline responses could provide a basis and outline for the discussions. The questionnaire is included as Appendix A to this report.

The first part of the questionnaire provided a format for listing the types of damage typically encountered in service for the various categories of aircraft parts, such as wing skins, wing substructure, control surface, etc. The format, given as Table A1 of Appendix A, provided for listing of typical defect sizes, location on the component, and type of maintenance action required. A List of Codes was attached to the questionnaire to expedite completion of this table by airline personnel. Codes were given for component types, defect types, and type of maintenance action required. The maintenance action categories included negligible damage requiring no repair; damage repairable at line station where down-time, facilities, equipment and specialized skills are severely limited; damage repairable only at the maintenance base using standard procedures from the maintenance manual; damage repairable only at the maintenance base using repairs developed by engineering for the specific repair situation; and nonrepairable damage requiring part replacement.

The remainder of the questionnaire covered the airlines maintenance facilities, equipment, and procedures. The questions covered detection of defects (whether at line stations or the maintenance base during a schedule check) and type of inspection procedure used; relative frequency of the maintenance action categories listed above; frequency of special repair situations at line stations and under what circumstances each are used; repair of removable components (whether removed for repairs or repaired on-aircraft); elapsed time available during periodic maintenance checks for repair; and availability of such equipment as autoclaves, ovens, vacuum pumps, freezers, and portable repair kits. An additional question asked verbally of the airlines was the relative frequency of damage caused by the three principal causes of damage: impact, fatigue, and corrosion.

Submittal of the questionnaire was followed about two months later by visits to the airline major maintenance bases by the Lockheed survey team. This team consisted of the Engineering Program Manager and a Structures Engineer with extensive experience in airline maintenance and repair. In all cases, discussions were held with airline engineering personnel with participation by maintenance personnel as well in some cases. Most of the airlines had filled out the questionnaire prior to the visit, but in all cases the questionnaire was reviewed item by item and provided an outline for the discussions.

Results of airline survey. - The airline questionnaire responses were summarized in two tables. Table III summarizes the airline damage experience with the data organized by defect type within each part category. Table IV

summarizes the responses to the questions on airline maintenance procedures and facilities.

The discussions with airline personnel provided additional information on airline maintenance operations and facilities, damage experience, and airline concerns and needs for the introduction of advanced composites into commercial transports. A summary of this information is given below:

- Aircraft damage and defects have three basic causes - fatigue, stress corrosion, and impact. The relative frequency of damage from these three causes varies widely from one airline and one aircraft type to another. The incidence of fatigue cracks obviously is related to the age and service history of aircraft, while corrosion is dependent on materials and design factors. A relatively new aircraft such as the L-1011 sees a relatively small proportion of fatigue and corrosion damage because of its shorter service life and use of improved alloys. Impact occurs to about the same degree on all aircraft, but the proportion varies with the other two factors.

- Corrosion damage typically occurs in the lower fuselage areas where water collects, while fatigue effects are not limited to any specific areas. Impact damage occurs principally in the lower fuselage area, flaps, and other areas subject to ground handling damage, with fuselage areas near cargo doors the most damage prone areas. The inboard flaps and inboard lower wing surfaces are subject to tire tread damage. In-flight damage such as hail and bird strikes are less significant causes of damage, and occur primarily on leading edges. The engine cowl door receives considerable damage resulting from its frequent removal for maintenance. Damage to wing skins and substructure is from a combination of fatigue and corrosion effects. The vertical stabilizer is a relatively damage-free area. Floor beams are a highly corrosion prone area, while floor posts see very little damage.

- The airlines had similar policies regarding line station repairs. These repairs are nearly always external aluminum patches, mechanically attached to the baseline part. These repairs are considered "airworthy" repairs permitting the continuation of revenue flights according to FAA requirements. The line station repairs are frequently but not always, replaced at the next maintenance check with an improved maintenance base repair which is more suitable from an aerodynamic, environmental, fatigue, or esthetic viewpoint.

- The incidence of line station damage or repairs requiring nonrevenue ferry flights is limited to two or three times a year. The use of crews flown in from the maintenance base for line station repairs is more common, but still occurs only a few times a year. These are both costly operations, and because of the need to minimize these situations, composite repair techniques suitable for line station operations are a necessary development.

- For composites, the line repairs bring up two potential problems. The drilling operations at line stations will always be made by untrained personnel without specialized tools. Subsequent inspection at the next maintenance check will be necessary to check for damage caused by the drilling and trimming operations. Drilling and trimming of composites will require training of maintenance base personnel, and this will initially be a problem. The other problem for line station repairs is the frequent omission of faying surface sealing and wet installation of fasteners, and the resultant galvanic problems when aluminum patches are attached to graphite structure.

- Airlines have widely differing attitudes on the issue of flush vs. external patches. In some cases, flush repairs are used in all areas except where back-side clearance or access problems prevent their use. In other cases, flush repairs are limited to aerodynamically critical areas such as leading edges, control surfaces, forward fuselage areas, etc. The percentages given for flush patches (see Table IV) vary from 10 percent to 80 percent.

- The airlines would prefer the use of metal patches and mechanical attachments for both external and flush repairs, as this merely extends their current practices to the new composite materials. However, the use of bonded repairs incorporating 121°C (250°F) curing adhesives with metal or precured graphite patches, or with cure-in-place graphite pre-preg patches is recognized by most of the airlines as a technique which will be required to a greater degree on future advanced composite and bonded structures. The cold bonding and wet layup techniques used on fiberglass repairs are generally considered to have limited applicability for the more highly loaded components on which graphite/epoxy will typically be used.

- Most of the airlines have some familiarity with the use of structural grade 121°C (250°F) curing pre-pregs and adhesives. Three of the airlines have autoclaves, and most of the others have ovens, freezers, cleaning tanks, and vacuum equipment. The airlines having less capability in this area frequently send components to outside facilities for repairs of this type, and several fabricators specialize in bonded repair for airlines. Some airlines with bonding capabilities perform these repairs for other airlines.

- The airlines usually remove bonded or fiberglass structures (such as control surfaces, fairings, and radomes) for repair, and replace with a spare. Fairings and radomes are generally repaired with wet layup fiberglass techniques, while control surfaces are usually given structural repairs using 121°C (250°F) curing, structural grade adhesives and pre-pregs cured under vacuum or autoclave pressure. Rebalancing and maintaining aerodynamic contour is critical for control surfaces, so these are usually given flush repairs. The airlines with autoclaves and extensive experience with bonding

operations make their own control surface repairs, while others send these components out for repair.

- The use of composites in nonremovable parts such as wings and stabilizers, and the need for on-aircraft structural bonded repairs is a new situation for the airlines. This will be one area requiring considerable development and training on their part.

- Maintenance down times are limited to a few hours, except for the "C" checks which occur on a roughly annual basis, and the major overhauls or "D" checks occurring at roughly 7 year intervals. Many airlines have segmented "C" checks where the aircraft is in 3 or 4 times a year and a certain percentage of the components are inspected in each segment. In some of these situations, down-time at "C" check is only a few hours, and bonded repairs could not be accomplished in that time.

- All of the airlines had full NDI capabilities, including ultrasonic, X-ray, and eddy current procedures. NDI in most cases is used to verify damage or defects which are detected visually (or occasionally by coin tapping). Components are generally not given periodic NDI over their entire surface area even at major overhauls. This is done only on certain specified critical areas, and generally on the basis of FAA directives or manufacturer instructions. This presents a potential problem with composites in that delamination initiated by impact damage might not be detected under current inspection procedures.

- Detection of nearly all defects resulting from fatigue and corrosion occurs at the maintenance base during scheduled checks, and as discussed above is mostly detected visually. Impact damage primarily occurs and is observed at line stations.

Task C - Defect Categorization Matrix

In Task C, the data from the Task A survey on composite defect sensitivity and the Task B survey of damage to existing aircraft were reviewed. The list of damage types and sizes from the airline survey was re-organized by defect type within each part category. The damage to existing metallic structures taken from this listing has been used to estimate the type of damage which would be expected to occur with comparable graphite/epoxy structure. The strength loss in the graphite/epoxy, the potential for growth of the damage, and the requirements for maintenance action have been estimated for generic types of components. In making these estimates, a considerable amount of judgment had to be used since comparative damage data for metallic and graphite structures are generally not available. In the cases where damage to metallic structures was incomplete or not clearly defined, estimates were not made for comparable graphite structures. The completed table, listing the damage types for metallic structures and the

comparable estimated composite damage is included herein as Table V, Defect Categorization Matrix.

A considerable listing of damage due to corrosion was obtained from the airline survey. Since this cause of damage is completely absent from composites, these damage listings are not included in Table V. Damage to metal structures caused by fatigue have been included, but since the growth of damage in composites from subsequent fatigue cycling is significantly less than metals, no attempt has been made to estimate composite damage size, strength reduction, or maintenance action required. In fact, fatigue cycling as the initiating cause of damage in composites appears to be a negligible factor, as long as design stresses are at the level typical of most composite applications (50% unnotched strength, 0.4% strain). Damage to honeycomb structure was also listed, but composite damage levels are not expected to differ significantly, as the bond line is assumed to be the point of failure rather than the adherend. Miscellaneous damage (lightning, fastener hole wear, and surface wear) have been handled in a similar manner as the fatigue listing, with composites assumed to react in a dissimilar manner to metal, such that damage extent can not be estimated.

Certain assumptions have been made in making estimates of impact damage to graphite structures. The first assumption, based on extensive test data for graphite structures reported in the literature, is that fatigue crack initiation and growth due to tension dominated spectrum load exposure typically does not occur for graphite/epoxy materials. However, graphite structures are more susceptible to delaminations, matrix cracking, and fiber failures due to foreign object impacts; and the damage typically spreads over a larger area than for the comparable metallic structures. In the present estimates it has been assumed that the damage from impact spreads an additional 5.1 cm (2.0 in.) for the graphite structures as compared to the metallic structures.

The estimates of the strength of impact damaged graphite/epoxy laminates as a percentage of undamaged laminate ultimate strength are based on data assembled during the Task A literature survey. In general, impact damage in graphite laminates which is at the threshold of visibility reduces the laminate strength to approximately 60-70% of the undamaged laminate strength. When the visible surface fiber cracks exceed 1.27 cm (0.5 in.) the laminate strength is reduced to 40% or less of the undamaged strength (see Figure 3) and further increases in damage area do not significantly lower this residual strength as long as the net area is not significantly reduced. In cases of extensive damage covering a large area of a particular component, the net area effect becomes significant and the damaged structure may be left with considerably less than 40% of the undamaged strength.

Test have shown that visible surface damage does not provide a good indication of the extent of internal delaminations and cracks because of the large variations in the size, shape and velocity of foreign objects causing impact damage. Therefore, it may be desirable to conduct periodic ultrasonic inspections of laminates which show indications of surface dents or damage,

to establish the extent of internal damage and repair requirements. In fact, tests have shown that extensive internal damage may occur with no visible surface damage or dents. In the present state-of-the-art, design ultimate strength requirements will normally be low enough so the structure can sustain ultimate loads with damage below the visual threshold. This fact may make it possible in some cases to operate without periodic ultrasonic inspections.

The potential for damage growth has typically been indicated as "low." Many tests have been made in which the size of internal delaminations and matrix cracks were determined by ultrasonic C-scans which were made both before and after spectrum load exposure. Little or no damage growth has been found with tentle or no damage growth has been found with tension spectrum strain levels in the range of 4000-4500 μm/m on room temperature specimens with no moisture conditioning and these strain levels are typical of most components for which composites are being considered. The effects of more severe environments on damage growth have not been determined at this time.

Maintenance actions which are required have been indicated in a general way. Where aerodynamic smoothness is important, requirements for a flush surface repair have been noted. In cases where restoration of a significant percentage of the strength would be required, the term "Structural Repair" has been used. In other cases repairs which may be primarily cosmetic in nature will frequently be adequate to provide the required smoothness, sealing or appearance.

Conclusions

The Task A survey of theoretical and experimental work on composite defect sensitivity provided significant information on the strength reduction in composites resulting from various types and sizes of flaws. The following significant conclusions were obtained from the survey results, and from the organization of defect data in Task C:

- The defect sensitivity of composites is being accounted for in current design practices by limiting design ultimate tensile and compressive strengths and strains to a level such that open holes and defects can be tolerated. This is typically 40-60% of unflawed strength and strains to failure, so that repairs of damage need restore only about 50% of unflawed tensile or compressive properties in order to restore design strengths and strains. This reduction of unflawed tensile and compression properties levels off in the 40-60% range as damage size is increased to about 1.27 cm. (0.5 in.).

- Tension dominated fatigue cycling does not cause flaws to grow to catastrophic sizes at the typical tensile strain levels (4000 - 4500 m/m) at which most composite components operate, nor does it cause further reduction of residual strength at these strain levels.

- The defect sensitivity of composites in compression loading is comparable to that in tensile loading at the lower load levels typical of most current composite applications. At higher compressive loads delamination growth can occur resulting in substantial reductions in compressive strength due to buckling.

The Task B airline survey provided data on the types, sizes, and origins of typical defects encountered by airlines on various categories of parts, as well as the type of maintenance action required for these defects. The survey results also provided information on airline repair and maintenance procedures, facilities and equipment, and the adaptability of airline operations to maintenance of composites. The following significant conclusions are summarized below:

- Airline damage results primarily from impact, fatigue, and corrosion. The introduction of composites can be expected to eliminate corrosion, and greatly reduce fatigue as causes of damage.

- The lower fuselage is the most damage-prone area, subject to both impact and corrosion, and most impact damage is from ground handling rather than inflight damage.

- All repairs are considered permanent repairs and must, according to FAA regulations, restore the full design strength of the component and must not adversely affect fail safe characteristics of the part. These criteria apply to repairs made at line stations as well as major maintenance bases.

- The only type of repair which can currently be accomplished at line staions is mechanically attached external patches. Potential problems with line repairs are galvanic corrosion and damage caused by drilling operations.

- Airlines use both flush, aerodynamic and external patch repairs, with widely varying proportions of each.

- Some airlines have excellent capabilities for structural bonded repairs, but others completely lack facilities and experience and utilize outside vendors for bonded repairs.

- Airlines have virtually no experience or capabilities for "on-aircraft" bonded repairs.

- Maintenance down times between major overhauls are too short in some cases to accomplish bonded repairs.

- Airlines have full NDI capabilities, but use NDI only to determine the extent of visually detected damage. Nonvisible delamination damage in composites would not be detected under this approach.

These results indicate a need for a variety of composite repair approaches including bonded and bolted repairs, and both external and flush patches.

PHASE 2 - DEVELOPMENT AND VERIFICATION OF REPAIR METHODS

Phase 2 consisted of a single Task in which selected repair concepts were screened using sandwich beam and monolithic laminate test specimens.

Selection of Repair Concepts

The selection of repair procedures to be screened and evaluated in Phase 2 was based on results of the Phase 1 surveys as discussed in the Introduction. The basic repair variables and the justifications for their inclusion in the Test Plan are as follows:

- Flush graphite patch repairs: For areas where aerodynamic smoothness is required; for critical structure requiring maximum joint efficiency; for critical structures where load concentrations and eccentricities must be avoided; for very thick structure where an external patch would involve excessive out of mold line thickness.

- External graphite patch repairs: For less critical structure and thinner laminates where the complexity of flush repairs is not required; for areas where back-side access limitations or sub-structure interference requires an external repair.

- Structural bonded repairs with heat-curing structural grade pre-pregs and adhesives: For critical and highly loaded composite structure; for maintenance base repairs where capability exists for a bonded repair; for composites where repair durability is critical.

- Cold-bonded and wet lay-up repairs with room temperature contact pressure curing systems: For non-critical, lightly loaded structure where little strength recovery is required and where repair durability is not a critical factor.

- Bolted metal repairs: For repair of all types of composite structure where limitations in facilities, personnel skills, down-time, or access prevent the use of bonded repairs.

Other variables included in the program were the use of pre-cured, bonded graphite patches and cure-in-place graphite patches. The cure-in-place patches can easily conform to contoured surfaces, are readily adapted to any size and shape of repair, and can be readily overlapped to form a scarf joint or stepped patch configuration. An external cure-in-place patch permits overlapping each ply over the preceding ply thus providing more effective bondline sealing. The pre-cured bonded graphite patch permits

autoclave cure of the patch material thus providing improved patch structural properties for a vacuum bonded repair. In a flush repair, the scarfed tapers of the patch and parent laminate must be matched which adds to the difficulty of a pre-cured bonded repair.

The bolted repairs included aluminum patches which are easier to drill and trim and are more readily available at all types of maintenance facilities, and titanium patches which provide a better match with the graphite composites galvanically and in thermal coefficient of expansion. For the limited number of bolted repairs included in this task, blind fasteners were used. These would be required where back-side access is unavailable, but standard fasteners provide improved pull-out strength and would likely be used where access permits.

All of the structural bonded repairs in this task used unaugmented vacuum pressure. This approach is feasible for on-aircraft repairs and for repairs at facilities lacking autoclaves. Additional structural efficiency can be achieved in bonded repairs through use of autoclave pressure or by combining with mechanical attachments.

The various repair approaches are shown schematically in Figure 7. Detailed descriptions of the repairs are given in the following paragraphs.

Test Plan

The Test Plan is outlined in Table VI for the sandwich beam test specimens with 16 ply laminates, Table VII for the sandwich beam specimens with 50 ply laminates, and Table VIII for the tabbed laminate specimens. The tables describe each repair concept, and the various repair and control specimens are assigned a code number. These tables also give the test results and failure modes. Selection of the various methods is discussed in the Introduction and in the preceding paragraph. The tests used to evaluate the repair procedures include static tensile and compressive strength and fatigue tests. These test procedures are discussed in the following paragraphs. Fatigue spectra were selected to be representative of a commercial transport wing cover component (for the 50 ply laminates) and the L-1011 vertical fin (for the 16 ply laminates), and are also discussed in the following paragraphs.

All parent laminates were conditioned to 1 percent moisture content by immersion in water at 82°C (180°F) prior to performing the repairs. This was done to simulate the condition of a typical composite part being repaired in service. This is significant for bonded repairs where entrapped moisture can affect the bonding surface condition or can cause blistering during elevated temperature cure. Laminates used for controls and for bolted repairs were also conditioned to provide direct comparisons with the bonded repairs. The repaired specimens were humidity conditioned for an additional 30 days at 60°C (140°F), 95 perent relative humidity to evaluate durability of the repair patch materials and adhesives.

Tests were performed at room temperature, -54°C (-67°F), and 82°C (180°F). The largest number of tests were performed at 82°C (180°F) since the presence of moisture produces the greatest strength reduction at elevatd temperature. This provides an evaluation of the durability of the graphite repair patch material and the repair adhesives.

The sandwich beam specimens included undamaged controls for both the 16 ply and 50 ply parent laminates. The tabbed laminate specimens permitted evaluation of a damaged, unrepaired control and this was included along with an undamaged control.

Design of Repairs

Flush repairs. - The development of the flush repair concepts was based on the scarf joint configuration studies done on the "Large Area Composite Structure Repair" (LACOSR) program, (reference 43). The basic concept of the scarf joint is simple; as the thickness of one side of the joint (for example the parent laminate) is diminished, the thickness of the opposite side (the patch) is increased. Load is transferred only through adhesive shear since the scarf length is large compared to the laminate thickness.

An elementary procedure was used for load transfer analysis based on the assumption that at any station the load in each adherend is proportional to the extensional stiffness. This procedure accounts for the heterogeneous nature of the laminate and gives a satisfactory description of the shear distribution in the splice when applied at each ply end in the splice.

The full thickness flush scarf concepts used in this program have identical parent and repair laminates with the same thickness and ply orientations. The relative stiffness (Et) values of each adherend (where E = Young's modulus and t = thickness) are determined by accumulating the relative values at each station as thickness is increased by one ply per station increment. Knowing the Et of each adherend, the total Et is found and the relative load in one adherend determined from the assumption that the load in each adherend is proportional to the adherend Et divided by the total Et.

The difference in the load fraction at two adjacent stations is the average relative shear (R.S.) loading for the increment, i.e.,

$$(R.S.)_{i,i-1} = (L/T)_i - (L/T)_{i-1}$$

where L_i = Left Et of station i

T_i = Total Et of station i.

The strength of the splice is inversely proportional to the maximum relative shear, i.e.,

$$P_{ULT} = F_{SU} (\Delta x)/M.R.S.$$

where F_{SU} = adhesive ultimate shear strength

Δx = station increment

M.R.S. = Maximum Relative Shear

Calculations as described were made in the previous Air Force LACOSR Program, and used to develop the basic joint configuration which has been used in the current program. Based on the experimental findings of the LACOSR program, a small number of cover plies have been added in most cases to relieve the stress concentrations at the ends of the scarf.

External repairs. - The external patch repairs were reviewed by Lockheed Structures Engineering prior to fabrication. While no formal analyses were conducted, the bonded repair designs were checked for adequate bond-line area so that the shear strength of the adhesive was not exceeded, and the bolted repairs were evaluated to ensure that the thickness of the metal patch provided adequate bearing strength for full laminate strength recovery. The overlap configuration of the pre-preg layer and pre-cured graphite layers was evaluated for effectiveness in reducing peak load concentrations at the patch edges.

Test Specimen Design

Sandwich beams. - The test specimen used for most of the repair tests was the honeycomb sandwich beam configuration shown in Figure 8. This specimen configuration was used for Specimen Types C-16, C-50, and I-XII (as identified in Tables VI and VII) incorporating both the 16- and 50-ply repaired laminates. This specimen was used because it provides a ready means of applying loads into thick laminates, because it provides a means of stabilizing the laminate during compression testing to prevent buckling, and is adaptable without modification for tensile, compression, or fatigue testing. This specimen configuration had been used successfully by Northrop on its previous Air Force program on Large Area Repair (ref. 3).

The beam configuration was selected to force a failure in the graphite face of the beam. This required careful design and selection of core density, slave skin material and thickness, and beam dimensions. The core splice configuration was used to allow heavy core outboard of the load application points to withstand the shear loading and the stress concentrations while supporting the test (repair) section with a core of realistic density for aerospace applications.

Core selection also influenced the beam dimensions. Since core shear is inversely proportional to the distance between load application and load reaction, the beam had to be long enough not to exceed the core strength.

This resulted in a considerable longer beam being required for the 50 ply laminates than for the 16 ply laminates. The adhesive bond strength was also a factor.

Finally, the slave skin was selected so that the failure stress in the slave skin would not be reached before the failure strain of the parent laminate. The parent laminate strength provided an upper-bound estimate of the predicted failure strain of a laminate in the repaired condition.

Tabbed laminates. - The Test Plan also includes several tabbed laminate specimens (Types C-U, C-D, XIII, and XIV as identified in Table VIII). This specimen configuration is shown in Figure 9, and was used for static tensile tests of 16 ply laminates. This specimen type with a 1.9 cm. (0.75 inch) hole in the center of the span, provides a more realistic geometric representation of an actual repair than the sandwich beam specimen in which the damage is represented by a cut completely across the specimen width. The tabbed laminate specimen also permits the testing of a damaged, unrepaired control. The laminate specimen prior to repair has a reduced strength and strain capability comparable to damaged components in service, and for repairs which restore only a small percentage of unflawed strength is likely to give more realistic values. Disadvantages are the greater difficulty in load introduction and stabilization against buckling. Two repairs, identical to repairs evaluated with the sandwich beam, were evaluated: one flush graphite repair and one external graphite patch repair.

Parent Laminate Fabrication

Two parent laminate lay-ups were used in the program as discussed previously. The 50 ply lay-up representing a highly loaded wing cover design had the following lay-up $(\pm 45, 90_2, +45, \pm 45, 0_4, +45, \pm 45, 0_3, +45, \pm 45, 0_2)_s$. This specific lay-up was developed by Northrop as a preliminary design for the B-1 program. The 16 ply lay-up representing a lightly loaded cover was taken from the L-1011 composite vertical fin cover design and had the following lay-up $(\pm 45, 0, \pm 45, +45, 0)_s$. In addition 4 ply pre-cured patch laminates were fabricated with a $0, 90_2, 0$ orientation. This orientation was selected as the thinnest possible unit which would be quasi-isotropic and symmetrical. These laminates were fabricated using Narmco 5208/T300 graphite/epoxy pre-preg tape, 0.127 mm (5 mils) pre-cured ply, 34 ± 3 percent resin content by weight conforming to a Lockheed Materials Specification. The laminates were fabricated using the following cure cycle.

1) Apply full vacuum

2) Heat to $171^{\circ}C \pm 2.8^{\circ}C$ ($175 \pm 5^{\circ}F$) at $1.1\text{-}1.7^{\circ}C$ ($2\text{-}3^{\circ}F$)/minute.

3) Dwell at 171°C ±2.8°C (275 ±5°F) for 45 minutes.*

4) Apply 689.5 ±34.5 kPa (100 ±5 psi), venting vacuum at 137.9 kPa (20 psi).

5) Heat to 179 ±2.8°C (355 ±5°F) at 1.1-2.2°C (2-4°F)/minute.

6) Cure for 120 + 10, -0 minutes at 179 ±2.8°C (355 ±5°F).

7) Cool to 79°C (175°F) under pressure.

An initial 50 ply trial laminate, 30.5 by 35.6 cm. (12 by 14 inches), was fabricated using this cycle and was satisfactory and void-free as determined by ultrasonic C-scan. Several subsequent 50 ply test laminates which were larger in area, had unacceptable voids however. Several other test laminates were satisfactory, and these were generally smaller and narrower than the panels which were unacceptable. The conclusion from these results was that when the transverse distance that the entrapped air and volatiles had to be moved was increased, the probability of their being entrapped was increased. The 50 ply lay-ups had been de-bulked prior to lay-up in four 12 and 13 ply units by exposure to full vacuum for 30 minutes at ambient temperature. Photomicrographic examination indicated most voids were at or within one ply of the boundary between these de-bulked units. Corrective action was therefore taken to eliminate the de-bulking operation, to reduce the area and width of the 50 ply laminates as much as possible, and to increase the vertical bleeding action by adding a breather ply between the laminate and the tool surface. This bleeder arrangement is shown in Figure 10.

The 16 ply parent laminates and the 4 ply pre-cured patch laminates were cured using the cure cycle given above with no de-bulking prior to cure. The bleeder arrangement consisted of one layer porous Teflon coated glass cloth over each surface of the lay-up; one layer of 120 glass bleeder over the lay-up followed by a caul plate covered with release film; a barrier film over the caul sealed to a Corprene dam with slits in each corner to provide a breather path; 2 layers polyester low absorption mat over the barrier film as a breather; and the vacuum bag. These laminates were all satisfactory as determined by ultrasonic C-scan, with no voids.

After fabrication and inspection, all parent laminates were conditioned to 1 percent moisture content by immersion in water at 82°C (180°F). Traveler coupons were used to monitor moisture pick-up of the laminates.

*Dwell time starts when temperature reaches 129°C (265°F).

A list of all the parent laminates used in the repair tests is given in Table IX, with resin content, density, calculated fiber volume and calculated void content. A similar list of the pre-cured patch laminates is given in Table X. The repair types for which each laminate was used is indicated by reference to the code numbers given in Tables VI, VII, and VIII.

Study of Cure Cycle Variables and Moisture Effects

During the course of the program, investigations were conducted to determine the cure cycle parameters that would be most suitable for the T300/5208 repairs and to study a blistering phenomenon which had occurred during the repair cure cycle of moisture conditioned laminates during a previous repair program.

Cure cycle variables. - Seven process development panels were fabricated to investigate cure cycle parameters for the T300/5208 material. The panels and the cure cycles for each panel are described in Tables XI and XII. Variables included (1) vacuum pressure versus 689.4 kPa (100 psi) autoclave pressure, (2) dwell at temperature (45 minutes at 135°C [275°F]) versus no dwell during temperature rise to the 177°C (350°F) cure temperature, (3) use of bleeder ply versus no bleeder, and (4) vertical versus horizontal orientation during cure. The panels were 7.8 inches (19.8 cm) wide, 16-ply $[(\pm 45/0/90)_2]_S$ and hexagonally shaped with stepped ply patterns and serrations to simulate a repair patch.

Based on previous Lockheed experience, two cure cycles were used, each with either vacuum pressure or with 689.4 kPa (100 psi) total pressure in an autoclave cure. These cure cycles are listed in Table XII. Because of concern about the amount of resin flow, two panels were cured in a vertical position. A single bleeder ply was used for one panel to compare with the no-bleed arrangement which is preferred to simplify the repair procedure.

Completed panels were inspected, physical properties were determined and matrix properties were compared using short beam shear specimens cut from the panels. Visual examination after cure showed no differences among the seven panels. Tapered edges where plies were dropped off appeared unaffected by the presence of one bleeder ply of 120 glass cloth. No sagging occurred for the panels cured vertically. The first two panels made under vacuum only with no dwell delaminated so that separation occurred during machining. A third panel cured in the same manner, but with a ply of glass bleeder, was free of delaminations. Two panels cured under vacuum only with a 45 minute dwell at 135°C (275°F) had voids. The two panels cured under 689.4 kPa (100 psi) autoclave pressure were void-free.

The panel quality of the vacuum bag cured laminates in the original set of seven panels was not satisfactory. Pre-preg quality was suspected as the cause. Since a major premise of the program is the use of vacuum pressure, two additional panels were fabricated from another pre-preg batch with and without dwell during temperature rise. Satisfactory test data were obtained

indicating that vacuum pressure curing could be used for repairs made out of T300/5208. Table XIII summarizes the results from the characterization of these nine laminates. Since the vacuum-with dwell and vacuum-without dwell cure cycles yielded satisfactory results, the latter was selected for use in the program based on simplicity.

Moisture effects. - Based on the results of the Air Force Large Area Composite Structure Repair Program (ref. 43), a concern existed that 50-ply parent laminates which had been conditioned to 1.0 percent moisture content might blister when exposed to the repair cure cycle. To address this issue, simulated cure cycles at 177°C (350°F) were run on spare moisture conditioned 50-ply pieces and a reduced cure temperature investigation was conducted.

The blistering investigation used four 50-ply pieces each 10.2 x 20.3 cm (4 x 8 inches). One wet (1.07 percent moisture content) and one dried (0.77 percent moisture content) piece were subjected to a simulated repair cure cycle [177°C (350°F) for one hour] and a simulated repair cure cycle with rapid heat-up [4.4°C (8°F) per minute]. None of the panels blistered.

The results suggested that blistering of parent laminates may not be as serious a problem as had been expected from the Air Force program experience. However, the small pieces used for this investigation may be less susceptible to blistering than the larger panels which previously blistered. Panels up to 35.6 x 127.0 cm (14 x 50 in.) did not blister when later repaired in the test specimens with a 177°C (350°F) cure cycle.

A reduced temperature cure cycle program accompanied the dry/wet blistering task. To evaluate the effects of a reduced temperature cure, panels were fabricated under vacuum pressure only at 149°C (300°F) for one, two, and three hours, and at 177°C (350°F) for one hour, which was the normal repair cure cycle for this program. Tension and compression coupons cut from the panels were tested at Northrop and results are tabulated in Table XIV.

The reduced temperature cure affects the matrix rather than the fibers, so that strength properties dependent on the matrix are more significant for evaluating the reduced temperature cure. The longitudinal compression strength depends on the ability of the matrix to prevent microbuckling of fibers and is therefore a better measure of cure cycle effects than the tension strength. However, the failure of the tension specimens cured at 149°C (300°F) for one hour resulted in extensive delamination over the full gage length, indicating very weak matrix strength. The specimens cured for two and three hours at 149°C (300°F) did not delaminate as much; the failure mode was the same as for the normal 177°C (350°F) cure. The strength values for the tension coupons reflect the lack of influence of the matrix since tensile load is largely carried by the fibers.

The compression data shows a definite trend, with all 149°C (300°F) cures weaker than the normal 177°C (350°F) cure. Failure modes for all compression coupons were the same, involving delamination and local

microbuckling of plies over a half-inch unsupported length at the mid-length of the specimen.

There was no significant difference in physical properties found by acid digestion. Values are shown in Table XV. Photomicrographs showed voids in all four specimens, as is to be expected with the vacuum bag cure. The appearance was the worst for the specimens cured at 149°C (300°F) for one hour, and the appearance improved progressively for the two and three hour cures.

Dynamic flexure tests (DMA) were also run on these four laminates in which the specimens were cyclically loaded in beam bending at 0.1 and 1.0 kHz frequency at various temperatures; and the dynamic modulus was determined. Glass transition temperatures (Tg) were determined as peaks in the phase angle of the time dependent response of the specimen to the induced load. The glass transition temperature was alternately determined by thermo-mechanical analysis (TMA) where the laminates response to a mechanical probe was measured. The results are summarized in Table XVI, and indicate that a 149°C (300°F) cure temperature is not adequate for complete cure of the 5208/T300 patches.

The specimens cured at Northrop were post-cured and changes in Tg determined. The changes observed upon post-cure of the 149°C (300°F) cured laminates further indicated the lack of complete cure, and softening of the 1 hour, 149°C (300°F) cure specimen occurred upon 172°C (350°F) exposure. Figure 11 shows dynamic modulus versus temperature as derived from the dynamic flexure tests, and illustrates the variation with cure condition on time-dependent material response to the cyclic loads. The loss of spring action indicated on this curve occurs above the Tg, which as mentioned above is taken as the phase angle peak. Spring action loss did not occur on the 177°C (350°F) cured, 177°C (350°F) post-cured specimen.

A decision was made to use a 177°C (350°F) cure temperature for the moisture-conditioned 50-ply laminates because (1) the reduced cure temperatures resulted in poorer quality material with reduced elevated temperature capabilities, and (2) the blistering investigation showed no blistering of moisture-conditioned parent laminates when exposed to 177°C (350°F).

Flush Patch Repairs

Repair Types I-V and XIII (see Tables VI, VII, and VIII for definition of repair codes) were all classified as flush repairs because the projection beyond the inner and outer mold line of the parent laminate was kept to a minimum. Three different classifications of flush repairs discussed below are cocured, precured and limited access. All repairs were performed on parent laminates containing 1.00 $\pm$0.05 percent moisture by weight. Conditioned laminates were stored in plastic bags between conditioning, machining and repair operations. Upon completion of the repair, the

specimens were reconditioned by exposure to 95 percent relative humidity at 60°C (140°F) for 30 days for the parent/patch combination.

The same general repair technique was used for all flush repairs. The parent laminates were removed from initial moisture conditioning and appropriate scarf surfaces were prepared using hand tools commonly found in the field, e.g., sanding disks, belt sanders, etc. The cure-in-place repairs (Types I, II, IV and XIII) were then laid-up onto the tapered bond line matching the orientation ply-by-ply of the removed parent material. These repair patches utilized the same Narmco 5208/T300 pre-preg used in the present laminates with the partial thickness repair (Type IV) matching the orientation of the laminate segment removed. A supplemental layer of Narmco M329 177°C (350°F) curing film adhesive 0.49 kg/m^2 (0.1 lb/ft^2) supported was used between the patch and the scarfed parent laminate surface. In every case cover plies (inner mold line, IML, and outer mold line, OML) extending beyond the repair area were used to increase the strength of the repair joint. The 0 degree OML plies were serrated at the edges by cutting with pinking shears to reduce bond concentrations.

The entire assembly made up of the IML, OML and replacement plies and adhesive was then oven cured using the following cycle without bleeding:

1. Apply full vacuum
2. Heat to 177°C (350°F) at 1.7-3.3°C/min (3-6°F/min)
3. Cure at 177 $\pm$5.6°C (350 $\pm$10°F) for 60 minutes after first thermocouple reaches 171°C (340°F)
4. Cool to 65.6°C (150°F) under full vacuum.

One additional tabbed laminate specimen was made for comparison of the cure-in-place graphite flush repairs (Type XIII) in which one layer of porous Teflon coated glass cloth was added over the repair as a breather.

Two of the flush repairs used pre-cured bonded graphite patches which were cured in the same manner and using the same 5208/T300 material as the parent laminates. These were Types III and V. Type III was a scarf repair with a precured patch. Scarfed surfaces with closely matched taper angles, were prepared on both the parent and the patch using hand tools. The patch was then bonded as the other specimens with IML and OML plies added before cure. The same cure cycle was used as described above for the cure-in-place repairs. Longitudinal movement was restrained during heat-up. Type V was a blind repair in which a 5-ply precured doubler was adhesively bonded with the M-329 adhesive for 60 minutes at 177°C (350°F) using pressure from Cleco mechanical fasteners. The fasteners were removed and a cure-in-place graphite repair assembled on the doubler and cured as in the other cure-in-place repairs. This procedure simulated the repair of structure with only one side accessible.

An attempt was made to evaluate the quality of the flush bonded repairs by NDI. Teflon disks had been placed in trim areas of the repair bond line as NDI standards. The results were inconclusive due to the complex geometry and the problem with extensive cure-in-place and fine bond-line porosity which masked any distinct voids. This fine, evenly dispersed porosity is the result of the unaugmented vacuum cure.

The specific details of these flush repairs are shown in Figures 12 through 16.

External Patch Repairs

Repair Types VI-T, VI-F, VII, VIII, IX, X, XI, XII, and XIV (as coded in Tables VI, VII, and VIII) are all external patch repairs in which the patch is entirely on the external surface with no internal doublers. The fabrication of these patches was performed in all cases to simulate a single-side access situation for repair. The types of external patch material used include:

- A cure-in-place graphite patch (Type VI-T) utilizing the 5208/T300 tape pre-preg used in the parent laminates, cured at 177°C (350°F) under vacuum pressure with a supplemental layer of M-329 adhesive 0.49 kg/m^2 (0.1 lb/ft^2) supported;

- A comparable cure in-place graphite patch (Type VI-F) utilizing a 5208/T300 fabric pre-preg in place of the tape. The graphite fabric is a 24 x 23 8-harness satin weave, 0.33 mm (13 mils) pre-cured ply nominal, 41 $\pm$3% resin content pre-preg.

- A pre-cured bonded graphite external patch (Types VII and XIV) with 5208/T300 patch material autoclave cured in the same manner as the parent laminate, and bonded with vacuum pressure at 177°C (350°F) using the M-329 adhesive;

- A similar pre-cured bonded external patch (Type IX) except bonded with EA 9330 2-part adhesive at room temperature and contact pressure;

- A wet lay-up graphite fabric patch (Type X) with EA 9313, a low viscosity 2-part resin, impregnated onto dry graphite fabric (24 x 23 8-harness satin), and cured at room temperature and contact pressure;

- Bolted metal patches using both titanium (Type XI) and aluminum (Type XII) and assembled with blind fasteners.

The cure cycles used for the bonded repairs described above are as follows:

- Bonding of precured 5208 graphite patches with M-329 adhesive using vacuum pressure:

Apply full vacuum

Heat to 177°C (350°F) at 3.3°C (6°F) minute or greater

Cure at 177°C (350°F) for 1 hour

Cool to 82°C (180°F) under full vacuum

Bleeder: 1 layer porous Teflon-coated glass over lay-up

- Bonding of 5208 graphite cure-in-place patches using vacuum pressure:

  Apply full vacuum

  Heat to 177°C (350°F) at 1.1 - 3.3°C (2-6°F)/minute

  Cure at 177°C (350°F) for 1 hour

  Cool to 82°C (180°F) under full vacuum

  Bleeder: Same as for the pre-cured graphite patch

- Bonding of precured 5208 graphite patches with EA 9330 room temperature adhesive and EA 9313 wet lay-up patches:

  24 hours at ambient temperature with weight used to apply contact pressure.

The graphite parent laminates and pre-cured patches were prepared for bonding by sanding lightly with 180-grit abrasive paper and wiping clean with a rag soaked with MEK. The surfaces were then air dried for 15 minutes.

The bolted metal patches were mechanically attached using MS21140 Huck stainless steel blind fasteners assuming single-side access. The fastener holes were drilled without back-up, supported only on honeycomb core, using high speed steel drills at low speeds (approximately 400 rpm). The blind fasteners were wet installed with sealant, and faying surface sealant was applied to patch and laminate surfaces prior to attachment of the patch. These measures were taken to prevent galvanic corrosion between the metal and graphite.

Each of the external patch repairs was used to rejoin two separate parent laminate separates. To simulate a cleaned-out damage area, the repair patch was centered over a 2.5 cm (1 inch) length of filler separating the two laminate segments. The filler was the EA9330 adhesive described above and was cured at room temperature as described. This material is thixotropic and could be used to fill a damage area in service prior to bonding of an external patch.

Detail configuration of each of the external patch concepts discussed above are given in Figures 17 through 21. The graphite repairs were all

applied in stepped layers with increments of two or four plies tape, one ply fabric, or one 4 ply pre-cured patch laminate as indicated in the figures. The pre-preg layers and pre-cured patches were cut with pinking shears to produce a serrated edge thus reducing load concentration at the patch edges. This has proven very effective in preventing premature peel failures. Each cure-in-place patch layer was draped over the layer beneath it to provide improved sealing of the bond line edges. Repaired laminates are shown in Figure 22 prior to bonding to the core material. Figure 23 shows a bolted repair with the back-side splitting resulting from drilling without back-up, and also shows the filler used between the parent laminate segments.

Specimen Fabrication and Machining

Two specimen configurations were used to evaluate the repair concepts as discussed previously. These are the sandwich beam specimen shown in Figure 8 and the tabbed laminate specimen shown in Figure 9.

Each individual sandwich beam test speciman is 2.54 (1 inch) or 5.08 cm (2 inches) wide as shown in Figure 8 with the repair in the center of the span extending across the full specimen width. The approach used in fabricating these specimens was to make a single repair rejoining two parent laminate segments of the proper length to obtain a 66 cm (26 inch) or 127 cm (50 inch) repaired specimen length as required. The width of the repair was made sufficient to obtain all the required replicate specimens plus a spare by subsequent machining. The repaired laminate specimen was bonded to the honeycomb core and slave skin in one piece to form a full width sandwich beam from which the 2.54 cm (1 inch) or 5.08 cm (2 inch) wide individual specimens were then cut. The steel and titanium slave skins were bonded as individual strips so that no cutting of the steel or titanium was required when the individual specimens were cut from the bonded sandwich panel.

The repaired laminates and slave skins were bonded to the honeycomb core using FM-400, a 177°C (350°F) curing film adhesive 0.29 kg/m^2 (.06 lb/ft^2) supported selected for its excellent hot/wet durability. The cure cycle was as follows:

- Apply full vacuum, then apply 241.3 kPa (35 lb/sq. in.) autoclave pressure venting the vacuum
- Heat to 177°C (350°F) at 3.3°C (6°F) minute or greater
- Cure at 177°C (350°F) for 1 hour
- Cool to 82°C (180°F) under full pressure

Bleeder: 1 layer porous Teflon coated glass over lay-up

The graphite parent laminates were surface treated for bonding by light sanding with 180 grit paper followed by an MEK wipe. The core was cleaned by carefully blowing clean, dry compressed air over the surface. The steel and

titanium were cleaned by Lockheed production processes defined in a Lockheed Process Specification for the steel and the titanium. The steel process involved degreasing, alkaline cleaning, followed by surface conditioning with Prebond 700 alkaline etch. The titanium process involved degreasing, alkaline cleaning, followed by a phosphate-fluoride conversion coat.

Northrop used comparable surface treatments for graphite, core, and steel surfaces but used the following surface treatment for the titanium.

- Mix 480-720 kg/m^3 (4-6 lb gallon) of TURCO 5578 alkaline etch powder into solution
- Heat to $93^{\circ}C \pm 2.4^{\circ}C$ ($200^{\circ}F \pm 5F$)
- Immerse part 5-7 minutes
- Rinse in cold deionized water for 5 min with spray or agitation
- Immerse the part in 10% HNO_3 (volume) for 2-3 mins at RT
- Rinse in deionized H_2O for 5 mins
- Dry in an air circulating oven for 30 mins $52-57^{\circ}C$ ($125-135^{\circ}F$)
- Prime coat within 2 hours.

All of the repaired specimens were conditioned for an additional 30 days at $60^{\circ}C$ ($140^{\circ}F$), 95% relative humidity to condition the patches, and this was done after bonding the beams. The bond lines were protected by sealing with lead tape. This proved to be inadequate for protection of the titanium bond line treated with the phosphate conversion coat (which is known to be highly moisture sensitive), and upon testing the first two or three of the Lockheed fabricated 16 ply beam specimens it was found that premature failures occurred at the titanium bond surface.

The affected specimens were returned to Lockheed, and the titanium skins were removed by immersion in a dry ice/acetone mixture. This was accomplished without damage to the core, repaired graphite skin, or graphite/core bond. The FM-400 adhesive was left on the core as the titanium pulled away clean, and this left an excellent surface for subsequent rebonding. Each titanium skin was recleaned and treated for bonding using the Northrop procedure described above, and was then rebonded as before to the same specimen from which it was removed. The repaired graphite/core segments were kept in sealed bags at all times except during cure to retain the moisture they had picked up during the 30 day conditioning of the beams. Monitoring of the traveler coupons indicated no significant loss of moisture, and so the re-bonded specimens were not given any further moisture conditioning. The rebonded specimens were subsequently tested without difficulty.

The tabbed laminate specimens shown in Figure 9 were machined to net size and a 1.9 cm (0.75 in.) hole was cut in the exact center of the span to

simulate a cleaned-out damage area. Fiberglass tabs 0.36 cm (0.14 in.) thick were fabricated using 6 plies of Hexcel F161/1581 or Narmco 8517/1581 fiberglass pre-preg cured at 177°C (350°F) for 1 hour. The 8517 tabs were used for the 180°F wet specimens because of its superior hot, wet properties. The tabs were bonded to the laminates using the same cure cycle given above for skin-core bonding of the sandwich beams. Surface treatment of tabs and laminate was by sanding and MEK wipe. The repair patches (Type XIII and XIV) as described previously were then applied to the specimens.

The completed sandwich beam with slave skin is shown in Figures 24 and 25. A tabbed laminate specimen with a repair patch is shown in Figure 26 and a typical individual sandwich beam specimen after trimming to net size is shown in Figure 27.

Static and Fatigue Testing

All mechanical testing for this program was conducted by the Engineering Test Laboratory of Northrop Corporation. The testing program basically consisted of three portions: static tensile tests of solid laminate specimens, and static and spectrum fatigue tests of honeycomb sandwich beam specimens. Elevated and reduced temperature cabinets were affixed to the test apparatus and the temperature monitored throughout the test where necessary.

Static tests. - The 16-ply solid laminate specimens, Types C-U, C-D, XIII and XIV, were monotonically loaded to tensile failure in a 2.76HN (600 kip) capacity Baldwin test machine as shown in Figure 28. Load was introduced through friction grips by means of glass loading tabs bonded to the test laminate. Strain measurements were taken at load increments such that at least ten data points were recorded during the test; the load increments varied between 8.9 and 22.2 kN (2000 and 5000 pounds) depending on the type of specimen being tested. Strain was measured on the quarter-length longitudinal centerline.

Both tensile and compressive static as well as spectrum fatigue tests were conducted on the honeycomb sandwich beam specimens. Load introduction was accomplished by four-point bending using a test fixture assembled specifically for that purpose (see Figure 29). The fixture was designed with freedom of rotation of all reaction points so that the test section was subjected to a constant bending moment. The beams were supported on the two ends and load applied by a load cell through a "T" fixture mounted on the center section of the specimen. Tensile or compressive static load was applied to the gage section of the beam depending upon whether the composite skin was the bottom or top surface of the beam when mounted in the fixture, respectively. Both 16-ply and 50-ply beams were tested in the same fixture by adjusting the span and using 44.48 kN (10 kip) and 111.2 kN (25 kip) capacity load cells, respectively. Strain gages were mounted within the constant-moment center portion of the beam; readings were taken at discrete intervals during the test with the failure strain linearly extrapolated to the failure load from the last strain measurement recorded.

Fatigue tests. - Fatigue test loads were appled to the specimen through a closed loop electro-hydraulic servo system actuated by the Northrop Fatigue Laboratory Control System. Load scaling and measurement were accomplished with a BA-13 bridge amplifier, load cell, and oscilloscope. The fatigue load spectra, taken from magnetic tapes, were stored on a disc extension memory of the control system. The maximum load for each specimen was determined by initially loading the specimens to half of the limit load design strain; the corresponding load level was then recorded and doubled to incorporate it into the control system. After two lifetimes had been applied to the beams, a standard beam static test was conducted on each specimen to measure residual strength.

Fatigue loading spectra. - Two random spectra were used for fatigue loading of sandwich beam specimens. The 50-ply specimens were exposed to two lifetimes of the "minitwist" spectrum, which was developed to represent the wing loading for typical commercial aircraft. The 16-ply specimens were exposed to two lifetimes of the fully-reversed L-1011 fin spectrum.

The definition of flight types and load cycles within each flight for the minitwist spectrum are shown in Table XVII. In addition to the loads shown, one ground-air-ground cycle per flight, equal to $-0.5\ S_m$, was added. The block of 4,000 flights shown in Table XVII was repeated 20 times to represent two lifetimes resulting in application of 1,208,400 cycles of loading to each 50-ply specimen. The L-1011 fin spectrum is defined for a 36,000 flight lifetime in Table XVIII. For two lifetimes, a total of 660,000 load cycles were applied to each 16-ply specimen.

Using the data in Table XVII and XVIII as supplied by Lockheed, Northrop generated random loads on magnetic tape for each of the spectra, which were then used to control test equipment. All loads were expressed as a percentage of the maximum load in the spectrum. A table of these loads was prepared, and a random number generator used to select individual load values sequentially which were then written on the tapes. Maximum loads in the spectra were set to cause maximum tensile strains of 2,000 $\mu\epsilon$ for the L-1011 fin spectrum and 3,000 $\mu\epsilon$ for the minitwist spectrum. These values, supplied by Lockheed, represent limit load design strains for the type of structure represented, e.g., fin and wing skins, respectively.

Discussion of Results

The test results are given in Table VI for the sandwich beam specimens with 16 ply laminates, Table VII for the sandwich beam specimens with 50 ply laminates, and Table VIII for the 16 ply tabbed laminate specimens. These tables also provide descriptions and code number for each repair concept.

As discussed previously, the primary test specimen used to evaluate and compare repair techniques was the sandwich beam specimen shown in Figure 8. The repair joint in the beam specimens extends across the complete width of the test laminate 2.54 cm (1 inch) for the 16 ply laminates; 5.08 cm

(2 inches) for the 50 ply laminates, and is joining two completely discontinuous adherends. Thus, the repair is providing recovery from zero strength as opposed to an actual component repair situation in which the damaged strength is typically 40 - 50% of unflawed strength. Joint efficiencies given in Tables VI and VII represent a comparison of the shear or bearing strength of the various repair techniques as compared to the unflawed tensile or compression strength of the parent laminate.

Flush repairs-sandwich beam specimens. - The flush bonded repairs incorporating structural grade graphite prepregs and adhesives bonded with tapered scarf joints represent the most complex, expensive, and time-consuming repair approach evaluated in this Task, and would be limited to properly equipped maintenance bases. They are also anticipated to be the most structurally efficient repairs. For these reasons, the flush repairs were used primarily for the 50 ply parent laminates which represent more highly loaded critical sructure. One specimen (Type I) was a flush repair of a 16 ply laminate. The results indicate that the flush, repairs provide the most effective restoration of unflawed strength. The joint efficiencies, which are the percentage of unflawed strength based on control specimen results, range from .647 to .897 in the static tests for the 80 ply laminate flush repairs (see Table VII). This recovery of 60% or more of unflawed strength is well above the typical design ultimate range of 40 - 60% unflawed strength and these results can be achieved for thick laminates representative of highly loaded components such as wing covers. This repair approach, while expensive and restricted to depot level facilities, does provide a means of restoring design strengths to highly loaded critical composite parts. These results were achieved using vacuum cure pressure only, indicating further improvements in strength recovery are possible when autoclaves are available for repair. The lower strengths achieved with the partial thickness repair and the flush repair with an internal doubler, as compared to the full thickness flush patches, is probably related to the greater complexity of these repairs. The unaugmented vacuum cure pressure may have been less effectively transmitted to the patch and bond line in these cases. For the partial thickness repair, another factor may have been eccentricity caused by the presence of both vacuum cured patch material and parent laminate across the repair section.

One flush, aerodynamic cure-in-place graphite repair was evaluated with the 16 ply laminate, (Type I) and joint efficiency was much lower than the other flush repairs and was lower in compression than the external patch repairs. A careful micrographic examination of the failure showed that the taper had not been machined properly. (Figure 30). The taper angle was too steep in some areas resulting in a high tensile load component which caused premature failure.

Fatigue tests as described previously were run on the undamaged controls, the full thickness pre-cured bonded patch (Type III) and the partial thickness cure-in-place repair (Type IV). Joint efficiency of the Type III repair determined by the residual tensile strength was over 70 percent, but the partial thickness fell below 50 percent. The factors discussed above which

caused the partial thickness repairs to have lower joint efficiencies based on static tests were the probable cause of the lower fatigue properties as well.

The failure modes for the flush repairs are given in Tables VI and VII and are described more fully in Appendix B. As expected the cure-in-place repairs with vacuum cured patches failed primarily by delaminations in the patch, whereas the pre-cured bonded repairs failed principally in the patch-parent bond line. It is significant, that despite the differences in failure modes, the two directly comparable full thickness repairs with cure-in-place and pre-cured patches (Types II and III) had comparable joint efficiencies. Figures 31 through 35 show typical flush repair specimens after testing.

External repairs-sandwich beam specimens. - The external repairs consisted of three basic concepts: 1) bonded or cure-in-place graphite repairs using structural grade pre-pregs and adhesives, 2) cold-bonded and wet-layup graphite patch repairs using room-temperature curing, two-part resins; 3) bolted metal repairs. These represent to varying degrees less complex, less costly, and less time-consuming repairs than the flush repairs discussed in the previous sections, and are more adaptable to maintenance base operations with limited facilities and to line station repairs. These repairs were all made to simulate a repair situation where no back-side access is available.

These repairs were used principally on the 16 ply laminates representing lightly loaded, less critical structure. One specimen type was included to represent an external bonded graphite repair of a 50 ply laminate. (Type VIII).

The external bonded and cured-in-place graphite patch repairs of the 16 ply laminates, utilizing structural pre-pregs and adhesives and cured under vacuum at 177°C (350°F), represent an intermediate level of complexity in the repair concepts being evaluated. This approach would be feasible for on-aircraft repairs where access is restricted and for airline maintenance operations where autoclaves are not available. The external repairs provided strength recoveries for the 16 ply laminates varying from 29 - 60 percent (see Table VI). This represents recovery from zero strength as the repair was used to rejoin two completely severed laminate segments. These results therefore indicate that in actual repairs where the unrepaired strength typically is 40 percent of unflawed strength, a partial recovery of unflawed strength could be achieved such that design strength (typically 40 - 60 percent of unflawed strength in the lightly loaded laminates represented by these specimens) is fully recovered. It appears therefore that a structurally bonded or cure-in-place graphite repair can restore design strength to lightly loaded components represented by the 16 ply laminates.

There was considerable variability in results with the external bonded specimens as compared to the flush repairs. This is likely the result of variability in the quality of the vacuum cured patches and bond lines accentuated by the inherent eccentricity and load concentrations of the external patch configuration.

Failure modes in the external bonded repairs were primarily delamination in the vacuum cured cure-in-place graphite tape patch (Type VI-T), but was primarily patch-parent laminate disbond for the cure-in-place fabric patch (Type VI-F). The pre-cured bonded graphite patch (Type VII) failed in a combined disbond - patch delamination mode. There were no significant differences in joint efficiencies for the three types of bonded external patches. A comparison of room temperature -54°C (-67°F) and 82°C (180°F) strengths on the structural bonded repairs indicated no significant temperature effects.

The external cold-bonded and wet lay-up graphite repairs, both incorporating two-part room temperature/contact pressure curing epoxy systems, achieved a significantly lower joint strength than the bonded patches which utilized structural grade systems. The failures were 100 percent patch disbond, and it appears that the very low peel strength of these resins made the joints particularly sensitive to the concentrated loads at the patch edges despite the measures taken to reduce edge load concentrations. These systems are very compatible with field repair capabilities, but it appears that their use is limited to repairs of small area non-critical damage where little or no strength restoration is required.

The results of the external mechanically attached metal doubler repairs were very low due to premature pull-out of the blind fasteners. There is considerable data from other programs at Lockheed and other companies showing that a bolted metal patch repair can provide significant strength recovery. (references 3 and 48). These other results, however, were obtained with standard titanium screws installed with nut plates. The results obtained in this program provide some indication of limitations in the use of blind fasteners for repair due to their low pull-out strengths. The higher results with the aluminum patches may be due to the greater flexibility and ductility of the aluminum patch material. The low joint efficiencies of the bolted repairs obtained with the sandwich beam specimens may be due in part to the beam specimens configuration, where only four-in-line fasteners are installed in the center line of the specimen to rejoin the two parent laminate segments. The lack of geometric representation of an actual repair and the absence of an alternate load path may have been particularly significant for these specimens.

The one specimen with an external patch repair of a 50 ply laminate (Type VIII) produced low joint efficiencies with bond line failure propagating at the patch edges. It appears that the excessive patch thickness required for the 50 ply laminates caused load concentrations at the patch edge resulting in premature failures. It appears that an external bonded patch, even with supplemental fasteners (titanium Hi-Loks) is not feasible for the thicker laminates, although a more geometrically representative bolted/bonded repair may have been more effective for the reasons discussed above.

Figures 36 through 44 show representative external patch repair specimens after testing.

Tabbed laminate specimens. - The program included a few laminate coupon type specimens, 15.2 cm (6 inches) by 50.8 cm (20 inches), with a center 3/4 inch hole representing cleaned-up damage, and with fiberglass tabs for load introduction. (See Figure 9). This type of specimen has the advantage of providing a geometric representation of actual damage and an actual repair patch, with unrepaired strength at the 40 - 60 percent level of unflawed strength typical of notched components; and permitting the testing of damaged, unrepaired controls. The introduction of loads, particularly in compression, is more difficult with this type of specimen, which is the principal reason the beam specimens were used. Results of these tests are given in Table VIII. A comparison of two flush repair concepts evaluated with each specimen type (Type I and XIII) indicates higher repaired strength with the laminate specimens but as discussed previously the Type I specimens had a badly machined scarf. Joint efficiencies of the Type XIII flush repair were comparable to joint efficiencies of comparable 50 ply flush repairs. A comparison of joint efficiencies for the external bonded repairs (Type VII vs Type XIV) show higher retentions (52 - 75 percent) were achieved with the laminate specimen. The most reasonable explanation is that the flush repair provided a very high restoration of unflawed strength, so that the initial unrepaired specimen condition (whether cut completely across the test section or with a hole in the center of the specimen) did not affect repaired strength. For the external bonded repairs, a lower percentage of unflawed strength is restored so that the initial unrepaired condition and the presence or absence of an alternate load path was significant.

An additional Type XIII cure-in-place repair was re-made by Northrop in an identical manner except that one layer of porous teflon coated glass cloth was added as a bleeder, as discussed in Section 2.7. Improved joint efficiencies were obtained indicating that a higher quality, more void-free vacuum and patch laminate was achieved. Despite the added cost and complexity of applying bleeder in a repair situation, it appears to provide a significant benefit to the repair.

Conclusions

The results of the Phase 2 coupon tests indicated the following primary conclusions: 1) the most effective repair was the flush, aerodynamic bonded graphite patch which restored design ultimate strength even for the thicker laminates representative of highly loaded structure; 2) unaugmented vacuum cure pressure proved satisfactory for both pre-cured bonded and cure-in-place graphite repairs using the structural grade systems; 3) the external bonded repairs utilizing vacuum cured structural grade pre-pregs and adhesives were adequate for restoration of design strengths in the thin laminates representative of lightly loaded structure; 4) the cold-bonded and wet lay-up external graphite repairs provided very little effective restoration of unflawed strength; 5) blind fasteners appear to have limited effectiveness for repairs, due to their reduced pull-out strength; and 6) the laminate coupon specimen, which geometrically represents an actual repair, is more suitable for evaluation of external bonded and bolted repairs than the sandwich beam specimen.

In summary, the various repairs evaluated are adequate for the typical lightly loaded composite components now being used. These parts are designed to account for the presence of fastener holes and undetectable internal delaminations, and for a typical flaw very little strength restoration is required for the repair. The airlines thus have the option for a very wide range of repair concepts for these components, and can select a repair procedure based on considerations of cost, down-time, access, facilities, and aerodynamic requirements. The flush, bonded graphite repairs are capable of providing a significant restoration of strength in the more highly loaded components being considered for future composite applications.

PHASE 3 - REPAIR OF COMPOSITE SUBELEMENT SPECIMENS

Selection and Fabrication of Test Components

The objective of the Phase 3 task was to validate selected repair concepts evaluated in Phase 2 by repairing structural element specimens representative of actual composite structure. The repair technology developed in Phase 2 was thus extended to geometrically representative components. In addition, these components provided an opportunity to evaluate repairs of stiffener elements and substructure, which have been evaluated much less frequently than skin cover repairs. Phase 2 evaluated repairs of two laminate thicknesses, 0.635 cm (0.25 in.) and 0.20 cm (0.08 in.), representative of highly loaded and lightly loaded structures, respectively. Structural elements were therefore selected to provide both highly loaded and lightly loaded structures in the Phase 3 tests as well.

Based on the above considerations, three components were selected: 1) an L-1011 composite vertical fin hat-stiffened cover (Type I), 2) a hat-stiffened wing cover (Type II), and 3) an L-1011 composite vertical fin spar segment (Type III). The two hat-stiffened cover components consisted of a single stiffener element with adjacent skin, while the spar specimen consisted of a cap segment (which is the most likely area to be damaged) along with a partial web segment. These are shown respectively in Figures 45 and 46.

The L-1011 vertical fin components were obtained from existing test segments fabricated under the advanced composite vertical fin (ACVF) program (NAS1-14000). Three segments were obtained for use as a repair article, a control specimen, and a spare. The cover segments were fabricated at Lockheed-California Company in accordance with the cover production procedures established for the ACVF program. The material used was the standard Narmco 5208/T300 pre-preg tape, 0.13 mm (5 mils) per ply, used in the fin program and also used for the Phase 2 coupon specimens in this program. These components (Figure 47) were free of voids as determined by ultrasonic inspection, but because of dimensional errors they were not acceptable for use as vertical fin test components. The parts were therefore made available to this program.

The spar segments (Figure 48) were fabricated by Lockheed-Georgia Company in accordance with the spar production procedures established for the ACVF

program, and also use the 5208/T300 pre-preg. The segments were part of a series of static test specimens. After static tests were completed, the failed spar specimens were inspected. Three components were selected in which the failure did not involve the test section shown in Figure 46. This provided the three specimens required for repair, control, and a spare. No untested spar segments were available for this program.

The use of existing L-1011 vertical fin components provided several advantages to this program. The principal advantage was eliminating the costs of fabricating a structural element specifically for the purpose of repairing it. In addition, components were obtained for which considerable background data and structural analyses were available.

The third component was the hat-stiffened wing cover. This was based upon a composite wing design developed by Lockheed-Georgia for another program. A bonding tool was developed, and several test components were fabricated under this program. None of the test parts were available, however, and it was necessary to fabricate a component from which the three test segments could be obtained (Figure 49). It was also necessary to modify the tool to eliminate two cocured rib segments that would have complicated the repair and testing of the part. The tool modification and part fabrication was performed at Lockheed-Georgia. The material was 5208/T300 pre-preg tape as for the other two components. The cure cycles for the three test components were based upon procedures developed under the ACVF program (NAS 1-14000) mentioned above. These cycles are detailed in the ACVF Phase II Final Report (Reference 49).

Test Plan

The Phase 3 Test Plan is defined in Table XIX. This activity consisted of static testing of one damaged/repaired and one undamaged control of each specimen type. The two test articles, along with a spare, were cut to net size from the components described in the previous paragraph, 2.1. The test segments were ultrasonically inspected for voids, damage, or other defects to ensure that no condition existed that would affect the test results. The components were then immersed in water at 82°C (180°F) until a weight gain of at least one percent was attained as determined by weighing traveler coupons. This brought the test segments to a condition typical of composite parts in service in which one percent equilibrium moisture content is typically attained. This is particularly significant for heat-cured bonded repairs where blistering of the parent laminate can be caused by application of heat or where moisture diffusion through the bond line can occur resulting in porosity.

After moisture conditioning, the repairs were accomplished as described in the following paragraphs.

Design of Repairs

The three structural subelements repaired and tested in Phase 3 represent the spectrum of bolted, bonded, and combined bolted/bonded approaches to substructure repair. The repair procedures selected were required to meet FAA guidelines for repair of structural components, which state that the design ultimate strength and remaining service life capability of the part must be restored. The procedures developed were designed to be compatible with the facilities and capabilities available at airline maintenance depots and were based on the repair concepts evaluated in Phase 2. These included cure-in-place and precured bonded graphite patches and bolted aluminum patches, and included both flush and external patch concepts. The specific repair configurations for each of the three specimens are as follows:

- Type I, hat-stiffened vertical fin cover (Figure 50) - A cure-in-place graphite external patch (Figure 51) for repair of the skin and a precured bonded graphite hat-section splice for repair of the hat (Figure 52)

- Type II, hat-stiffened wing cover (Figure 53) - A cure-in-place graphite flush patch for repair of the skin (Figure 54) and a precured bonded graphite hat-section splice for repair of the hat (Figure 55)

- Type III, vertical fin spar - A bolted aluminum splice patch repair with multiple splice plates for repair of the cap and a single splice plate for repair of the web (Figure 56).

Design criteria for each of the repairs is given in the following subparagraphs.

Fin cover specimen. - The skin for the fin cover specimen is 16 plies thick, so an external patch was considered to be the most feasible approach and would be within typical aerodynamic smoothness criteria. The cure-in-place patch selected was a 20-ply lay-up (Figure 51) that was tested in the Phase 2 coupon tests.

The hat stiffener was repaired with a precured hat bonded to the basic stiffener. It was considered that precured hat sections could be readily stored by the airlines and cut to length as required. For this repair to work well the basic hat outer surface and the repair hat inner surface must be accurately tooled. The precured hat patch is shown in Figure 52. The overall repair is shown in Figure 50.

Wing cover specimen. - This repair concept is similar to the fin cover repair. The difference is that the skin repair has to be flush because of the increased skin thickness. An external patch would exceed aerodynamic limits and would also result in excessive load concentrations and eccentricity. The lay-up of the skin repair is identical to the basic skin except for the added

0/±45 outer mold line plies shown in Figure 54; each ply in the flush patch matches a corresponding ply in the parent. The hat stiffener was repaired using a precured hat bonded to the basic stiffener, the same concept used for the fin cover specimen. The precured hat patch is shown in Figure 55. The overall repair is shown in Figure 53.

Spar cap specimen. - The spar cap repair (Figure 56) was designed to match the EA of the severed Gr/Ep component. The modulus (E) of the cap is approximately that of aluminum, so 2024-T3 was selected as the repair material. The repair to the cap required approximately 0.51 cm (0.20-in.) thick aluminum and the repair to the web approximately 0.36 cm (.14 in.) thick aluminum. In order to introduce the load to the repair, the 0.51 cm patch had to be stepped so as to eliminate machining and forming. The repair was built up from 0.18 cm (0.07 in.) thick plate stock as shown on Figure 56. The fastener loads were determined by using a strain compatability analysis, and a factor of two was applied to account for bolt bending.

Fabrication of Repairs

Each of the subelement specimens was trimmed to net size from the larger components as described previously and was then ultrasonically and/or radiographically inspected prior to repair to ascertain the prerepair condition of the article. All specimens including the control were then moisture conditioned by immersion in 82°C (180°F) deionized water to saturation. Initial moisture content was determined by back-drying travelers of the specimens under vacuum at 88°C (190°F). Average final moisture content is reported herein for each specimen type. Repairs were then accomplished as described below.

Vertical fin cover panel, Type I. - The repair of the vertical fin cover panel element consisted of precuring a graphite/epoxy hat-section patch and vacuum curing repairs to the hat section and skin of the specimen in a single operation.

A 96.52 by 17.78 cm (38.0 x 7.0 in.) hat section was removed from a larger multistiffened cover panel as shown in Figure 57 and moisture conditioned to 1.45 percent by weight. Included was one control specimen in addition to the specimen being repaired. This section was subsequently cut in half laterally to provide two stiffened segments, 48.26 by 17.78 cm (19.0 by 7.0 in.), for the purpose of rejoining to simulate repair of a hat section of zero bypass load capability. The two 48.26 cm (19.0 in.) segments were then ultrasonically inspected, which revealed resin-rich regions at the flange ply drop-offs and minor delaminations extending from 3.81 to 10.16 cm (1.5 to 4.0 in.) from one end along one edge of the flange on one segment. The inspection of the hat portion of the plan view of the specimen was indistinct because of the limitations of the inspection technique. These anomalies were not adequate to prevent repair and test of the article.

A 22.86 cm (9.0 in.) hat-section patch was laid up out of T300/5208 pre-preg tape and cured using another graphite/epoxy hat section as the tool. The patch section duplicated the ply orientation of the original hat as shown in Figure 52. Ply lengths at the ends of the patch were staggered 0.25 cm (0.10 in.) per ply to provide a taper to each end of the patch. The cure cycle and cure configuration used for the patch are shown in Figure 58. After cure, the width of the patch was machined to match that of the parent hat section, approximately 11.68 cm (4.6 in.).

The hat section patch was assembled by placing the parent halves skin side down end to end with a 2.54 cm (1.0 in.) separation between them. A layer of M-329 supported film adhesive was applied to the parent hat cap and flanges over which the precured hat-section patch was placed. The assembly was inverted (i.e., skin side up), and a precured plug of glass/epoxy was placed in the gap in the skin to support the lay-up of the full width external skin patch as shown in Figure 51. The external plies were assembled on a layer of M-329 adhesive as shown in Figure 51.

The entire assembly was envelope bagged and vacuum cured to the following cycle:

- Apply full vacuum.
- Heat to 177°C (350°F) at 3.3°C (6°F) per minute.
- Cure at 177° (350°F) for one hour.
- Cool to 82°C (180°F) under full vacuum.
- Apply one layer of porous Teflon-coated glass bleeder over lay-up.

Figure 50 shows the complete assembled repair schematically.

Postrepair radiographic inspection showed lengthwise disbonds in the radius regions of the hat. This was probably caused by a mismatch of radii between the parent and the patch resulting from bridging of the patch plies during precure and by normal variations in dimensions between the hat section used for the lay-up tool and the hat section being repaired. The bond in the flat area was judged adequate for testing. The article was moisture reconditioned at 60°C (140°F) and 95 percent relative humidity for 30 days to simulate additional service exposure after repair.

Figures 59 and 60 are photographs of the finished hat-section and external skin patch repairs.

Wing cover panel, Type II. - The repair of the wing panel element consisted of precuring a graphite/epoxy hat-section patch and bonding it to the parent hat section under vacuum pressure while cocuring a flush skin patch in the same operation. Fasteners were installed in the flange to supplement shear transfer into the repair.

Two 96.52 x 17.78 cm (38.0 x 7.0 in.) hat-stiffened wing cover specimens were removed from a larger, multistiffened panel as shown in Figure 61 and were moisture conditioned to 1.41 percent by weight. These included one control specimen and one repair specimen. The repair specimen was then cut in half laterally to provide two stiffened segments 48.26 by 17.78 cm (19.0 by 7.0 in.) for the purposes of rejoining to simulate repair of a hat section with zero bypass load capability. Radiographic inspection of the multistiffened panel was performed by Lockheed-Georgia Company before delivery to Northrop. The x-rays showed no significant internal anomalies.

A 35.56 cm (14.0 in.) hat section patch was laid up and cured using a section of another hat stiffener as the tool (See Figure 55). The orientation was the same as the parent hat and the patch material was unidirectional T300/5208 pre-preg tape. Special effort was made to ensure that ply bridging in the radii was avoided. The same cure configuration and cure cycle was used as with the fin cover panel (Figure 58). The cured hat section was machined to match the width of the parent sections, and a 2.54 cm (1.0 in.) taper was machined to each end.

A 19 to 1 slope was machined on one end of the skin side of each parent half to facilitate the flush skin patch. A silicone rubber plug was cast inside the hat section and removed and machined to be used to support the skin repair and to seal the hat section for vacuum bagging.

The precured hat-section patch was lined with one layer of M-329 film adhesive, as shown in Figure 62, extending 0.51 cm (0.2 in.) beyond the ends of precured hat. The parent halves, skin side up, were then fitted into the hat patch cavity and clamped in place using a hot air gun to aid assembly (Figure 63). The gap between the scarved ends of the parent halves was 4.06 cm (1.6 in.) A bead of ECN 1299 room-temperature curing adhesive paste thickened with Cab-O-Sil powder was placed around the ends of the parent hat sections and cured overnight to provide a seal at the bondline during cure (Figure 64). The rubber plug was inserted (Figure 65) and the skin patch replacement plies laid up matching the parent skin orientation (Figure 66). The replacement plies, along with film adhesive and cover plies, as shown in Figure 54, were assembled, clamped together, and vacuum cured as described in Section 2.4.1 for the Type I repair.

Initially, attempts were made to vacuum bag the circumference of the repairs since this most closely resembles the in situ repair situation (i.e., air was allowed to remain inside the hat section). Because of cracking of the adhesive seal around the rubber plug and other fit-up problems, however, adequate vacuum pressure could not be applied with this approach, so the entire assembly was evelope bagged for cure, as was done for the Type I repair.

After cure, 0.483 cm (0.19 in.) diameter holes were drilled at 1.91 cm (0.75 in.) intervals along the flanges and 100-degree countersunk on the skin surface to accommodate a reduced shear head bolt. Flush shear head bolts, washers, and steel nuts were installed dry in the holes to enhance the shear

transfer from parent to patch to parent as shown in Figure 53, which illustrates the entire repair assembly schematically.

Postrepair nondestructive inspection was not performed because of the difficulty in interpreting the NDT results of such a complex internal configuration. The completed repair was moisture reconditioned for a period of 30 days in 82°C (140°F)/95 percent relative humidity air to simulate additional service exposure after repair.

Vertical fin spar segment, Type III. - The purpose of the vertical fin spar repair effort was to demonstrate the feasibility of mechanically fastened metal repairs to a graphite/epoxy sub-structure. Depot-level repair facilities were assumed and 2024-T3 aluminum sheet selected as the repair material because of its wide availability. The substructure selected for repair was a 96.52 cm (38.0 in.) long portion of the L-1011 vertical fin spar cap as shown in Figure 67.

The specimuns used for the Type III repair were segments taken from static test specimens in Lockheed's advanced composite vertical fin program (NAS 1-14000). To verify that failure occurred away from the segment to be used in the repair test program, radiographic inspection was performed on the selected "T" sections. The results of this inspection showed no internal damage to the spar cap segments other than minor delaminations around the cap fastener holes, which could have resulted from manufacture as easily from the previous static test of the spar.

The control and repair specimens were cut from the spar "T" sections as shown in Figure 67. The repair specimen was cut into two equal segments by making two lateral cuts; the web stiffener was removed at that location providing room for the aluminum splice plates. These segments were then moisture conditioned to 1.34 percent by weight along with the control specimen.

The design philosophy of the repair was to use the existing fastener holes in the cap and to use a fastener spacing of 4D in the web section. The existing holes in the cap were not equally spaced, so the cap splice plates on either side of the web were made different lengths in order to provide the required number of fasteners for shear transfer. The repair configuration is shown in Figure 56. The aluminum plates were cut to size, clamped in place on the spar segment, and match drilled using hand-held equipment. The repair was assembled using MIL-8802-B2 polysulfide faying surface sealant for corrosion protection. Forty-eight fasteners were installed as detailed in Figure 56. Because of the nature of the repair, no postrepair moisture reconditioning was performed on the specimen. Figure 68 shows the completed repair.

Testing Procedure

The vertical fin and wing cover specimens, Types I and II, respectively, were tested in static compression, and the vertical fin spar segment, Type III, was tested in static tension. Strain gages were used in all tests to

monitor strain response both in the patch and parent portions of the specimens. One repaired and one control specimen of each type was tested in order to generate repair efficiency data in terms of percent strength restoration.

The compression tests were conducted in a 889.68 kN (200,000 pound) capacity Tinius-Olsen test machine. Stabilization was supplied by a fixture that provided support only to the flanges as shown in Figure 69. Teflon tape was placed between the specimen and fixture at the points of contact to minimize friction loading of the fixture during specimen shortening. Lateral support for the fixture was provided by three sets of lateral rollers. The ends of the specimens were potted in TE4351 aluminum-filled epoxy tooling compound to prevent end crushing during load application. Longitudinal strain gages were placed back-to-back at the midlength of all compression specimens as shown in Figure 70. In the repaired specimens, these gages were placed on the hat section and skin repairs; an additional gage was placed on the hat crown at quarter length to measure the far field, parent strain. As indicated in Figure 70, some gages in the repaired specimens were located away from the centerline by mistake. Figure 69 shows a compression specimen mounted in the fixture ready for load application. The potted ends of the specimen can be seen protruding from either end of the fixture. Specimens were sealed in plastic bags until mounted in the test fixture to retain the moisture conditioning.

The static tension tests of the vertical fin spar segment wre conducted on a 222.42 kN (50,000 pound) capacity Baldwin-Emery test machine. Hardened steel test fixtures were fabricated to introduce tension load through the centroid of the "T" section. These fixtures were compatible with the existing fastener hole pattern of the spar segments. Strain was measured at midlength on the web and flange on the control specimen (Figure 71); on the repaired specimen, strain was measured in three locations on the repair patch (gages 1,2,3) and one far-field location (gage 4) as shown in Figure 72. The specimen mounted in the test machine ready for load application is shown in Figure 73.

Discussion of Results

Test Results - One control (unrepaired) and one repaired specimen of each of the Types I, II, and III were tested to failure under axial load. The strain gage locations for Type I and II specimens are shown in Figure 70; the locations of gages for the Type III control and repaired specimens are shown in Figures 71 and 72, respectively. Each failure will be briefly described below; the failure measurements taken for all substructure tests are summarized in Table XX.

The Type I, vertical fin cover panel segment, control specimen failed at a load of -160.1 kN (-36,000 pounds). The strain differential measured by the back-to-back gages was not considered to be indicative of out-of-plane bending since a small differential existed from the onset of load application and since the stiffnesses of the hat and skin sections differ. Figure 74 shows the failure location in the hat section of the control specimen. The absence of hat/skin interfacial shear failure implies that failure occurred simultaneously in both sections.

The Type I repaired specimen failed at a load of -146.3 kN (-32,900 pounds). The primary failure occurred in adhesive shear between the parent and precured patch hat sections. This failure allowed the parent sections to displace resulting in a butt compression failure of the parent skin against the plug used to support the cocured skin patch. Figure 75 shows the minor external signs of falure in the skin patch.

The Type II, wing cover panel segment control specimen failed at a load of -398.5 kN (-89,600 pounds). The resulting failure surface displayed severe skin/stiffener separation terminating in coincident compression failure of both the skin and hat section as shown in the lower portion of Figure 76. There was also severe midplane delamination in the skin at the location of the compression failure. Since the graphite/epoxy failures in Figures 74 and 76 did not occur in the vicinity of the potting compound failures, it was assumed that the potting failures did not precipitate structural failure.

The Type II repaired specimen failed at a load of -314.9 kN (-70,800 pounds). Postfailure examination of the specimen provided evidence that the sequence of failure may have been failure of the cocured flush skin repair in interlaminar tension resulting in load eccentricity and redistribution through the precured hat-section patch causing subsequent adhesive shear and fastener bearing failures. The failed specimen is shown in Figures 77 and 78.

The Type III, vertical tail spar segment specimens were tested to failure in tension. The Type III control specimen failed at a load of +182.4 kN (+41,000 pounds) and strain magnitudes of 5215 and 6415 μm/m in the cap and web, respectively. Failure occurred in net tension through the row of fasteners in the loading fixture closest to the center of the specimen. This was at strain levels corresponding to that of flat panels containing unloaded circular holes, so the influence of the loading fixture was judged to be minimal, i.e., failure was expected to occur at this strain magnitude because of the existing holes in the structure.

The Type III repaired specimen failed at a load of +168.1 kN (+37,800 pounds). A net tension failure through the first row of fasteners in the web repair and subsequent web/cap separation resulted as is shown in Figure 79.

Analysis of Results - The most significant test results were the strength resolution percentages, which showed that all three of the repairs achieved values well above design strength levels. Percentages ranged from 79 percent of unflawed strength on the highly loaded Type II wing cover specimen to over 90 percent unflawed strength for the two vertical fin components. Design ultimate strengths in composites are typically around 50 percent of unflawed strength to account for notch effects. Since the three specimens were taken from actual hardware components, it was possible to compare results against design strength as determined analytically and verified by structural tests. The repair, in fact, did exceed these established design strengths in all cases. The control unflawed specimen results also conformed closely to predicted values.

Failure modes in all cases were typical for these types of components. The two undamaged Type I fin cover and Type II wing cover controls showed typical compression failures. As mentioned previously, the failures did not appear to have intiated from potting compound failure at the specimen ends. Type III spar control failed in the grip area in net tension, but this occurred at predicted load levels.

The failures in all three repaired specimens initiated through the patch areas, as would be expected. It is interesting that failure in the repaired fin cover initiated in the precured hat-splice-to-parent-hat bondline, while the repaired wing cover failure initiated in the cocured skin splice. The initiation of the wing cover failure at less that full unflawed strength (79 percent) in the cure-in-place skin patch may indicate some limitations in the use of vacuum-cured graphite patches at high loads levels. The initiation of failure in patch interlaminar tension may have been related to the less than optimum quality of the vacuum-cured composite patch. The net tension failure of the Type III spar component across the bolted web repair was the expected mode of failure.

The strain measurements show a reasonable correlation between gages on the control specimens and far-field gages (located away from patch effects) on the repaired Type I fin cover and Type II wing cover specimens. These comparative values of the Type I fin cover specimens are -5272μm/m control and -5058μm/m repaired. These gages were both on the hat crown. For the Type II wing cover specimen, comparative strains on gages located on the hat crown are -4334μm/m control and -3258μm/m repaired. These values give strain recovery percentages comparable to the strength recovery percentages given in Table II. The correlation between far-field strains and control strains is not as good for the Type III spar specimen. The response of the far-field gage in this specimen may have been influenced by some patch effects due to its location (see Figure 72).

Strain measurements taken from gages located on the patches show significant reductions compared to control and far-field gages. On the Type I and Type II specimens, some gages were located directly over the filled gap between the parent skin and hat sections (see Figure 70). These gages were

therefore not in the area of increased cross-section where external skin and/or hat patches are bonded to the parent laminates. Other gages on the Type I and Type III specimen (Figures 70 and 72) were located in areas where the cross-section consisted of combined external patch plus parent laminate thickness. The same degree of strain reduction occurred in both cases, however, indicating that strain readings for gages located over the gap were affected by the proximity of the increased sections.

Conclusions

The test results indicated the following basic conclusions:

1) The use of graphite patch repairs, either precured bonded or cure-in-place, is satisfactory for the repair of lightly loaded and highly loaded parts. These repairs can be satisfactorily accomplished using unaugmented vacuum pressure, although there may be some limitations on use of vacuum cure-in-place graphite patches for very high load levels.

2) The use of bolted repairs is satisfactory for lightly loaded structural components.

3) The repair of composite substructures can be accomplished using comparable approaches to those evaluated for skin cover repairs in many previous programs.

4) Repair of composite structures can be accomplished under the limitations of field repair facilities or on-aircraft repairs, where either vacuum bonded or bolted repair approaches will be required.

PHASE 4 - REPAIR OF FULL-SIZE COMPOSITE STRUCTURE

Phase 4 Activities in Relation to L-1011 Vertical Fin Ground Tests

The objective of Phase 4 is to extend the repair technology developed in the Phase 2 coupon tests and the Phase 3 subelement tests to repair of large-area damage on full-size structure. As discussed in the Introduction, the vertical fin ground test article (GTA) was selected as the test component, and the Phase 4 activities consisted of post-repair fatigue cycling which supplemented the repair activities planned as part of the vertical fin ground tests (Reference 50). Table XXI summarizes the fin ground test activities, and indicates how the Phase 4 activity is incorporated into the ground test plan.

Application of Large-Area Damage

The fin ground test plan called for a damage area, 12 inches by 4 inches, to be representative of lightning strike damage. The location of this damage

on the vertical fin is indicated in Figure 80. The location and orientation of the damage in relation to the adjacent hat stiffeners is shown in Figure 81. The damage extends nearly across the full width of the two adjacent hat stiffeners, thus fulfilling one of the requirements specified by NASA for the large-area damage in Phase 4 that it extend across two adjacent elements of a stiffened cover.

Simulated lightning strike damage was inflicted to the fin cover at an area selected as the most critical for large area damage. This was on the left hand cover between VSS 97.19 and VSS 121.1 (see Figure 80) approximately 12 by 4 in. and at a 45^{o} angle to the rear spar. The cover was first damaged by impacting at 13.3 ft-lbs to obtain delaminations. A hole was then burned through the skin using an electric arc from a 3/16 in. diameter welding rod. The area of delamination was determined by ultrasonic inspection, and was then burned with an oxygen/acetylene flame torch to char the outer plies.

Figure 82 shows the 3/16 inch hole produced by the welding rod and shows the marked delamination area. Figure 83 shows the 12 inch by 4 inch charred area which was slightly larger than the delamination.

Repair Patch Design and Fabrication

The repair concept used for the damaged skin was a precured bonded external graphite patch similar to the configuration evaluated in the Phase 2 coupon tests. This repair concept is shown in Figure 81. The edges are step tapered for aerodynamic considerations as well as to reduce peel loads at the patch edges. The patch dimensions, thickness and ply orientations were developed using the following analytical procedure. The patch was sized to approximately match the EA of the skin and the stiffener flanges. No 90^{o} plies were included because this would give a large difference in Poisson's ratio between the patch and the fin cover.

The length of the patch was sized on the conservative assumption that the maximum average shear stress in the bond must not exceed 500 psi. This assumption was made because the fin cover contained an unknown moisture content which combined with the vacuum-only cure at 350^{o}F would cause porosity in the bondline. The repair was sized to carry 150% of design ultimate load for the fin cover to ensure that it would not fail during the residual strength.

The 4 ply (45, -45, -45, 45) precured patch layers were obtained from patch stock fabricated for the Phase 2 precured bonded graphite repairs and were made from the Narmco 5208/T300 pre-preg material which has been used in the first three program phases as well as in the vertical fin program. The three ply (0_3) patch layers were fabricated specifically for the Phase 4 repair. There was no suitable 5208/T300 pre-preg available at Lockheed at that time, and the (0_3) patch stock was therefore fabricated from Hercules 3502/AS4 pre-preg. The Hercules pre-preg has been qualified to a Lockheed Materials Specification used to procure the 5208/T300 pre-preg used in this

program and the vertical fin program, and was therefore acceptable for use in combination with the 5208 material.

Cure cycles used for fabrication of the precured patches are given in Appendix C. The patches were autoclave cured, and were ultrasonically inspected and found void-free. After inspection the patch layers were trimmed to net size as shown in Figure 81. The 4 ply patches were trimmed with pinking shears to produce a serrated edge which assists in reducing peel loads at the patch edges. The three-ply unidirectional patches were cut with a band saw, as they were too sensitive to edge delamination for use of the pinking shears.

Bonding of Graphite Patch to Fin Surface

The damage area on the fin surface was prepared for bonding using the procedure outlined in Appendix C. This basically involved cleaning of the bonding surface on the fin; cleaning out the hole with a sander; filling the hole with a precured graphite disc, bonded in place with Hysol EA 9330 which is a two-part room temperature curing epoxy resin; and final sanding and cleaning.

A layer of Narmco Metlbond 329 adhesive was then applied to one surface of each of the five precured patch layers as shown in Figure 81. The patch layers were laid-up maintaining the 1/4 inch step dimensions and the location in relation to the damaged fin area as indicated in Figure 81.

The patch was then bagged and cured under vacuum at 350^{o}F using a heater blanket for application of heat. The bagged patch is shown in Figure 84 prior to application of the heater blanket. The bleeder arrangement and cure cycle are described in Appendix C. A leak check was performed prior to start of cure. Vacuum was monitored throughout the cure, and patch temperature was monitored by thermocouples at the patch edges.

Upon removal of the heating blanket and vacuum bag it was apparent that the center area of the patch had overheated. The vacuum bag had melted onto the silicone rubber heating blankets. The vacuum had only dropped to 18 in. of Hg as a result. The top stack was bulged upwards from the skin contour indicating it had expanded away from the stack below it. The edges all appeared well bonded as they were only heated to 355^{o}F as indicated by the two edge thermocouples. This top stack of 4 plies was scraped off and a bulged area with a split in the 0^{o} direction was found on the fourth stack. The area was approximately 1 by 1-1/2 inches. This stack of three 0^{o} plies was also scraped off. In the process a gouge was made in the third stack so it also was removed. It appeared to be of the proper contour and was tightly adhering to the second stack.

Three new patches were cut to size to replace the three top patch layers which had been removed. These patches were bonded in place using the procedure described above. An additional thermocouple was placed over the nylon bag under the heating blanket. The two edge thermocouples were located in the

adhesive at the bottom of the stack no. 3. This bonding operation was done at a slower heat-up rate to avoid an excessive temperature. The heating was very uniform edge to edge but the center top thermocouple read 355°F when the edges read 273-276°F. Narmco indicated that Metlbond 329 would cure in 90 minutes at 275, so the heat on the patch was held for 2 hours to ensure a full cure. The vacuum held at 28" Hg throughout the bonding cycle. After cooldown and removal of the bag the surface of the top stack was in good condition with no discoloration and an acceptable contour. The two edges which were not thermocoupled appeared slightly soft as the heating blankets were elevated slightly in these edges to prevent bag sealant burn through. It was felt these edges were not fully cured and they were heated with a heat gun at approximately 350°F for 15 minutes to obtain fully cured adhesive.

The cured patch was ultrasonically inspected, and bondline porosity was detected. This condition was expected with an unaugmented vacuum cure. The analysis described previously used data obtained on vacuum cured adhesive specimens, and thus accounted for the reduced properties resulting from this condition.

The two damaged and disbonded hat stiffeners were repaired by mechanically attaching the hat flanges to the repaired skin after inspection of the graphite patch. NAS 4502U flush head stainless steel screws and HL94 stainless steel collars were installed at 1 inch intervals as shown in Figure 80, with the countersink in the graphite patch. Fastener holes were drilled with back-up using standard carbide twist drills, and the fasteners were wet installed with sealant. The completed repair patch is shown in Figure 85.

Post-Repair Fatigue Cycling

After completion of the repair, the vertical fin GTA was subjected to one lifetime of fatigue cycling using the same spectra (see Table XXII) as in the two lifetimes of cycling which preceded the damage. Strain gage locations on the lefthand cover during this cycling are indicated on Figure 80. As noted previously, this was the supplemental activity covered by this program.

Static Testing to Failure

After completion of fatigue cycling, the fin GTA was loaded to failure as described in the vertical fin Ground Test Plan (Reference 50). Strain gages were retained at the same locations as for the fatigue cycling as indicated in Figure 80.

Discussion Of Results And Conclusions

The post-repair lifetime of fatigue cycling was accomplished with no detectable effect on the patch. The patch remained intact and fully bonded. The gages indicated no anomalous readings or any significant variations from

readings at comparable loads in the pre-repair cycling. There were no adverse effects on the fin component resulting from the presence of the patch.

The final static loading of the fin produced a failure at 120% of design ultimate load. The failure occurred in the front spar-cover area indicated on Figure 80, which was well away from the repair. The repair patch remained intact and fully bonded after failure, and did not in any way contribute to the failure mode. Strain measurements were in accord with predicted values, and no anomalous strain readings were noted.

The tests verified that the patch met and exceeded the design requirements of restoring the capability of the damaged area to withstand design loads for the fin. The results also validated the concept of repairing lightly loaded components such as the vertical fin using vacuum cured, external bonded patches. This approach is relatively simple to accomplish in any type of repair situation likely to be encountered in commercial aircraft service.

REFERENCES

1. "Repair Technology for Boron/Epoxy Composite", AFML-TR-71-270, G. Lubin et. al., Feb. 1972, Grumman Aerospace Corp., Bethpage, New York.

2. "Repair Procedures for Advanced Composite Structures, Volume 1 General Study", AFFDL-76-57, V. J. Studer and R. M. LaSalle, Dec. 1976, General Dynamics Corp., Fort Worth, Texas.

3. "Large Area Composite Structure Repair", AFFDL-TR-77-5, AFFDL-TR-77-121, AFFDL-TR-78-83, J. D. Labor, Northrop Corp., Hawthorne, California.

4. "Bolted Field Repair of Composite Structures", NADC-77109-30, J. C. Watson et. al., March 1979, McDonnell Corp., St. Louis, Missouri.

5. "Composite Repair Procedures", Lockheed Report 27863, December 1976, R. H. Stone, Lockheed-California Company.

6. "Composite Repair", Lockheed Report 28934, R. H. Stone, January 1979, Lockheed-California Company.

7. "Structural Criteria for Advanced Composites", R. M. Verette and J. D. Labor, AFFDL-TR-76-142.

8. "Effects of Manufacturing and In-Service Defects on Composite Materials", R. M. Verette and E. Demuts, Army Symposium on Solid Mechanics, Cape Cod, Mass., September 1976. Proceedings published as AMMRC-MS-76-2, Army Materials and Mechanics Research Center, Watertown, Mass.

9. "Environmentally Controlled Fatigue Tests of Box Beams with Built-In Flaws", J. D. Labor and R. M. Verette, Journal of Aircraft, May 1978, pp. 257-263.

10. "Uniaxial Failure of Composite Laminates Containing Stress Concentrations", R. J. Nuismer and J. M. Whitney, ASTN-STP-593, 1975, pp. 117-142.

11. "Evaluation of Flawed Composite Structure under Static and Cyclic Loading", T. R. Porter, Boeing Aerospace Company.

12. "A Correlation for the Fracture of Filamentary Composites", J. W. Mar and K. Y. Liu, M.I.T. preprint of a note.

13. "Evaluation and Expansion of an Analytical Model for Fatigue of Notched Composite Laminates", R. L. Ramkumar, S. V. Kulkarni, and R. B. Pipes, NASA CR-145308, March 1978.

14. "Fatigue of Notched Fiber Composite Laminates, Part II: Analytical and Experimental Evaluation", S. V. Kulkarni, P. V. McLaughlin, Jr., and R. B. Pipes, NASA CR-145039, April 1976.

15. "Advanced Composite Serviceability Program", Rockwell International Corporation, AFML Contract F33615-76-C-5344, Quarterly Progress Reports No. 1 through 8.

16. "Stress Fracture Criteria for Laminated Composites Containing Stress Concentrations", J. M. Whitney and R. J. Nuismer, J. of Composite Materials, Vol. 8 (July 1974) p. 253.

17. "The Determination of Fracture Strength in Orthotropic Graphite/Epoxy Laminates", H. J. Konish, Jr. and T. A. Cruse, AFML Contract No. F33615-73-C-5505.

18. "Tensile Strength of Notched Composites", T. A. Cruse, J. of Composite Materials, Vol. 7, April 1973.

19. "Compression Effects on the Fatigue of Notched Boron/Epoxy Composites", E. C. Durchlaub and R. B. Freeman, presented at the Second Conf. on Fibrous Composites in Flight Vehicle Design, 22-24 May 1974, Dayton, Ohio.

20. "Impact Damage Characteristics of Graphite/Epoxy Laminates", N. M. Bhatia, Northrop Corp. NOR-76-186, June 1977.

21. "Service/Maintainability of Advanced Composite Structures", J. D. Labor, AFFDL-TR-155, November 1978.

22. "Investigation of Damage Tolerance of Graphite/Epoxy Structures and Related Design Implications", N. R. Adsit and J. P. Waszczak. NADC-76387-30, December 1976.

23. "Impact Fracture of Composite Sandwich Structures," M. D. Rhodes, AIAA paper 75-748.

24. "Low Velocity Transverse Normal Impact of Gr/Ep Composite Laminates", E. J. McQuillen, B. W. Gause, and R. E. Llorens, J. of Composite Materials, Vol. 10, pp. 79-91, January 1976.

25. "Effect of Low Velocity Impact Damage on the Compressive Strength of Graphite/Epoxy Hat-Stiffened Panels", M. D. Rhodes, J. G. Williams, and J. H. Starnes, Jr., NASA TMX-73988, December 1976.

26. "Evaluation of Ballistic Damage Resistance and Failure Mechanisms of Composite Materials", E. F. Olster and H. A. Woodbury, AFML-TR-72-79, 1972.

27. "Evaluation of Fracture in Notched Composite Laminates", S. V. Kulkarni and B. W. Rosen, Materials Sciences Corporation Report No. MSC/THR/606/1031, October 1976.

28. "Some Observations on Fracture Behavior of Advanced Fiber Reinforced Laminates", C. P. Sendeckyj, Proc. of 12 Annual Meeting of Society of Engineering Science, Austin, Texas, 20-22 October 1975.

29. "Investigation of Failure Mechanism in Fiber Composite Laminates", P. V. McLaughlin, Materials Sciences Corporation, TFR/7508, Final Report on NADC Contract N62269-74-C-0662, 1975.

30. "Characterization of Composites for the Purpose of Reliability Evaluation", J. C. Halpin, K. L. Jerina, and T. A. Johnson, ASTM STP 521, 1973.

31. "Fatigue of Notched Composites", P. V. McLaughlin, Jr., S. V. Kulkarni, S. N. Huang, and B. W. Rosen, Third Conference on Fibrous Composites in Flight Vehicle Design, NASA TM X-3377.

32. "Fracture Mechanics and Composite Materials: A Critical Analysis", C. Zweben, ASTM STP 521, 1973.

33. "Residual Strength Characterization of Laminated Composites Subjected to Impact Loading", G. E. Husman, J. M. Whitney, and J. C. Halpin, ASTM STP 568, 1975, pp. 92-113.

34. "Investigation of Brittle Fractures in Graphite/Epoxy Composites Subject to Impact", L. B. Greszczuk and H. Chao, USAAMRDL-TR-75-15, May 1975.

35. "Structural Integrity Requirements for Projectile Impact Damage - An Overview", J. G. Avery, T. R. Porter, and R. W. Lauzze, AGARD Conf. Proc. No. 186, Specialists Meeting on Impact Damage Tolerance of Structures, October 1975.

36. "Impact Behavior of Polymeric Matrix Composite Materials", Peichichon and R. Mortimer, AFML-TR-76-242, December 1976.

37. "Hard Object Impact Damage of Metal Matrix Composites", J. Awerbuch and H. T. Hahn, J. of Comp. Materials, Vol. 10, July 1976.

38. "Impact Behavior of Graphite/Epoxy Simulated Fan Blades", T. S. Cook and J. L. Preston, Jr., Paper Submitted to the AIAA Journal of Aircraft (Paper No. 77-365).

39. "Material Variables Affecting the Impact Resistance of Graphite and Boron Composites", R. C. Novak, AFML-TR-74-196, June 1975.

40. "A Scanning Electron Microscopic Study of Hybrid Composite Impact Response", D. F. Adams, J. of Materials Science, Vol. 10, pp. 1591-1602, 1975.

41. "Dynamic Response of Anisotropic Laminated Plates under Initial Stress to Impact of a Mass", C. T. Sun and S. Chattopadhyay, AFML-TR-74-258, March 1976.

42. "Large Area Composite Structure Repair", A. L. Scow and R. W. Kiger, AFFDL-TR-77-5, First Interim Report, May 1977, Northrop Corp.

43. "Large Area Composite Structure Repair", R. W. Kiger and S. H. Myhre, AFFDL-TR-77-121, Second Interim Report, November 1977, Northrop Corp.

44. "Advanced Development of Conceptual Hardware Horizontal Stabilizer", Grumman Aerospace Corp., AFML contract.

45. "Macroscopic Fracture Mechanics of Advanced Composite Materials," M. E. Waddoups, J. R. Eisenmann, and B. E. Kaminski, Journal of Composite Materials, Vol. 5, 1971, pp. 446-454.

46. "Fatigue Characteristics of Graphite/Epoxy Laminates Under Compression Loading", M. S. Rosenfeld and S. L. Huang, AIAA J. Aircraft, Vol. 15, No. 5, May 1978.

47. "Some Observations on Fracture Behavior of Advanced Fiber-Reinforced Laminates", Sendeckyj, G. P., Proceedings of the 12th Annual Meeting of the Society of Engineering Science, University of Texas at Austin Press, 1975, pp. 625-634.

48. "Advanced Composite Aileron for L-1011 Transport Aircraft, Quarterly Technical Report - No. 9", Contract NAS1-15069, LR 29352, Lockheed-California Company, prepared for NASA-Langley Research Center, January 1980.

49. "Advanced Manufacturing Development of a Composite Empennage Component for L-1011 Aircraft, Phase II - Final Report, Design and Analysis", NASA CR-165634, A. C. Jackson et. al., Lockheed-California Company, Burbank, California, April 1981.

50. "Ground Test Plan - Advanced Manufacturing Development of a Composite Empennage Component for L-1011 Transport Aircraft", Lockheed Report LR 29583, January 1981.

APPENDIX A
AIRLINE SURVEY QUESTIONNAIRE

1. Using the attached Table A-1, please indicate the types of damage or defects typically encountered in service for the various part categories listed. Indicate typical defect sizes and the frequency of occurrence of each type of defect to the best of your knowledge. Where applicable, define locations on the part where defects are most frequently noted. Define the defect and component types using the codes given in the attached Code List. Indicate the probable cause of damage to the best of your knowledge.

   For the various damage situations indicated on the table, please categorize defects according to the maintenance action required using the codes given in the attached Code List. Indicate the effect of size and location of the defect on categorization of the defect and action required.

   Completion of this table may be based on personal knowledge and judgment of Engineering and Shop personnel, but where possible answers based on documented service data are preferred.

   Other codes may be added as necessary. If information in certain categories is unavailable, or if not applicable please indicate. Priority should be given to wing and empennage skins, stiffeners, and substructure; control surfaces; and fairings, since these are the most likely candidates for composite applications.

2. Indicate for each of the damage and defect types listed in the Code List, whether visual inspection, NDI, or a combination of the two is used for detection; and indicate the percentage of each defect type that is detected in-service at line station and at the major maintenance base during scheduled checks.

Defect Type	% Detected at Line Station	% Detected at Maintenance Base

APPENDIX A. - AIRLINE SURVEY QUESTIONNAIRE Continued

TABLE A-1. - DAMAGE AND DEFECTS NOTED IN SERVICE (1)

Component Type (Code No.)	Type of Defects Noted (Code Nos.)	Typical Defect Size or Range of Sizes Noted	Location of Defect on Component	Probable Cause of Damage	Maintenance Action Required (Code No.)	Remarks

(1) See pg. for list of Codes

3. Indicate the relative frequency of occurrence of each of the maintenance action categories given in the Code List.

   Also indicate the relative frequency of occurrence of the following situations:

   1) Temporary repair of defects at line stations followed by a ferry flight to the maintenance base for permanent repairs.

   2) Repair of defects at a line station using personnel and/or equipment flown in from the maintenance base.

4. Are external patches considered acceptable as permanent repairs?

   Indicate in which areas and component types external patches are acceptable, and where flush aerodynamic repairs are required.

   What percentage of repairs are aerodynamic repairs?

5. Are removable components, such as control surfaces and fairings generally removed for repair or are repairs made on the aircraft?

6. Which of the following equipment are available?

	Major Maintenance Base	Line Station
Autoclave	_____	_____
Large Ovens	_____	_____
Vacuum Pumps	_____	_____
Heat lamps, heater blankets	_____	_____
Freezers	_____	_____

7. Are your maintenance people familiar and proficient with standard wet layup patch fiberglass repair techniques?

   Adhesive bonded repairs of metal structure, both hot bond and cold bond?

8. Would you consider the use of portable repair kits (vacuum pump, heater blanket, rheostat, along with patch material, adhesives, bagging and bleeder material), for composite repair, when there is widespread usage on aircraft?

   Would you foresee their use at line stations as well as maintenance bases?

9. What is the maximum feasible elapsed time for completion of a repair during maintenance checks?

LIST OF CODES

DAMAGE AND DEFECT TYPES

a) Cracks
b) Delaminations
c) Disbonds
d) Impact damage
e) Corrosion effects
f) Wear
g) Lightning strike
h) Elongated fastener holes

COMPONENT TYPES

Wing	Horiz. Stab.	Vert. Stab.	Item
W1	HS1	VS1	Skins, doublers
W2	HS2	VS2	Skin stiffener elements
W3	HS3	VS3	Leading edge members
W4	HS4	VS4	Trailing edge members
W5	HS5	VS5	Control surfaces
W6	HS6	VS6	Substructure (spars, ribs)
W7	HS7	VS7	Fairings
W8	HS8	VS8	Fuselage joint
W9	HS9	VS9	Other joints (hinges, actuators, etc.)

APPENDIX A. - Concluded

Fuselage	Item	Other	Items
F1	Skins	M1	Engine Cowling, Support Str.
F2	Frames	M2	Langing Gear Members
F3	Stringers	M3	Pylon
F4	Bulkheads		
F5	Doors		
F6	Floor Beams & Posts		
F7	Floor Panels		
F8	Fairings		
F9	Radomes		

MAINTENANCE ACTION CATEGORIES

1. Negligible damage. Repair not required.
2. Can be permanently repaired in line stations.
3. Can be permanently repaired at maintenance base only using standard repair.
4. Can be permanently repaired at maintenance base only and requires Engineering disposition.
5. Not repairable. Part replacement required.

APPENDIX B
FAILURE MODES - PHASE 2

STATIC TESTS

C-50 RT Tension -1, -2

-1 Interlaminar shear failure near the core side (0.13 cm [.05 in.] from core) at one end of the laminate at 0 degree ply in both specimens. Failure of core splice and partial disbond of steel (non-critical).

-2 top 3 plies separated from rest of laminate at 90 degree ply

RT Compression -5, -6

-5 interlaminar shear failure near center on core side. Core disbond on end probable cause.

-6 good failure - center section, multiple ISF* fiber failure of outermost plies.

ET tension -3, -8

-3 ISF near core side on one edge (at 0 degree ply); splice failure, partial core/composite and core/steel disbond in center.

-8 fiber crushing through entire thickness at one core splice. Four separate pieces after failure. Top 3 plies separated from rest of laminate at 90 degree ply.

ET Compression -4, -7

-4 steel disbond on one end, composite disbond in center and ISF of 1 or 2 plies nearest core.

-7 failure identical to -6

C-16 RT Tension -1, -2

Fiber splitting and breakage primarily along $\pm$45 degree plies. Core splitting and separation from Ti after failure

*ISF = Interlaminar Shear Failure

ET Tension -3, -8

Same as RT Tension. Failure occurred more toward the center of the beam.

RT Compression -5, -6

Severe delamination, fiber crushing through entire thickness. Many fiber fragments.

-5 delamination and local buckling away from primary failure location but still in test section.

ET Compression -4, -7

-7 same as RT Compression. More buckling after delamination.

-4 fiber failure through 1/3 to 1/2 of thickness on core side in two places in test section. Remainder failed between these locations in fiber crushing and breakage along ±45 degree plies.

CU Fiber breakage across specimen center section
Fiber splitting in ±45 degree laminate

CD ±45 degree fiber splitting
-45 degree fiber breakage
Failure surface began at edge of hole and progressed at a ±45 degree angle to the sides of the coupon

I The failure of these laminates both in tension and compression was due primarily to extensive delamination in the cocured patch. The adhesive was left intact with no evidence of bondline failure. The failed surface in the joint region showed longitudinal fiber splitting in the ±45 degree plies with no apparent fiber failure.

II Both tension and compression failure surfaces showed cohesive bondline failure becoming patch material delamination toward the honeycomb core end of the scarf joint. Slightly more evidence of delamination existed in compression than in tension.

III Both specimens showed evidence of a core bond failure with no delamination in the precured patch. Failure initiated near the outside edge of the scarf joint within the adhesive and propagated as delamination into the parent laminate. Severe fiber breakages occurred in the cover plies at the location of bondline failure.

Compression - Again the bondline failure occurred near the outside tip of the scarf resulting in delamination of both parent and patch. Failed material was confined to the outermost 1/3 of the laminate

thickness with the core-side 2/3 still apparently intact. Fiber breakage again occurred in cover plies.

IV Tension - Cohesive failure of one scarfed edge of the patch was followed by severe delamination of the parent material at the depth to which damage was removed. Portions of 90 degree plies remained attached to the adhesive surface while all other plies separated at the adhesive.

Compression - Intrapatch delamination caused sub-surface fiber failure (crushing) within the patch resulting in parent laminate delamination. There was no bondline failure.

V ET Tension -1, -2

-1 shear failure of scarf joint terminating at fracture of the cover plies at top end of the bondline. Core separation of composite and steel at center portion of beam.

-2 ISF at end on core side at 0 degree location through thickness as did C-50-1, -2, -3.

ET Compression -3, -4

-3 shear failure of bondline resulting in fiber breakage through the thickness of patch near core end of bondline and moderate patch delamination.

-4 Severe waviness of plies near core end of bondline possibly causing poor alignment with parent. Failure started at this location (end of bond) and progressed as ISF through patch and to a lesser degree through parent. Waviness caused severe thickness variation near bondline.

Waviness true for all Type V specimens.

VI-T ET Tension -1, -2

Primarily interlaminar shear failure in patch beginning at the end of patch and propagating through patch - not through adhesive. Ply breakage in each near bondline.

RT Compression -5, -6

Complete patch separation and disintegration with remnants of patch ply tips remaining on parent. Combination of adhesive and composite interlaminar shear separation primarily at the $\pm$45 degree plies.

ET Compression -7, -8

Composite/core separation in center and cohesive bondline failure.

Reduced Temperature -3, -4

Cohesive bondline failure at tips of patch becoming core/composite separation at plug. Parent delamination away from ply beginning on core side.

VI-F ET Tension -1, -2

Interlaminar tensile failure of surface plies of parent directly under bondline in what appears to be ± 45 degree plies. No bondline failure. Ply breakage of separated plies at end of patch. Plug fractured.

ET Compression -3, -4

Same failure as ET Tension tests.

VII ET Tension -1, -2

Shear separation through book of plies closest to parent. No bondline failure. Plug fractured and honeycomb core failure in center section.

RT Compression -5, -6, -7

-5 composite/core separation caused parent bondline failure

-6 discrete sections of bondline throughout patch failed adhesively as though there was a poor bond or poor surface wetting of the composite by the adhesive.

-7 no parent bond failure. Failed same as ET Tension with a massive single delamination in parent through a 0 degree ply.

ET Compression -8, -9

-8 failed through the first book as did ET Tension. Composite/honeycomb separation

-9 top plies of parent delaminated under patch. Composite/core separation

Reduced Temperature -3, -4

-3 interlaminar shear failure through first book of plies -across total section.

-4 shear failure in first book beginning at tip of external patch but propagating into parent on way to plug. At plug, failure becomes core/composite separation and more parent delamination further from plug.

VIII ET Tension -1, -2

Identical shear failures beginning at the bondline near the tip of patch, progressing along bond then progressing into parent laminate where thickness of patch steps up. Failure progressed to plug then through thickness at plug interface.

ET Compression -3, -4

Identical failures - shear initiates at patch tip, jumps into patch between first and second plies and proceeds to plug, then propagates through thickness.

IX ET Compression -1, -2

Identical failures - shear failure between patch and parent - cohesive bondline failure and plug pull-out. Large voids in bondlines. Interleafing (domino) effect in adhesive common in shear failures.

-2 had less voids and went to a 30 percent higher load so the voids could have caused failure in -1.

X ET Compression -1, -2

Identical failures - cohesive shear failure between patch and parent. Failure surface very topographic due to internal ply terminations - some ply tip breakage. Plug pulled out.

XI ET Tension -1, -2

Combination bearing and fastener pull-through in composite. -2 had fastener separation.

ET Compression -3, -4

Subtle bearing failure in composite and faying surface sealant fracture.

APPENDIX B. - Concluded

XII ET Tension -1, -2

Separation at faying surface sealant. Fastener pull-through of the composite at one end of the metal patch. Combination pull-through and bearing failure in composite.

ET Compression -3, -4

-3 very subtle bearing failure in composite. Almost no visible sign of failure. Plug buckling (slight).

-4 stability failure of metal plate. Out of plane deformation of metal caused composite/core separation and parent delamination on both sides of patch.

XIII Failure occurred cohesively through one of the scarfed longitudinal surfaces. Adhesive failure.

XIV Corner delamination in patch becoming adhesive failure in bondline. Failure of composite progressed laterally from side of hole after patch disbond (at half length of patch).

FATIGUE TESTS

C-16-9 -10 In both specimens a through the thickness fiber splitting type failure resulting in ply separation, composite/core and titanium/core separation. Failure progresses through gage section honeycomb to titanium face sheet disbond.

VI-T-9 Failure progressed through first patch ply to plug fracture. Very similar to static tension failures. Both sides of external patch failed.

VI-F-5 Failure progressed through top ply of parent to plug fracture. Only one side of external patch failed.

C-50-9 Failure occurred as through the thickness fiber splitting (as C-16) at the location of core splice. Scattered delamination close to top and bottom of composite in various locations along laminate.

IV-5 Parent interlaminar tensile failure at maximum depth of part-through repair. Failure of one patch scarfed surface.

III-5 Adhesive bondline failure resulting in cover ply fracture at top of scarf.

APPENDIX C
CURING AND BONDING PROCEDURES FOR
GRAPHITE SKIN PATCH - PHASE 4

A. Cure Cycle and Bleeder Arrangement for Precured Patch Laminates

CURE:

1. Apply full vacuum. Heat to 275°F at 2-3°F/minute.
2. Dwell at 275° ±5°/minute for 45 minutes starting dwell time when part reaches 270°F.
3. Apply 100 ±5, -10 psi, venting vacuum when pressure reaches 20 psi.
4. Heat to 355°F at 2-4°F/minute, start cure timing when part reaches 350°F.
5. Cure at 355° +10, -5°F for 120 ±5 minutes.
6. Cool to 175°F or below under full pressure at 3°F/minute maximum.

BLEEDER ARRANGEMENT:

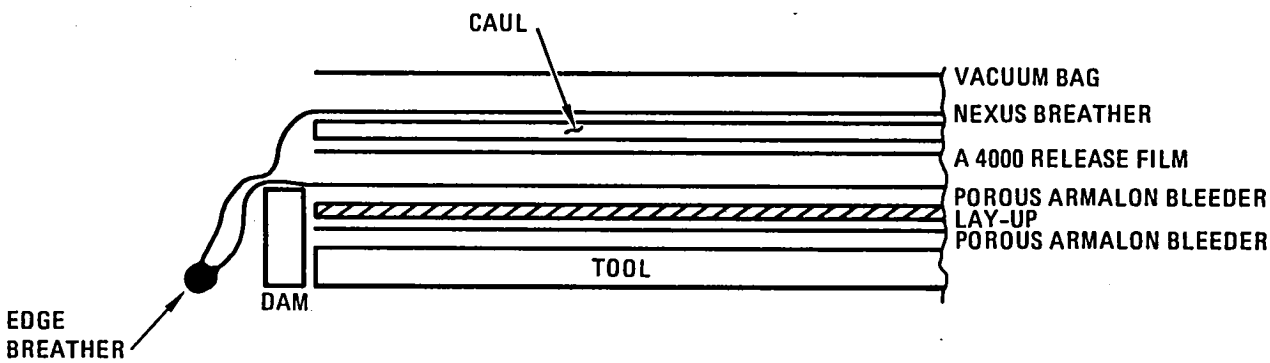

B. Cure Cycle and Bleeder Arrangement for Patch Bonding with M329 Adhesive

CURE CYCLE - M329 Adhesive

1. Apply full vacuum (20 in. Hg minimum)
2. Heat to 350°F ±5°F at 6°F/minute or greater.
3. Cure at 350°F ±5°F for 60-65 minutes.
4. Cool to 180°F under full vacuum.

BLEEDER ARRANGEMENT:

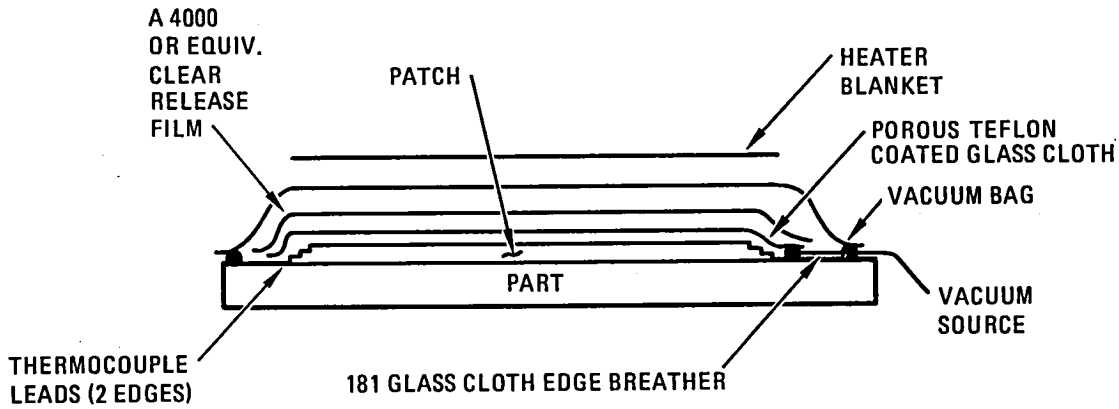

C. Fin Surface Preparation Procedures

1. Clean ultrasonic couplant off surface.
2. Scotchbrite surface in damage area.
3. Clean out hole with small drum sander.
4. MEK wipe damage area. Cut G/E disc to plug hole.
5. Apply teflon tape to inside skin over hole.
6. Cast EA 9330 epoxy around G/E disc to seal hole.
7. After RT cure, sand or file smooth.
8. Layout white pencil lines for positioning the repair stack patches.
9. Clean surface with MEK.
10. Apply teflon tape edge protection and 181 edge breather. Tape in place.

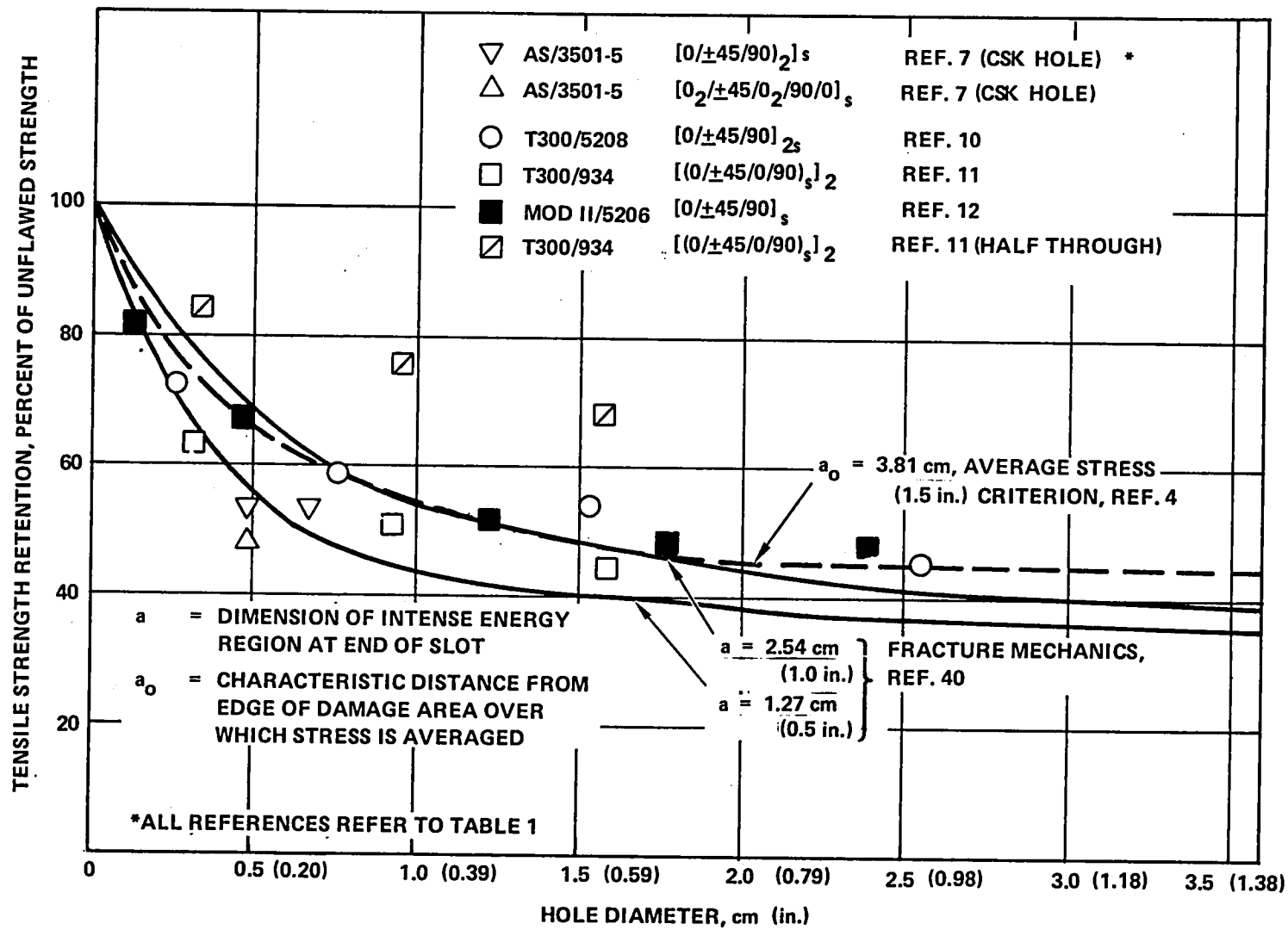

Figure 1. - Tensile strength retention of laminates with a hole.

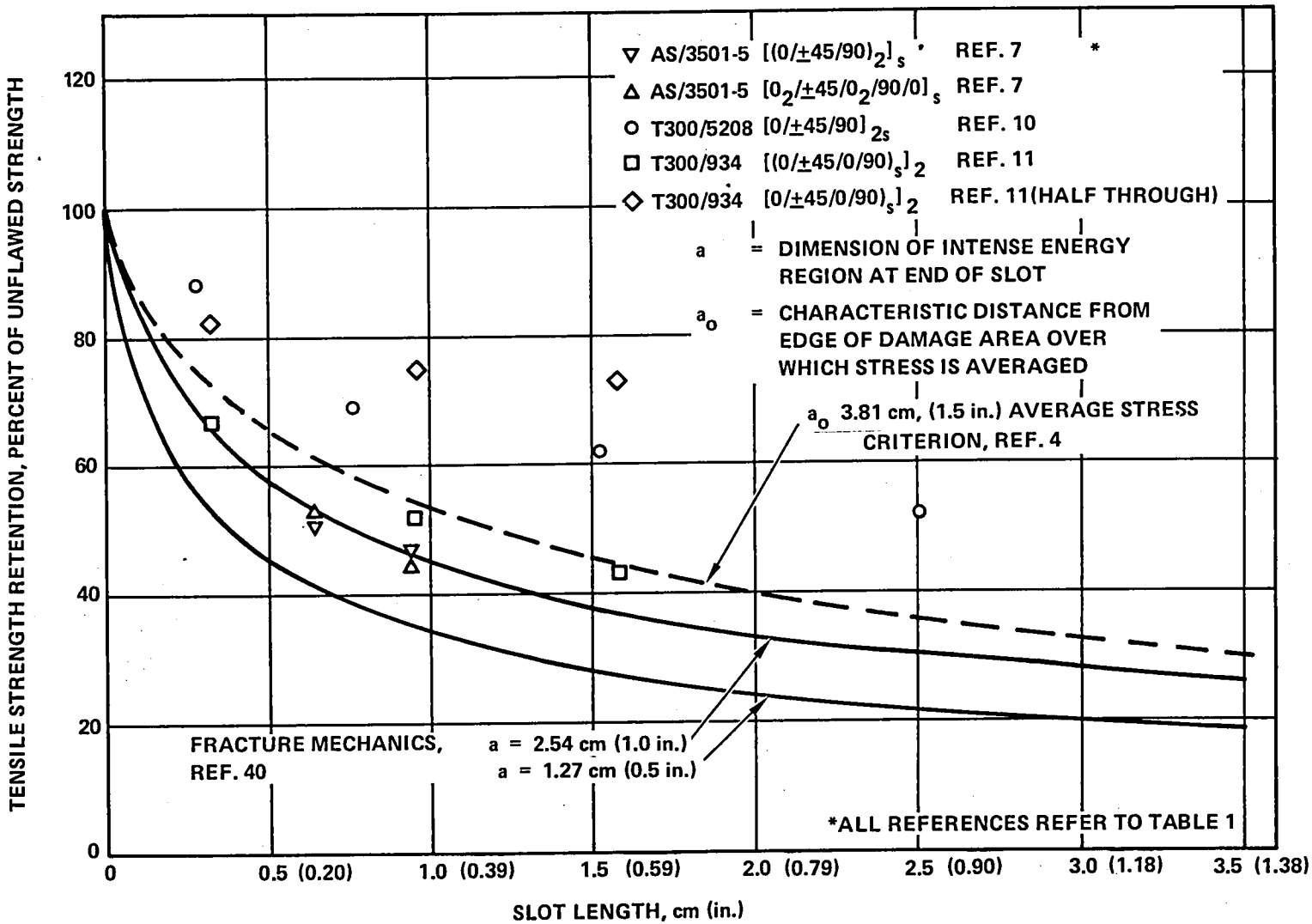

Figure 2. - Tensile strength retention of laminates with a slot.

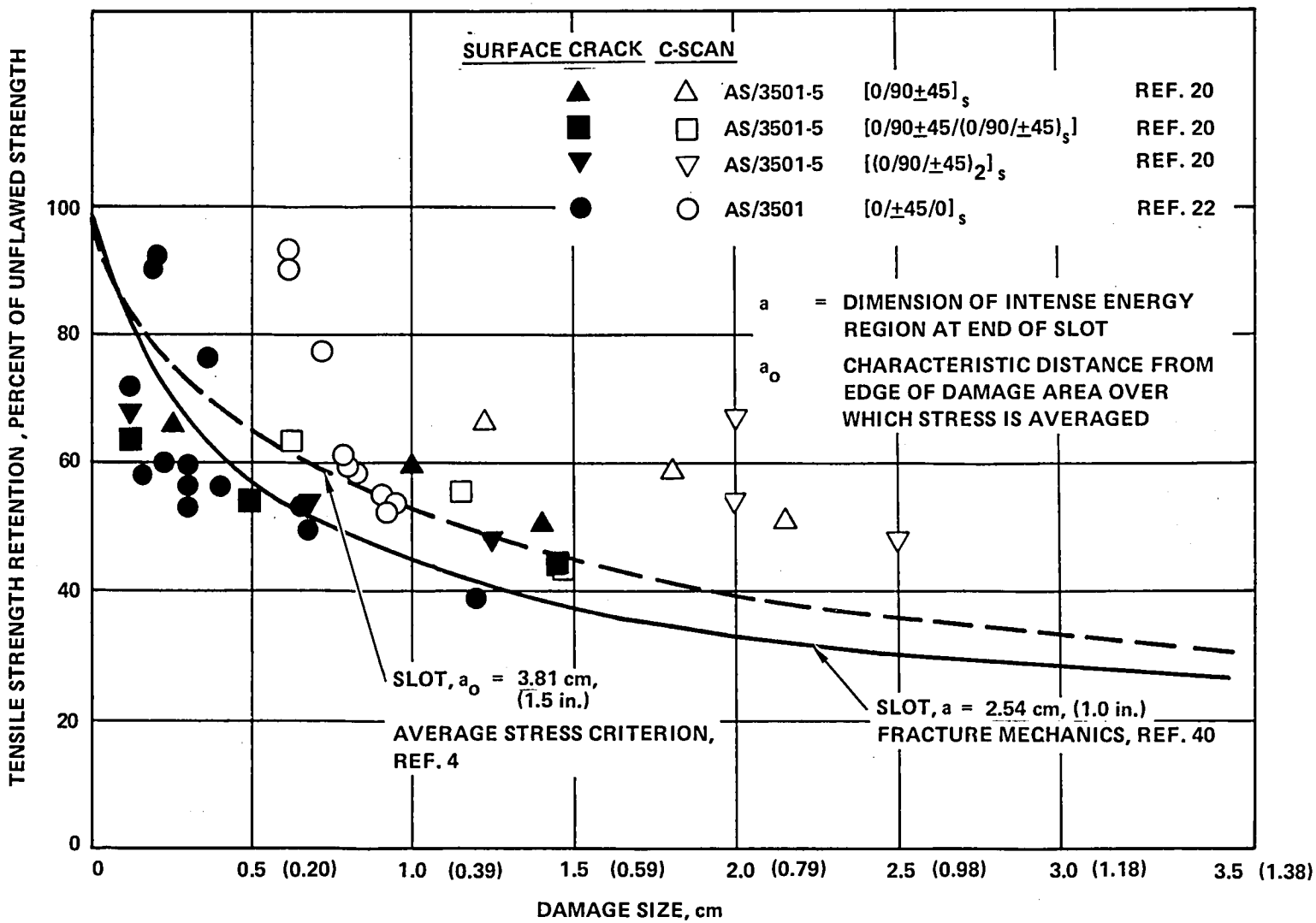

Figure 3. - Tensile strength retention of impacted laminates vs. damage area.

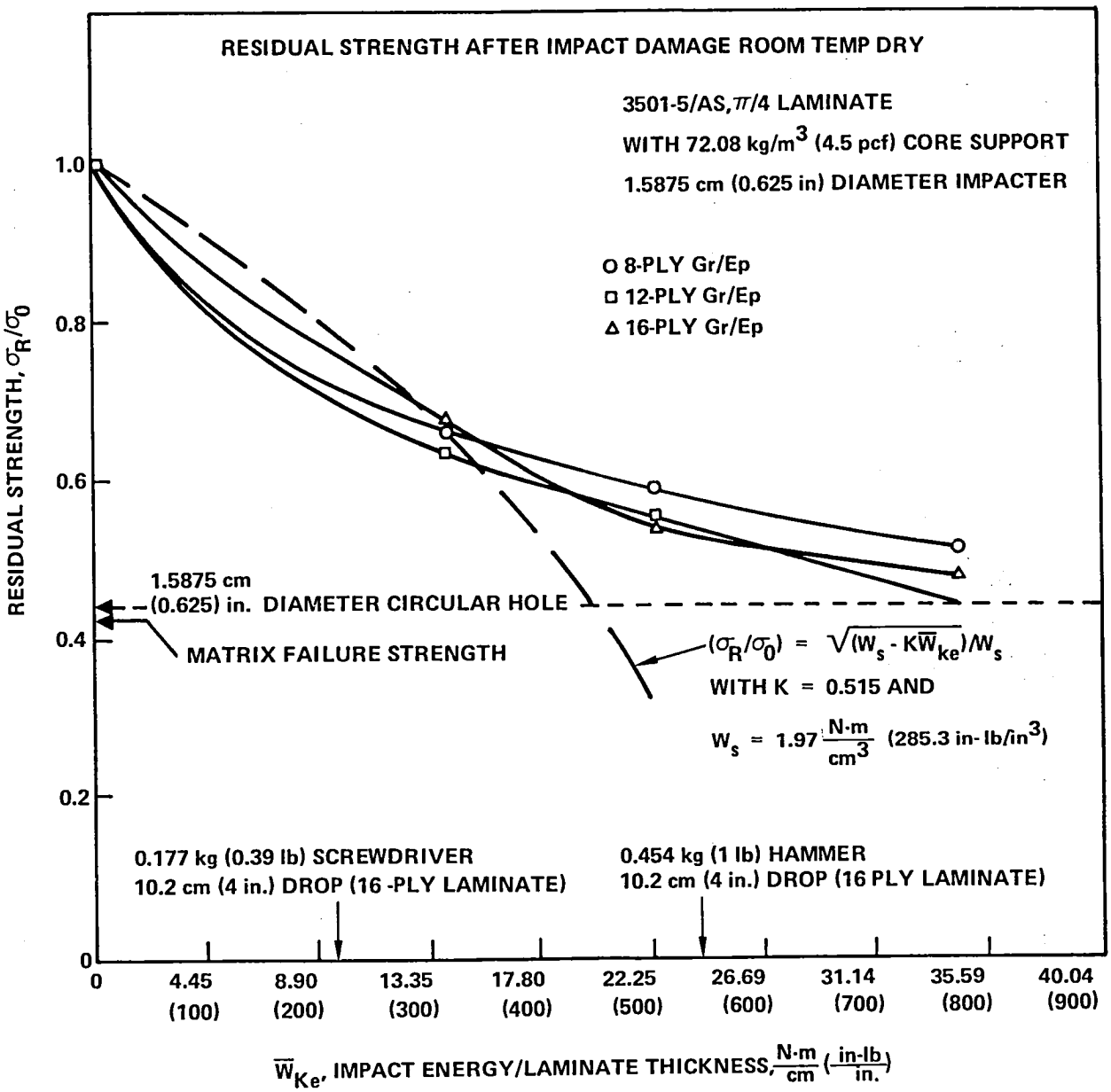

Figure 4. - Residual tensile strength of impacted laminates vs. impact energy.

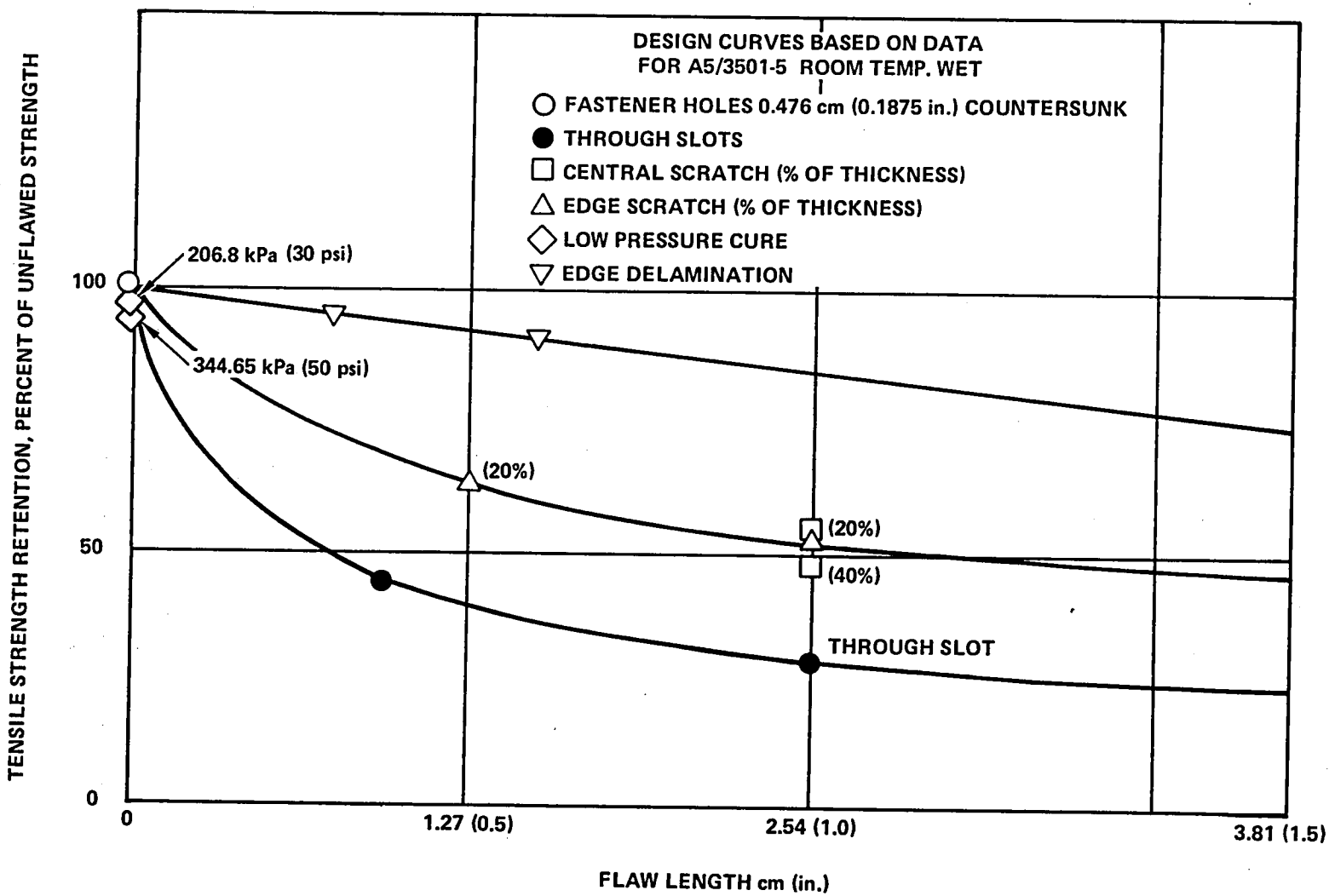

Figure 5. - Residual tensile strength for graphite/epoxy laminates with flaws.

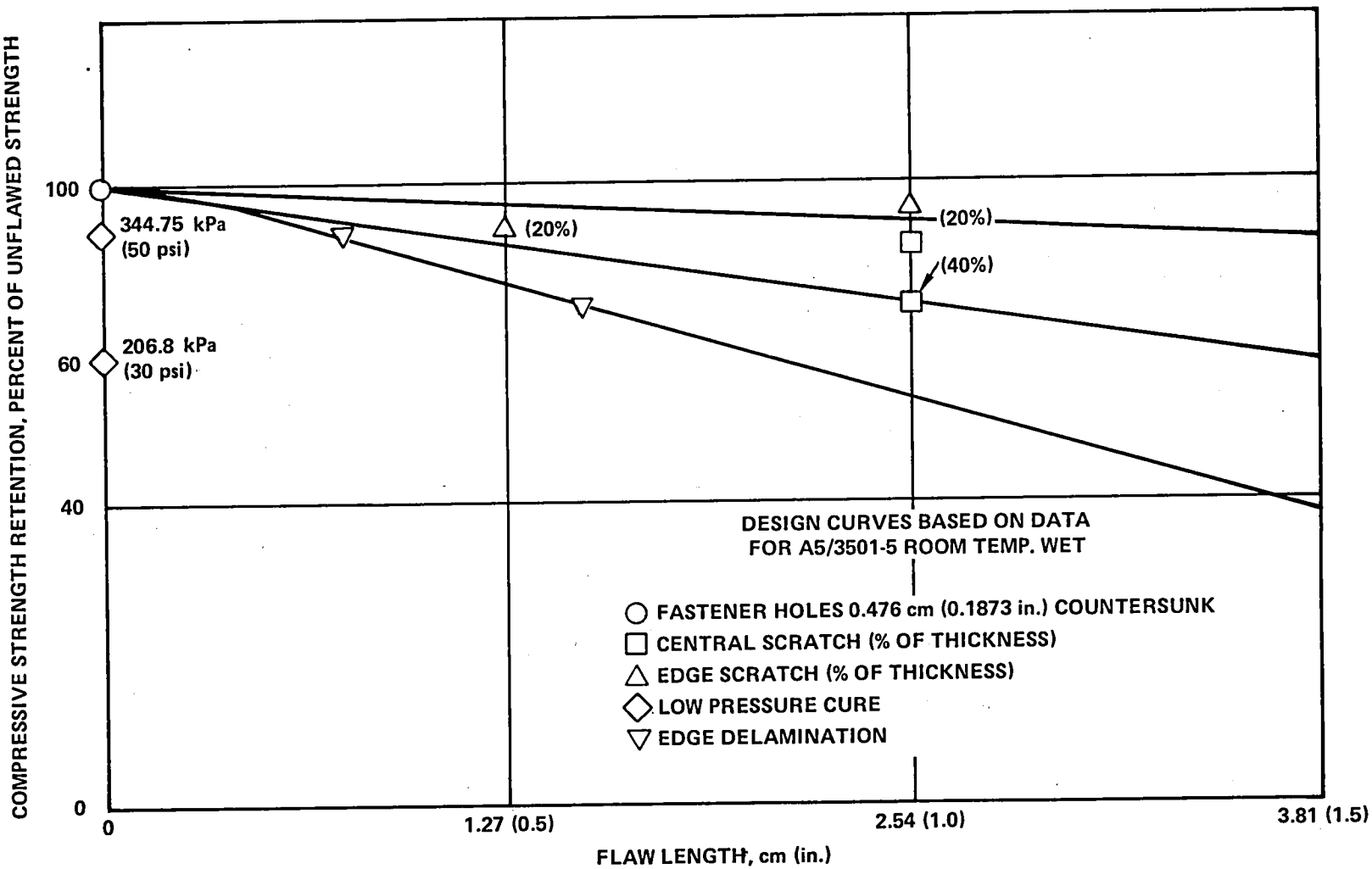

Figure 6. - Residual compression strength for graphite/epoxy laminates with flaws.

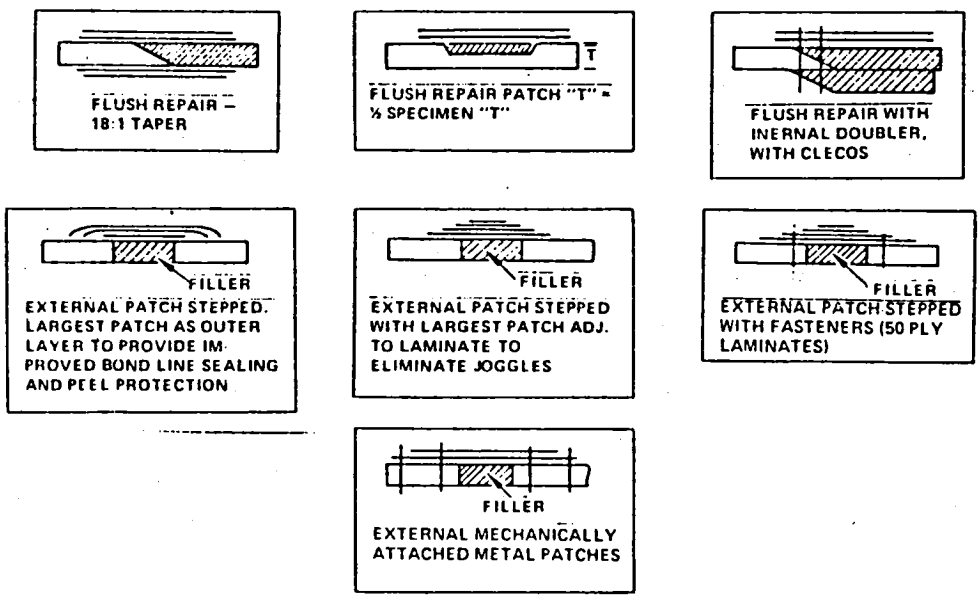

Figure 7. - Repair concepts.

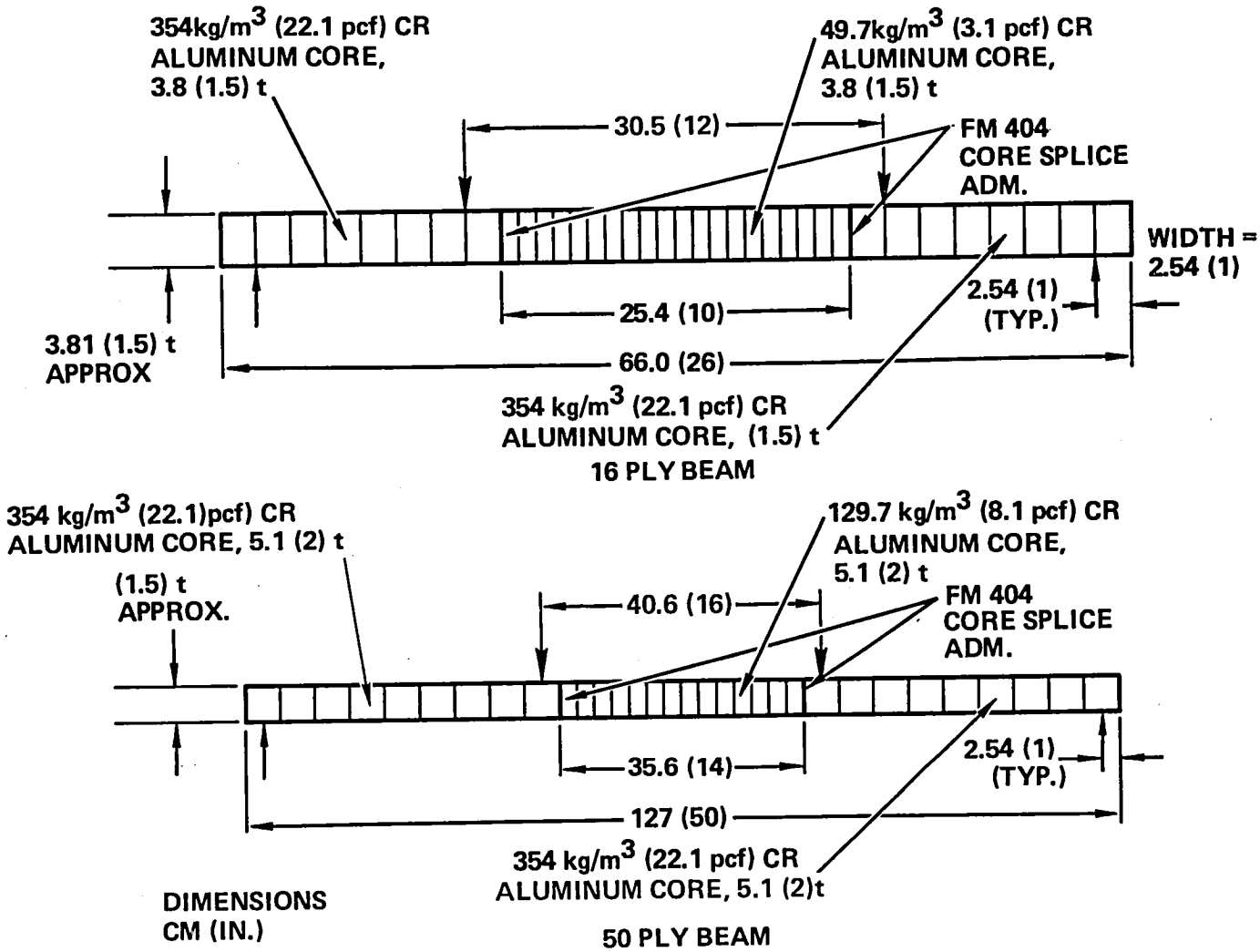

Figure 8. - Sandwich beam specimen.

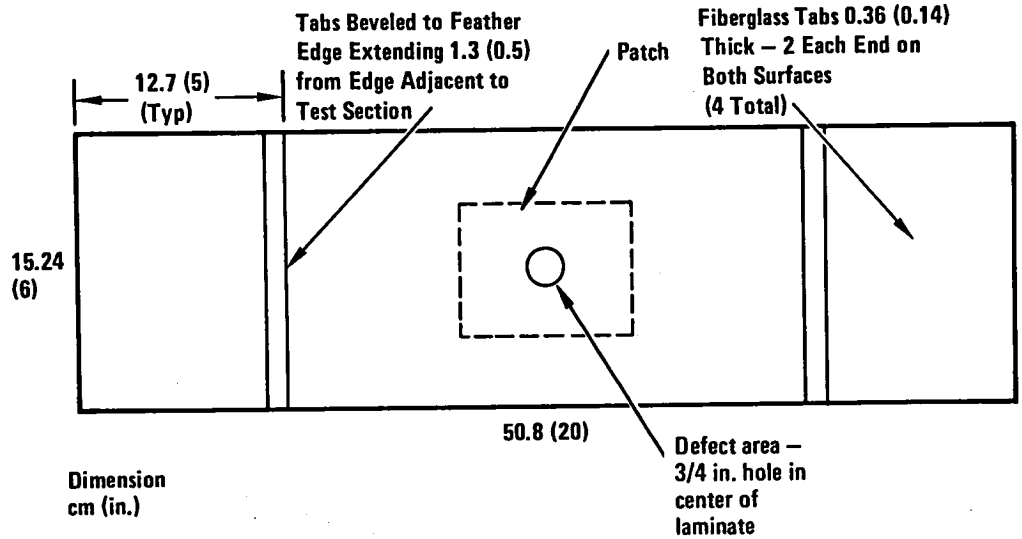

Figure 9. - Laminate specimens.

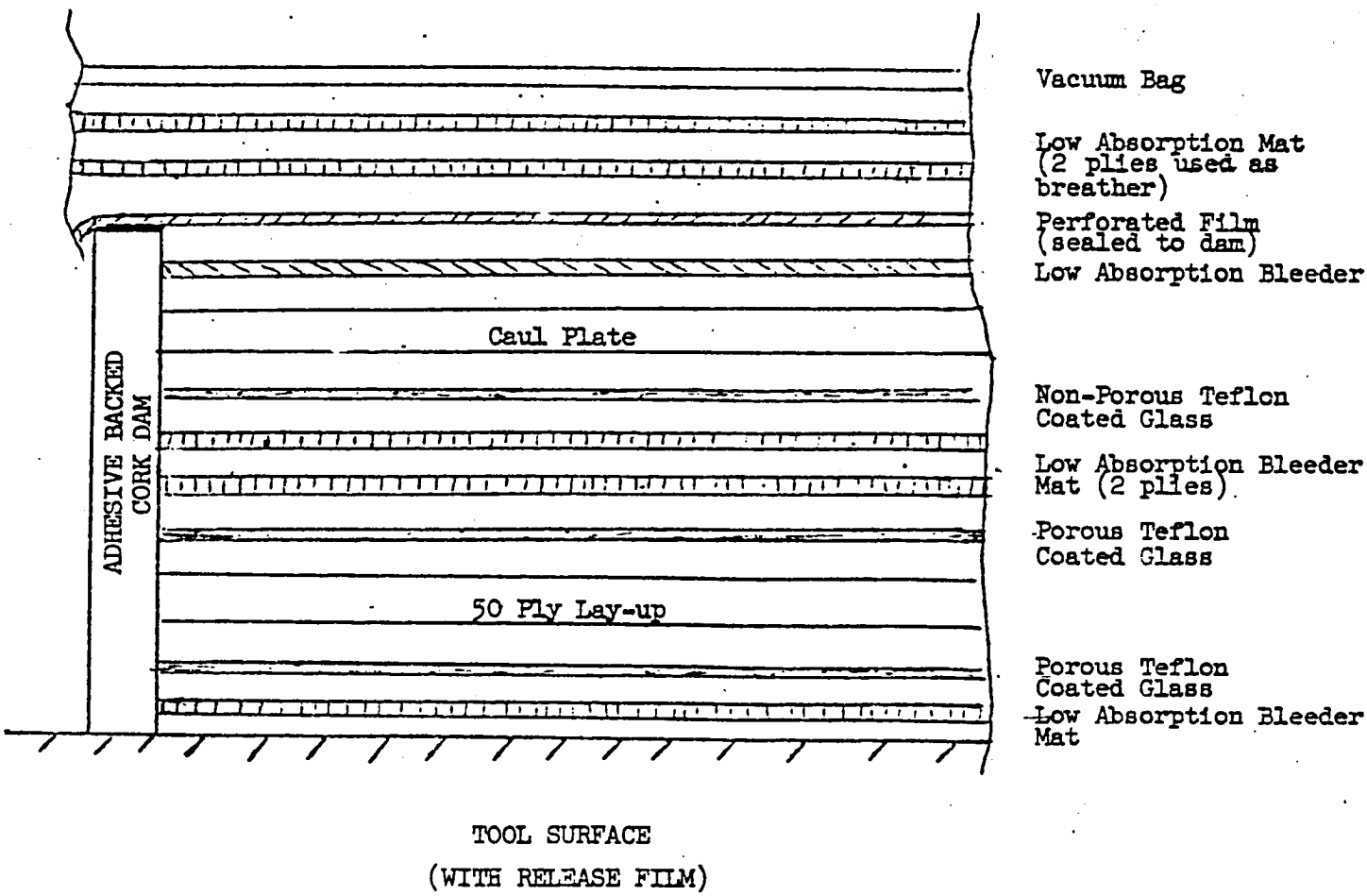

Figure 10. - Modified bleeder arrangement for 50 ply laminates.

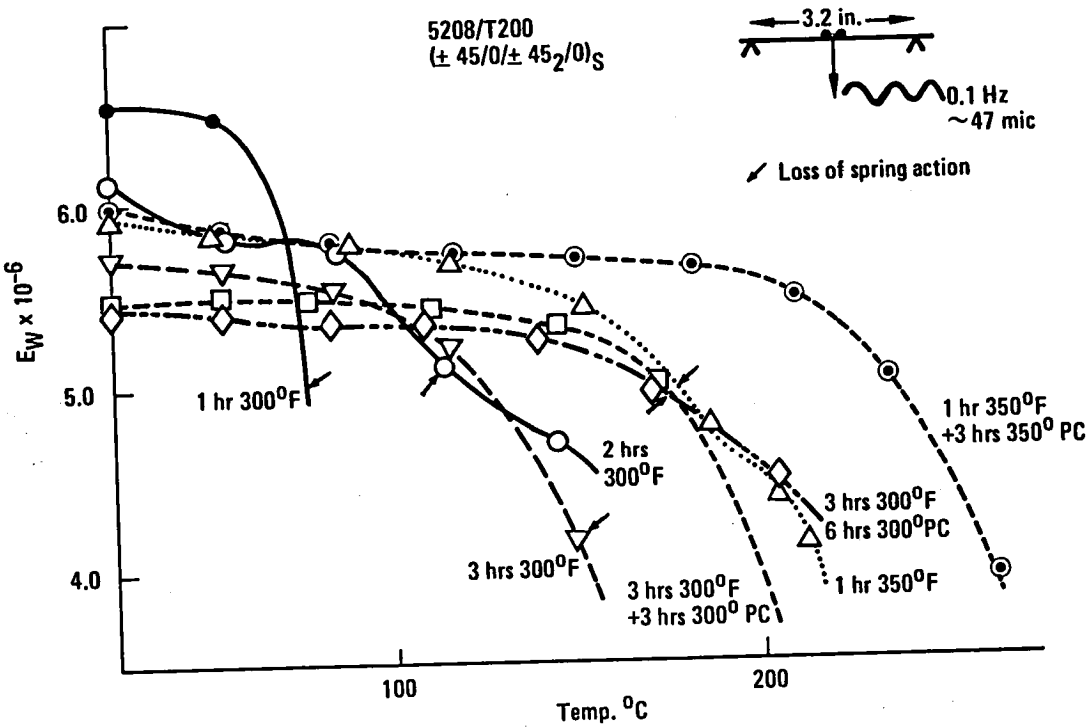

Figure 11. - Dynamic modulus vs. temperature.

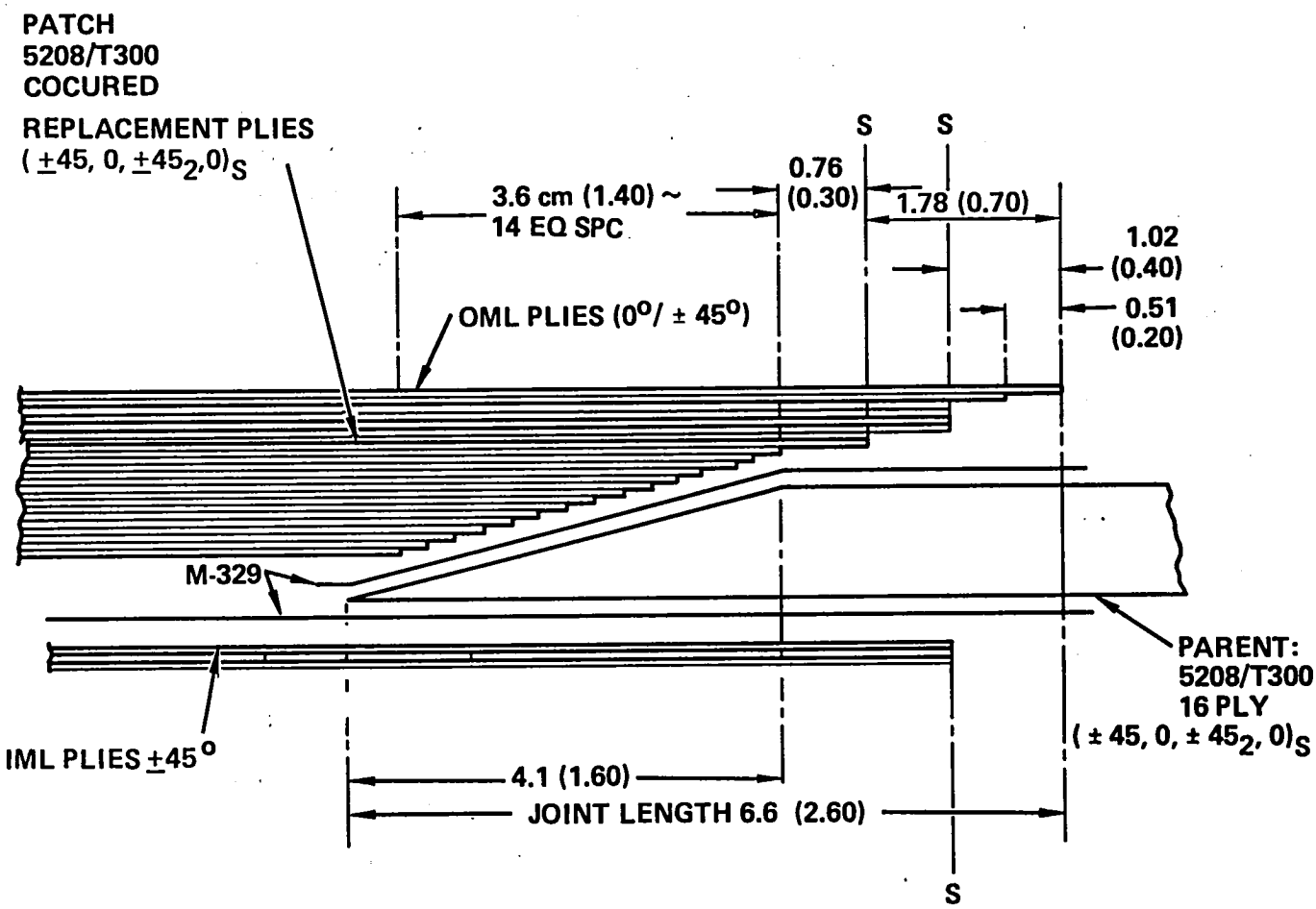

NOTE: TYPE I - SANDWICH BEAM SPECIMEN PER FIG. 8
TYPE XIII- TABBED LAMINATE SPECIMEN PER FIG. 9

Figure 12. - Flush cure-in-place graphite repairs - 16 ply parent laminate (Types I and XIII)

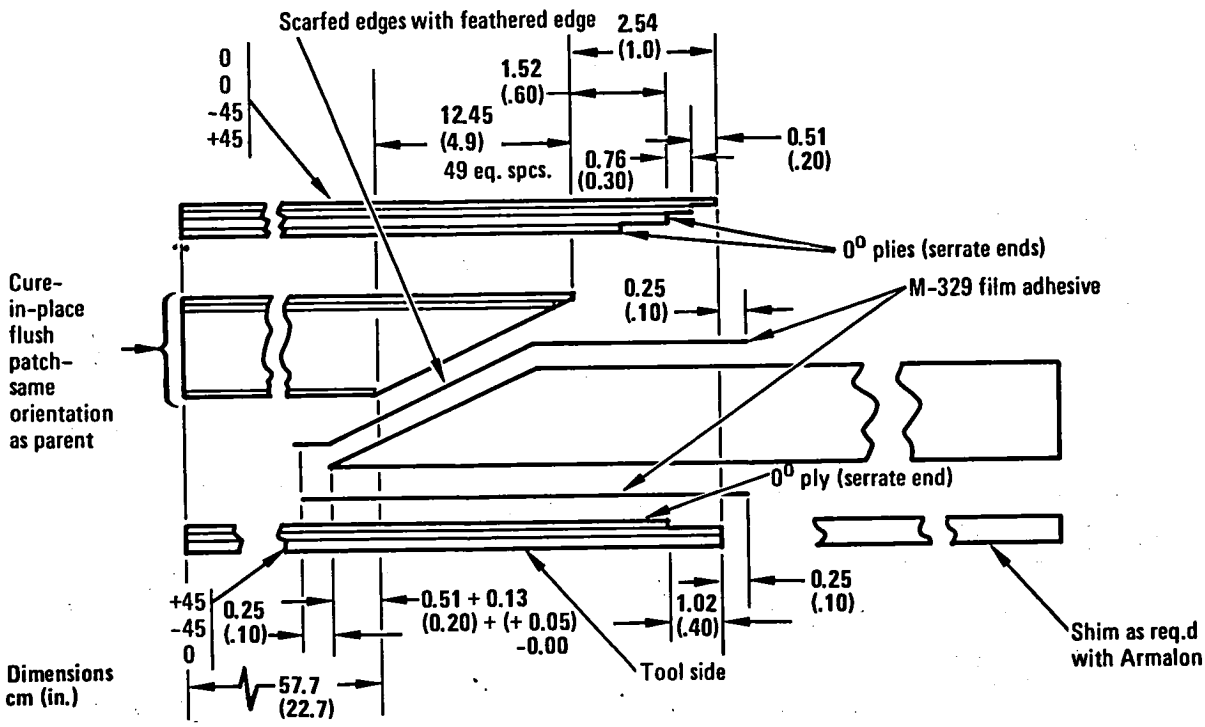

Figure 13. - Flush cure-in place graphite repair - 50 ply parent laminate - (Type II).

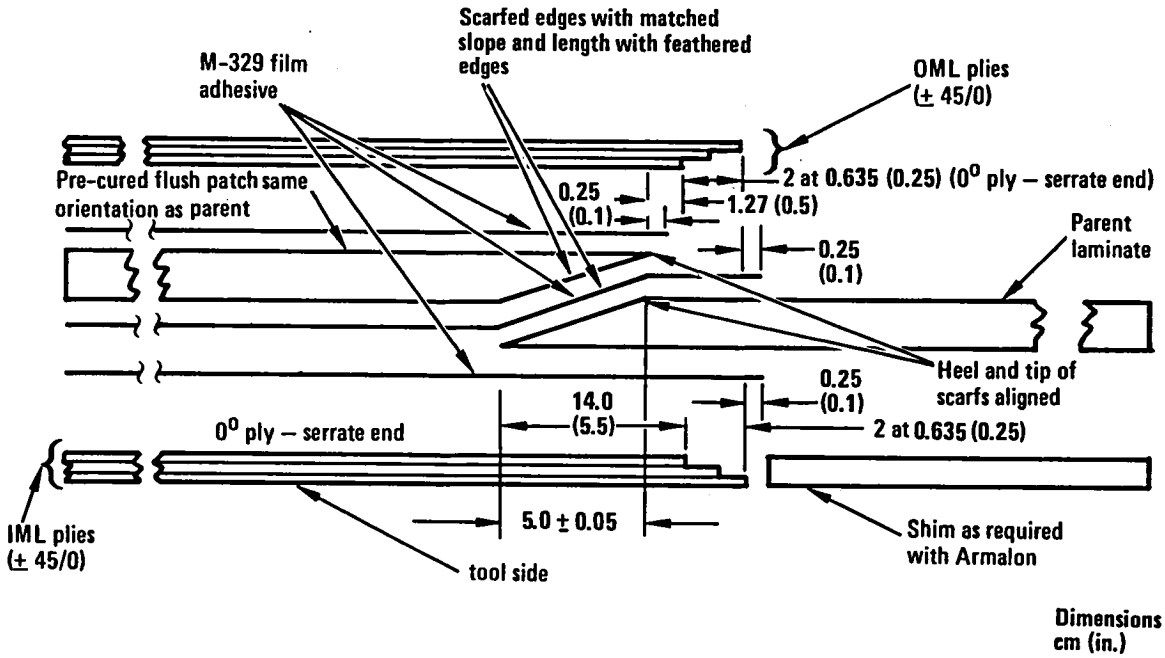

Figure 14. - Flush pre-cured bonded graphite repair - 50 ply laminate (Type II).

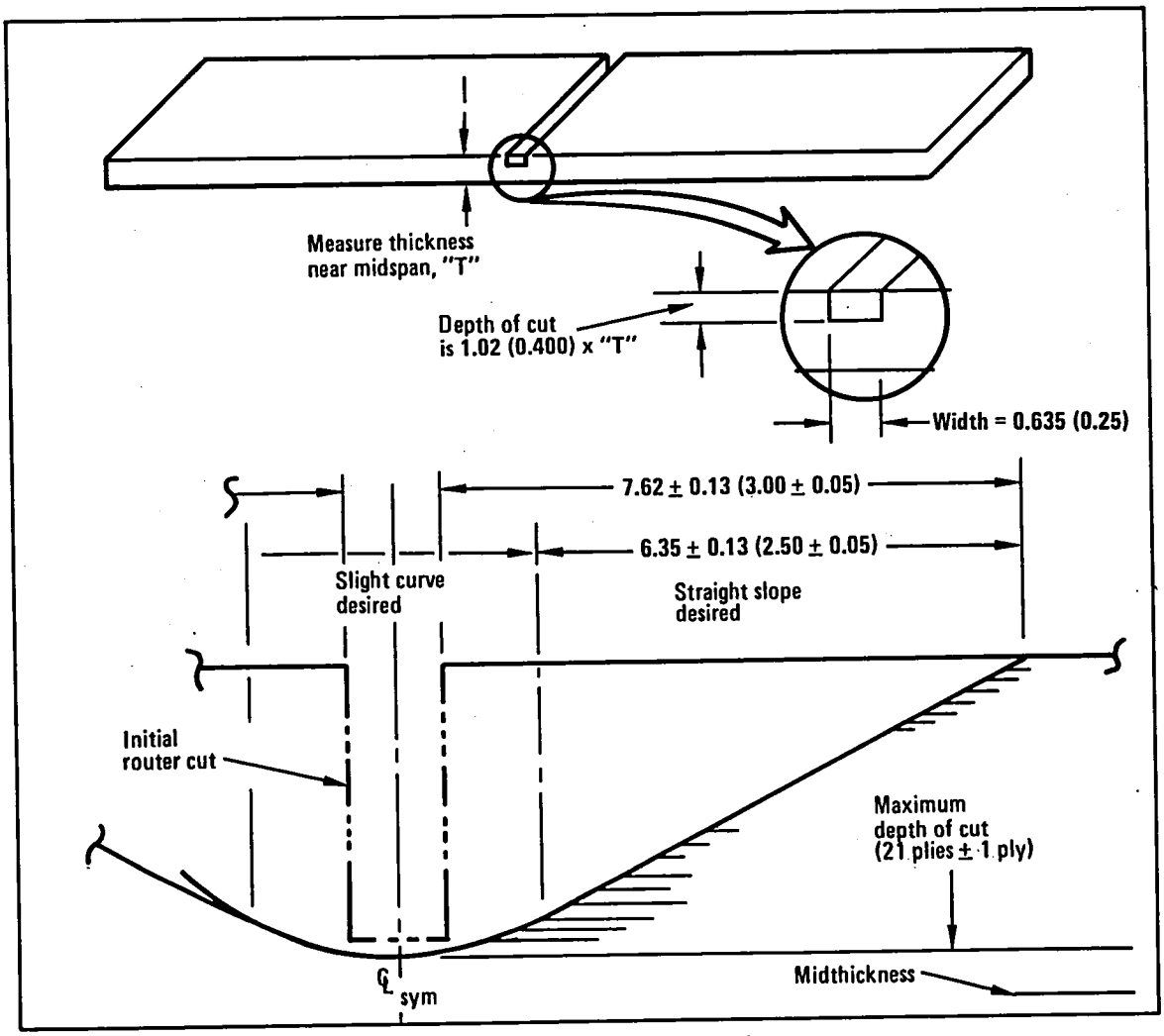

a. Machining and scarf surface preparation

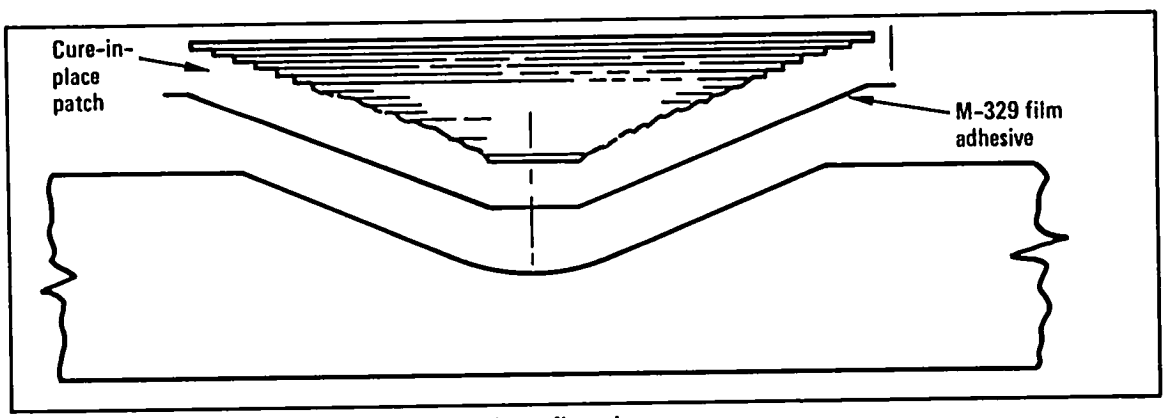

b. Repair ply configuration

Dimensions
cm (in.)

Figure 15. - Flush cure-in-place partial thickness graphite repair - 50 ply laminate (Type IV).

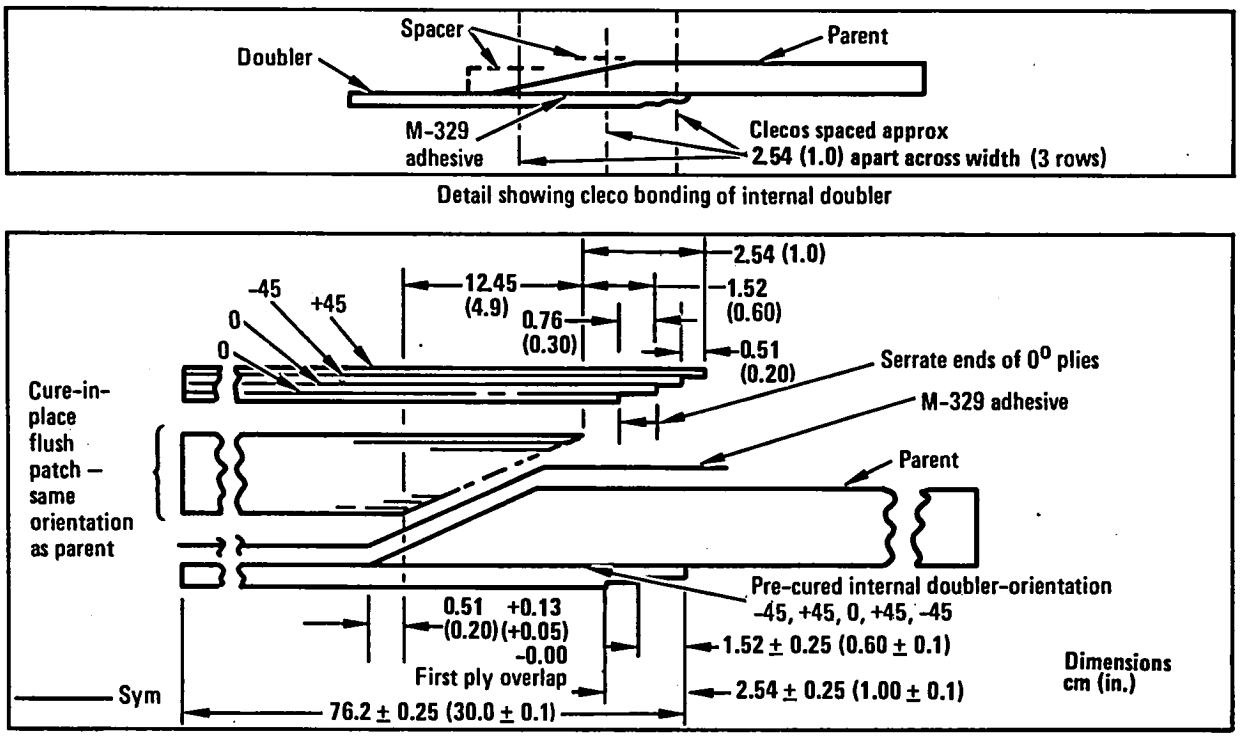

Figure 16. - Flush cure-in-place graphite repair with pre-cured internal doubler 50 ply laminate (Type V).

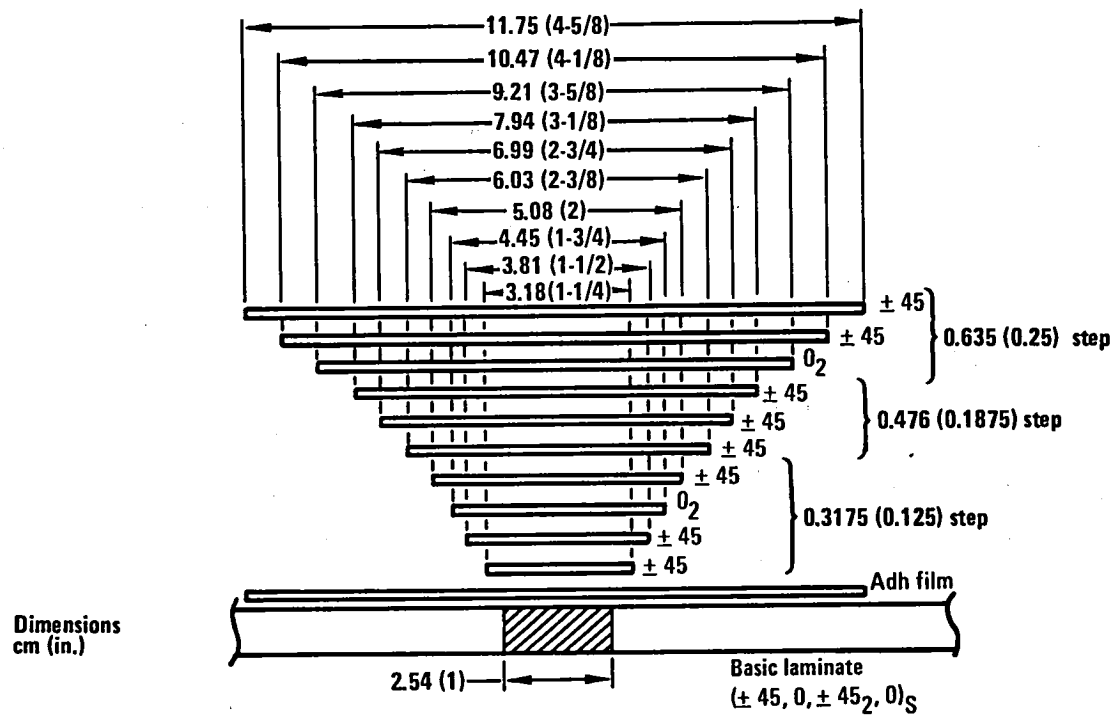

Figure 17. - Patch configuration - specimen VI-T.

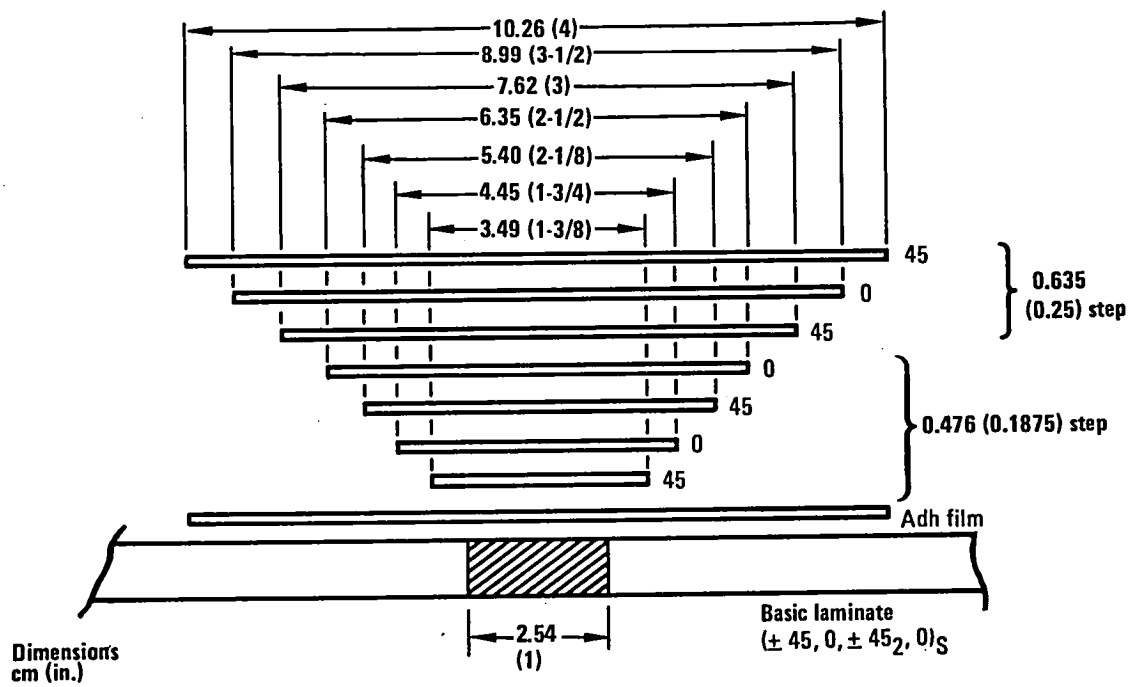

Figure 18. - Patch configuration - specimens VI-F and X.

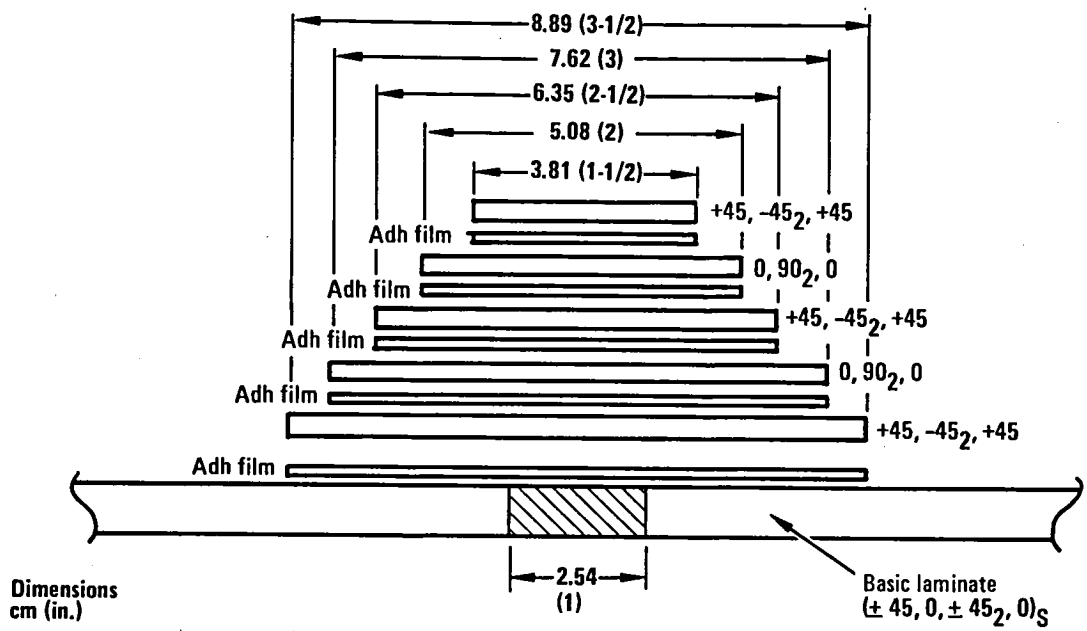

Figure 19. - Patch configurations - specimens VII, IX, and XIV.

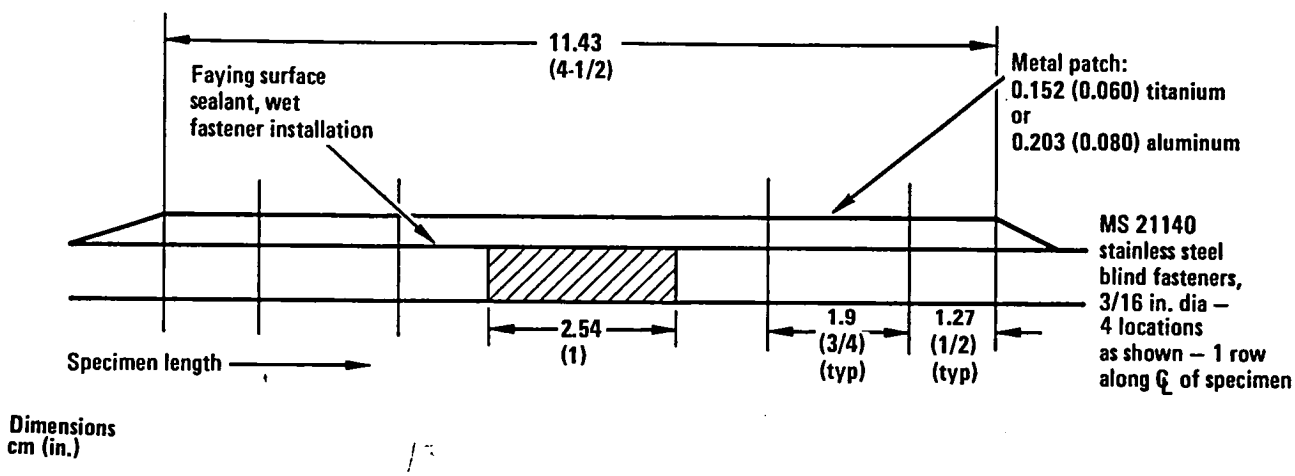

Figure 20. - Patch configuration - specimens XI and XII.

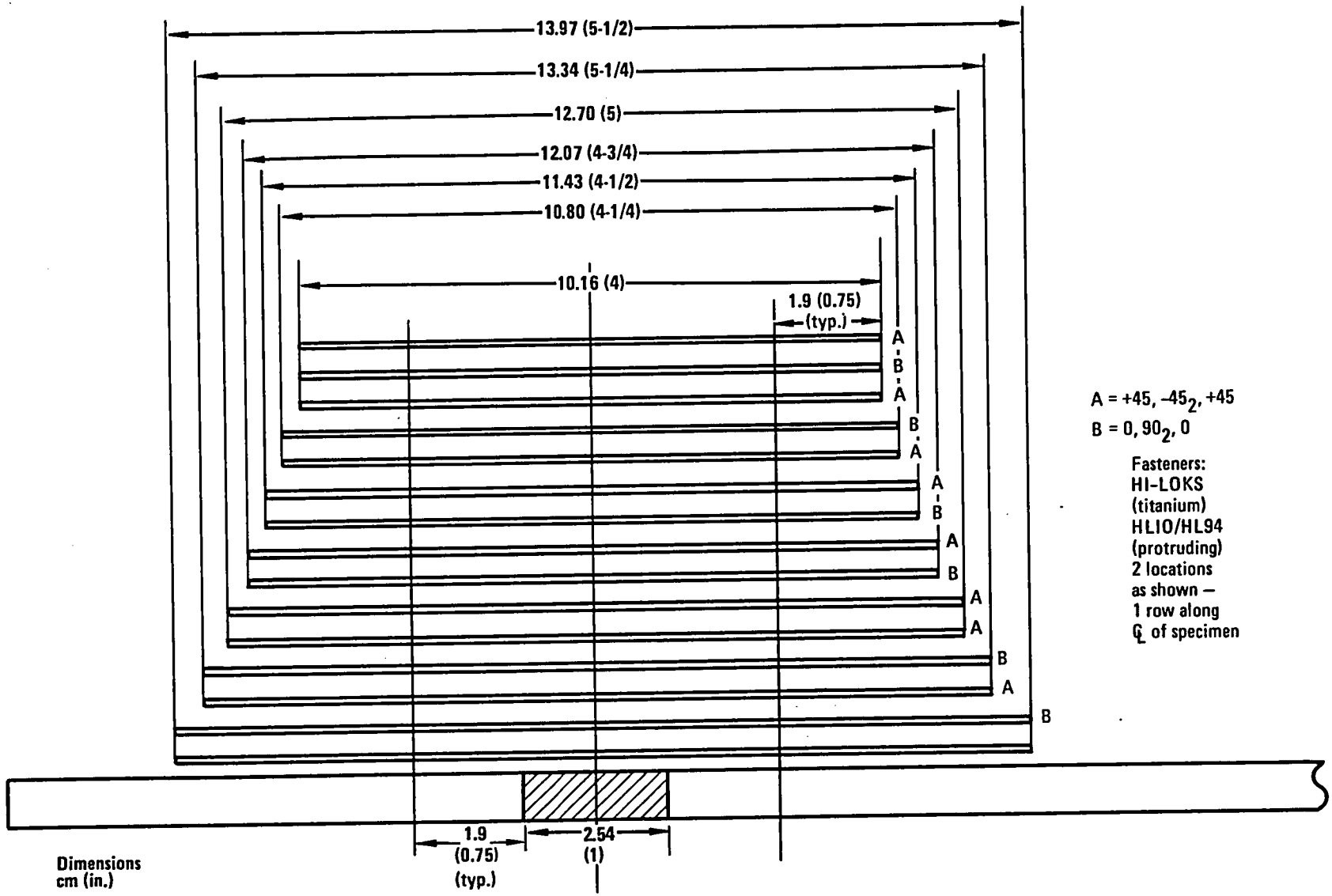

Figure 21. - Patch configuration - specimen VIII.

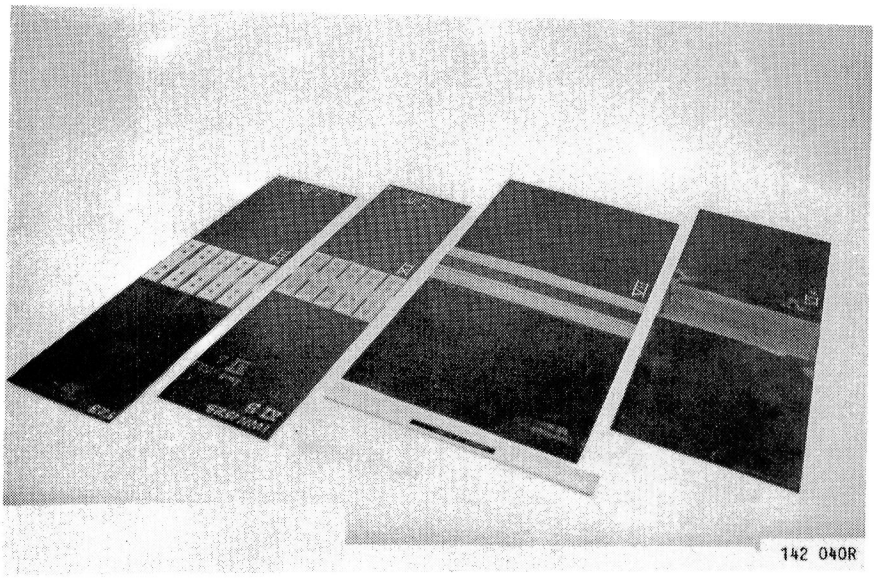

Figure 22. - Repaired parent laminates prior to bonding
To core (Types VI-F, VII, XI, XII).

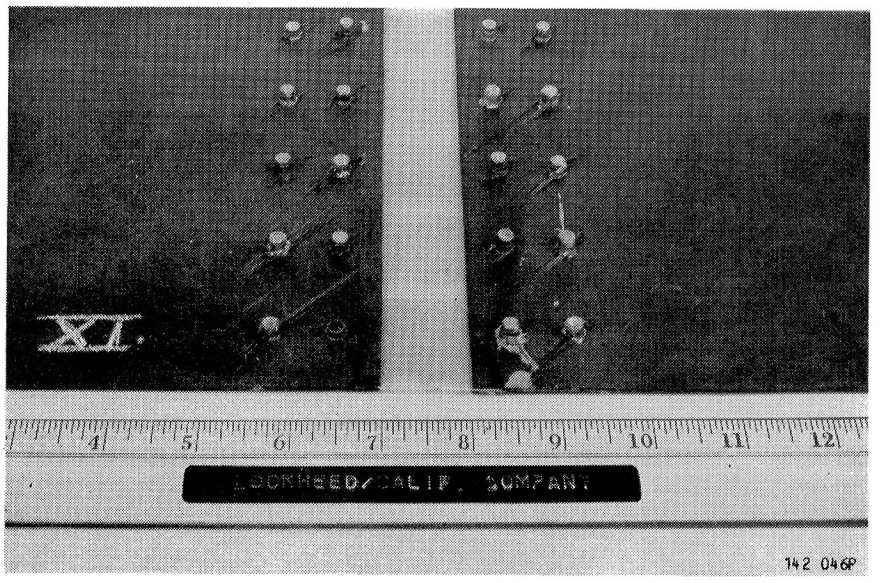

Figure 23. - Back-face of bolted repair (Type XI) showing splitting
from single-side drilling and showing filler.

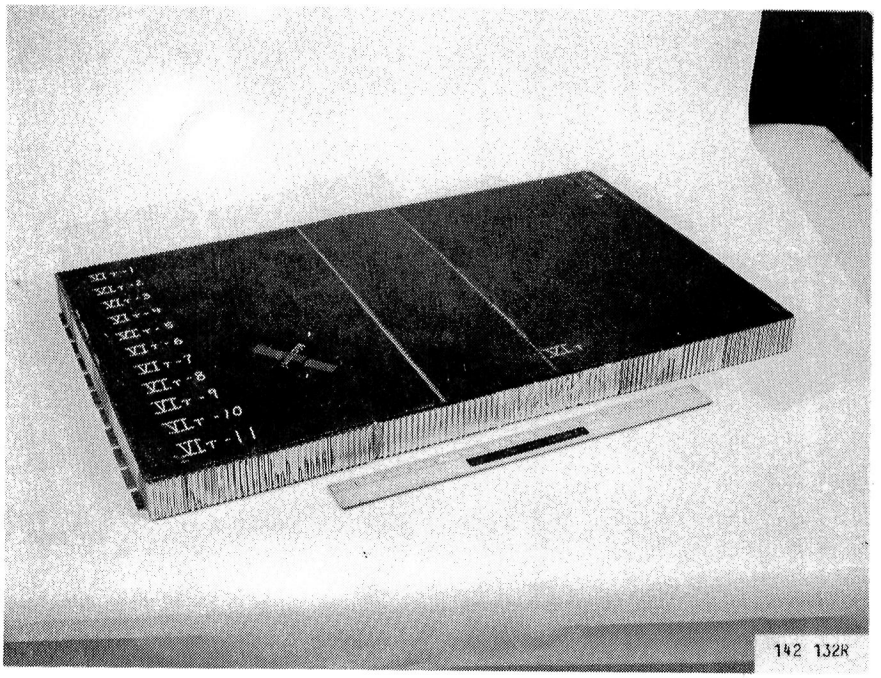

Figure 24. - Sandwich beam specimen with slave skins (type VI-T).

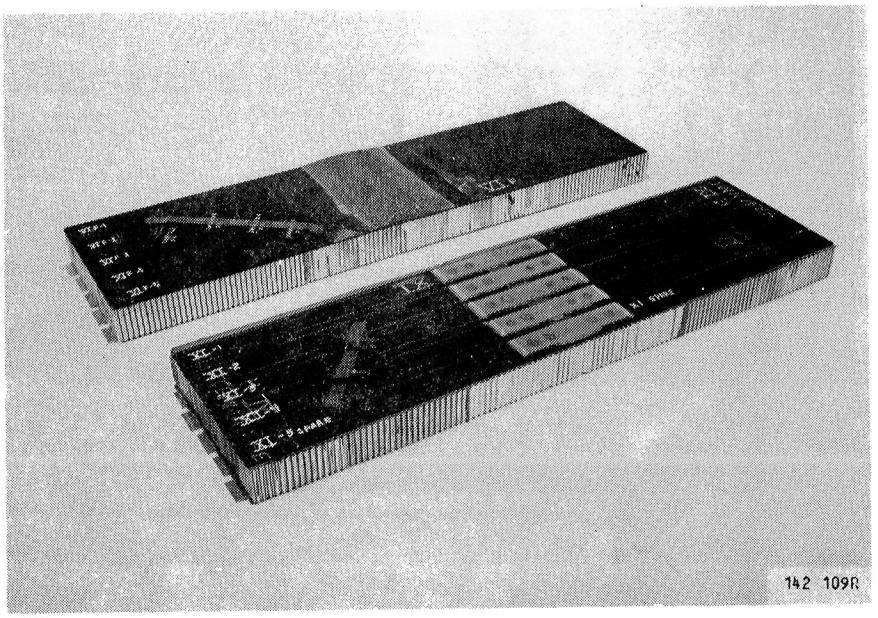

Figure 25. - Sandwich beam specimens with Slave skins (types VI-F, XI)

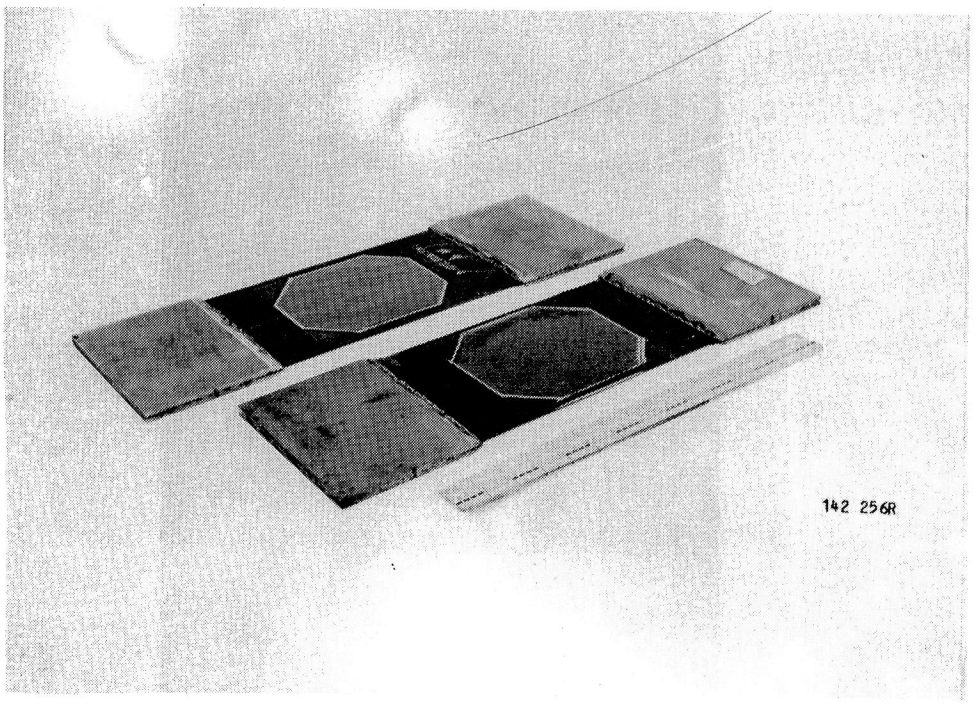

Figure 26. - Tabbed laminate specimen with Repair patch (type XIV).

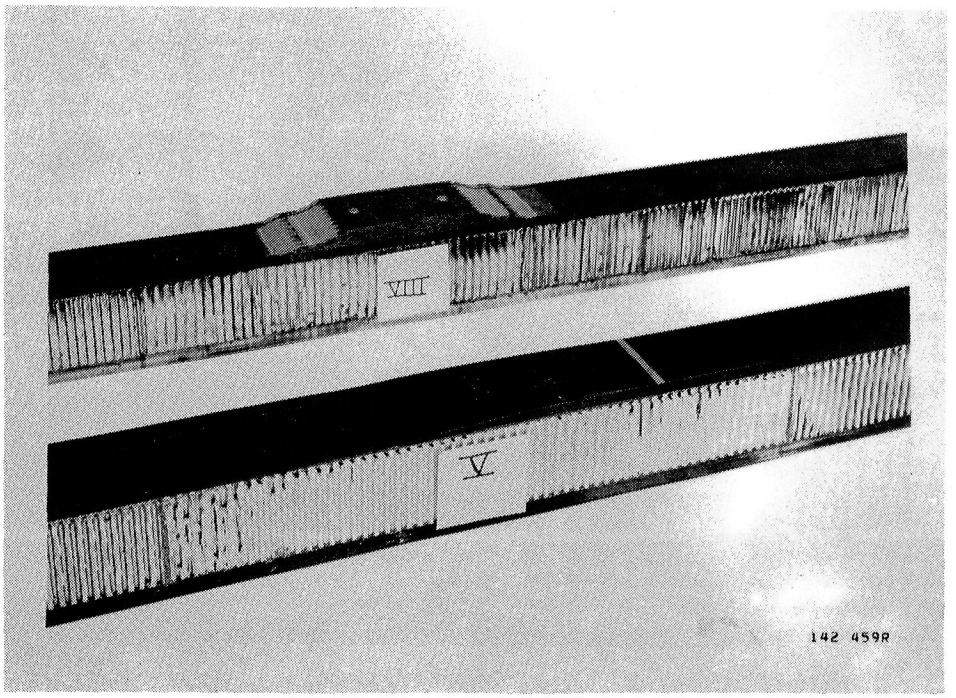

Figure 27. - Individual sandwich beam specimens With repair patches.

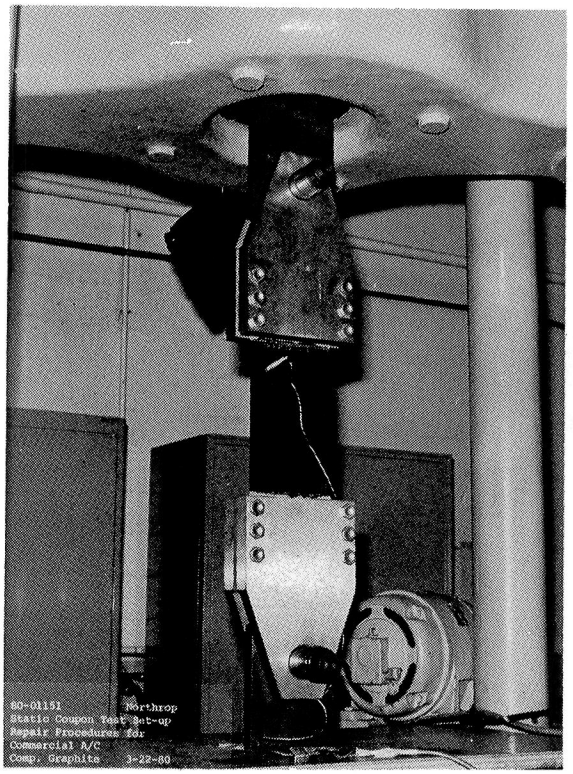

Figure 28. - Test set-up for tabbed laminate specimen.

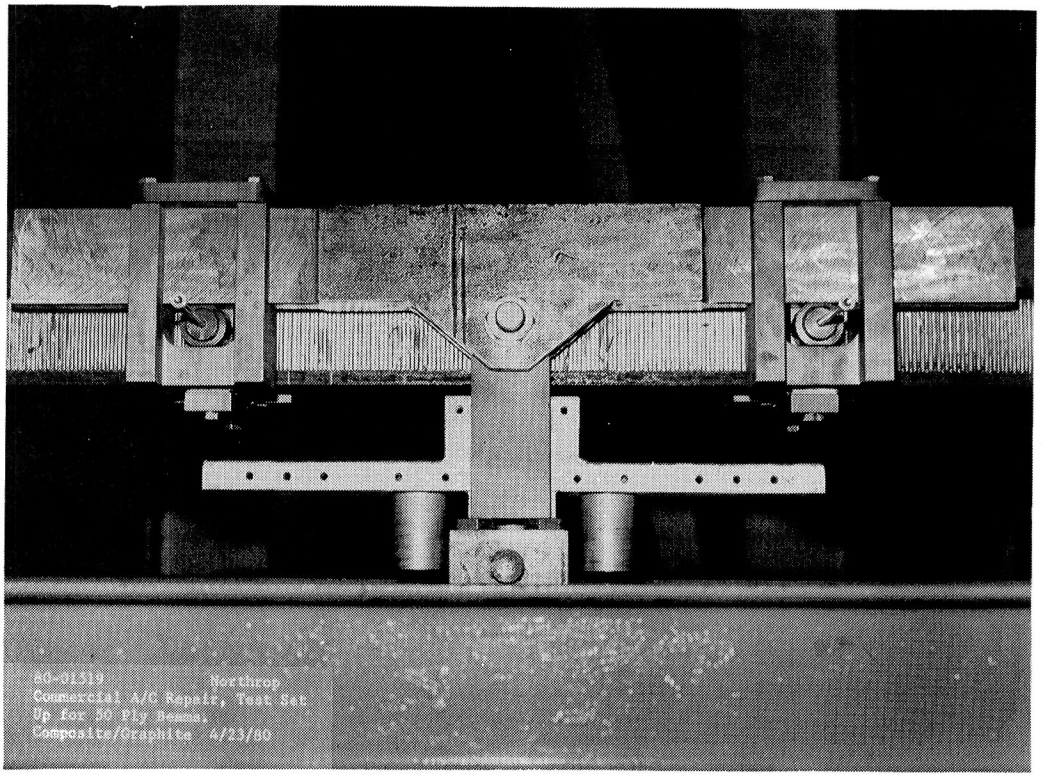

Figure 29. - Test set-up for sandwich beam specimen.

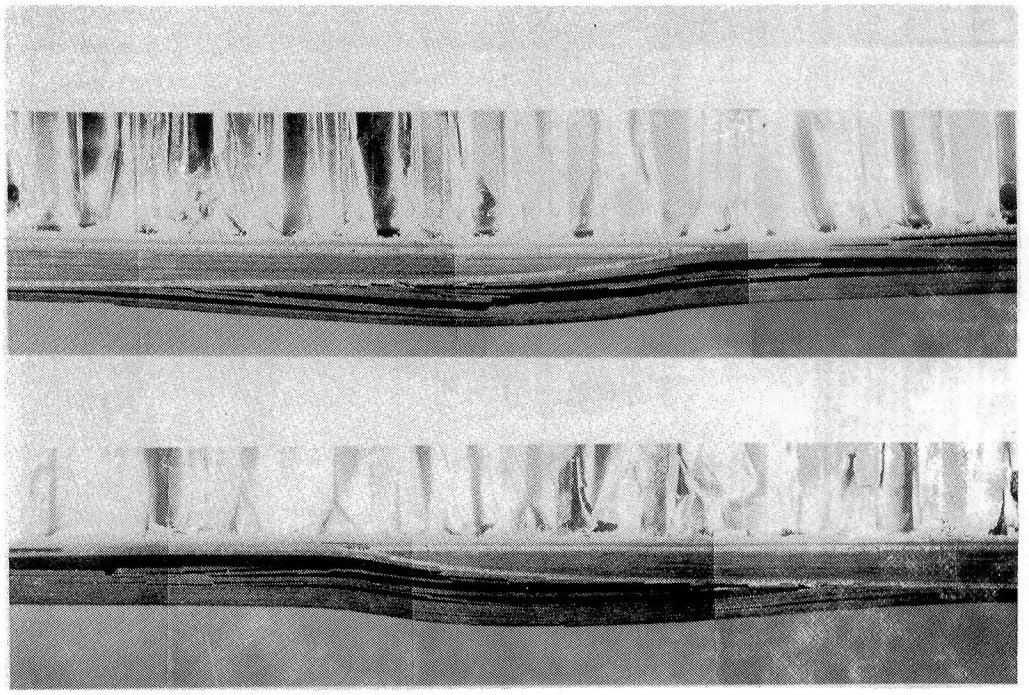

Figure 30. - Type I specimen after test showing poorly machined scarf taper.

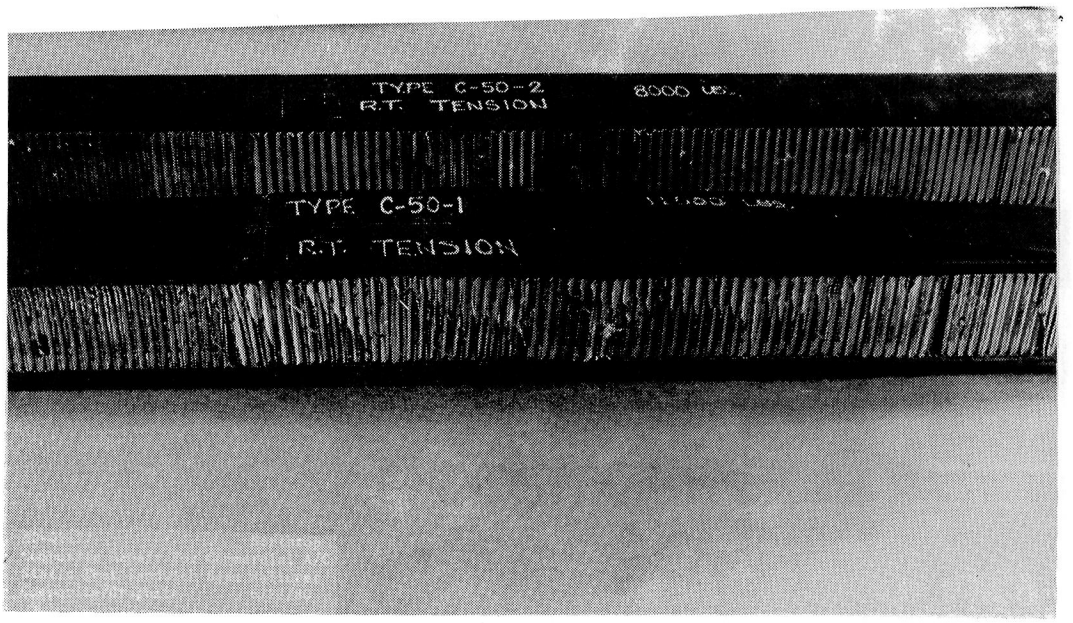

Figure 31. - Type C-50 specimens after testing.

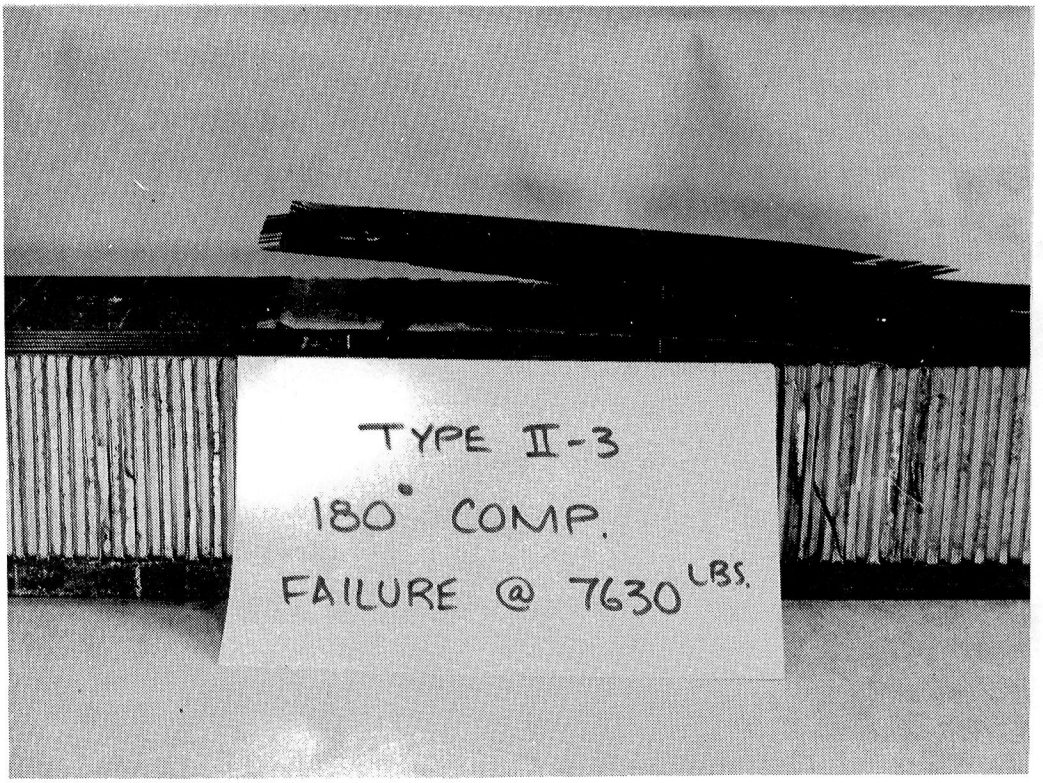

Figure 32. - Type II specimens after testing.

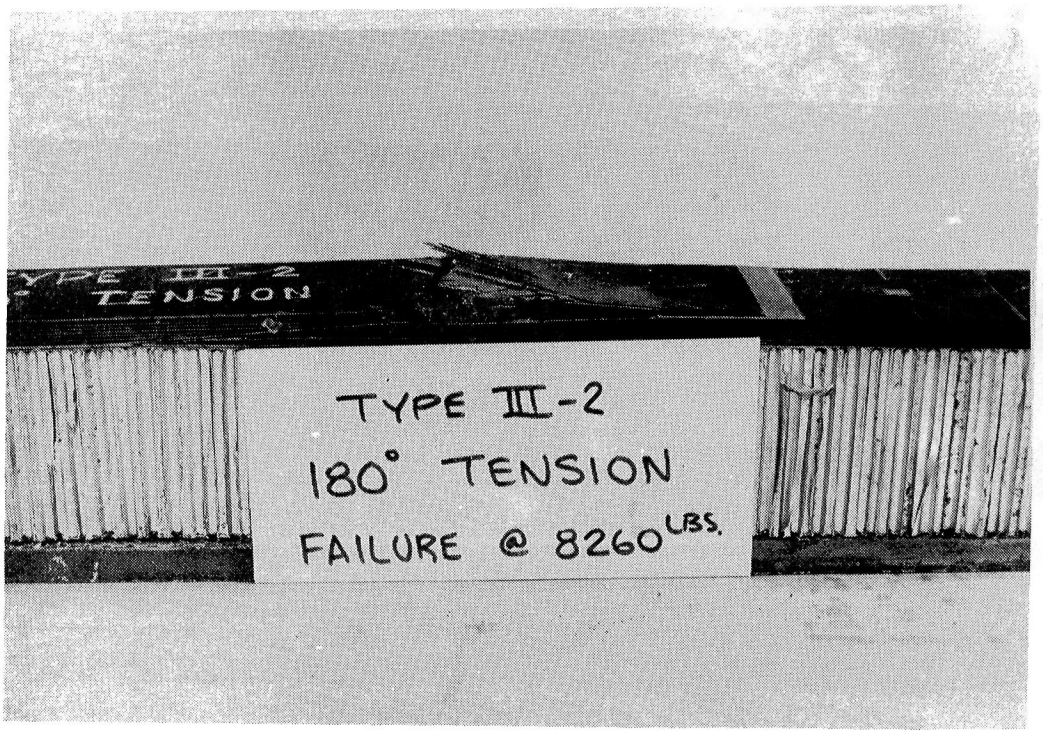

Figure 33. - Type III specimens after testing.

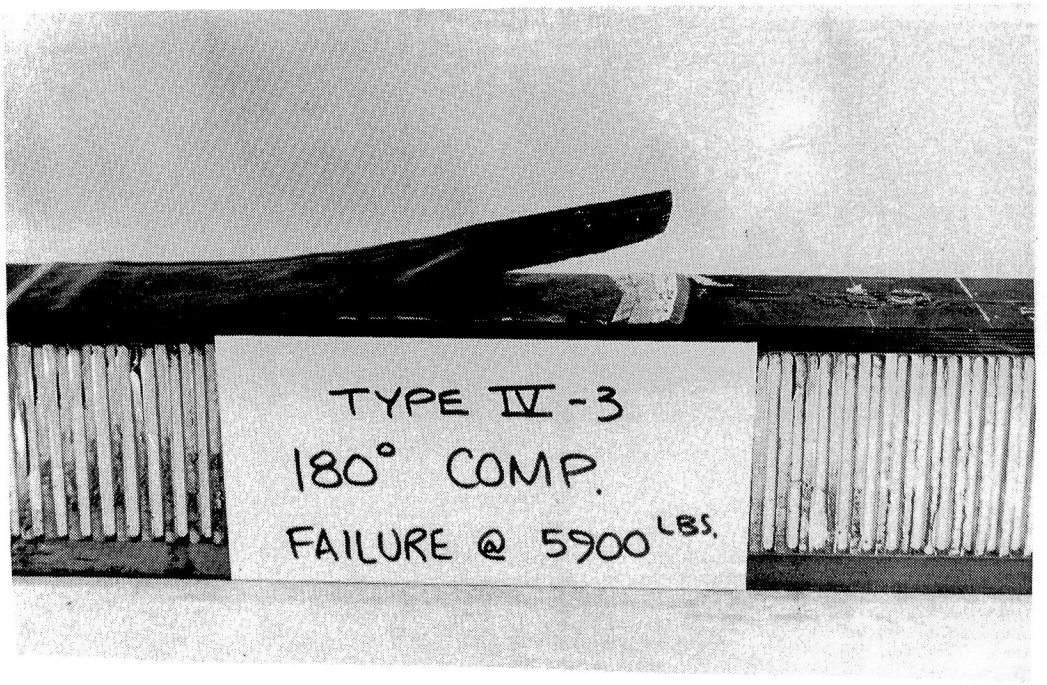

Figure 34. - Type IV specimens after testing.

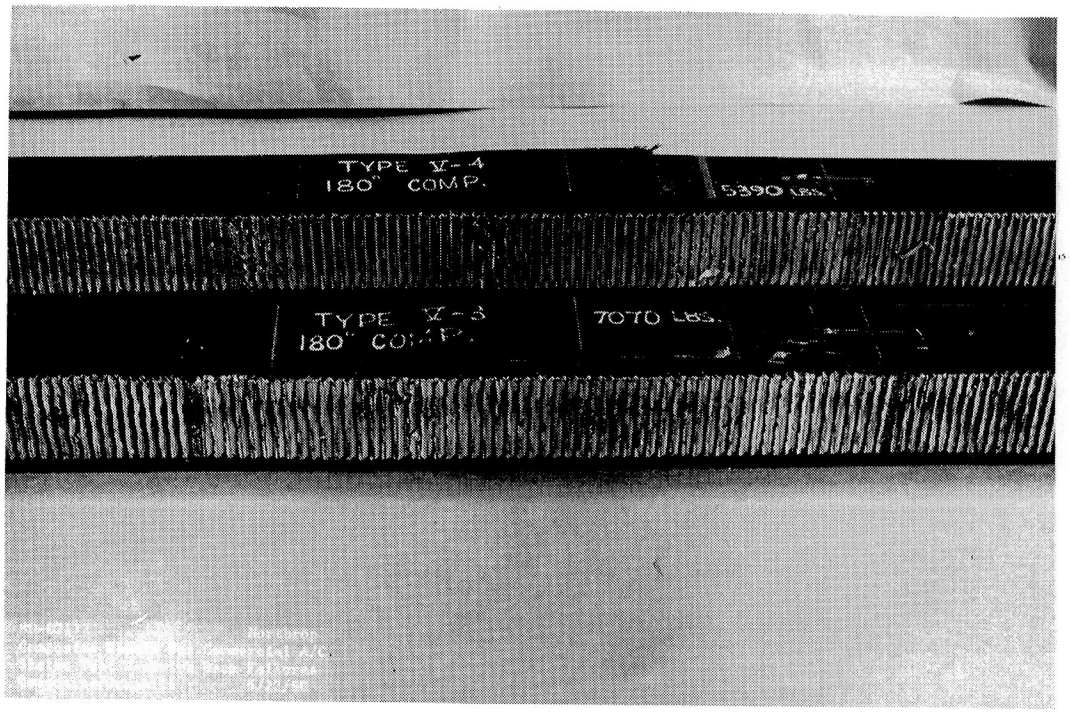

Figure 35. - Type V specimens after testing.

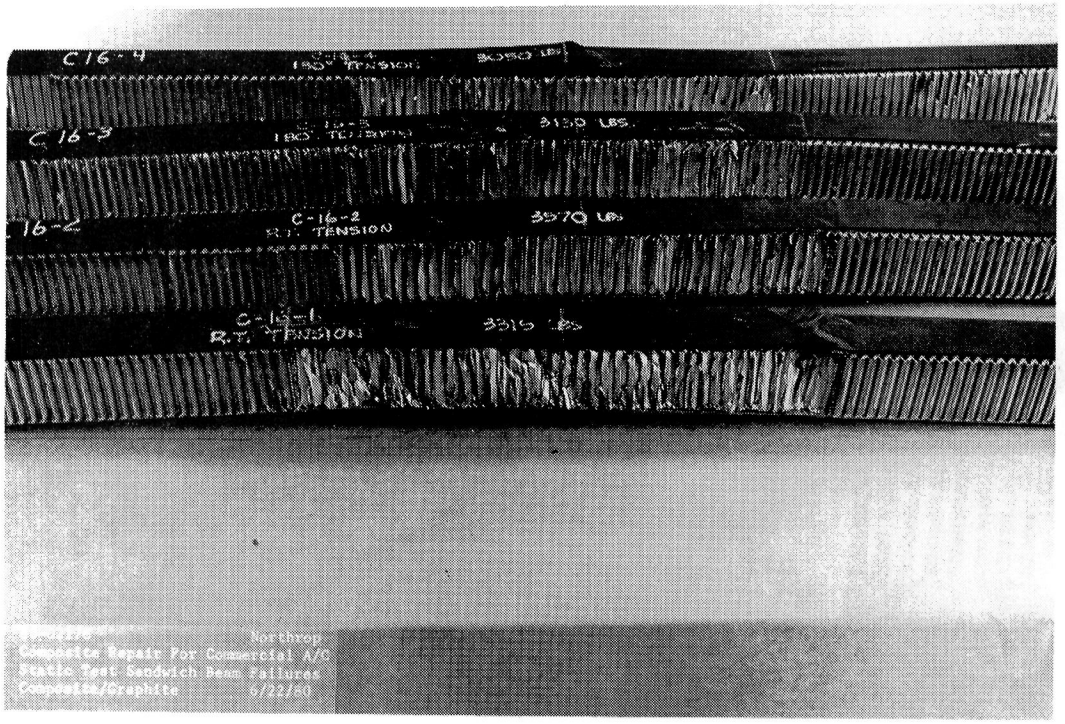

Figure 36. - Types C-16 specimens after testing.

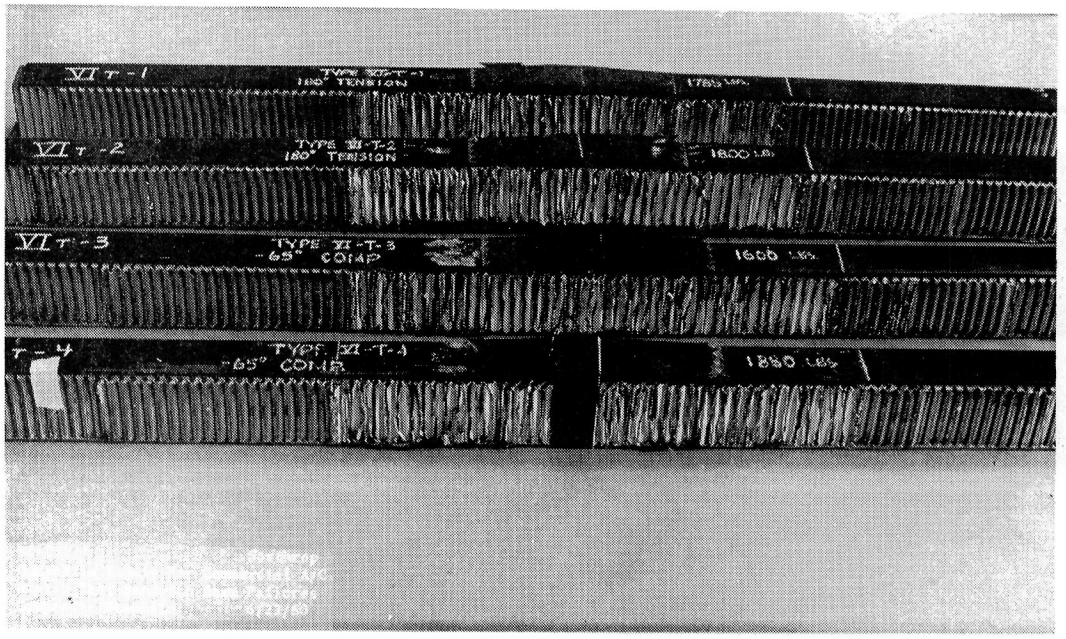

Figure 37. - Type VI-T specimens after testing.

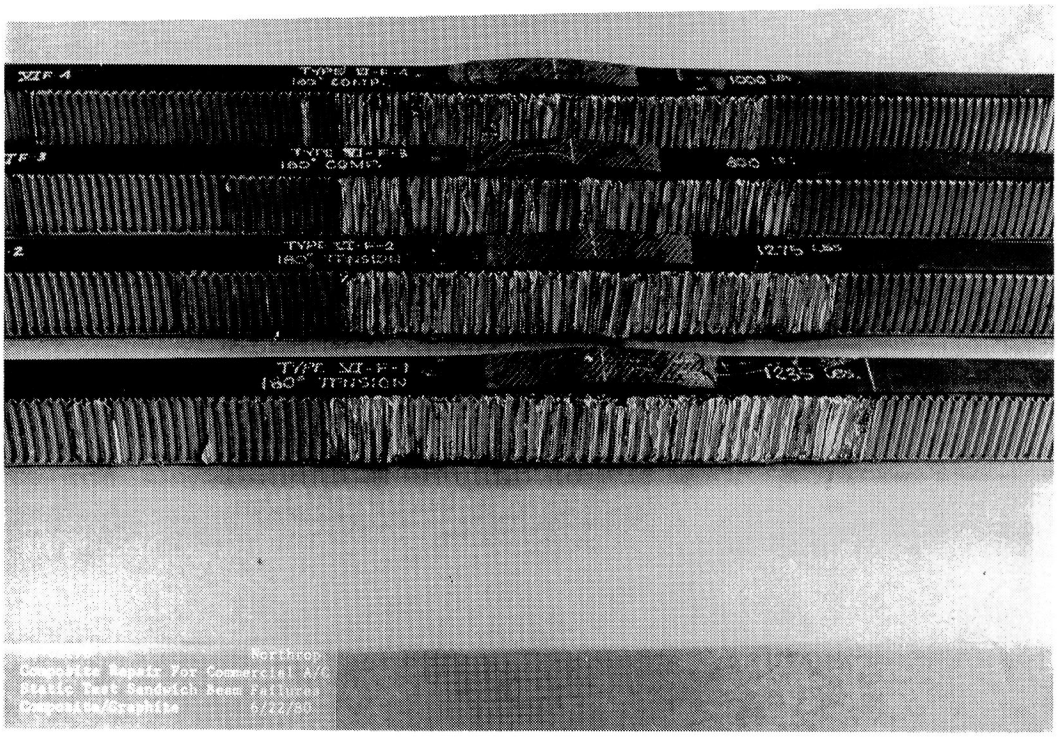

Figure 38. - Type VI-F specimens after testing.

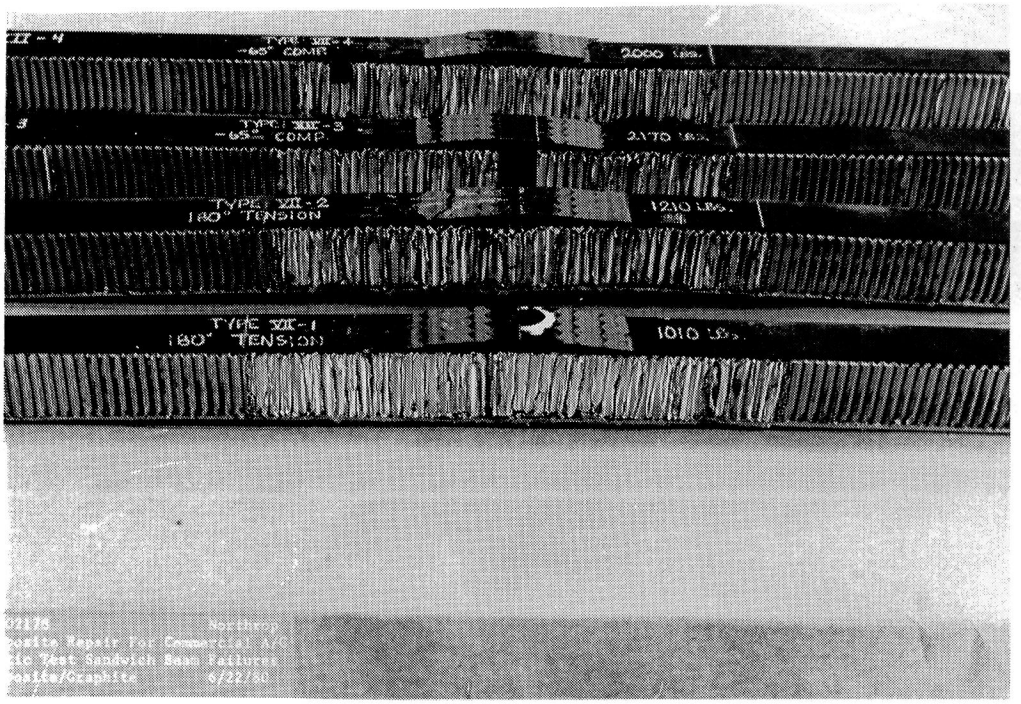

Figure 39. - Type VII specimens after testing.

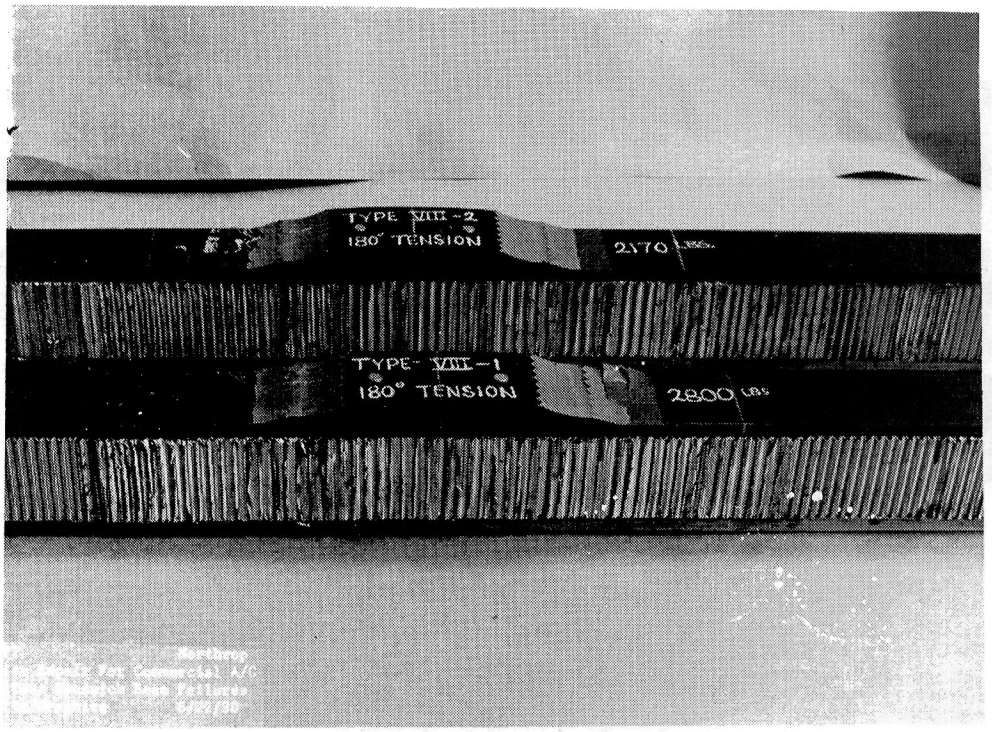

Figure 40. - Type VIII specimens after testing.

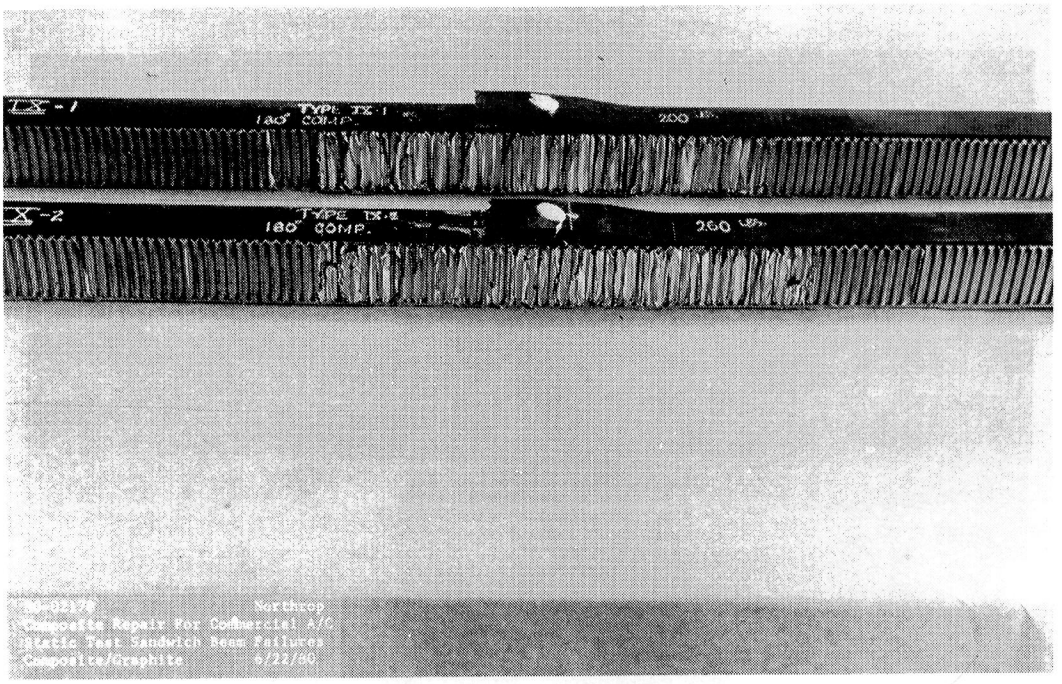

Figure 41. - Type IX specimens after testing.

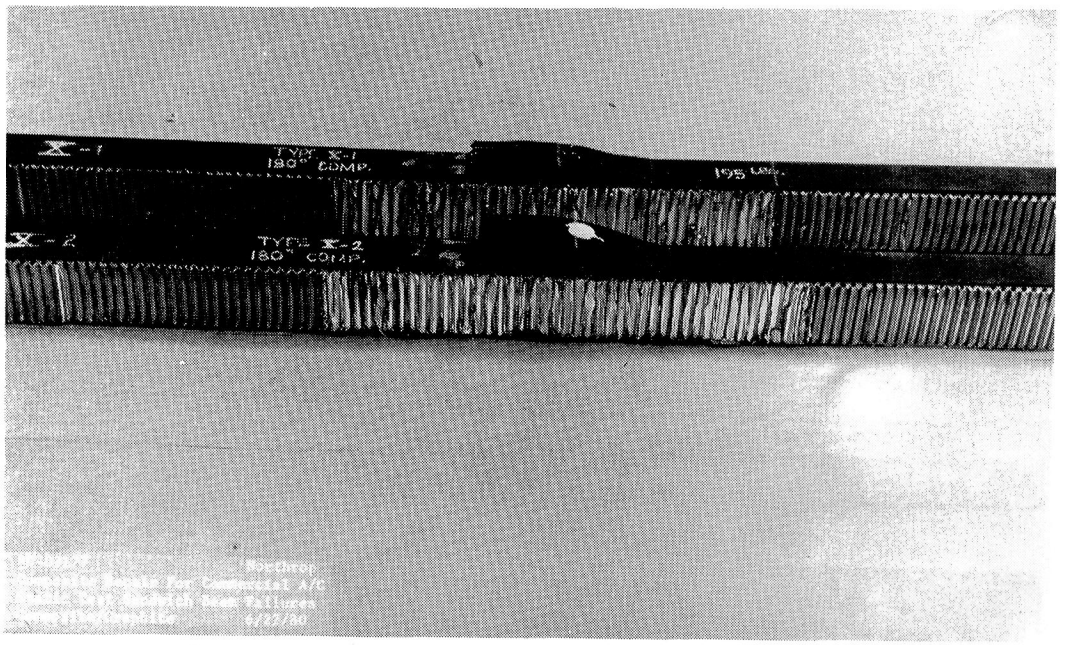

Figure 42. - Type X specimens after testing.

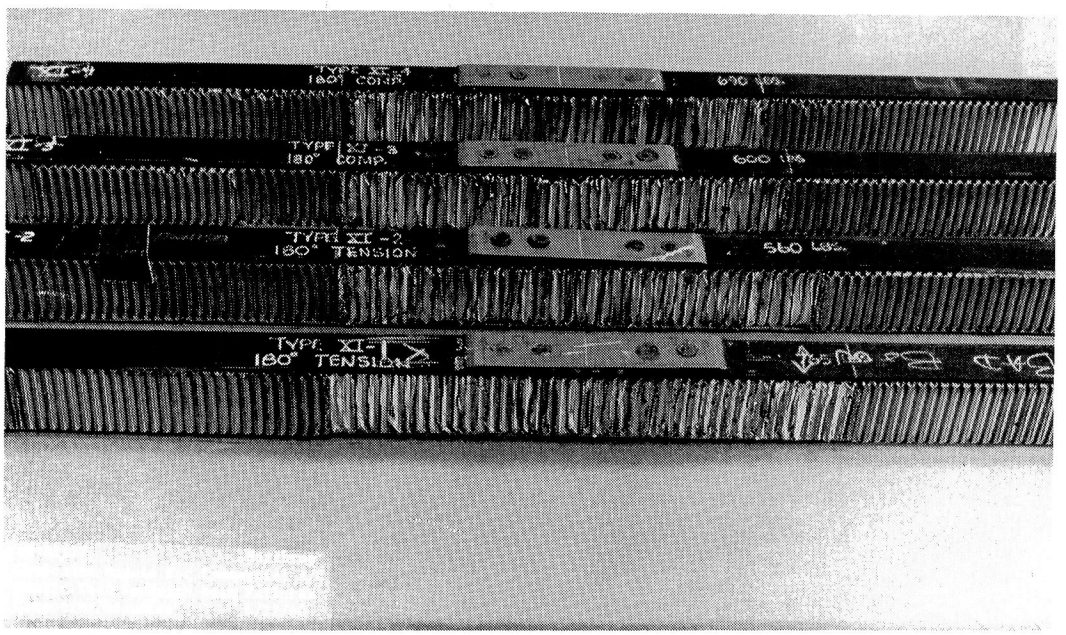

Figure 43. - Type XI specimens after testing.

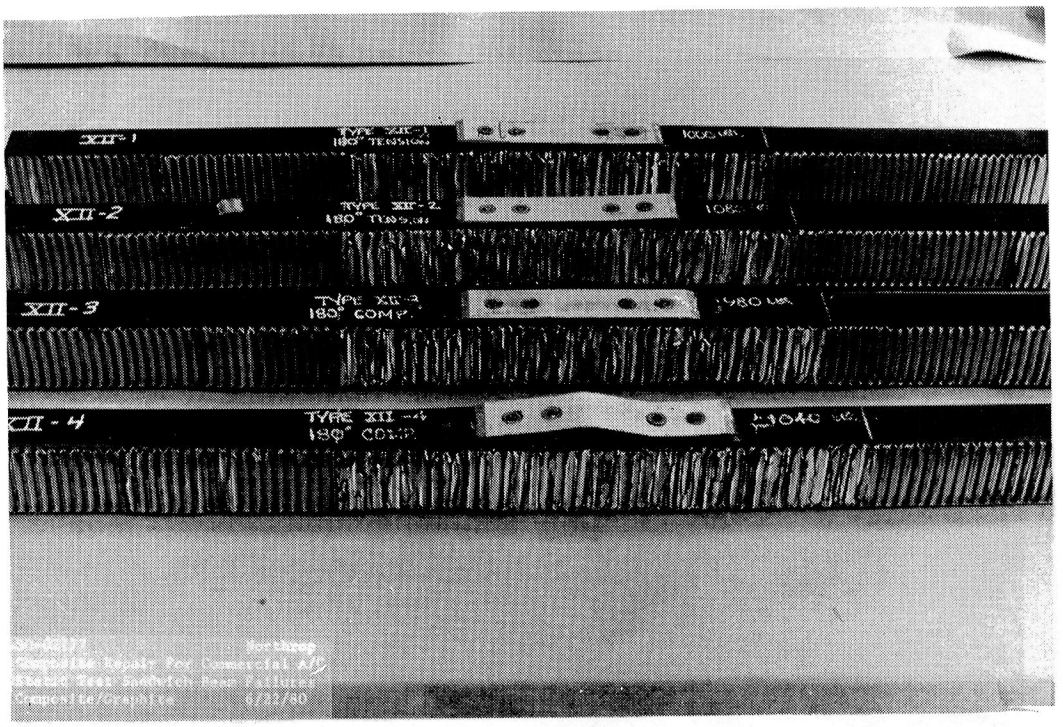

Figure 44. - Type XII specimen after testing.

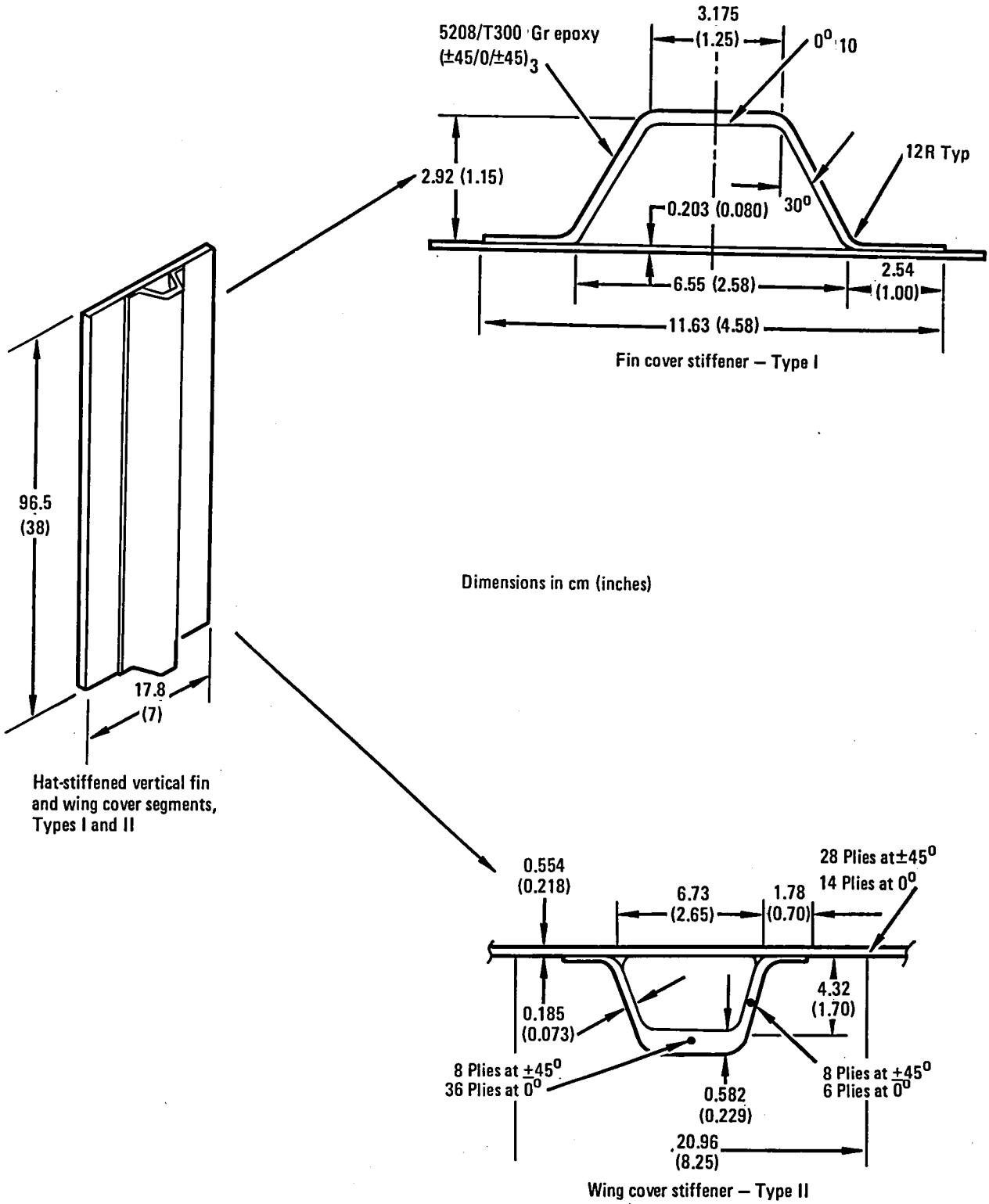

Figure 45. - Structural element configurations - hat-stiffened vertical fin and wing covers.

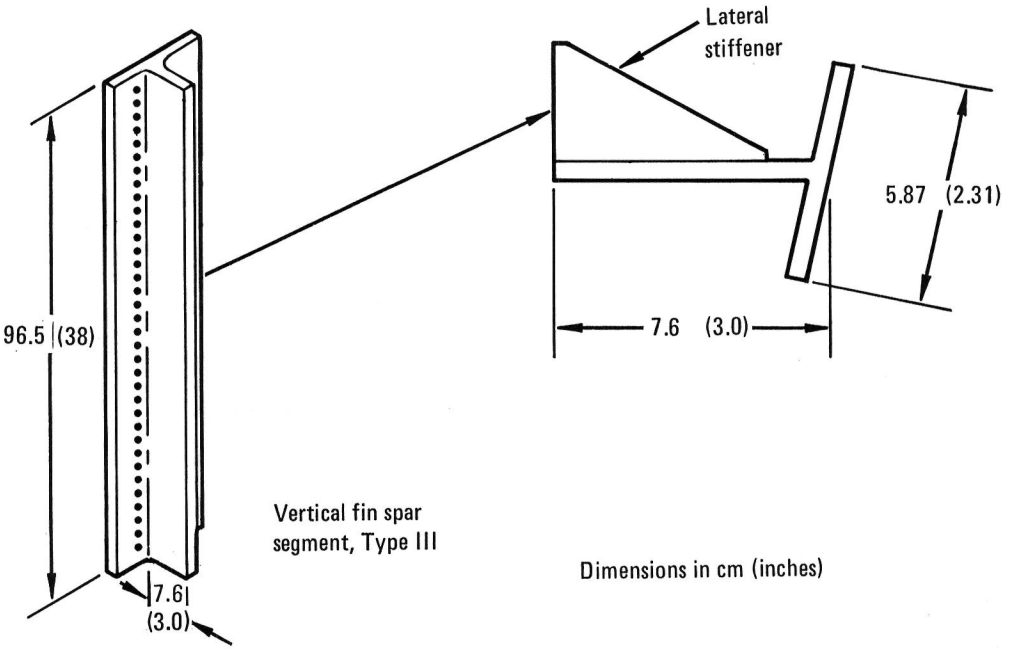

Figure 46. - Structural element configuration - vertical fin spar.

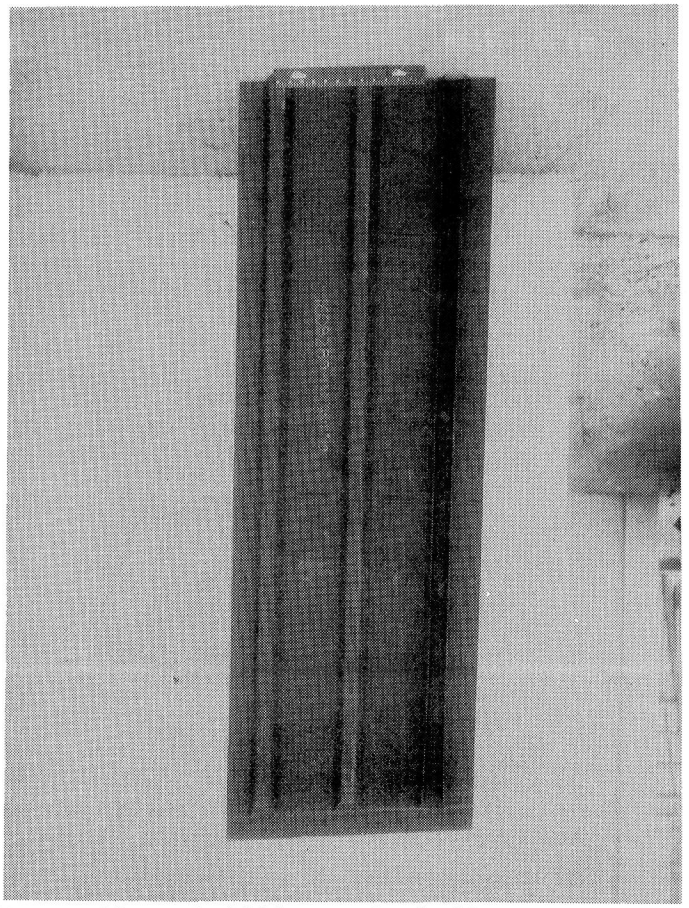

Figure 47. - L-1011 vertical fin curve segment.

Figure 48. - L-1011 vertical fin spar test segment.

Figure 49. - Hat stiffened wing cover panel.

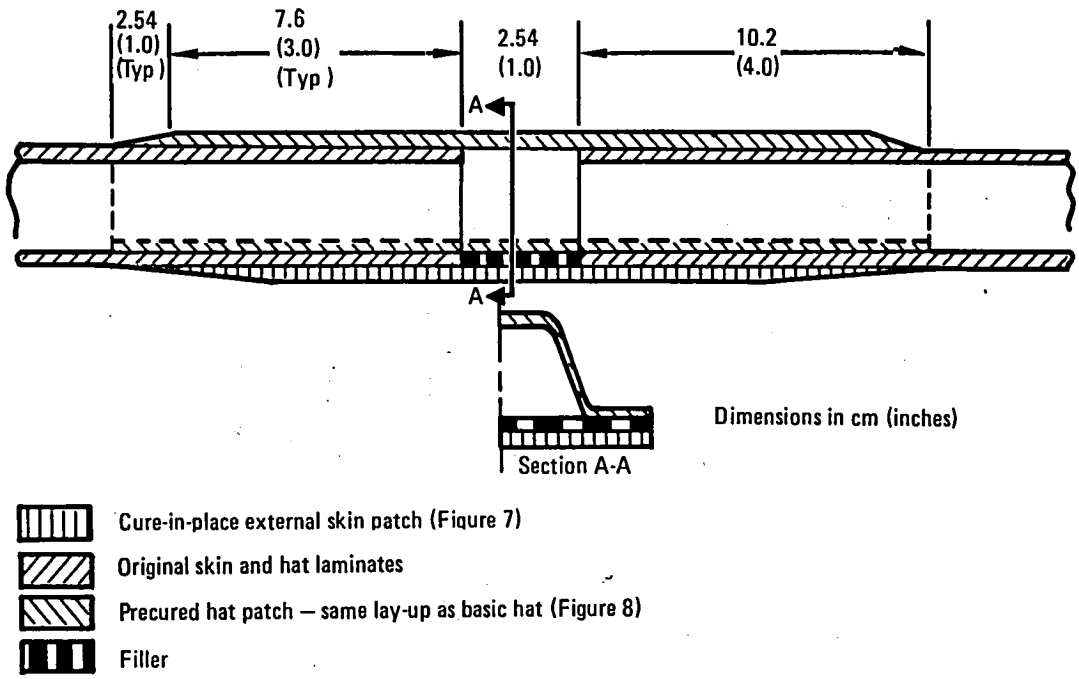

Figure 50. - Repair configuration - Type I fin cover.

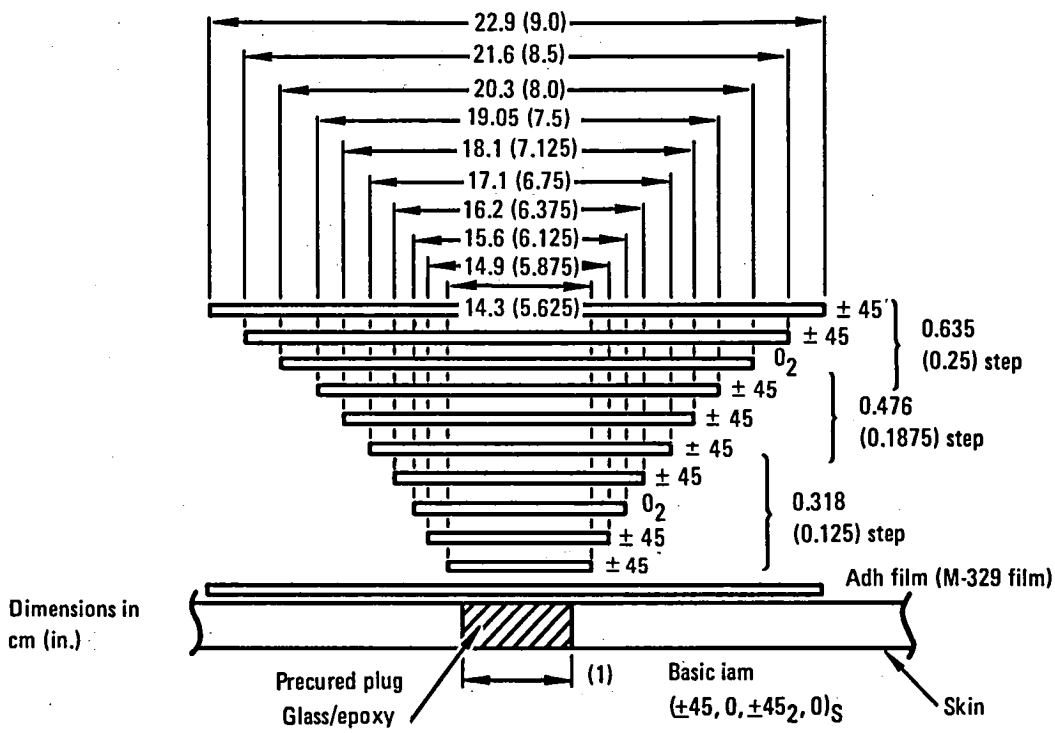

Figure 51. - Skin patch lay-up.

PATCH ORIENTATIONS	
+45	+45
-45	-45
0	0
-45	-45
+45	+45
+45	0_5
-45	0_5
0	+45
-45	-45
+45	0
	-45
	+45
B-B	C-C

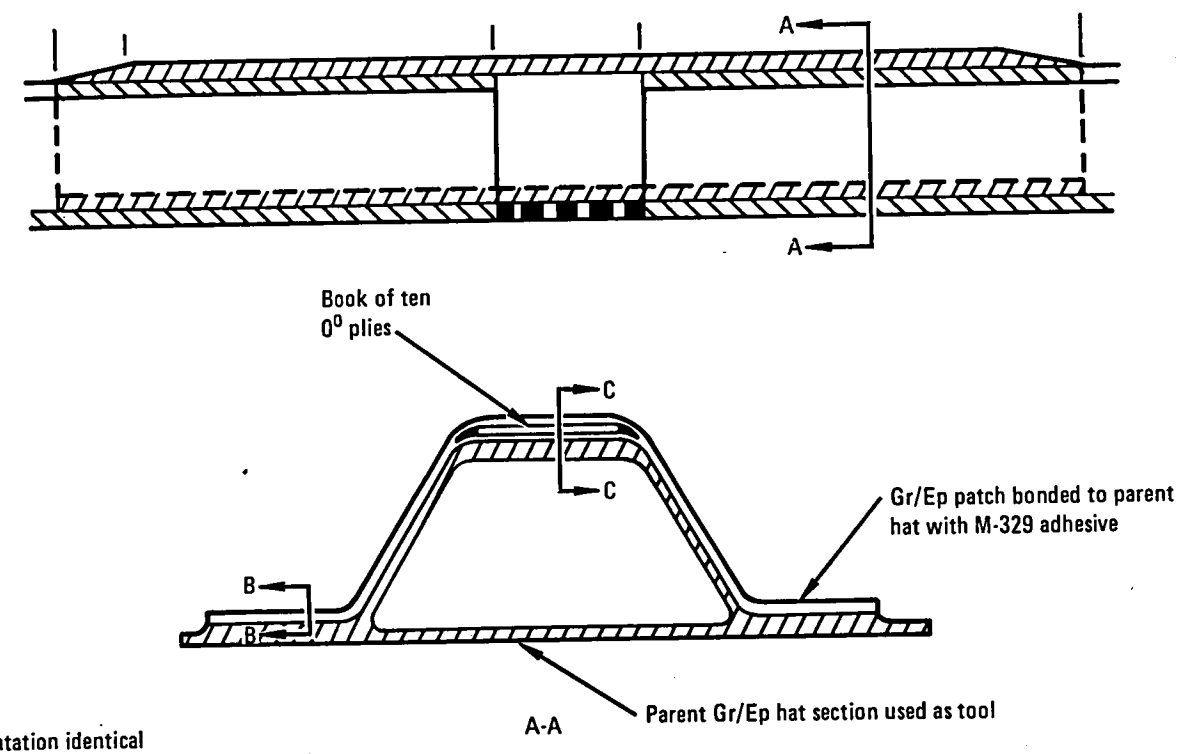

Note: Patch orientation identical to parent hat

Figure 52. - Fin cover repair configuration showing tool and patch ply orientation.

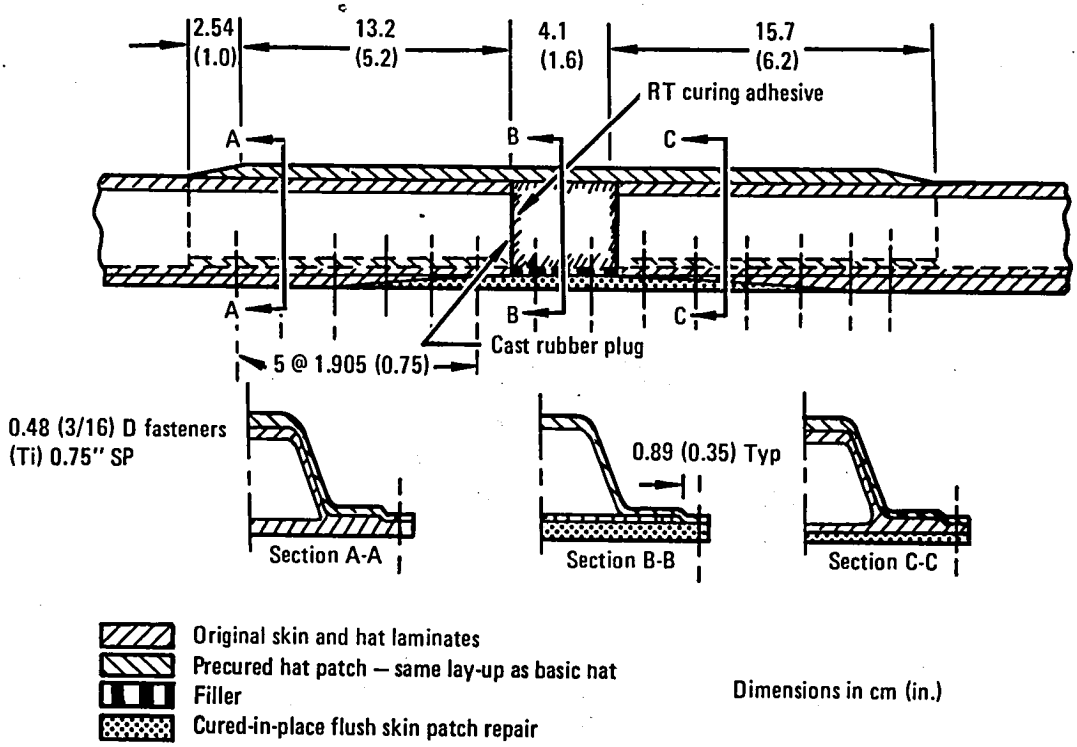

Figure 53. - Hat-section repair assembly - Type II wing cover.

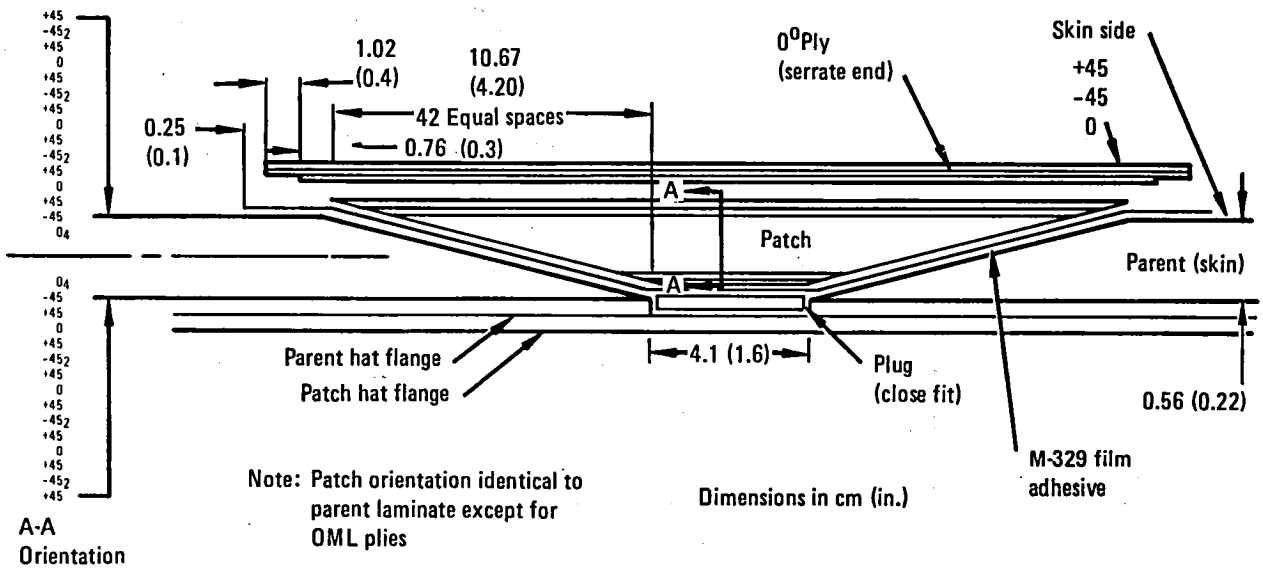

Figure 54. - Flush patch repair of skin - Type II wing cover.

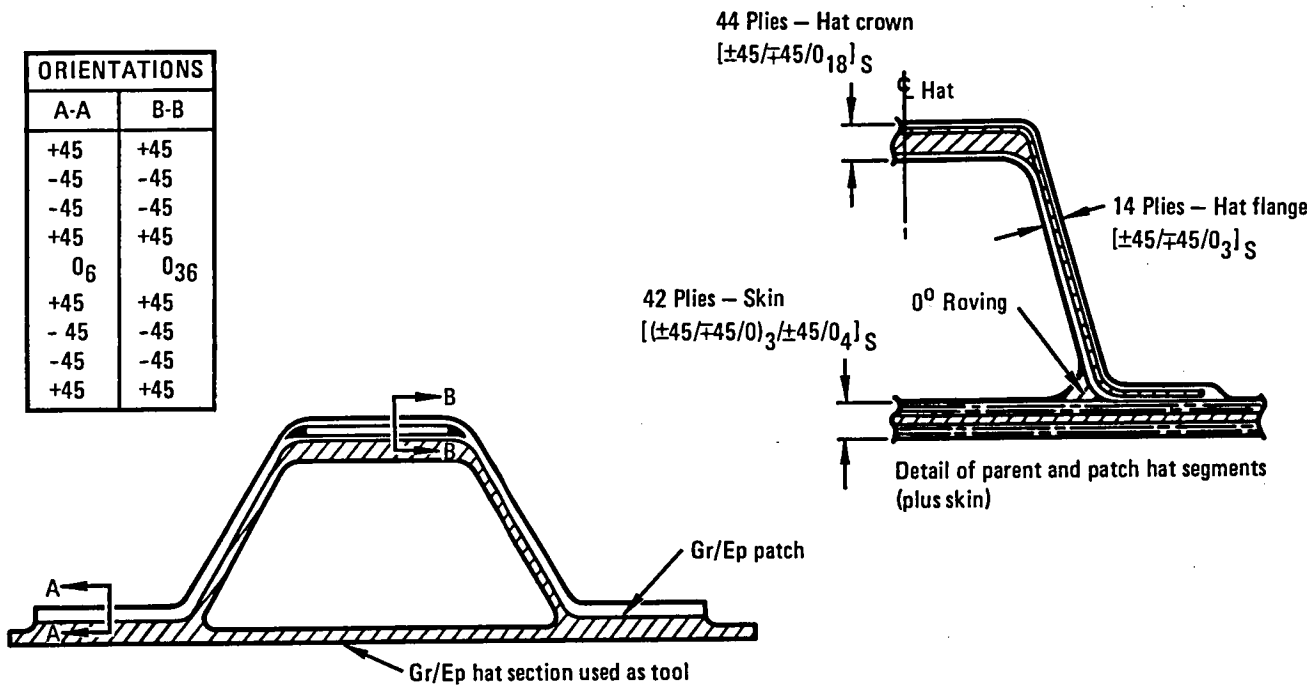

Figure 55. - Configuration of precured hat-section splice - Type II wing cover.

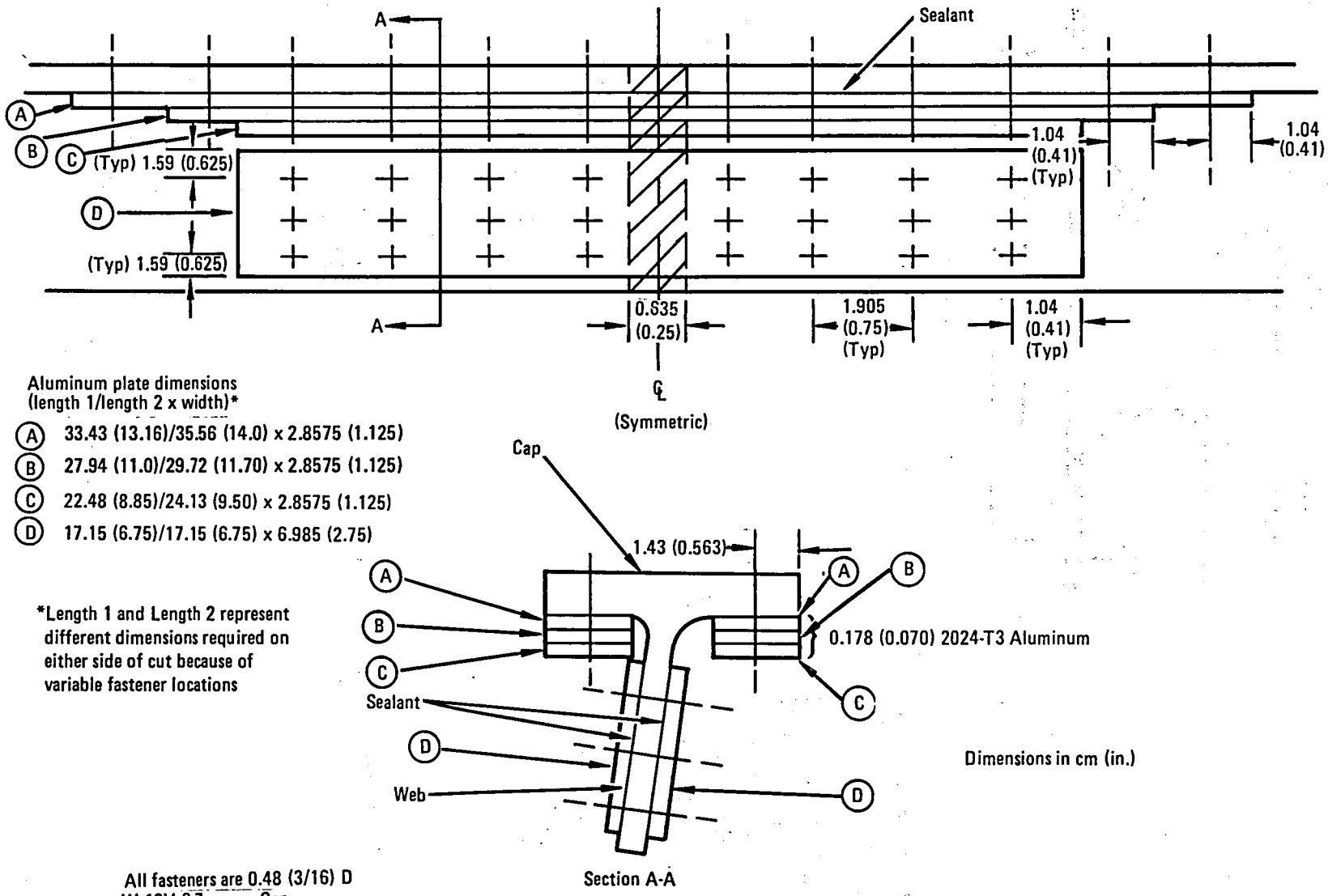

Figure 56. - Spar cap repair configuration.

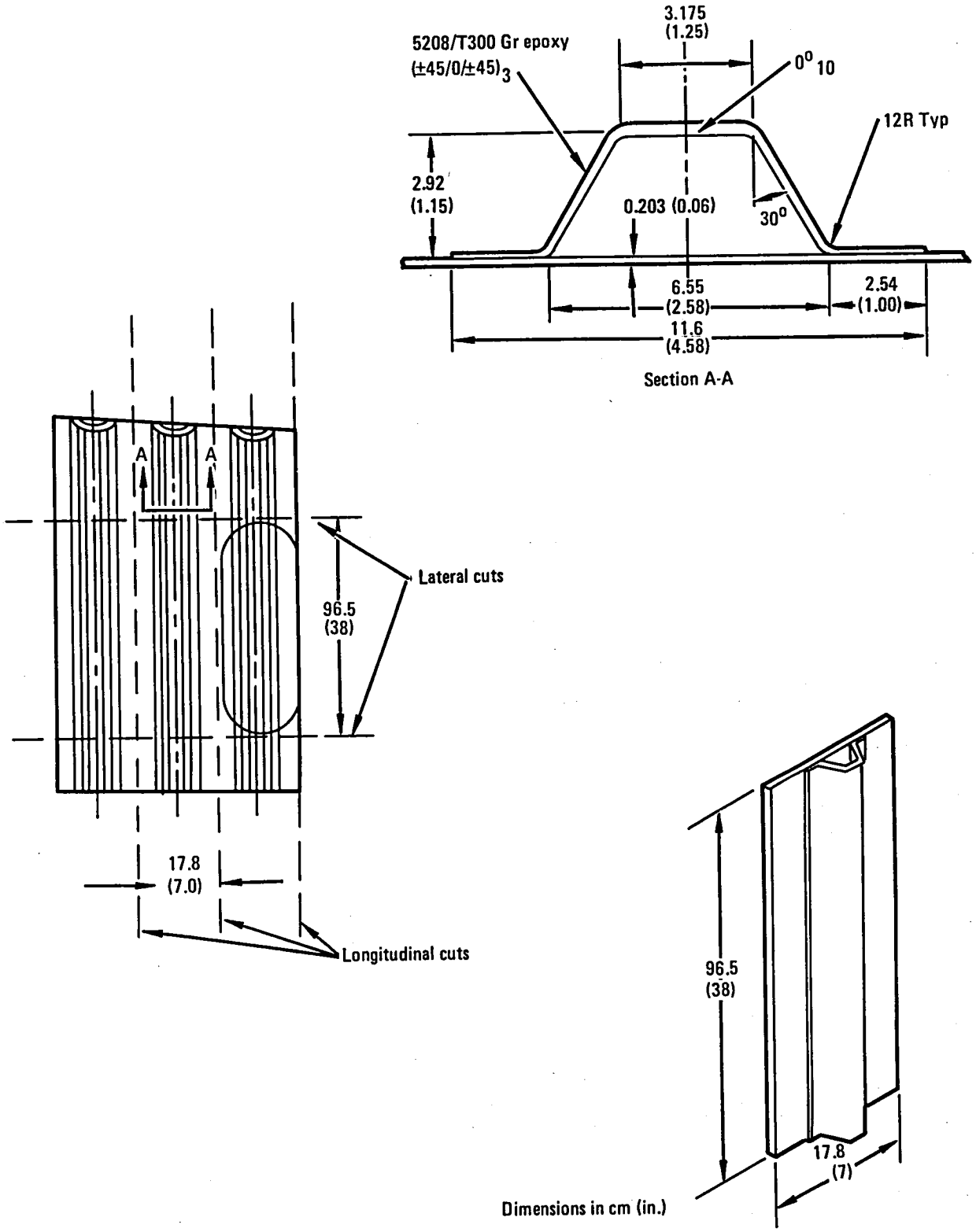

Figure 57. - Sectioning diagram for L-1011 fin cover panel.

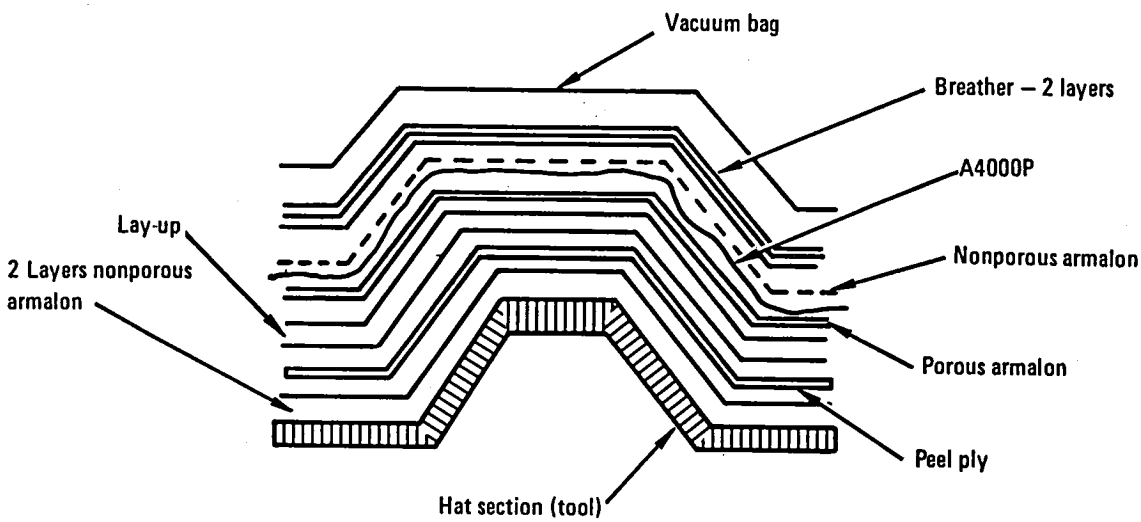

CURE SEQUENCE		TIME – MINUTES	
PRESSURE KPA±34.5 (PSI±5)	TEMPERATURE °C±5.5°C (°F ±10°F)	MINIMUM	MAXIMUM
345 (50)	Ambient – 66 (150)	–	10
138 (20)	66-99 (150-210)	50	80
	99 (210)	20	30
	99-127 (210-260)	45	60
	127 (260)	105 TOTAL { 30	105 { 45
138-586.5 (20-85)	127 (260)	105 TOTAL { 10	105 { 20
586.5 (85)	127 (260)	105 TOTAL { –	105 { –
	127-177 (260-350)	60	90
	177 (350)	105	150
	177-71 (350-160)	30	–
138-0 (20-0)	71 (160) – R.T.	–	–

Figure 58. - Cure configuration and cure cycle.

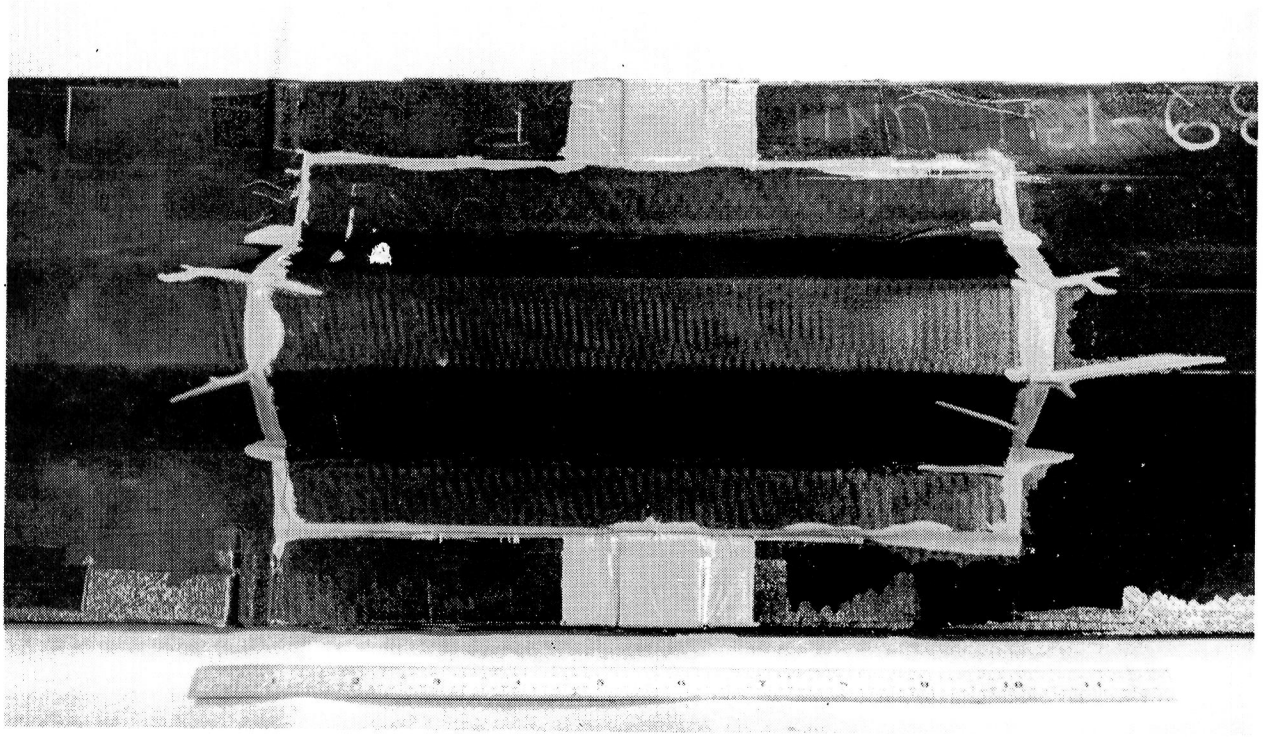

Figure 59. - Completed hat-section repair for the vertical fin cover panel specimen (Type I).

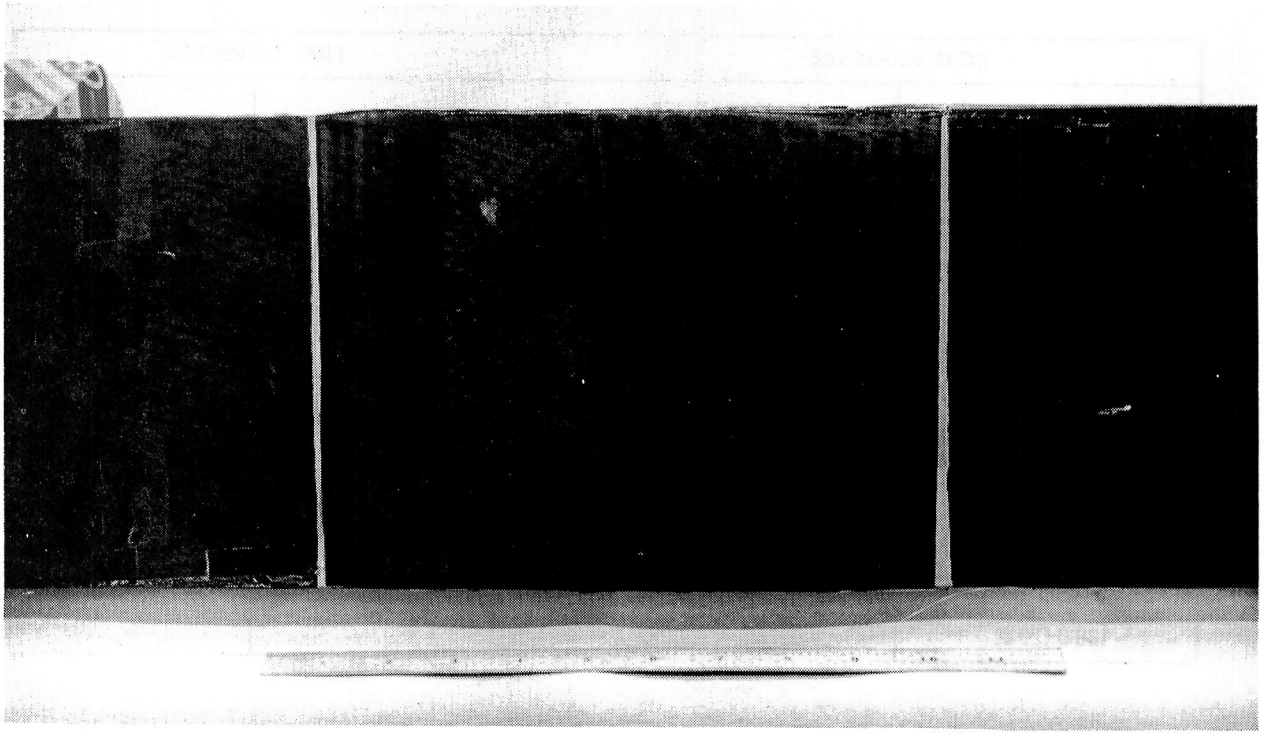

Figure 60. - Completed external skin repair of the vertical fin cover panel specimen (Type I).

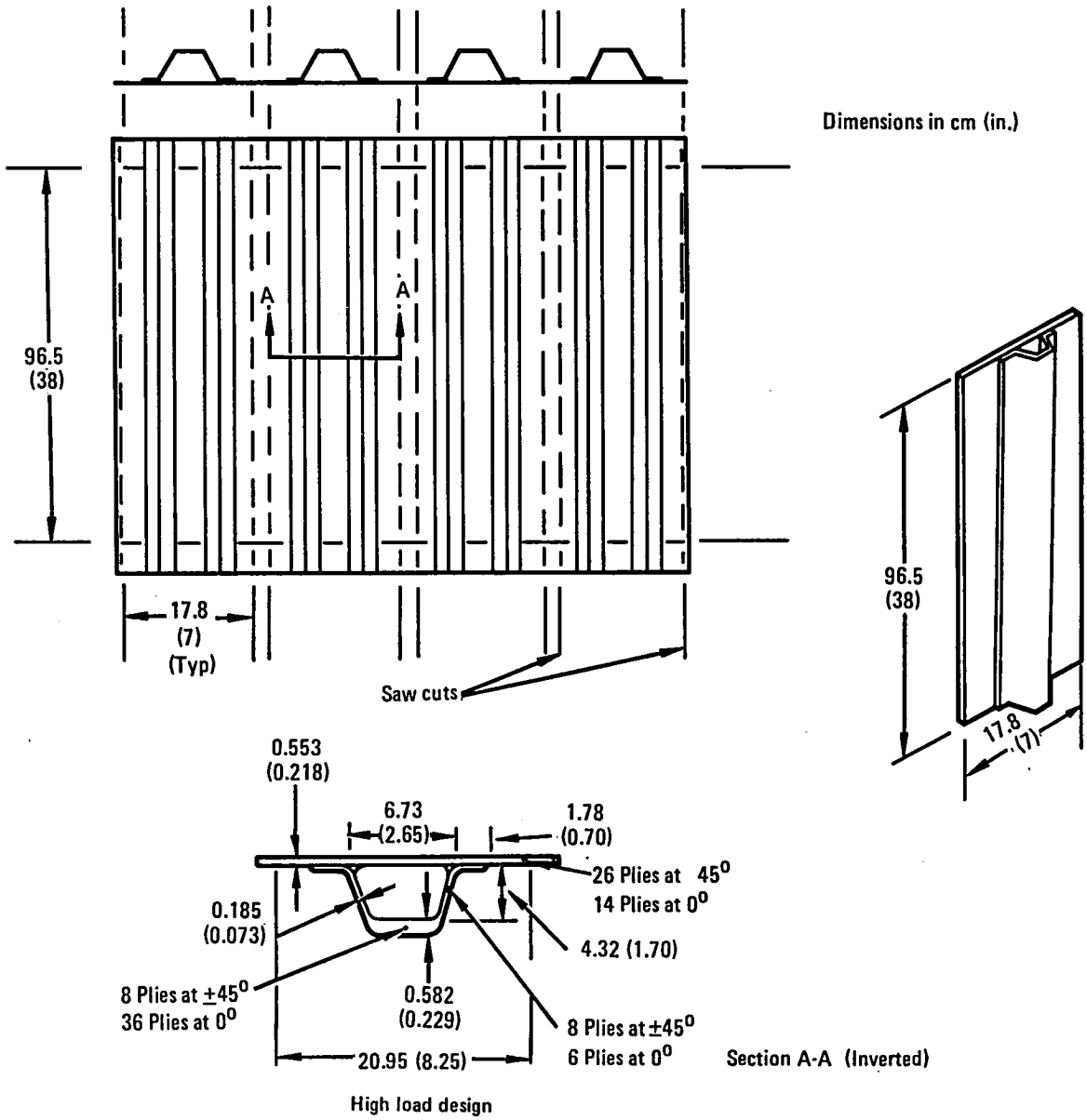

Figure 61. - Sectioning diagram for Type II specimens.

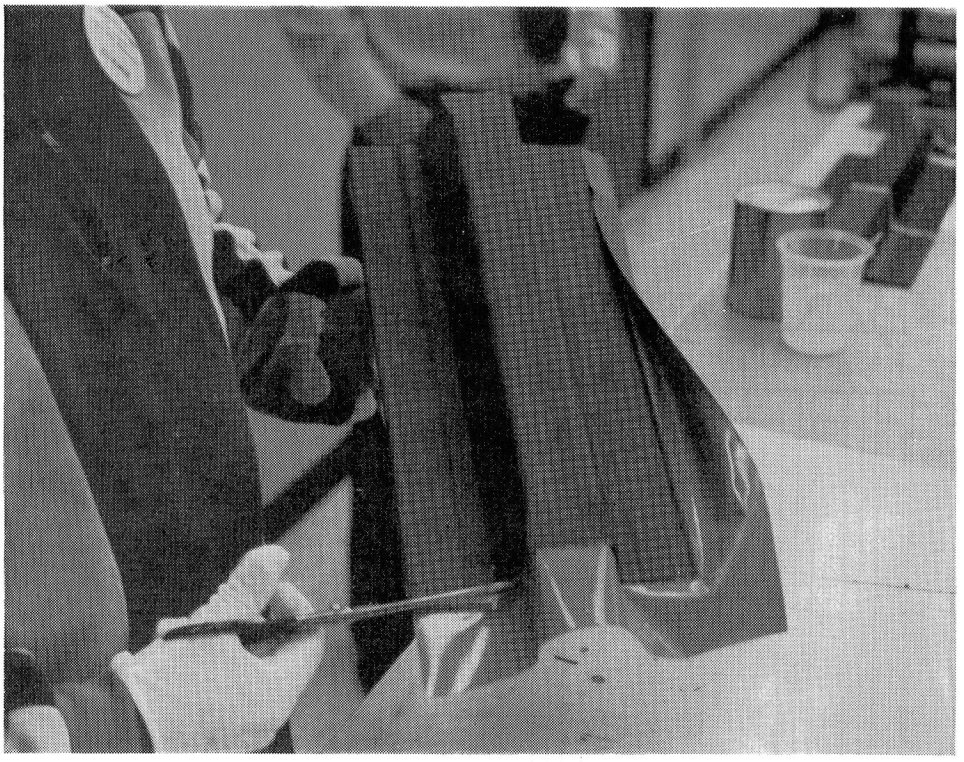

Figure 62. - Application of adhesive film to hat section.

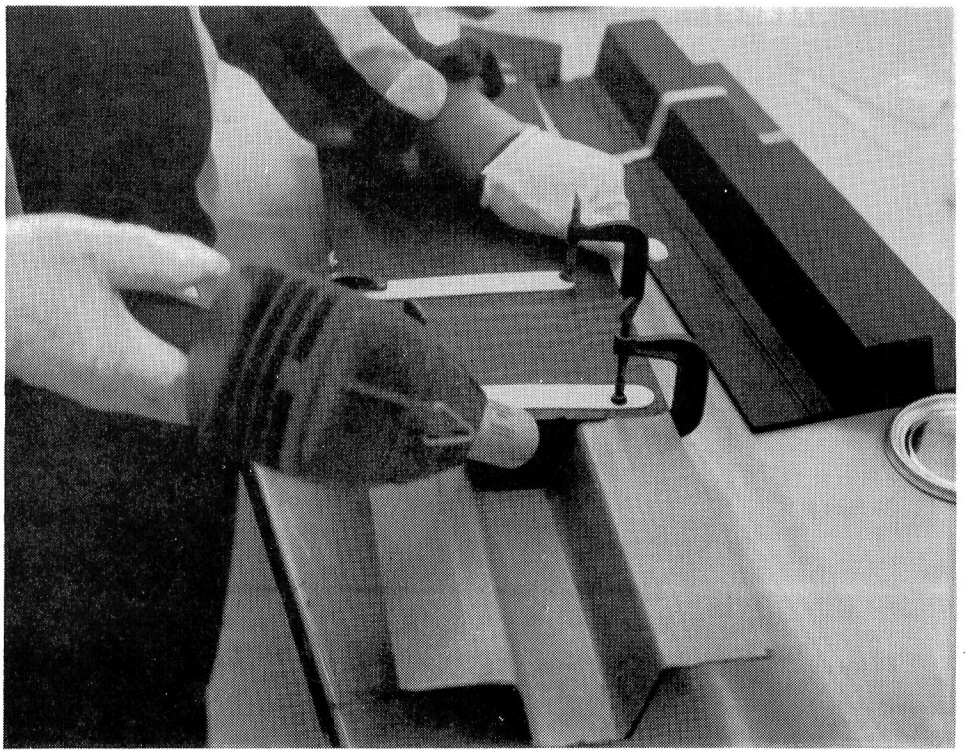

Figure 63. - Fitting of parent segments to hat splice plate.

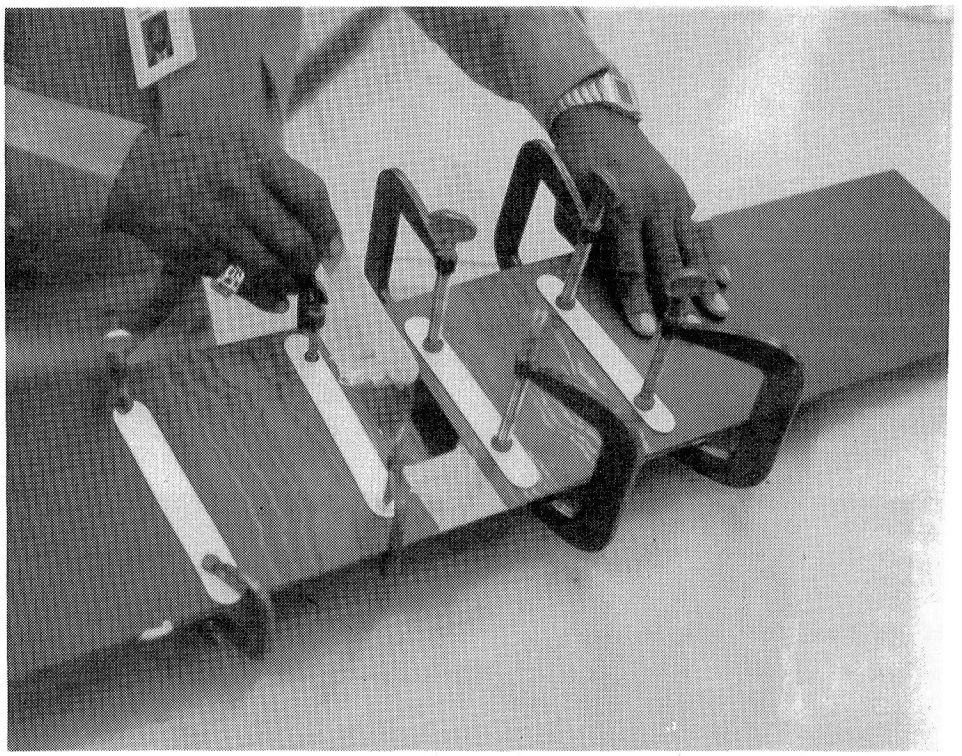

Figure 64. - Application of adhesive paste to seal hat segment ends.

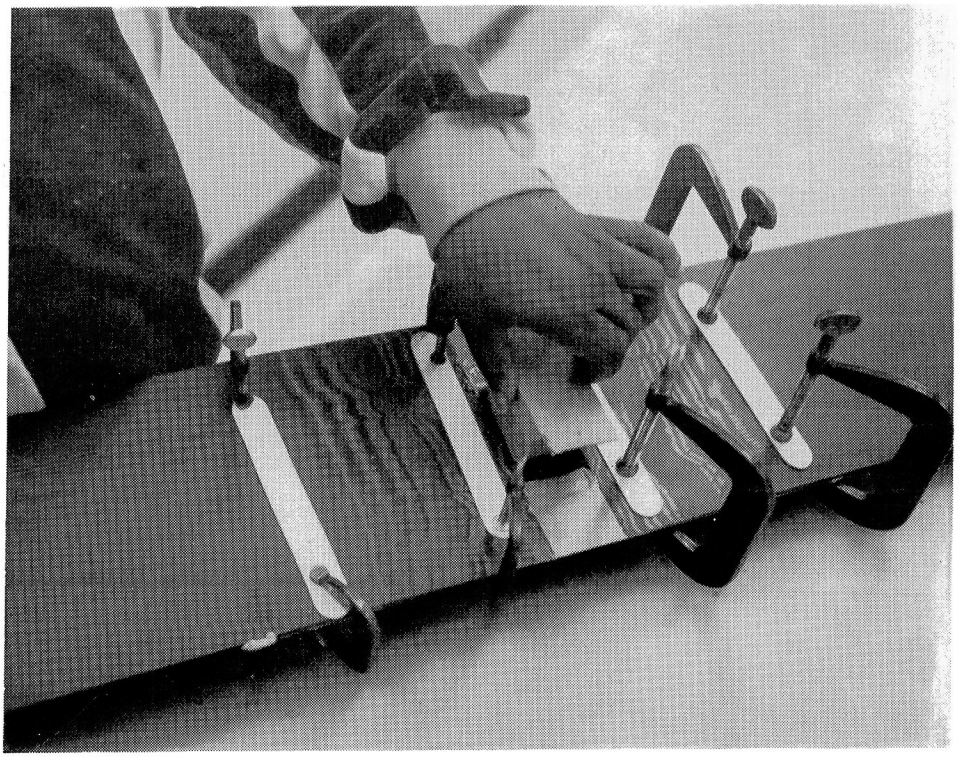

Figure 65. - Placement of silicone plug into hat cavity.

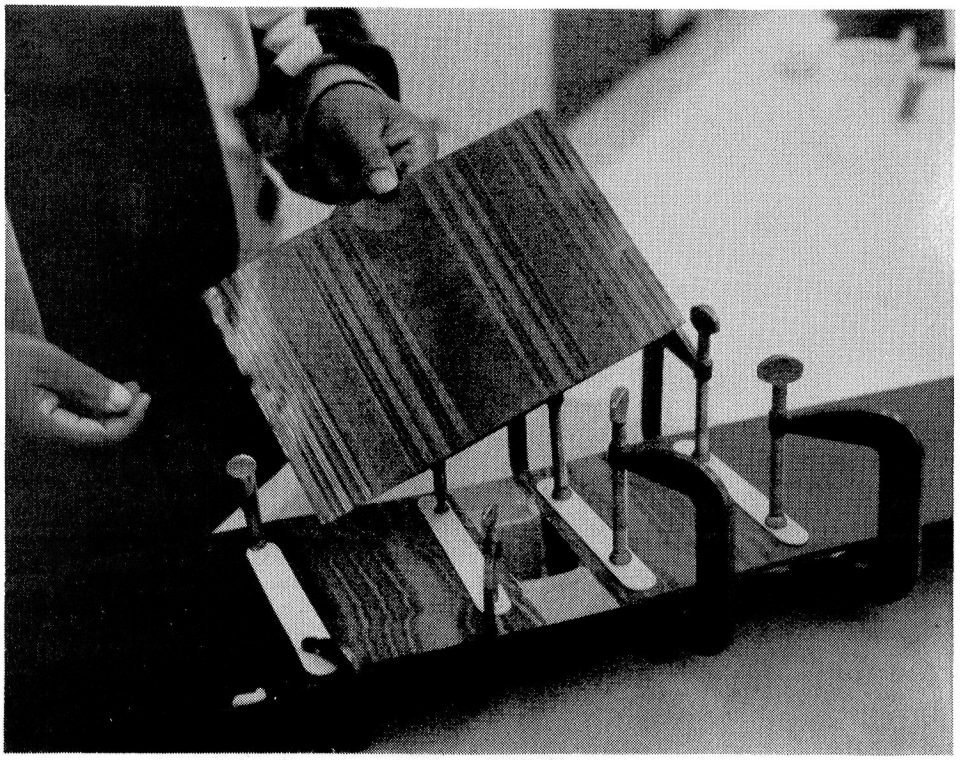

Figure 66. - Skin patch replacement plies.

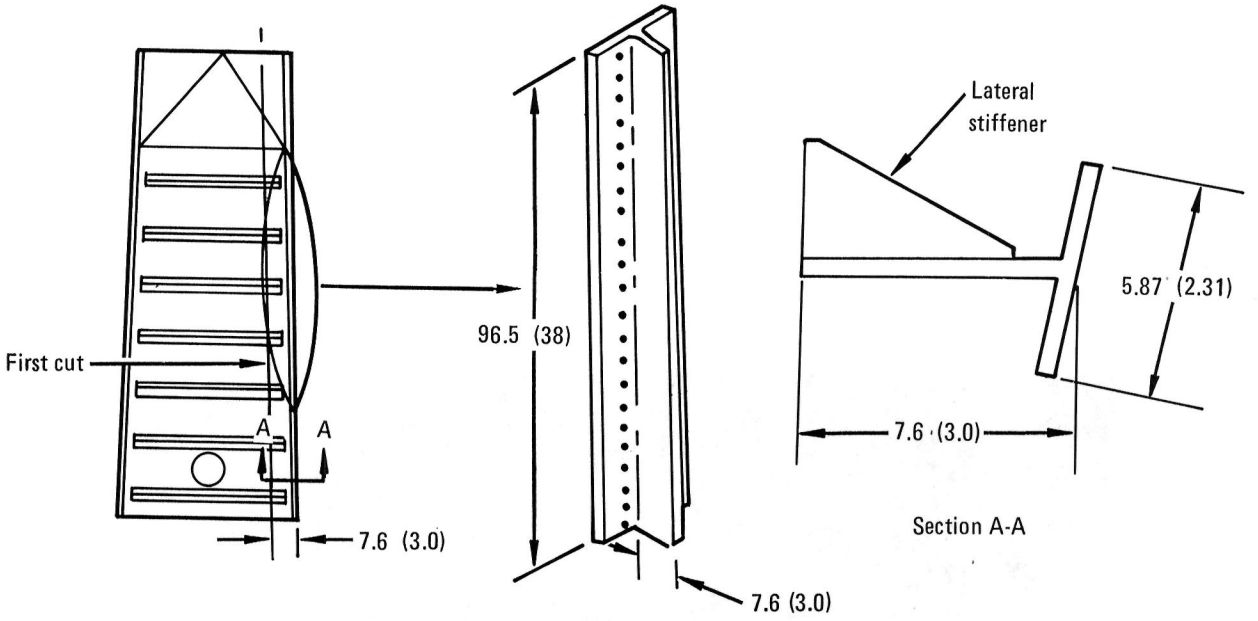

Figure 67. - Vertical fin spar sectioning diagram.

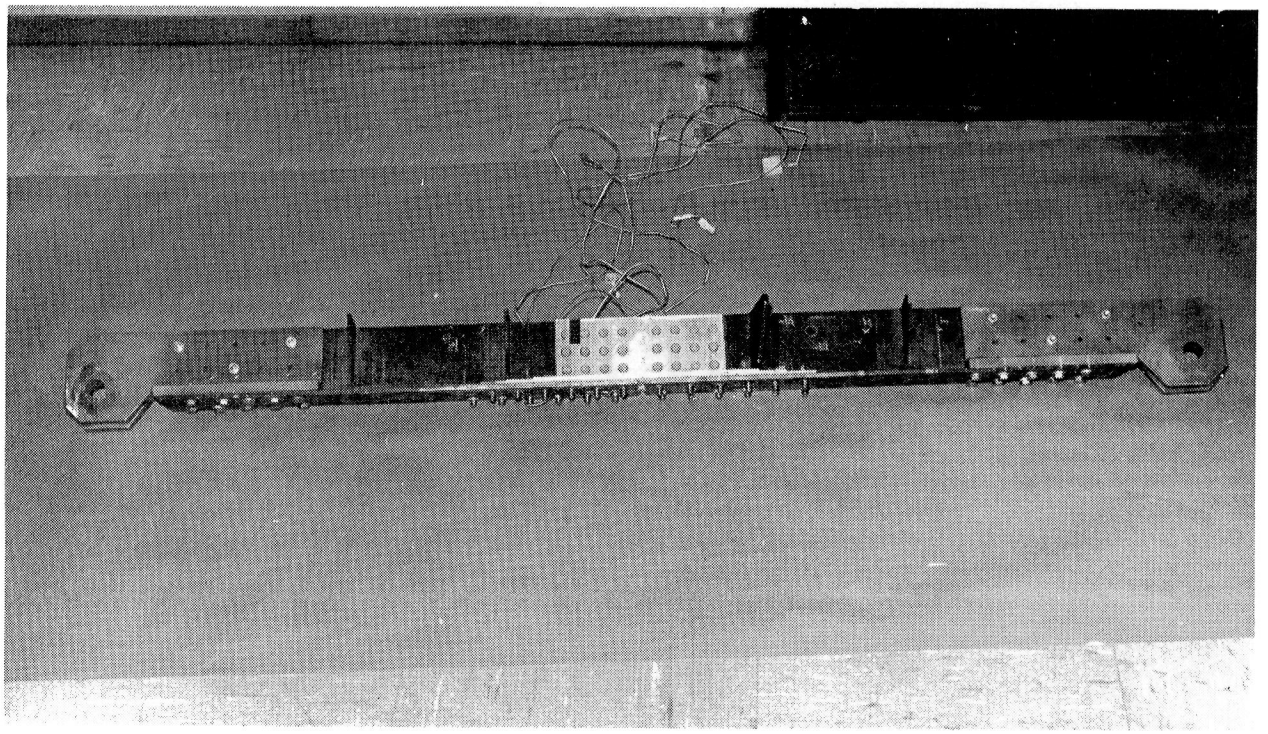

Figure 68. - Completed vertical fin spar segment repair (Type III).

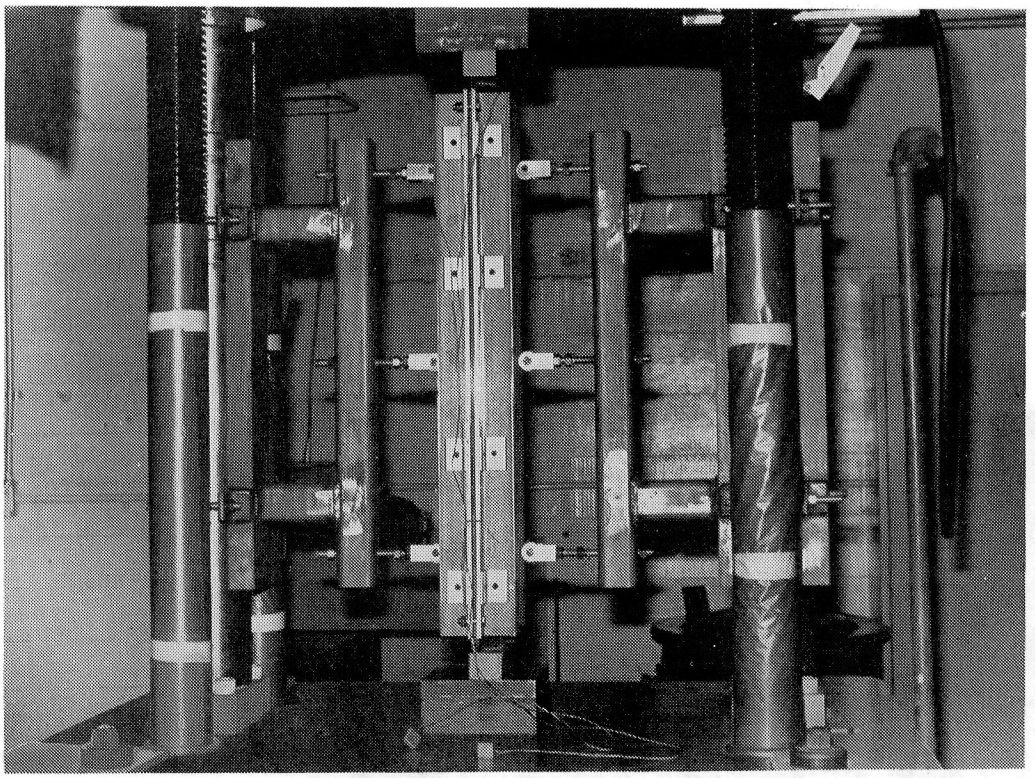

Figure 69. - Compression specimen in stabilization fixture ready for testing.

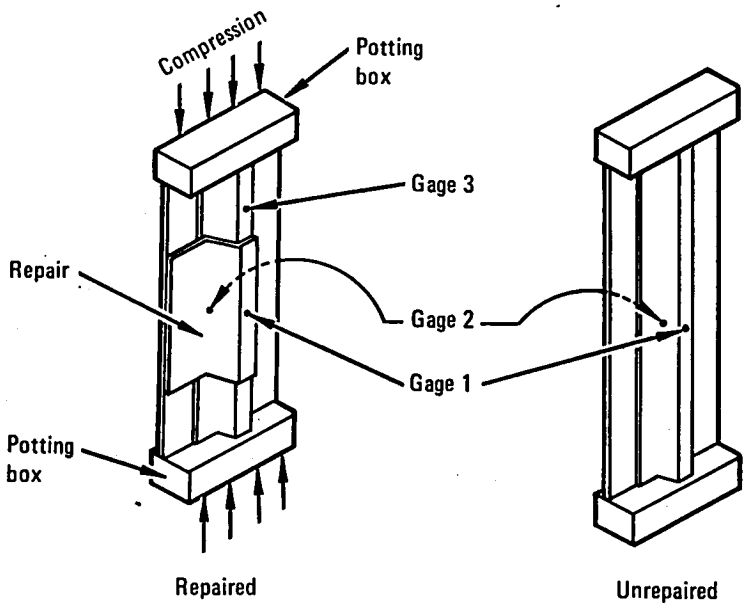

Gage 1: Hat side on horizontal and vertical centerlines
Gage 2: Skin side on horizontal and vertical centerlines
Gage 3: Hat side on longitudinal centerline, 7.62 cm (3.0 inches) from end of patch

NOTE: Gage 2 on skin side of repaired Type I fin cover specimen was mislocated 0.633cm from edge of center gap and 1.905 cm from vertical center line of specimen

Figure 70. - Strain gage locations for Type I and II cover specimens.

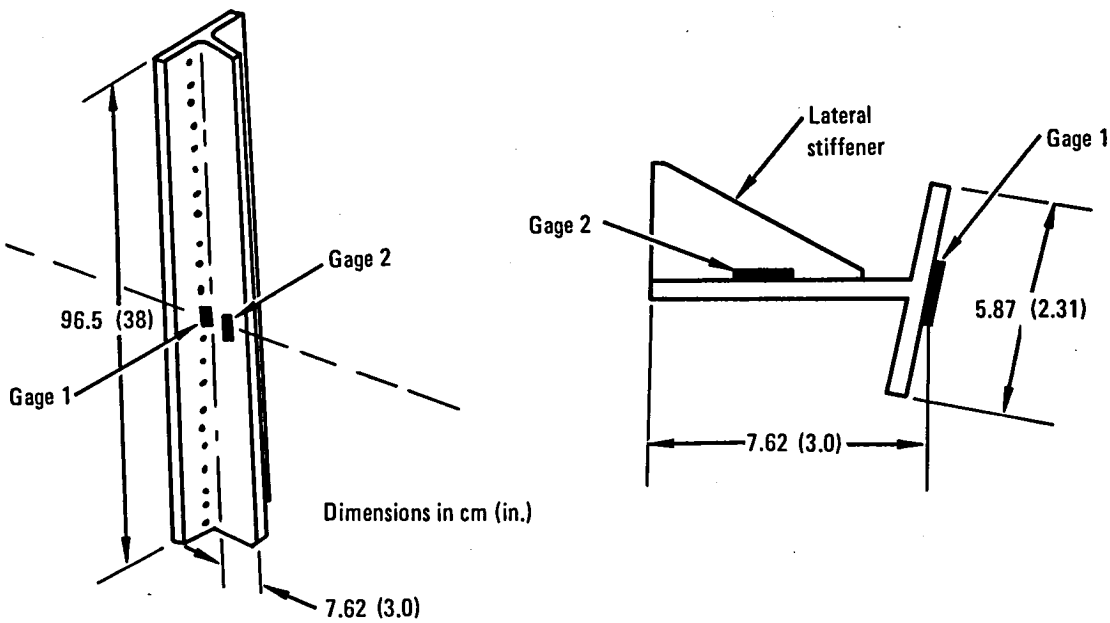

Figure 71. - Strain gage locations for Type III control specimens.

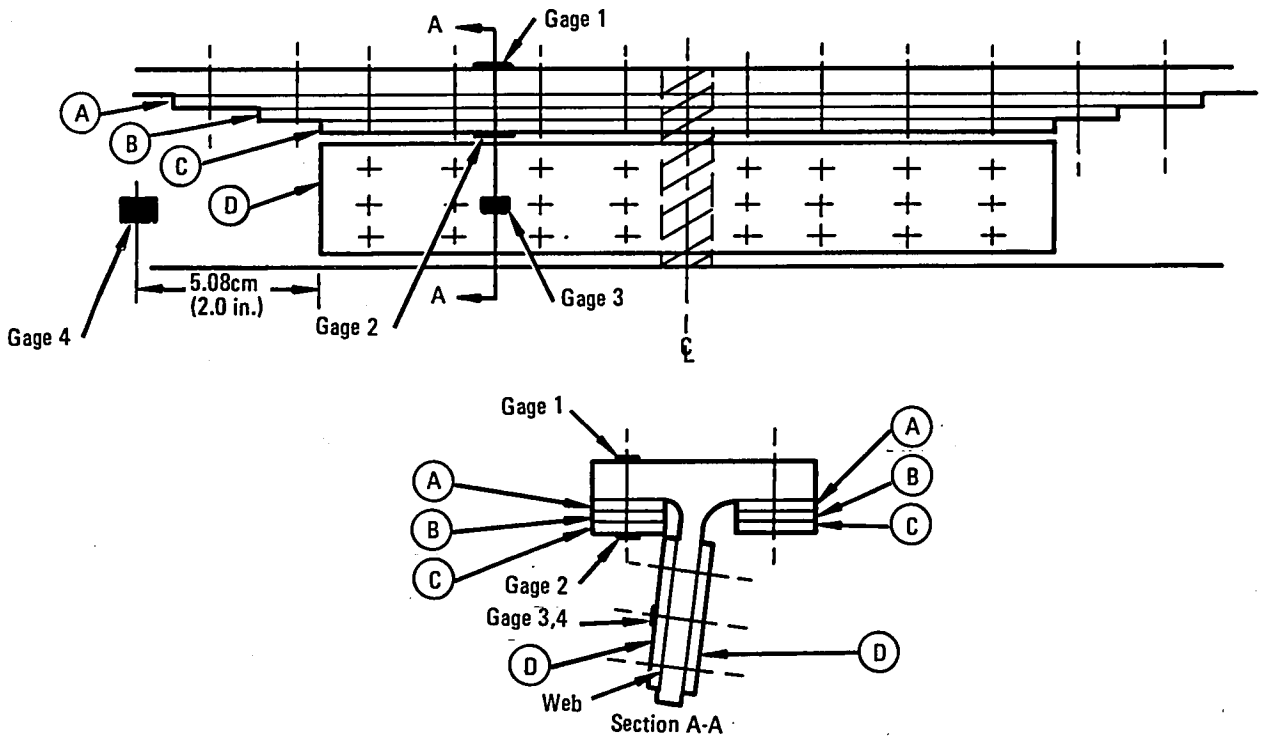

Figure 72. - Strain gage locations for Type III spar specimen.

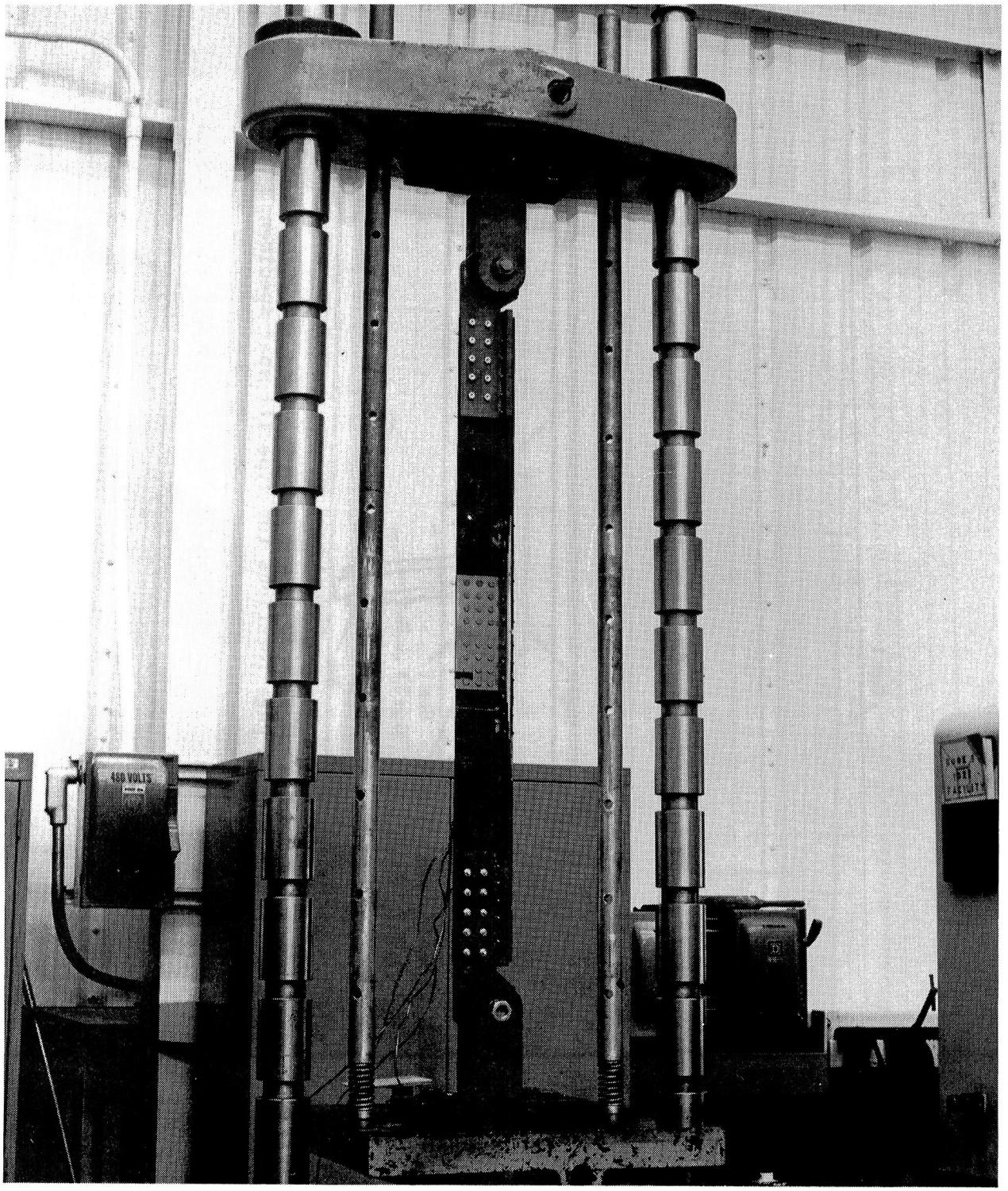

Figure 73. - Type III, vertical fin spar segment specimen ready for testing.

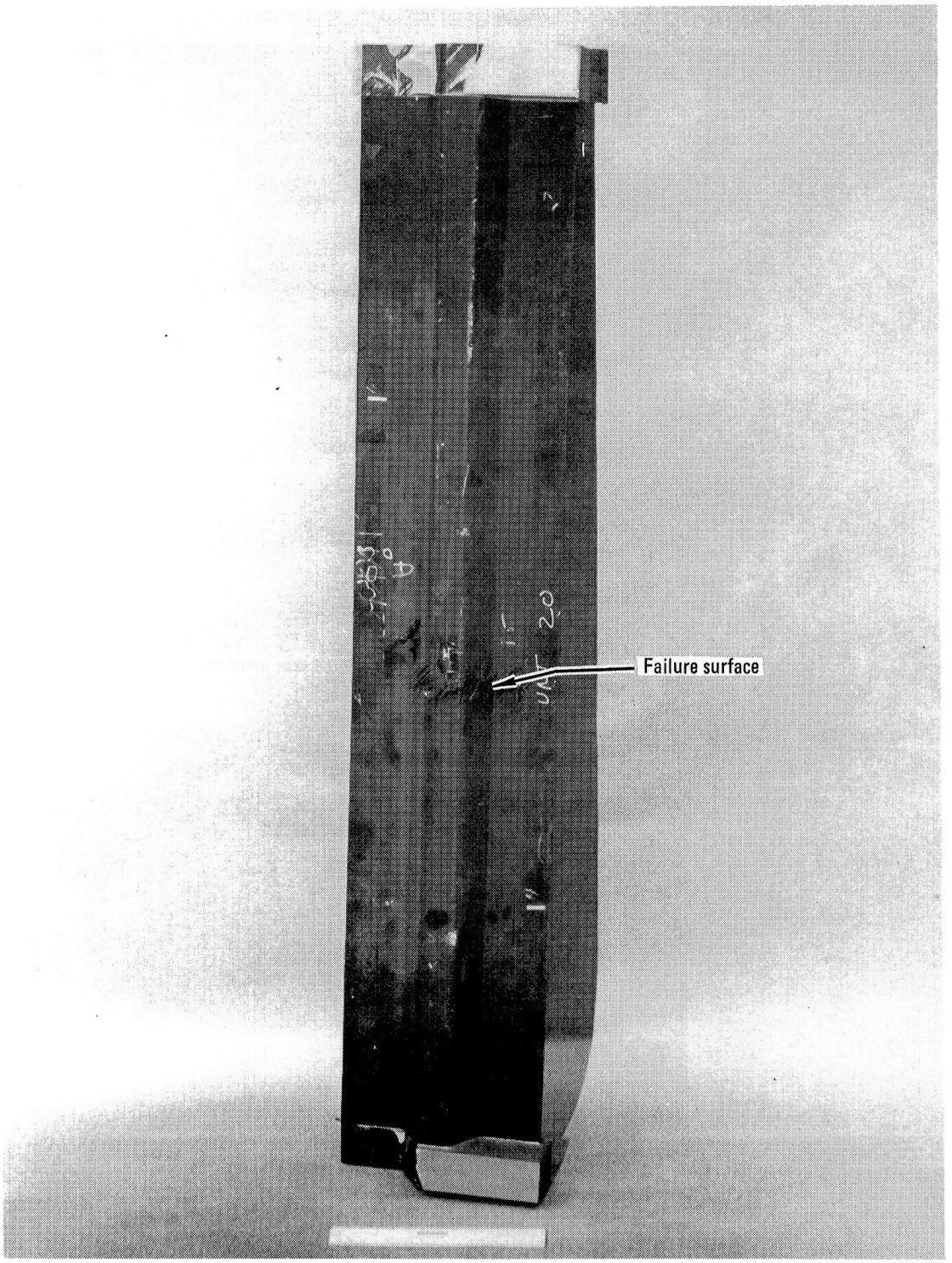

Figure 74. - Failure of the Type I control specimen.

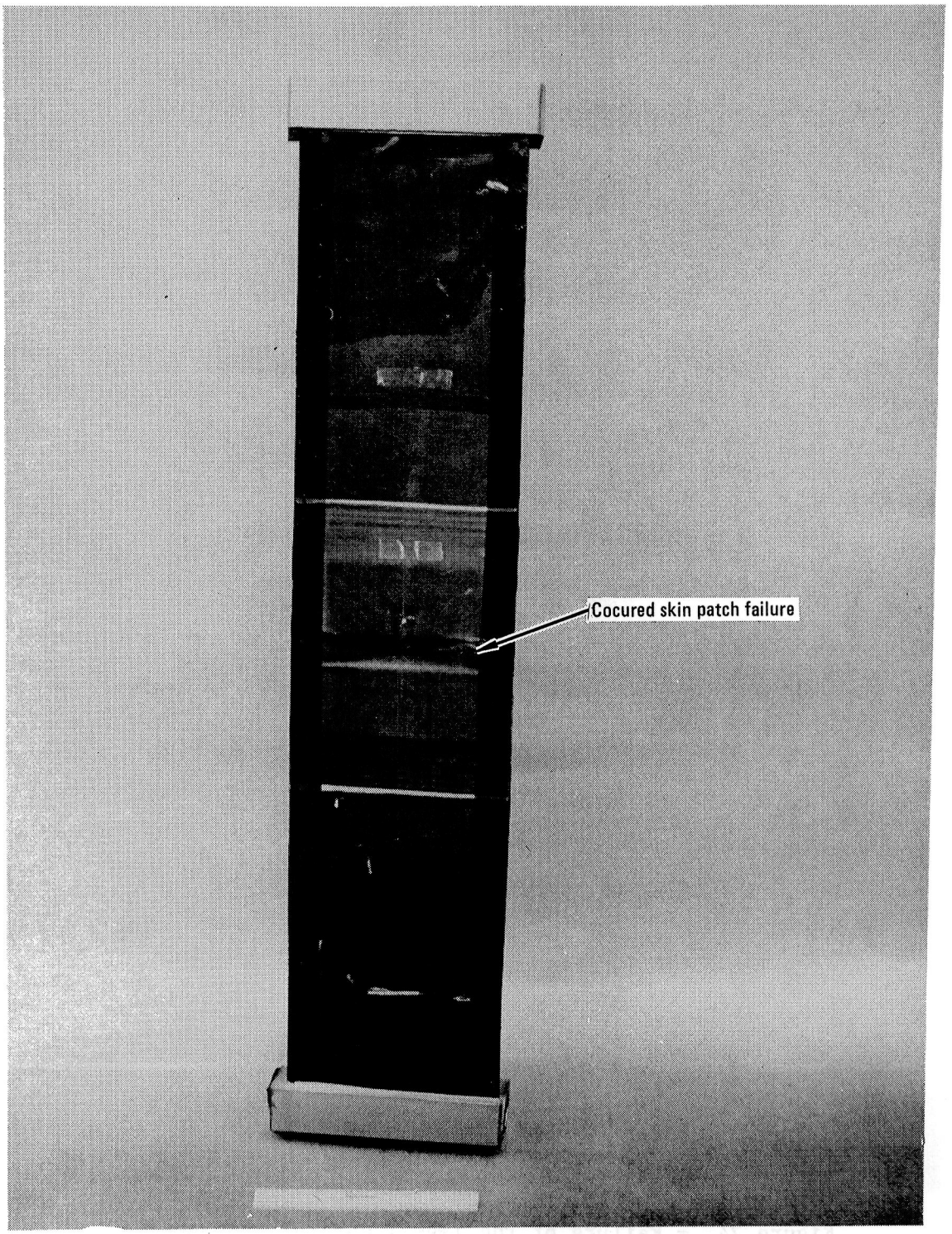

Figure 75. - Failed Type I repaired specimen.

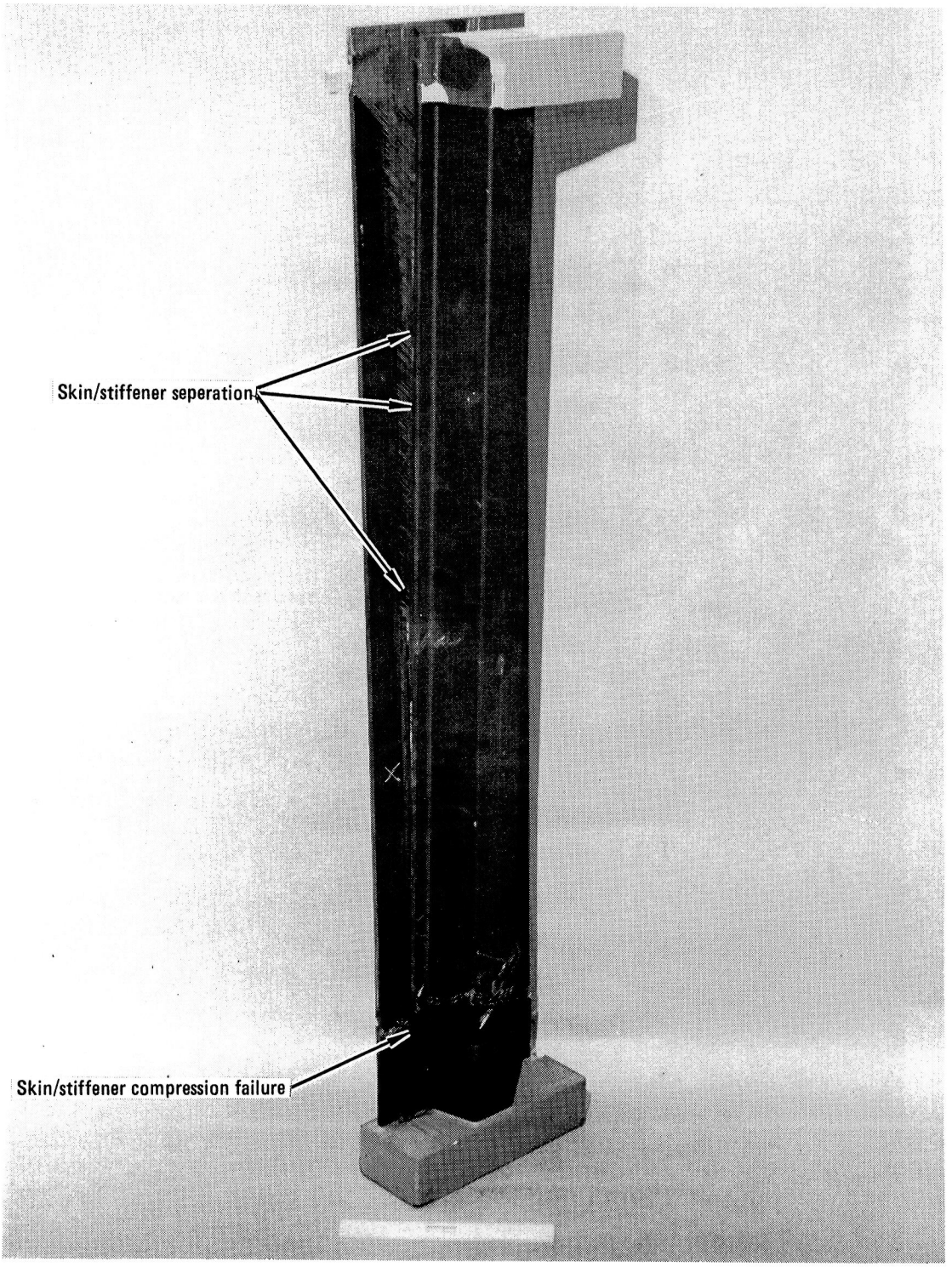

Figure 76. - Failure of the Type II control specimen.

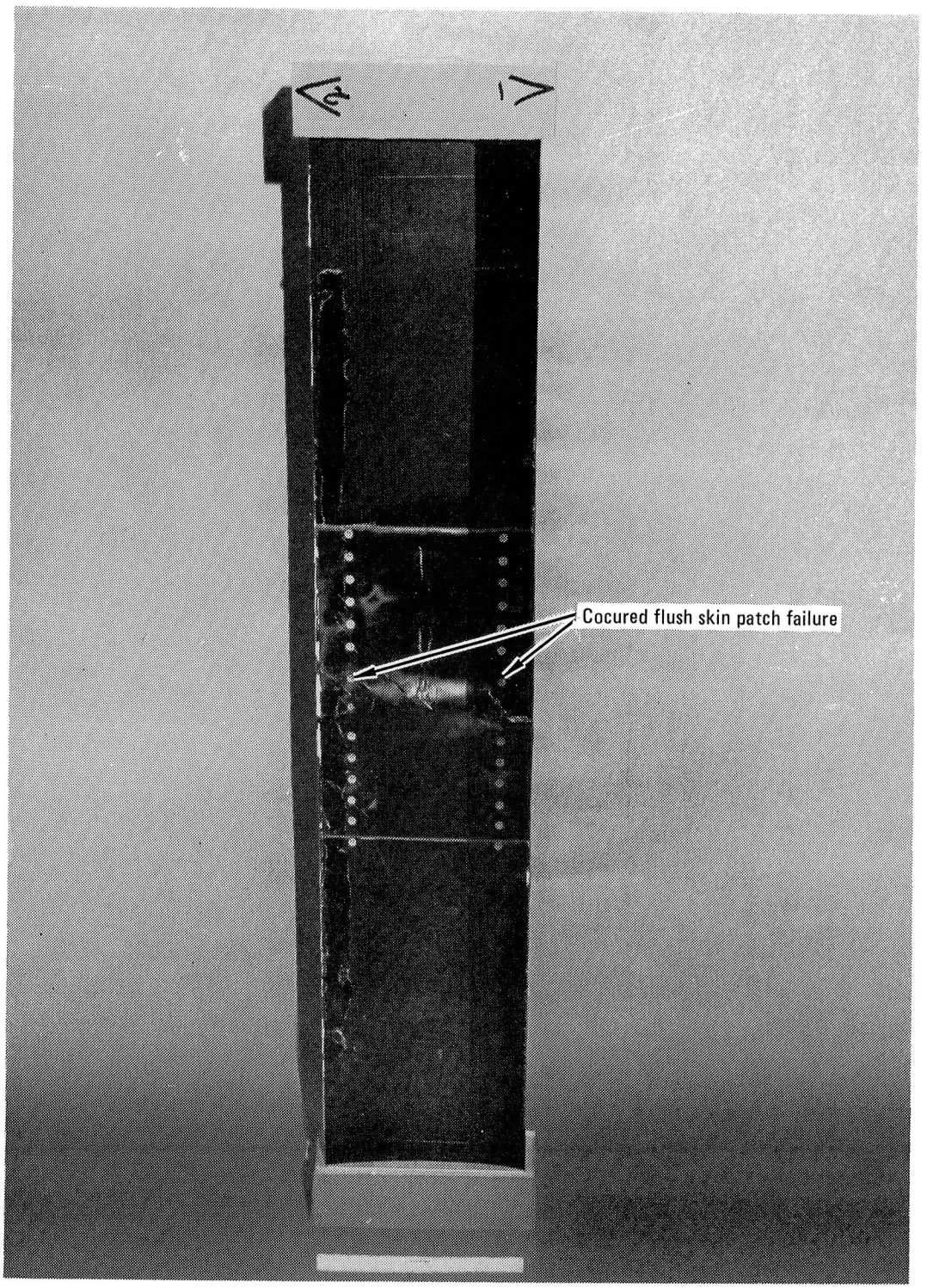

Figure 77. - Skin patch side of Type II repaired specimen failure.

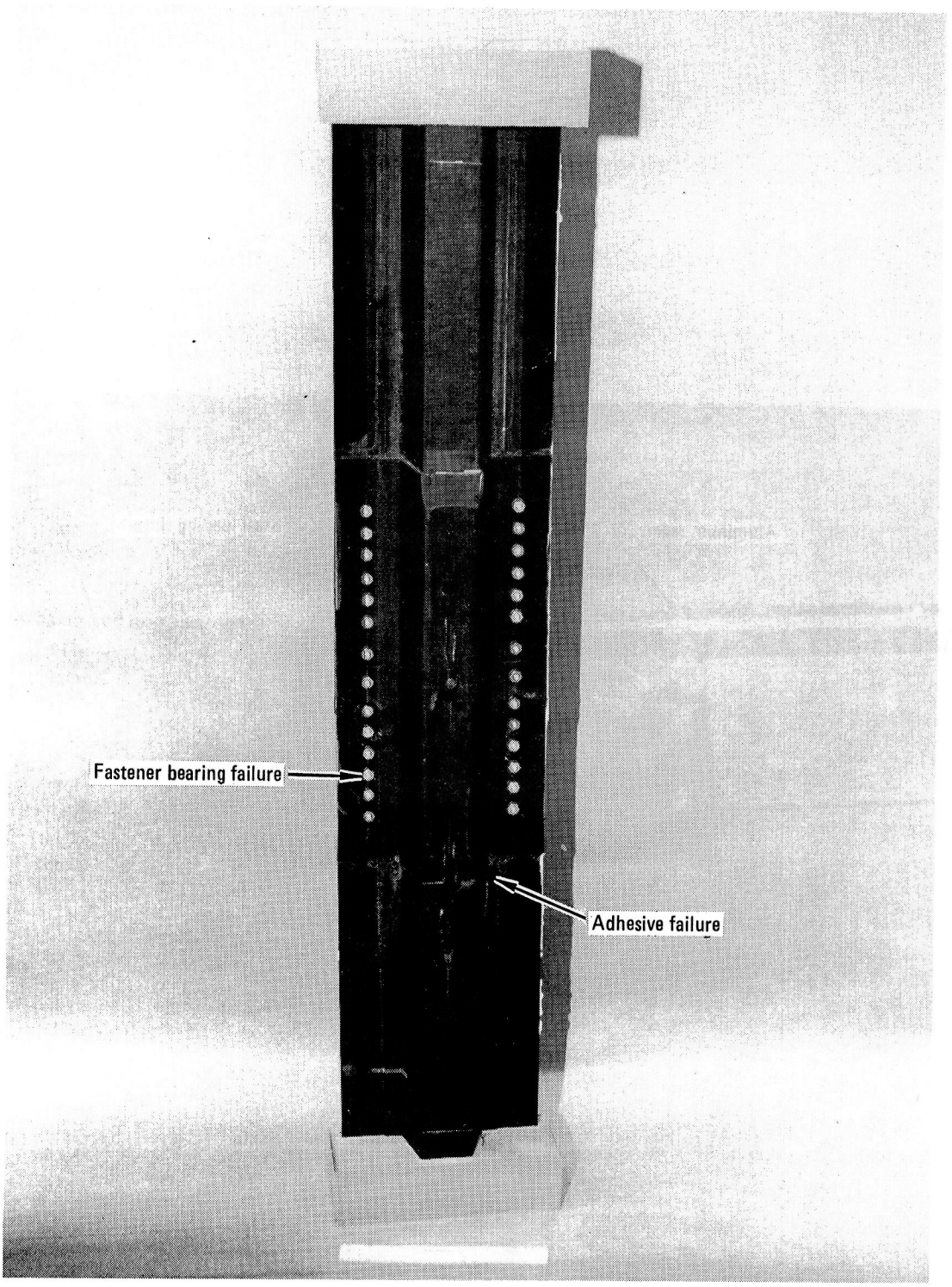

Figure 78. - Hat side of Type II repair specimen failure.

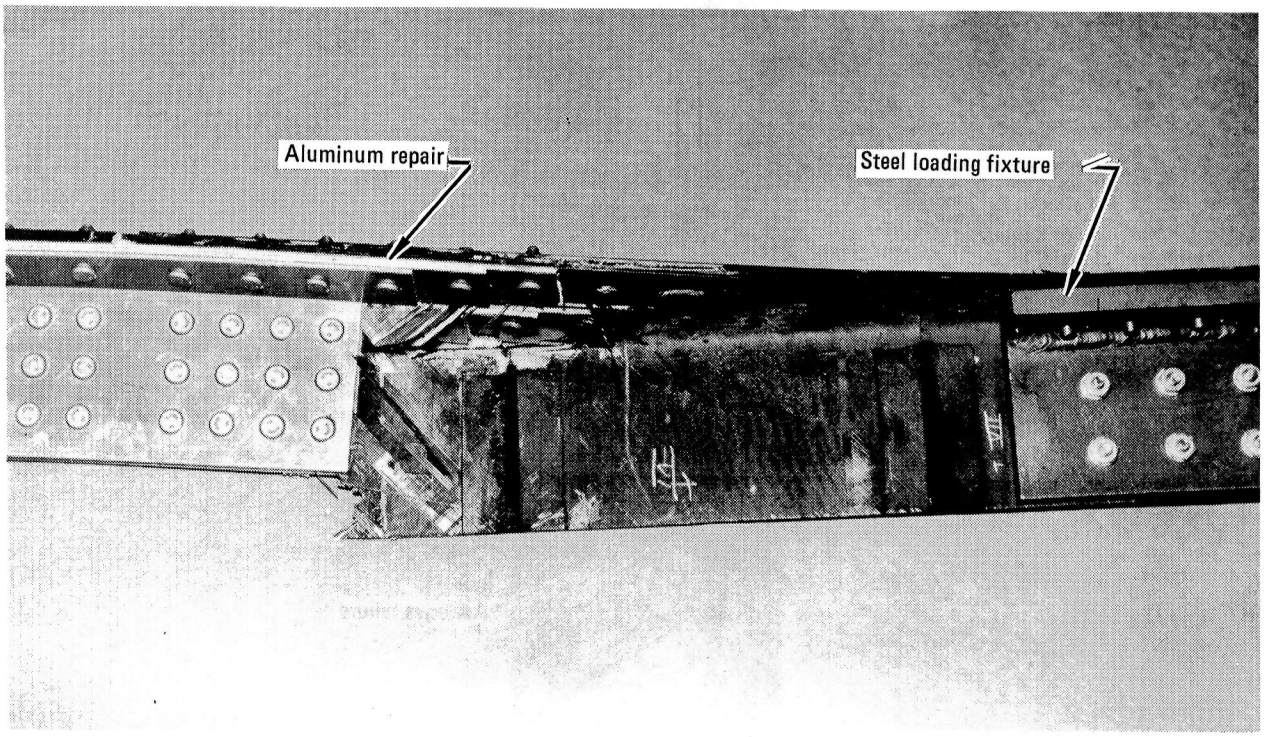

Figure 79. - Type III repaired specimen failure.

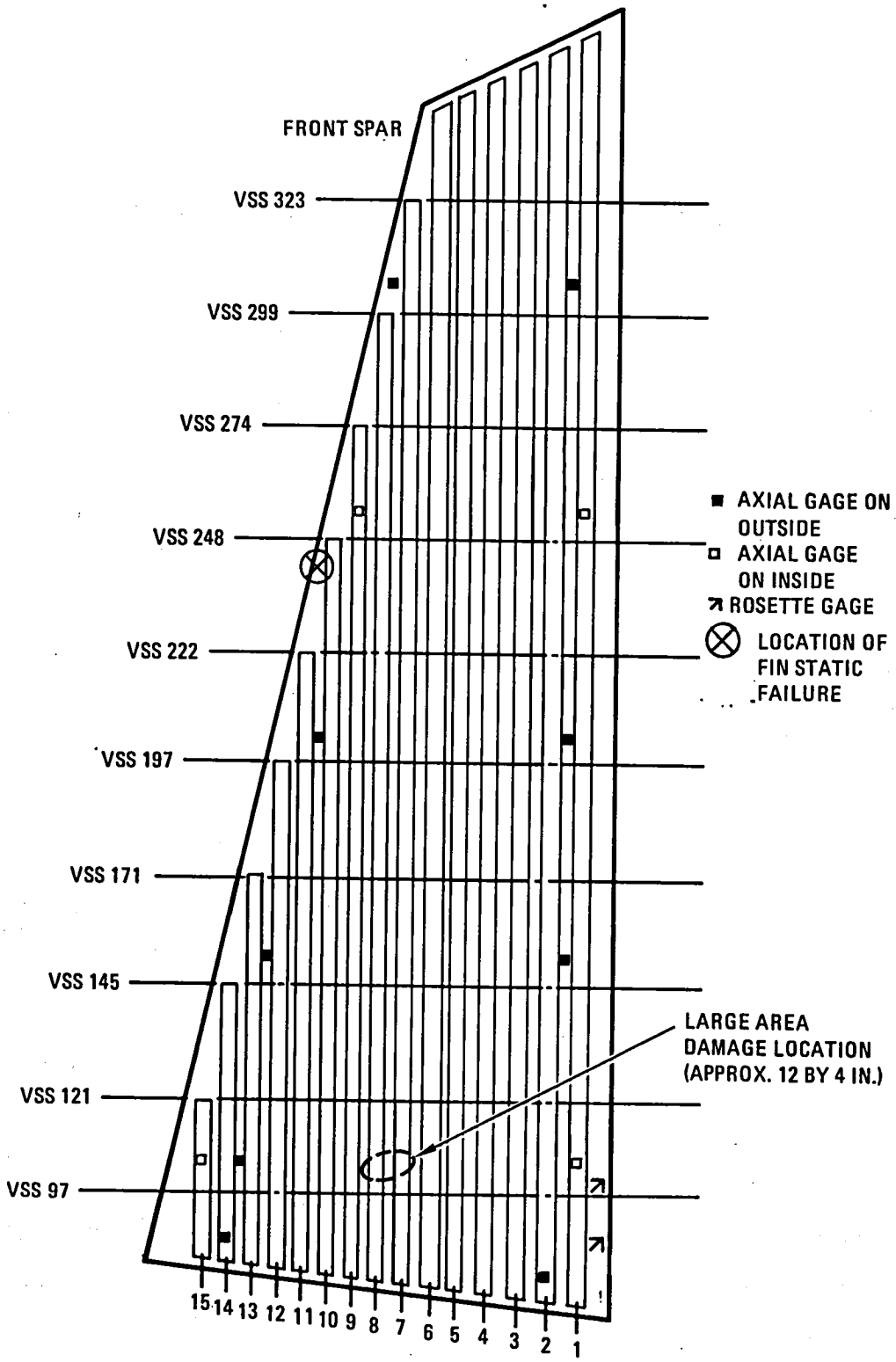

Figure 80. - Large area damage location on vertical fin GTA.

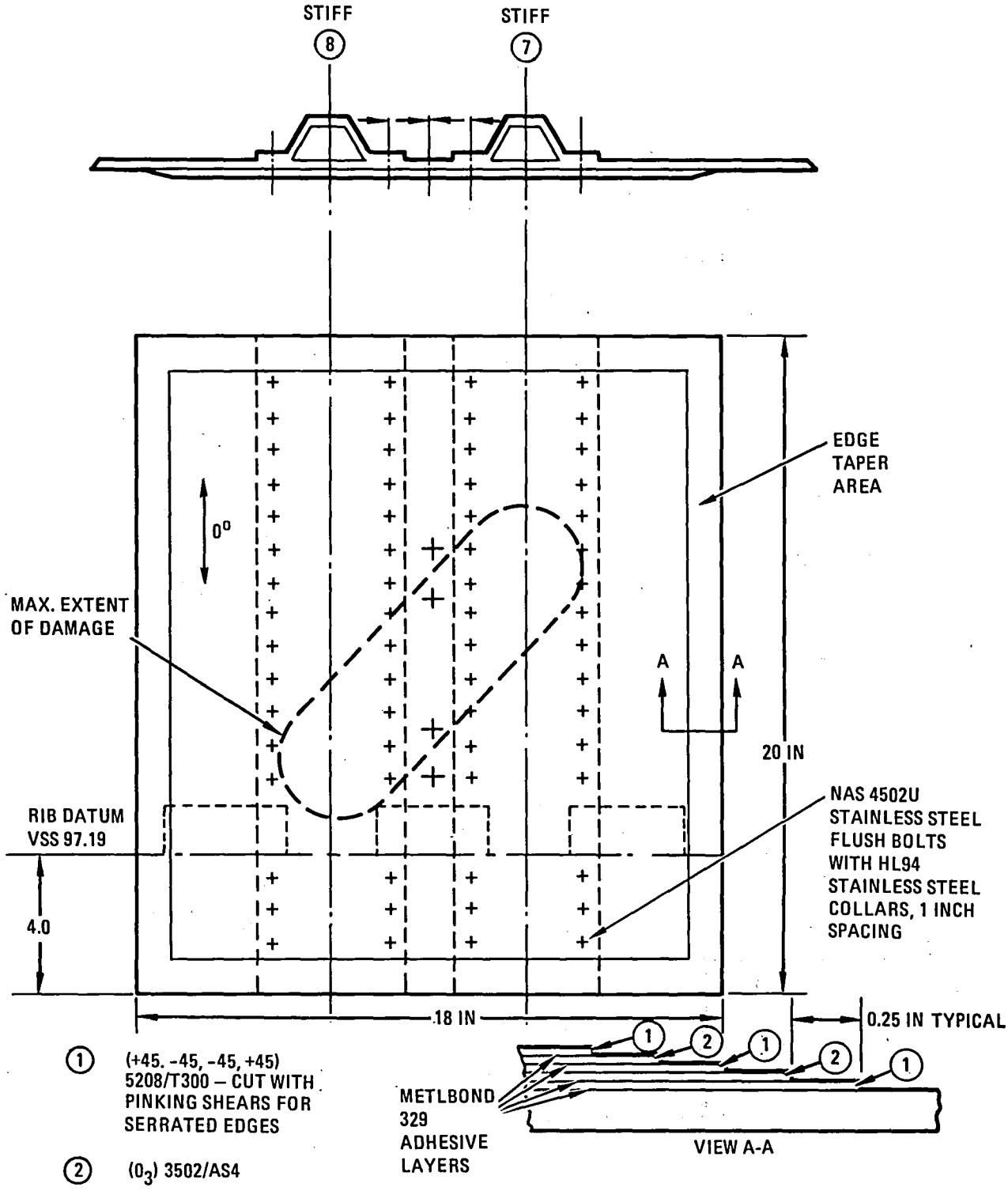

Figure 81. - Repair patch and damage area on fin component.

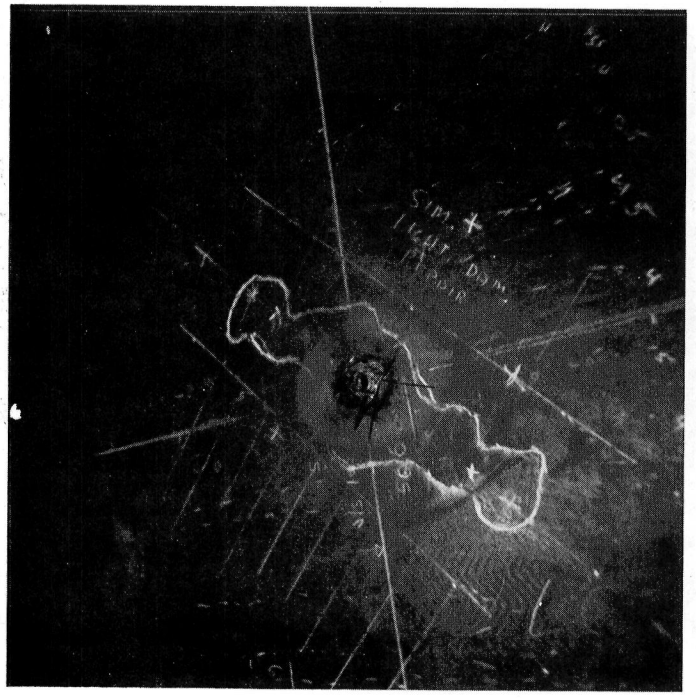

Figure 82. - Through penetration damage and marked area of delamination (before charring).

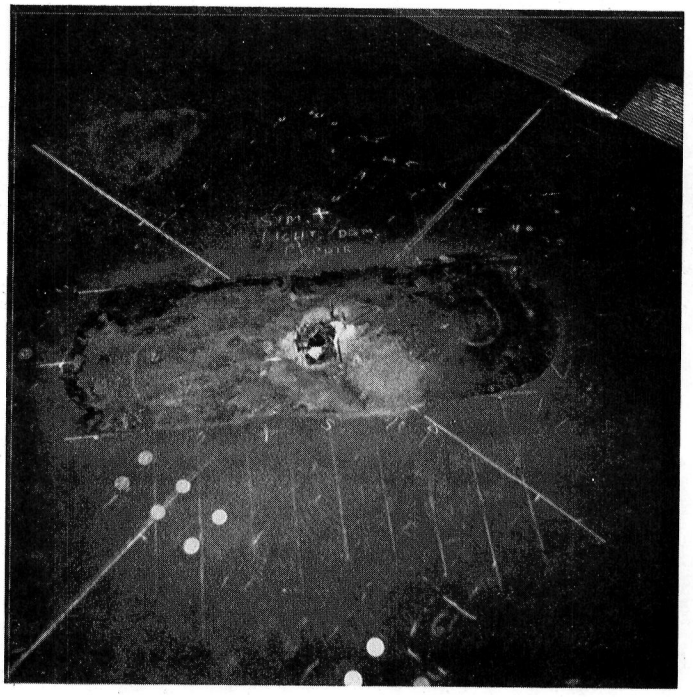

Figure 83. - Through penetration damage surrounded by charred area.

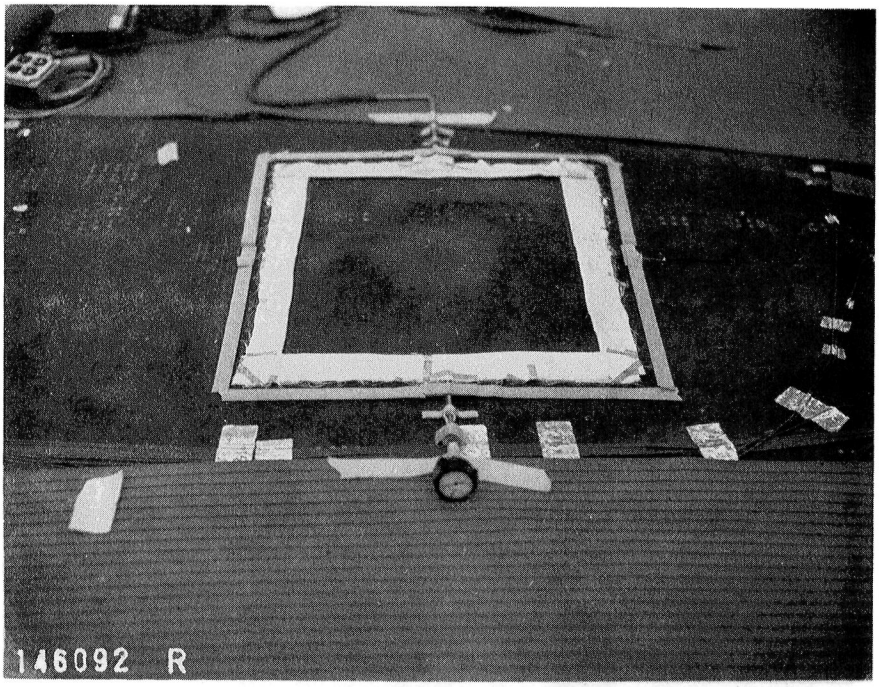

Figure 84. - Bonded patch lay-up with vacuum bag.

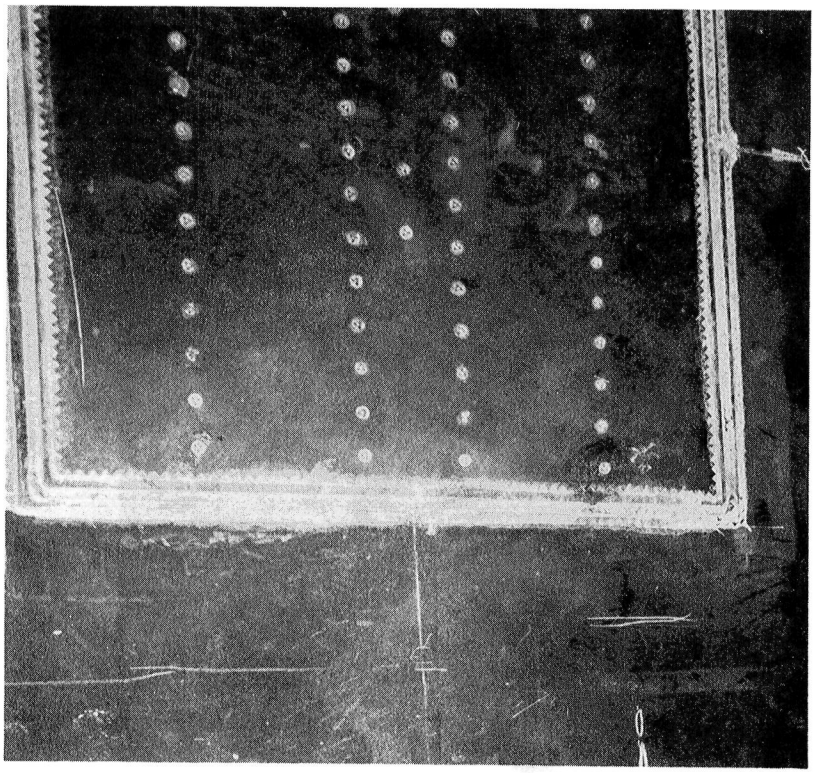

Figure 85. - Repair patch on vertical fin ground test article.

TABLE I. - SUMMARY OF DOCUMENTS DESCRIBING FLAWS IN COMPOSITE STRUCTURES

Documents		Flaw Type	Experimental Data	Analysis Methods	Notes
Ref.	Title				
7.	"Structural Criteria for Advanced Composites," R.M. Verette and J.D. Labor, AFFDL-TR-76-142.	Voids, 1.52 cm (0.6 in.) Diam. Edge Delaminations, Scratches 3 and 6 Plies Deep, FOD Impact, Oversized 0.476 cm (3/16 in.) Fastener Holes, Over-torqued 0.476 cm (3/16 in.) Flush Fasteners	Coupons $(0/\pm45_2/0/\pm45)_s$ $(0_2/\pm45/0_2/90/0)_s$ $(0/\pm45/90)_{2s}$ Tens. & Compr, Static & Fatigue Room Temp. Wet	None	AS/3501-5
8.	"Effects of Manufacturing and In-Service Defects on Composite Materials," R.M. Verette and E. Demuts, Army Symposium on Solid Mechanics, Cape Cod, Mass., Sept. 1976. Proceedings published as AMMRC MS 76-2, Army Materials and Mechanics Research Center, Watertown, Mass.				
9.	"Environmentally Controlled Fatigue Tests of Box Beams with Built-In Flaws," J.D. Labor and R.M. Verette, Journal of Aircraft, May 1978, p. 257-263	(Same as No. 1 and 2 above)	Monolithic Panels, 50.8 cm x 152.4 cm (20 in. x 60 in.) $(0_{20}/\pm45_4/90_4)_T$ Tens. & Shear Static & Fatigue on 2 Multi-flawed box beam skins	None (Used to verify applicability of coupon data to larger structure)	AS/3501-5, with Glass/Epoxy buffer strips & softening strips
10.	"Uniaxial Failure of Composite Laminates Containing Stress Concentrations," R.J. Nuismer and J.M. Whitney, ASTM STP 593, 1975, pp 117-142.	0.254 cm to 2.54 cm (0.1 to 1.0 in.) diam. holes nad through slots	Coupons $(0/90)_{4s}$ & $(0/\pm45/90)_{2s}$ Static Tension Room Temp. Dry	Test data were used to correlate with average stress & point stress criteria (See Ref. No. 16)	Scotchply 1002 glass/epoxy and T300/5208 Gr/Ep

TABLE I. - Continued

Documents		Flaw Type	Experimental Data	Analysis Methods	Notes
Ref.	Title				
11.	"Evaluation of Flawed Composite Structure under Static and Cyclic Loading," T.R. Porter, Boeing Aerospace Co.	0.3175 cm - 1.587 cm (1/8 to 5/8 in.) diam. holes, slots and countersunk holes	Coupons $[(0/\pm45/0/90)_s]_2$ $[(0_3/\pm80)_2]_s$ $[(0/+30/0*/-30/0)_2]_s$ Tens. static and Fatigue	Fracture mechanics procedures applied to test data.	T300/934 *S-glass ply. C-scan data. Proof loads defined for qualification.
12.	"A Correlation for the Fracture of Filamentary Composites," J.W. Mar and K.Y. Liu, M.I.T. preprint of a note.	Up to 7.62 cm (3 in.) diam holes.	$(\pm45/0)_s$ $(0/\pm45)_{2s}$ $(0/\pm45/90)_{2s}$ $(0/\pm45/90)_s$ $(0/\pm45/90)_{3s}$	Laminate strength with holes based on fracture mechanics.	Boron/Aluminum and Gr/Ep
13.	"Evaluation and Expansion of an Analytical Model for Fatigue of Notched Composite Laminates," R.L. Ramkumar, S.V. Kulkarni, and R.B. Piples, NASA CR-145308, March 1978.	Holes & slots	Coupons of several orientations. Tens & Compr. Static & Fatigue.	Analytical Model includes interlaminar effects near the hole.	T300/5208 C-scan data
14.	"Fatigue of Notched Fiber Composite Laminates, Part II: Analytical and Experimental Evaluation," S.F. Kulkarni, P.V. McLaughlin, Jr., and R.B. Pipes, NASA CR-145039, April 1976.	0.635 cm (0.25 in.) diam. holes.	Coupons of several 8 ply orientations. Tens. Static & Fatigue. Crack growth rate & wearout curves.	Analytical Model based on "wearout" of the laminate around the hole.	3M boron 0.010 cm (0.004 in.) diam. and SP 296 resin. C-scan data.

TABLE I. - Continued

Documents		Flaw Type	Experimental Data	Analysis Method	Notes
Ref.	Title				
15.	"Advanced Composite Serviceability Program," Rockwell Intern. Corporation, AFML Contract F33615-76-C-5344, Quarterly Progress Reports No. 1 through 8.	0.673 cm (0.265 in.) diam hole. 0.94 x 0.94 cm (0.37 x 0.37 in.) inclusion & delaminations. 2.54 cm (1.0 in.) long scratch, and gaps in layup.	3.81 cm (1.5 in.) wide coupons $[(0/\pm45/90)_2]_s$ $[(0/\pm45/0)_2]_s$ $[(90/\pm45/90)_2]_s$ Tens & Compr. Static & Fatigue (Data not yet available)	Strength predicted with flaws using various failure criteria for tension and shear only.	AS/3501-5A, T300/5208 and Hybrid
16.	"Stress Fracture Criteria for Laminated Composites Containing Stress Concentrations," J.M. Whitney and R.J. Nuismer, J. Composite Materials, Vol 8 (July 1974) p 253.	0.127 to 2.54 cm (0.05 to 1.0 in.) diam. holes and slots.	$(0/\pm45)_s$ $(0/\pm45/90)_s$ Static Tens. Limited test data used to verify analytical method	Initial description of "Average Stress Criterion" and "Point Stress Criterion"	Scotch ply glass/epoxy T300/5208 Gr/Ep.
17.	"The Determination of Fracture Strength in Orthotropic Graphite/Epoxy Laminates," H.J. Konish, Jr. and T.A. Cruse, AFML Contract No. F33615-73-C-5505.	0.51 to 2.54 cm (0.2 to 1.0 in.) slots.	Range of orientations, Static Tens.	Fracture mechanics approach. Critical strain energy release rate.	T300/5208
18.	"Tensile Strength of Notched Composites," T.A. Cruse, J. of Com. Materials, Vol. 7, April 1973.	Circular hole and rectangular notch.	$(0_2/+45/0_2/-45)_s$ $(0/\pm45)_{2s}$	Model for crack growth, fracture toughness, critical strain energy release rate.	T300/5208 Primarily an analytical study.

TABLE I. - Continued

Documents		Flaw Type	Experimental Data	Analysis Methods	Notes
Ref.	Title				
19.	"Compression Effects on the Fatigue of Notched Boron/Epoxy Composites," E.C. Durchlaub and R.B. Freeman, presented at the Second Conf. on Fibrous Composites in Flight Vehicle Design, 22-24 May 1974, Dayton, Ohio.	0.051 cm (0.02 in.) slot 1.22 cm (0.5 in.) diam. hole	$(0/\pm45/90)_s$ $(+45/0/-45/90)_s$ R = 10 and R = -2 constant amplitude fatigue	S-N fatigue data	Boron/Epoxy
20.	"Impact Damage Characteristics of Graphite/Epoxy Lamintes," N.M. Bhatia, Northrop Corp. NOR-76-186, June 1977.	Impact 1.5875 cm (0.625 in.) diam., steel)	Coupons, monolithic and sandwich panels, $\pi/4$ orientation, tens, static and fatigue	Fracture mechanics model, crack size vs. impact energy	AS/3501-5, hybrids with E-glass and Kevlar-49. Design curves for damage size vs. impact energy, strength vs. impact energy.
21.	"Service/Maintainability of Advanced Composite Structures," J.D. Labor, AFFDL-TR-155, November 1978.	Impact 1.5875 cm (0.625 in.) diam. spherical, plus "sharp" 1.5875 and 0.9525 cm (0.625 and 0.375 in.) in. diam.	Monolithic (8-32 ply) Sandwich (4-8 ply) $(0/\pm45/90)$ Impact energy vs. damage level data. Strength data being obtained.	None (limited correlation or impact test data with analytical prediction methods)	AS/3501-5, Boron/Ep, and hybrids. Instrumented impact data.

TABLE I. - Continued

Documents		Flaw Type	Experimental Data	Analysis Methods	Notes
Ref.	Title				
22.	"Investigation of Damage Tolerance of Graphite/Epoxy Structures and Related Design Implications." N.R. Adsit and J.P. Waszczak. NADC-76387-30, December 1976.	Impact 0.635 to 2.54 cm (0.25 to 1.0 in.) diam., steel. FOD less than 0.635 cm (0.25 in.) diam. stone	Stiffened Panel $(\pm 45/0_2/\mp 45)_s$ Sandwich panel $(0/\pm 45/0)_s$ Tens. & Compr. Static & Fatigue.	-	AS/3501-5. Plots of damage vs. impact energy. Residual strength vs. impact energy.
23.	"Impact Fracture of Composite Sandwich Structures," M.D. Rhodes, AIAA paper 75-748.	FOD 1.27 cm (0.5 in.) diam. Al sphere, 170.8 - 722.6 m/sec. (52 to 220 fps)	Sandwich panel 4 to 12-ply (0/90) Tens. & Compr. static	-	Type "A" & T300 Gr/Ep, Kevlar-49/Ep hybrids
24.	"Low Velocity Transverse Normal Impact of Gr/Ep Composite Laminates," E.J. McQuillen, L.W. Gause, and R.E. Llorens, Jol. of Composite Materials, Vol. 10, pp. 79-91, January 1976.	Impact 0.51 cm (0.2 in.) diam sphere and rod	Wide beam $(\pm 45/0_2/\mp 45)_s$ Short beam shear static	Modal solution for transient response of beam.	Gr/Ep, theory-experimental correlation shown to be good.
25.	"Effect of Low Velocity Impact Damage on the Compressive Strength of Graphite/Epoxy Hat-Stiffened Panels," M.D. Rhodes, J.G. Williams, and J.H. Starnes, Jr., NASA TMX-73988, Dec. 1976.	FOD 1.27 cm (0.5 in.) diam. Al sphere, 54.8 m/sec (180 fps) Hole 1.27 cm (0.5 in.) diam.	Minimum weight hat stiffened, $(\pm 52/\mp 52)_{2s}$ $(\pm 45/\mp 45)_{2s}$ Compr. static, buckling strength	-	T300/5208 Strength reduction up to 50% observed.

TABLE I. - Continued

Documents		Flaw Type	Experimental Data	Analysis Methods	Notes
Ref.	Title				
26.	"Evaluation of Ballistic Damage Resistance and Failure Mechanisms of Composite Materials," E.F. Olster and H.A. Woodbury, AFML-TR-72-79, 1972.	Ballistic Impact (30 & 50 caliber projectiles)	Panels, several orientations, Tens., Static, fracture toughness. Residual strength of preloaded panels.	Fracture mechanics approach to predict residual strength.	T50S/5206, Boron/Ep, S901/Glass/5209, Al 6061-T6. High speed photos of crack growth.
27.	"Evaluation of Fracture in Notched Composite Laminates," S.V. Kulkarni and B.W. Rosen, Materials Sciences Corporation Report No. MSC/TFR/606/1031, October 1976.	Idealized holes and slots.	None (Data from other sources used)	Tension strength prediction model.	Computer program "LACA" for strength prediction.
28.	"Some Observations on Fracture Behavior of Advanced Fiber Reinforced Laminates," G.P. Sendeckyj, Proc. of 12 Annual Meeting of Society of Engineering Science, Austin, Texas, 20-22 October 1975.	Idealized scratch and slot	None (Data from other sources used)	Tension strength for scratch, fracture toughness vs. slot size.	Theory-experimental correlation shown to be good.
29.	"Investigation of Failure Mechanism in Fiber Composite Laminates," P.V. McLaughlin, Materials Sciences Corporation, TFR/7508, Final Report on NADC Contract N62269-74-C-0662, 1975.	Scratch (1-ply deep across entire width)	None	Model considers interlaminar stresses in region of flaw and stress concentration in adjacent plies to predict ultimate failure.	$[90/0]_s$ under tension, $[\pm 45]_s$ under tension, $[0/\pm 45]_s$ under biaxial tension and shear.

TABLE I. - Continued

Documents		Flaw Type	Experimental Data	Analysis Methods	Notes
Ref.	Title				
30.	"Characterization of Composites for the Purpose of Reliability Evaluation," J.C. Halpin, K.L. Jerina, and T.A. Johnson, ASTM STP 521, 1973.	No specific type.	Some wearout and open hole data.	Wearout procedure	Good overview, provides overall philosophy for design.
31.	"Fatigue of Notched Composites," P.V. McLaughlin, Jr., S.V. Kulkarni, S.N. Huang, and B.W. Rosen, Third Conference on Fibrous Composites in Flight Vehicle Design, NASA TM X-3377.	Idealized slots.	None	A procedure for predicting static and fatigue strength outlined.	Axial, transverse and off-axis failure stresses are computed to predict laminate failure.
32.	"Fracture Mechanics and Composite Materials: A Critical Analysis," C. Zweben, ASTM STP 521, 1973.	Slots	-	Discussion of several hypotheses for fracture	Primarily a survey and fracture mechanics model development effort.
33.	"Residual Strength Characterization of Laminated Composites Subjected to Impact Loading," G.E. Husman, J.M. Whitney, and J.C. Halpin, ASTM STP 568, 1975, pp. 92-113.	FOD 0.45 cm and 0.61 cm (0.177 in. & 0.24 in.) diam. steel projectile, 45.7 to 304.8 m/sec. (150 to 1000 fps)	Coupons 12-ply (0/90) orientations. Tens., static strength.	Fracture mechanics based model to predict residual strength. Bowie solution used for laminate with hole.	Several Gr/Ep and Gl/Ep systems. Application of analysis procedure limited to damage considerably less than through penetration.

TABLE I. - Continued

Documents		Flaw Type	Experimental Data	Analysis Methods	Notes
Ref.	Title				
34.	"Investigation of Brittle Fractures in Graphite-Epoxy Composites Subject to Impact," L.B. Greszczuk and H. Chao, USAAMRDL-TR-75-15, May 1975.	FOD 3.8 cm (1.5 in.) diam. steel sphere, velocities up to 91.4 m/sec (300 fps.) Damage varied from none to 7.6 cm (3 in.) long cracks.	Panels 0.168, 0.353, and 0.660 cm (0.066, 0.139, and 0.260 in.). Cylinders 7.6 and 15.2 cm (3 and 6 in. size), (0/90) orientation. Threshold energy level to cause initial damage.	Theory to relate impact velocity and energy to damage zone. No strength prediction.	Several Gr/Ep systems and hybrid laminates.
35.	"Structural Integrity Requirements for Projectile Impact Damage - An Overview," J.G. Avery, T.R. Porter, and R.W. Lauzze, AGARD Conf. Proc. No. 186, Specialists Meeting on Impact Damage Tolerance of Structures, Oct. 1975.	Ballistic Damage (wide range of sizes)	-	Design methodology for damage tolerance including fatigue and fail-safe criteria.	Composite and metal structures.
36.	"Impact Behavior of Polymeric Matrix Composite Materials," Peichichon and R. Mortimer, AFML-TR-76-242, Dec. 1976.	FOD (Gelatin, Al and steel projectiles).	Cantilever plate $[(0/45/0/-45)_6/0]_s$	One-degree-of-freedom impact model, finite-difference model.	AS/3501 Fan blade applications.
37.	"Hard Object Impact Damage of Metal Matrix Composites," J. Awerbuch and H.T. Hahn, J. of Comp. Materials, Vol. 10, July 1976.	FOD 0.45 cm (0.177 in.) diam. steel. Velocities from 15.2 to 274.3 m/sec (50 to 900 fps).	Cantilever beam, 6 to 8 ply. Tens., static residual strength.	Crack size and residual strength vs. impact energy.	B/Al and Borsic/Ti, photomicrographs of impact damaged cross-sections.

TABLE I. - Continued

Documents		Flaw Type	Experimental Data	Analysis Methods	Notes
Ref.	Title				
38.	"Impact Behavior of Graphite/ Epoxy Simulated Fan Blades," T.S. Cook and J.L. Preston, Jr., Paper Submitted to the AIAA Journal of Aircraft (Paper No. 77-365).	FOD (spherical projectiles) - 1.27 cm (0.5 in.) diam. gelatin and ice, 0.635 cm (0.25 in.) diam. steel)	Cantilever Beam, diamond shaped cross-section, level of damage determined.	-	Modmor II/286 Gr/Ep, fan blade application
39.	"Material Variables Affecting the Impact Resistance of Graphite and Boron Composites," R.C. Novak, AFML-TR-74-196, June 1975.	FOD 1.27 cm (0.5 in.) diam. gelatin projectiles, velocities from 30.5 to 274.3 m/ sec (100 to 900 fps)	Cantilever beam, diamond shape, (±45/0/±45) ply orientation. Tens. static, bending, charpy and ballistic impact tests.	None	Several Gr, Boron, S-glass, and Kevlar 49 fibers in polysulfone and epoxy matrix. Fan blade.
40.	"A Scanning Electron Microscopic Study of Hybrid Composite Impact Response," D.F. Adams, J. of Materials Science, Vol. 10, pp. 1591-1602, 1975.	Notch	Notched and unnotched charpy specimens, unidirectional and (0/±45/90) orientations. Instrumented impact tests.	None	Rigidite 5206 Gr/Ep, hybrids with glass, Kevlar 49 and nylon fibers. Macrophotographs of failure zones provided.
41.	"Dynamic Response of Anisotropic Laminated Plates under Initial Stress to Impact of a Mass," C.T. Sun and S. Chattopadhyay, AFML-TR-74-258, March 1976.	Impact	None	Modal response solution, Hertz contact force.	-

TABLE I. - Continued

Documents		Flaw Type	Experimental Data	Analysis Methods	Notes
Ref.	Title				
42.	"Large Area Composite Structure Repair," A.L. Scow and R.W. Kiger, AFFDL-TR-77-5, First Interim Report, May 1977, Northrop Corp.	None	Lap joints and scarf joints in monolithic and sandwich panels. Tens. static, exposed to fuel, moisture, and hydraulic fluid at room temp. and 130°C (265°F).	Bonded joint design using relative adherend stiffness of each ply.	Primarily reports development of repair methods rather than effect of defects
43.	"Large Area Composite Structure Repair," R.W. Kiger and S.H. Myhre, AFFDL-TR-77-121, Second Interim Report, November 1977, Northrop Corp.	None			
44.	"Advanced Development of Conceptual Hardware Horizontal Stabilizer," Grumman Aerospace Corp., AFML contract.	Voids 1.27 x 1.27 cm (0.5 x 0.5 in). Spread tows less than 0.635 cm (0.25 in.). Gap 7.6 cm (3 in.) long. Scratch (2-ply deep). Fillet radius void 0.127 cm x 20.3 cm (0.05 x 8 in.). Fiber breakout (drilling), and thick bondline.	Flaws incorporated in test elements of stabilizer torque box. Failure loads shown to exceed design ultimate load.	None	AS/3501-5 and Gr-Boron Hybrid

TABLE I. - Concluded

Documents		Flaw Type	Experimental Data	Analysis Methods	Notes
Ref.	Title				
45.	"Macroscopic Fracture Mechanics of Advanced Composite Materials," M.E. Waddoups, J.R. Eisenmann, and B.E. Kaminski, Journal of Composite Materials, Vol 5, 1971, pp. 446-454.	Holes 0.15 to 7.6 cm (0.06 to 3.0 in) diam. slots	$\left[0/\pm45\right]_{2s}$	Analytical model based on linear elastic fracture mechanics applied to holes & slots.	Graphite/epoxy
46.	"Fatigue Characteristics of Graphite/Epoxy Laminates Under Compression Loading," M.S. Rosenfeld and S.L. Huang, AIAA J. Aircraft, Vol. 15, No. 5, May 1978.	Holes 0.635 cm. (0.25 in.) diam.	$\left[0/\pm45)_s\right]_3$ compression fatigue S-N data		Narmco 5209 and AS/3501-6 Graphite/Epoxy
47.	"Some Observations on Fracture Behavior of Advanced Fiber-Reinforced Laminates," Sendeckyj, G.P., Proceedings of the 12th Annual Meeting of the Society of Engineering Science, University of Texas at Austin Press, 1975, pp. 625-634.	Scratches	None	Analytical model based on net section strength including bending effects.	Graphite/Epoxy

TABLE II. - RESIDUAL STRENGTH OF GRAPHITE/EPOXY LAMINATES WITH FLAWS (From Ref. 1)

Flaw Type	Flaw Size[3]	Laminate[1] Type	% of Unflawed Strength (Tension)			% of Unflawed Strength (Compression)		
			Static	2 LT T[4]	2 LT C[5]	Static	2 LT T[4]	2 LT C[5]
Through Slots	0.9525 cm (0.370 in), 45°	A	53	-	-	-	-	-
	0.9525 cm (0.370 in), 90°	A	44	-	-	-	-	-
	0.9525 cm (0.370 in), 45°	B	51	-	-	-	-	-
	0.9525 cm (0.370 in), 90°	B	47	-	-	-	-	-
Surface Scratch, Center	2.54 cm (1.0 in), 3-ply	A	69	69	69	103	92	100
	2.54 cm (1.0 in), 3-ply	B	55	63	62	103	90	94
	2.54 cm (1.0 in), 6-ply	B	50	53	54	88	84	81
Fastener Holes,(2) Countersunk	Two 0.476 cm (3/16 in)	A	48	49	51	82	75	79
	Two 0.476 cm (3/16 in)	B	52	56	58	91	83	81
	Two 0.635 cm (1/4")	B	53	55	-	94	-	86
Surface Scratch, Edge	2.54 cm (1.0 in), 3-ply	B	53	58	59	104	96	96
	1.27 cm (0.5 in), 3-ply	B	64	70	67	100	93	94
Low Pressure Cure	206.8kPa (30 psi)	A	110	112	98	88	78	93
	206.8kPa (30 psi)	B	97	102	99	88	85	73
	344.65kPa (50 psi)	B	101	94	106	106	104	99
Edge Delamination	1.524 cm (0.6 in), radius	A	91	103	-	81	-	101
	1.524 cm (0.6 in), radius	B	99	107	-	91	-	98
	0.762 cm (0.3 in) radius	A	95	106	-	92	-	101

NOTES: Material AS/3501-5 Graphite/Epoxy (Room temperature, Wet)
Cure Condition: 127°C (350F) for 30 minutes at 689.3K Pa (100 psi) pressure (Postcured 188°C (370F) for 4 hours)

(1) Laminate Types: A- 16-ply $(0_2, \pm 45, 0_2\ 90, 0)_s$

B- 16-ply $(0, \pm 45, 90)_{2s}$

(2) Test runs with fasteners installed.

(3) All specimens 5.1 cm (2 inches) wide.

(4) 2 LT T = 2 lifetimes of tension dominated fatigue, F-5E wing.

(5) 2 LT C = 2 lifetimes of compression dominated fatigue, F-5E wing.

TABLE III. - SUMMARY OF AIRLINE DAMAGE EXPERIENCE

Component Type	Defect Type	Probable Cause of Damage	Typical Defect Size cm (in.)	Typical Location of Defect on Component	Maintenance Action Required	Airline Code, Remarks ⚠
Wing skins	Cracks	Fatigue	1.27 - 3.8 (0.5-12.5)	Lower Skin	Maint. base - std. repair or Engr. disposition	E
			0.15 - 41 (0.06-16)			C
			2.54 - 12.7 (1-5)	Spar areas; rear spar	Maint. base - Engr. disposition	J, D
			2.54 - 7.6 (1-3)	Lower skin around access holes	Maint. base - std. repair	K
	Corrosion effects	Stress corrosion	1.27 - 2.54 (0.5-1)	Lower skin	Maint. base - std. repair or Engr. disposition.	E (Fairly infrequent);
					Line station or negligible	C (No sizes given)
			2.54 (1) dia.	Edges, around fasteners	Maint. base - Engr. disposition	B
			7.6 - 152 (3-60)	Lower skin, fwd. edge	Maint. base - std. repair	H (Large defects - infrequent occurrence)
			0.635 - 30.5 (1/4-12)	Upper and lower skins	Maintenance base repairs: 70% std. repairs, 30% Engr. dispositioned repairs	I
	Impact damage	Tire treads	7.6 x 15.2 (3 x 6)	Lower skin	Maint. base - std. repair or Engr. disposition	E (Fairly low frequency)
			Dings 5.1 (2) deep	Lower skin	Maint. base - Engr. disposition	A
		Ground equipment	-	Lower skin	Varies from negligible to line station repair to maint. base repairs	C
Wing stiffener elements	Cracks	Fatigue			Line station repairs, also maint. base repairs, both std. and Engr. dispositioned	C
		Stress Corrosion				
		Fatigue	5.1 - 10.2 (2-4)	Stringers	Maint. base - std. repair	J
			2.54 - 12.7 (1-5)	Stringers		D
			2.54 - 7.6 (1-3)	Stringers, lower skin		K
			5.1 (2) typ.	Radii	Maint. base - std. repair	G
			0.635 - 7.6 (1/4-3)	Spars, webs	Maintenance base repairs: 70% std. repairs, 30% Engr. dispositioned repairs	I
	Corrosion effects	Micro-organisms	-	Fuel tanks	Line station or maint. base repairs	C
		Stress corrosion	-	Surface area	Maint. base - Engr. repair	B (infrequent)

TABLE III. - Continued

Component Type	Defect Type	Probable Cause of Damage	Typical Defect Size cm (in.)	Typical Location of Defect on Component	Maintenance Action Required	Airline Code, Remarks ⚠
Wing leading edges	Cracks	Impact, wear	22.9 x 30.5 (9 x 12)	Leading edges	Maint. base - std. repair, occas. line station	E (occurrence in moderate freq.)
			5.1 x 12.7 (2 x 5)	Leading edge	Maint. base - std. repair	J
			2.54 - 12.7 (1-5)	Leading edge slats	Line station repair	D
			2.54 - 12.7 (1-5)	Fwd. edge	Negligible or line sta. repair	G (erosion major cause)
		Fatigue	5.1 (2) (typ.)	Fixed leading edge around access doors	Maint. base - std. repair	A
	Disbonds	Fatigue	50% of area	Leading edge	Replacement req'd	A
Wing trailing edges	Cracks	Poor bonding, excessive rigidity of core	5.1 to 1.5 meters (2-5 feet)		Maint. base - Engr. repair	F
		Impact	22.9 - 30.5 (9-12)	Trailing edge member	Maint. base - std. repair	E
		Fatigue	2.54 - 12.7 (1-5)	Trailing edge member	Line repair	D
		Fatigue	7.0 (2-3/4) typ.	Lower caps of trailing edge	Maint. base - Engr. repair	A
	Delaminations, disbonds	Poor bonding	25.81 cm^2 - 2580 cm^2 (4 in^2 - 400 in^2)		Maint. base - Engr. repair	F
		Impact, corrosion, lightning, wear	7.6 - 10.2 (3-4)		Line repair; maint. base repair, std. and Engr.; part replacement	J
		Fatigue	2.54 - 12.7 (1-5)	Trailing edge member	Line repair	D
		Impact (tire recaps), wear	2.54 - 17.8 (1-7)	Panel center	Maint. base - std. and Engr. repair	G
		Tire impact	40.6 x 40.6 (16 x 16) typ.	Upper inboard area	Maint. base - std. repair	A
		Impact, lightning	7.6 - 76.2 (3-30)	Trailing edge member	Line station repair; replace part	B
Wing control surfaces	Cracks	Fatigue, corrosion			Line repair; maint. base std. and Engr. repair	C
		Fatigue	10.2 - 15.2 (4-6)	Trailing edge flaps, leading edge slats	Maint. base - std. repair	A
		Fretting Fatigue	Variable	Spoiler along wings attach fitting	Part replacement	H

TABLE III. - Continued

Component Type	Defect Type	Probable Cause of Damage	Typical Defect Size cm (in.)	Typical Location of Defect on Component	Maintenance Action Required	Airline Code Remarks ⚠
Wing control surfaces (cont.)	Impact damage	-	15.2 x 15.2 (6 x 6) typ.	Trailing edge areas	Maint. base - std. repair; line station	E (moderate frequency
		Ground equipment			Negligible: line repair; maint. base repair - std. and Engr.	C
		Tire tread loss	Variable	Trailing edge flap, leading edges	Maint. base - std. repair; interim line repairs	H
		Tire	Up to 50% of area		Maint. base - Engr. repair	A
		Hail (cracks, dents all over area)			Part replacement	K
	Delaminations, disbonds	Corrosion	10.2 (4) dia. typ.	Trailing edge areas	Maint. base - std. repair	E
			-	-	Maint. base - std. or Engr. repair.	C
			2.54 - 20.3 (1-8)	Skin		B
			Extensive	Upper and lower skins	Maint. base - std. repair	K
			25.8 cm^2 - 2580 cm^2 (4 in^2 - 400 in^2)	Random	Maint. base - Engr. repair	F
		Poor factory bond	Variable	Trailing edge flaps	Part replacement	H
		Impact, lightning	7.6 - 10.2 (3-4) dia.	Honeycomb areas	Negligible: line repairs; maint. base std. repairs	J
		Impact	5.1 - 15.2 (2-6)	Flaps	Line repairs; maint. base std. repairs	D
		Impact (tires); wear; corrosion	30.5 (12) typ.	Panel center	Line repairs; maint. base std. and Engr. repairs	G
	Corrosion effects	-			Negligible; line repairs; maint. base std. and Engr. repairs	C
			30.5 (12) typ.	Panel center	Line repairs; maint. base std. and Engr. repairs	G
			5.1 - 15.2 (2-6)	Flaps	Line repairs; maint. base std. repair	D
Wing sub-structure	Cracks	Fatigue	3.8 - 7.6 (1-1/2 - 3)	Flange radii	Maint. base - std. repair	E (moderate frequency)
			5.1 - 15.2 (2-6)	Spars, rib		D
			2.54 - 7.6 (1-3)	Spar lower chord		K
			0.635 - 20.3 (1/4 - 8)	Spars, webs	Maintenance base repair; 30% std. repairs, 70% Engr. dispositioned repairs	I

TABLE III. - Continued

Component Type	Defect Type	Probable Cause of Damage	Typical Defect Size cm (in.)	Typical Location of Defect on Component	Maintenance Action Required	Airline Code Remarks ⚠
Wing sub-structure (cont.)	Cracks (cont.)	Fatigue and corrosion			Maint. base - std. and Engr. repair	C
	Corrosion	Coating breakdown		Surface	Maint. base - Engr. repair	B
Wing fairings	Cracks	Fatigue, corrosion			Negligible; line repair; maint. base repairs - std. and Engr.	C
		Impact	5.1 - 30.5 (2-12)		Maint. base - std. repair	D
		Aerodynamic vibration loads	Up to 1.5 meters (5 feet)		Maint. base - std. repair or part replacement	H
			0.16 - 2.54 (1/16 - 1)	Skin	Negligible. Repair not required	I
	Delaminations, disbonds	Corrosion			Negligible; line repairs; maint. base - std. and Engr. repairs	C
		Impact	5.1 - 30.5 (2-12)		Maint. base - std. repair	D
		Aerodynamic vibration loads	Up to 3.65 meters (12 feet)		Maint. base - std. repair or part replacement	H
	Wear; Fastener hole elongation	Design problems			Negligible; line repair; maint. base - std. and Engr. repairs	C
	Wear	Vibration	0.16 - 2.54 (1/16 - 1)	Skin	Negligible. Repair not required	I
	Impact	Tire	22.9 x 61.0 (9 x 24)	MLG hinge strut door	Maint. base - std. repair	A
Wing - fuselage joint	Cracks	Corrosion effects initating fastener peel. Wear.	Varies	Attachment holes	Line repair. Maint. base std. repair	J
		Fatigue, resulting from poor design	2.54 - 20.3 (1-8)	Drag angle upper wing; fuselage - to wing center	Maint. base - std. repair	K
	Corrosion effects		5.1 - 15.2 (2-6)	Fuselage joint	Maint. base - Engr. repair	D
		Stress corrosion		Attach TEE	Maint. base - Engr. repair or part replacement	B
Wing, Hinge and actuator joints	Wear		61.0 (24) length	Hinges	Maint. base - engr. repair	D
Horizontal stabilizer skins	Cracks	Fatigue, stress corrosion, impact	0.15 - 40.6 (0.06-16)		Maint. base - std. and Engr. repairs	C
		Fatigue	2.54 - 12.7 (1-5)	Spar skin area	Maint. base - std. repair	D

TABLE III. - Continued

Component Type	Defect Type	Probable Cause of Damage	Typical Defect Size cm (in.)	Typical Location of Defect on Component	Maintenance Action Required	Airline, Code Remarks ⚠
Horizontal stabilizer skins (cont.)	Impact damage (puncture)	DLC struct door lost in flight		Horizontal stabilizer lower surface	Maint. base - Engr. repair	A
Horizontal stabilizer stiffener elements	Cracks	Strain corrosion			Maint. base - std. and Engr. repair	C
		Fatigue	5.1 - 10.2 (2-4)	Stringers	Maint. base - std. repair	J
			2.54 - 12.7 (1-5)	Stiffeners		D
			1.27 - 2.54 (0.5-1)	Stiffeners		K
	Disbonds	Fatigue	5.1 - 10.2 (2-4)	Stringers	Maint. base - std. repair	J
Horizontal stabilizer leading edges	Impact damage (cracks, dents, punctures)		22.9 x 30.5 (9 x 12)	Leading edge	Maint. base - std. repair; occasional line repair	E (moderately frequent occurrence)
			2.54 - 12.7 (1-5)	Leading edge skins	Line repair	D
		Hail; sonic fatigue	2.54 - 20.3 (1-8)	Panel edges	Negligible; line repair: maint. base std. repairs	G
		Bird impact	2.54 - 10.2 (1-4)	Leading edge	Maint. base - std. repair (riveted, flush)	K
	Wear		2.54 - 20.3 (1-8)	Panel edges	Negligible; line repair; maint. base - std. repairs	G
		Rain, sand		Nose	Maint. base, Engr. repair or part replacement	B (continuous problem)
Horizontal stabilizer trailing edges	Cracks	Fatigue	2.54 - 12.7 (1-5)	Trailing edge stiffeners	Line repairs	D
			7.6 x 2.54 (3 x 1) typ.	Inboard closure rib, aft end	Maint. base - std. repair	A
		Impact	2.54 - 25.4 (1-10)	Panel edges and center	Negligible; line repair; maint. base - std. repair	G
	Corrosion effects		1.27 - 2.54 (1/2 - 1)	Trailing edges	Maint. base - std. repair	E (moderate frequency)
	Delaminations, disbonds		5.1 - 15.2 (2-6)	Trailing edges	Maint. base - Engr. repair	B
	Cracks, punctures	Lightning	5.1 x 15.2 (2 x 6)	Trailing edge	Maint. base - Engr. repair	B
Horizontal stabilizer control surfaces	Cracks	Fatigue; corrosion			Line repairs; maint. base std and Engr. repairs	G
		Impact	2.54 - 50.8 (1-20)	Edges	Negligible; line repairs; maint. base - std. repairs	G
	Impact damage	Ground equipment			Negligible; line repair; maint. base std and Engr. repairs.	C
		Ground equipment	5.1 x 21.7 (2 x 5)	Elevator trailing edge	Maint. base - std. repair	A

TABLE III. - Continued

Component Type	Defect Type	Probable Cause of Damage	Typical Defect Size cm (in.)	Typical Location of Defect on Component	Maintenance Action Required	Airline Code, Remarks ⚠
Horizontal stabilizer control surfaces (cont.)	Impact damage (cont.)	Ground equipment (cont.)	12.7 x 17.8 (5 x 7)	Elevator upper skin	Maint. base - Engr. repair	A
	Delaminations, disbonds	Poor factory bonds corrosion	12.9 cm^2 - 25.8 cm^2 (2 in^2 - 4 in^2)		Maint. base - Engr. repair	F
			10.2 (4) dia.	Trailing edges	Maint. base - std. repair	E (moderate frequency)
					Maint. base - std. and Engr. repairs	C
			5.1 - 15.2 (2-6)	All areas		B
			2.54 - 50.8 (1-20)	Edges	Negligible; line repairs: maint. base std. repairs	G
			5.1 - 15.2 (2-6)	Honeycomb area	Maint. base - std. repair	D
Horizontal stabilizer sub-structure	Cracks	Fatigue	3.8 - 7.6 (1-1/2 - 3)	Flange radii	Maint. base - std. repair	E (moderate frequency)
			5.1 - 12.7 (2-5)	Spars		D
		Fatigue; corrosion (general corrosion effects)			Maint. base - std. and Engr. repairs	C
		Stress corrosion	3.8 - 7.6 (1-1/2 - 3)	Spars	Maint. base - Engr. repair	B
Horizontal stabilizer fairings	Fatigue; corrosion				Negligible; line repairs; maint. base std. and Engr. repairs.	C
	Impact		7.6 x 30.5 (3 x 12)	All areas	Maint. base - std. repair	D
	Delaminations, disbonds	Wear; lightning; corrosion			Negligible; line repairs; maint. base std. and Engr. repairs	C
		Poor factory bond		Lower face, upper trailing edge panel	Part replacement	H
	Wear	-		Leading and trailing edges	Maint. base - std. repair	K
Horizontal stabilizer - fuselage joint	Cracks	Corrosion		Attachment holes	Line repairs; maint. base std. repairs	J
	Wear			Attachment holes		
	Corrosion effects	Condensation	5.1 - 15.2 (2-6)	Bolted joint area	Maint. base - std. repair	D
	Elongated holes	Wear			Line repair; maint. base - std. repair ; part replacement	B

TABLE III. - Continued

Component Type	Defect Type	Probable Cause of Damage	Typical Defect Size cm (in.)	Type Location of Defect on Component	Maintenance Action Required	Airline Code, Remakrs ⚠
Horizontal stabilizer - hinge actuator joints	Wear	-	61.0 (24) typ.	Hinges	Maint. base - Engr. repair	D
	Cracks; elongated holes	Wear			Line repairs; maint. base std. repairs	B
Vertical stabilizer - skins	Cracks	Fatigue; stress corrosion	0.15 - 40.6 (0.06-16)		Maint. base - std. or Engr. repair	C
		Fatigue	5.1 - 15.2 (2-6)	Entire skin area	Maint. base - std. repair	D (occurs very seldom)
			2.54 - 7.6 (1-3)			K (stiffness/frequency problem)
		Fatigue; impact	2.54 - 20.3 (1-8)	Center	Line repair; maint. base std. repair	G
Vertical stabilizer - stiffener elements	Cracks	Fatigue; corrosion			Maint. base - std. or Engr. repair	C
		Fatigue	5.1 - 15.2 (2-6)	Stiffeners	Maint. base - std. repair	D (occurs very seldom)
Vertical stabilizer - leading edges	Cracks	Fatigue	2.54 - 5.1 (1-2)	Leading edge	Line repair	D (occurs very seldom)
		Impact	2.54 - 20.3 (1-8)	Leading edge	Negligible; line repair	G
		Impact (bird strike)	2.54 - 10.2 (1-4)	Leading edge	Maint. base - std. repair	K (flush, riveted patch)
	Wear	Rain/sand		Nose	Maint. base - Engr. repair; part replacement	B
		Erosion	2.54 - 20.3 (1-8)	Leading edges	Negligible; line repair	G
Vertical stabilizer - trailing edges	Cracks	Fatigue	2.54 - 10.2 (1-4)	Trailing edge	Maint. base - std. repair	D
Vertical stabilizer - control surfaces	Cracks	Fatigue; corrosion			Line repair; maint. base std. and Engr. repair	C
		Impact; fatigue	2.54 - 25.4 (1-10)	Center area, rudder	Line repair; maint. base std. repair	G
	Corrosion effects				Negligible; line repair; maint. base std. and Engr. repair	C
	Impact damage	Ground equipment			Negligible; line repair; maint. base std. and Engr. repair	C
	Delaminations, disbonds	Corrosion	10.2 (4) dia.	Trailing edges	Maint. base - std. repair	E (moderate frequency)
					Maint. base - std. and Engr. repairs	C
			5.1 - 25.4 (2-10)	Honeycomb	Maint. base - std. repair	D

TABLE III. - Continued

Component Type	Defect Type	Probable Cause of Damge	Typical Defect Size cm (in.)	Typical Location of Defect on Component	Maintenance Action Required	Airline Code, Remarks ⚠
Vertical stabilizer - control surfaces (cont.)	Delaminations, disbonds (cont.)	Corrosion (cont.)	5.1 - 15.2 (2-6)	All areas	Maint. base - std. and Engr. repairs	B
Vertical stabilizer - sub-structure	Cracks	Fatigue	3.8 - 7.6 (1-1/2 - 3)	Flange radii	Maint. base - std. repair	E (Moderate frequency)
			5.1 - 15.2 (2-6)	Spars	Maint. base - std. repair	D (very seldom)
			15.2 (6) typ.	Ribs, doublers	Maint. base - Engr. repair	B
		Corrosion; fatigue			Maint. base - std. and Engr. repair	C
Vertical stabilizer - fairings	Cracks	Fatigue; corrosion			Negligible; line repair; maint. base - std and Engr. repairs	C
		Fatigue	10.2 - 30.5 (4-12)	Trailing edge, top	Maint. base - Engr. repair (Part rebuilt)	B
	Wear		5.1 - 25.4 (2-10)	Entire area	Line repair	D
	Wear, elongated fastener holes	Poor design			Negligible; line repair; maint. base - std. and Engr. repair	C
	Delaminations, disbonds	Corrosion			Negligible; line repair; maint. base - std and Engr. repairs	C
		Fatigue	10.2 - 30.5 (4-12)	Trailing edge, top	Maint. base - Engr. repair	B
	Corrosion effects				Negligible; line repairs; maint. base - std. and Engr. repairs.	C
Vertical stabilizer - fuselage joint	Corrosion			Joint	Maint. base - std. repair	D
	Cracks	Fatigue	10.2 (4)	Radius of attach angle	Maint. base - Engr. repair	B (minor problem)
Vertical stabilizer - hinge actuator joints	Cracks	Fatigue	5.1 - 15.2 (2-6)	Fittings	Maint. base - std. repair	D
Fuselage skins	Impact	Ground equipment		Around doors	Line repair; maint. base std. and Engr. repairs	J
			10.2 x 30.5 (4 x 12)	Exterior	Maint. base - Engr. repair; occas. line station repair	E (low frequency)
			5.1 - 61.0 (2-24)	Near doors	Line repair; maint. base std. repairs	D

TABLE III. - Continued

Component Type	Defect Type	Probable Cause of Damage	Typical Defect Size cm (in.)	Typical Location of Defect on Component	Maintenance Action Required	Airline Code, Remarks ⚠
Fuselage skins (cont.)	Impact (cont.)	Ground equipment (cont.)	2.54 - 17.8 (1-7) (occas. up to 91.4) (36)	Below cabin floors	Negligible; line repair; maint. base - std. repair	G
			5.1 - 190.5 (2-75)	RH lower area, cargo, service areas	Maint. base - Engr. repair	B (frequent)
			0.159 - 10.2 (1/16 - 4)	All skin areas	80% line repairs; 30% maintenance base std. repairs	I
	Corrosion effects	Water, fluids collecting	7.6 - 15.2 (3 x 6)	Faying surfaces	Maint. base - std. repair	E (fairly high frequency)
				Around doors	Line repairs; maint. base std. and Engr. repairs	J
			5.1 - 61.0 (2-24)	Bilge	Line repair; maint. base std. repair	D
			2.54 - 17.8 (1-7)	Below cabin floor	Negligible; line repair; maint. base std. repair	G
			2.54 - 20.3 (1-8)	Bilge	Maint. base Engr. repair	E (frequent)
				Lap seams (intergranular corrosion)	Line repair	H
	Cracks	Fatigue	2.54 - 10.2 (1-4)	Sides, overwing area	Maint. base - Engr. repair	B (rare, results from hard landings)
			0.159 - 10.2 (1/16 - 4)	All skin areas	80% line repairs, 30% maintenance base, std. repairs	I
		Corrosion (moisture, fluids)		Lower lobe	Maint. base - std. repair	K (poor drainage)
		Corrosion (intergranular)		Along stringer rivet line	Line repairs	H
Fuselage frames	Cracks	Fatigue	7.6 - 10.2 (3-4)	Flange radii	Maint. base - std. repair	E (fairly high frequency)
			5.1 - 10.2 (2-4)	Complete area	Line repair; maint. base std. repair	D
			3.8 (1-1/2)	Brace at lower end	Maint. base - Engr. repair	A
		Corrosion	5.1 - 10.2 (2-4)	Upper and lower areas	Line repair; maint. base Std. repair	D
			2.54 - 30.5 (1-12)	Radii (All areas on 7079 alloys 727; other A/C in lavatory areas)	Maint. base - Engr. repair	G (stress corrosion)
			2.54 - 30.5 (1-12)	Overwing Tee	Maint. base - Engr. repair	B (stress corrosion)
Fuselage stringers	Cracks	Impact			Line repair; maint. base Std. and Engr. repairs	J
	Impact damage		30.5 (12)		Maint. base - std. repairs; line station repair on rare occasions	E (fairly low frequency)

TABLE III. - Continued

Component Type	Defect Type	Probable Cause of Damage	Typical Defect Size cm (in.)	Typical Location of Defect on Component	Maintenance Action Required	Airline Code, Remarks ⚠
Fuselage stringers (cont.)	Impact damage (cont.)		7.6 - 30.5 (3-12)	Chordwise location	Maint. base - Engr. repair	G
	Corrosion				Line repairs; maint. base std. and Engr. repairs	J
		Poor insulation		Upper and lower areas	Line repairs; maint. base std. repairs	D
	Cracks	Fatigue	5.1 - 10.2 (2-4)	Complete area	Line repair; maint. base std repairs	D
Fuselage bulkheads	Cracks	Fatigue	5.1 - 15.2 (2-6)	Complete area	Line repair; maint. base std. repairs	D
		Fatigue; impact corrosion	7.6 - 30.5 (3-12)	Around doors	Maint. base - Engr. repair	B
	Corrosion effects	Poor drainage	15.2 - 50.8 (6-20)	Lower section	Maint. base - Engr. repair	B
Fuselage doors	Cracks	Fatigue	3.8 - 7.6 (1-1/2 - 3)	Flange radii	Maint. base - std. repair	E (fairly low frequency)
			5.1 - 61.0 (2-24)	Outer frame	Line repair; maint. base std. repair	G
			5.1 - 20.3 (2-8)	Pan	Maint. base - Engr. repair	B
		Impact			Line repair; maint. base std. repair	J
	Impact damage	Ground handling	5.1 - 15.2 (2-6)	Complete area	Maint. base - std. repair; Part replacement	D
			5.1 - 61.0 (2-24)	Outer frame	Line repair; maint. base - std. repair	G
			0.159 (1/16) up to 20.3 x 20.2 (8 x 8) area	Skin and frame	70% line repairs; 30% Engr. base maint. repair	I
	Wear				Line repair; maint. base - std. repair	J
	Corrosion effects (incl. cracks)			Full panel	Maint. base Engr. repair	B
Floor beams and posts	Cracks	Fatigue	5.1 - 15.2 (2-6)	Complete area	Maint. base - Engr. and std. repairs	D
			2.54 - 15.2 (1-6)	Web	Maint. base - Engr. repair	B (minor problem)
				Beam web	Line repair; maint. base - std. repair	H
		Corrosion	2.54 - 5.1 (1-2)	Under galleys at entrance	Maint. base - std. repair	K (poor sealing, galvanic action steel fasteners to aluminum)
	Wear; corrosion effects		2.54 - 15.2 (1-6)	Web	Maint. base - Engr. repair	B (minor problem)

TABLE III. - Continued

Component Type	Defect Type	Probable Cause of Damage	Typical Defect Size cm (in.)	Typical Location of Defect on Component	Maintenance Action Required	Airline Code Remarks ⚠
Floor panels	Impact		30.5 (12) dia.		Part replacement	E (fairly high frequency
		Normal service; also wear effects		Galley and lavatory areas	Part replacement	J
		Ground handling	25.4 x 30.5 (10 x 12)	Cargo compartment	Maint. base - std. repair	A
		Normal service	15.2 - 61.0 (6-24)		Part replacement	D
	Corrosion effects; cracks		Full panel		Part replacement	B
		Waste water leakage	Entire part	Cabin floor support hat	Maint. base - std. repair	A
	Delaminations, disbonds	Normal service	15.2 - 61.0 (6-24)		Part replacement	D
				Galley and lavatory areas	Part replacement	J
				Upper face	Part replacement	H
		Corrosion		Entire panel	Part replacement	G
Fuselage fairings	Impact; wear		2.54 - 15.2 (1-6)	Center	Negligible: line repair; part replacement	G
			15.2 - 61.0 (6-24)	Adjacent to doors	Maint. base - std. repair; part replacement	D
		Ground vehicle	2.54 x 15.2 (1 x 6)	Near galley service door	Maint. base - std. repair	A
			2.54 - 15.2 (1-6)	Entire area	Maint. base - Engr. repair	B
		External forces			Negligible; line repair	H
	Delaminations, disbonds		30.5 (12) dia.		Maint. base - std. repair	E (fairly low frequency)
			15.2 - 61.0 (6-24)	Adjacent to door	Maint. base - std. repair; part replacement	D
		Poor landing	25.8 cm^2 - 0.74 m^2 (4 in^2 - 8 ft^2)	Panel center	Maint. base - Engr. repair	F
		Impact, fatigue	2.54 - 15.2 (1-6)	Entire area	Maint. base - Engr. repair	B
	Cracks	Air loads		Attach points, supports	Line repairs	H
	Elongated fastener holes				Negligible; line repair; part replacement	G
		Fatigue		Entire area	Maint. base - Engr. repair	B (minor problem)

TABLE III. - Continued

Component Type	Defect Type	Probable Cause of Damage	Typical Defect Size cm (in.)	Typical Location of Defect on Component	Maintenance Action Required	Airline Code Remarks ⚠
Radomes	Delaminations, disbonds	Water ingestion	15.2 - 61.0 (6-24)	Entire area	Maint. base - std. repair; part replacement	D
		Impact	2.54 - 17.8 (1-7)	Center	Negligible; part replacement	G
		Moisture	15.2 (6)	Nose	Maint. base - Engr. repair	B
	Impact damage		15.2 - 61.0 (6-24)	Entire area	Maint. base - std. repair; part replacement	D
		Hail, bird strike	2.54 - 17.8 (1-7)	Center	Negligible; part replacement	G
	Lightning		2.54 - 17.8 (1-7)	Center	Negligible; part replacement	G
	Cracks	Hail, moisture			Maint. base - std. repair	K
Engine cowling, support structure	Cracks	Heat	25.8 cm^2 - 0.74 m^2 (4 in^2 - 8 ft^2)	Center of panel	Maint. base - Engr. repair	F
			10.2 - 15.2 (4-6)	Back-up structure	Maint. base - Engr. repair	E
		Impact, wear			Line repair; maint. base - std. repair	J
		Fatigue	5.1 - 30.5 (2-12)	Complete area	Line repair; maint. base - std. repair	D
			7.6 (3)	Nose cowl aft bulkhead stiffeners	Maint. base - std. repair	A
Engine cowling, support structure	Impact		5.1 - 30.5 (2-12)	Complete area	Line repair, maint. base std. repair	D
		Ground vehicle	35.6 (14) Tear	Outer skin	Maint. base - std. repair	A
		Hangar collision	91.4 (36)	Center engine nose cowl lip	Maint. base - Engr. repair	A
	Disbonds	Heat	25.8 cm^2 - 0.74 m^2 (4 in^2 - 8 ft^2)	Center of panel	Maint. base - Engr. repair	F
	Wear	Interference with engine components			Line repair	H
	Elongated fastener holes	Fatigue			Maint. base - Engr. repair	B
Landing gear	Cracks	Corrosion			Maint. base - Engr. repair	J
		Hydrogen embrittlement	2.54 (1)	Main landing gear	-	K
		Fatigue	5.1 - 30.5 (2-12)	Doors	Line repair; maint. base std. repair	D

TABLE III. - Concluded

Component Type	Defect Type	Probable Cause of Damage	Typical Defect Size cm (in.)	Typical Location of Defect on Component	Maintenance Action Required	Airline Code, Remarks ⚠
Landing gear (cont.)	Corrosion effects			MLG logic pivot pin - entire part	Maint. base - Engr. repair	A
			1.27 - 10.2 (1/2-4)	Trunnion and struts	Maint. base - Engr. repair	B
	Delamination		5.1 - 30.5 (2-12)	Doors	Line repair; maint. base - std. repair	D
	Wear				Maint. base - Engr. repair	J
	Elongated fastener holes		1.27 - 10.2 (1/2-4)	Trunnion and struts	Maint. base - Engr. repair	B
Pylon	Cracks	Wear		Skin	Line repair; maint. base std. and Engr. repairs	J
		Fatigue	5.1 - 30.5 (2-12)	Skin and stringers	Line repair; maint. base std. repair	D
			5.1 - 50.8 (2-20)	Wing pylon glove fairing	Maint. base - std. repair;	A
			1.27 - 5.1 (1/2 - 2)	Spar	Maint. base Engr. repair; part replacement	B
			3.8 - 7.6 (1-1/2 - 3)	Lower spar web	Line repair	H
			2.54 - 20.3 (1-8)	Aft engine mount support rib	Line repair	H
	Delamination	Heat	90% of area	Wing pylon trailing edge fairing	Maint. base - std. repair	A
	Wear	Wind	2.54 - 12.7 (1-5)	Access door leading edge	Maint. base - std. repair	A
	Elongated fastener holes	Wear		Skins	Line repair; maint. base std. and Engr. repair	J

⚠ Participating airlines were randomly coded by the letters A through K

TABLE IV. - SUMMARY OF AIRLINE MAINTENANCE AND REPAIR PROCEDURES

Questions	Airline Responses △										
	A	B	C	D	E	F	G	H	I	J	K
For various types of damage, indicate percentage detected at line station and at the maintenance base. Is detection visual or by NDI?	1) Cracks: 30% line, Visual △	1) Cracks: 20% line, Visual, NDI	1) Cracks: 10% line, Visual, NDI	75% of all defects at line: 25% at maintenance base. 95% of detections are visual; 5% NDI	1) Cracks: 10% line, Visual, NDI	1) Cracks: 20% line	1) Cracks: 20% line, Visual NDI	1) Cracks: 0% line, Visual	1) Cracks: 15% line, Visual, NDI	1) Cracks: 30% line, NDI, Some Visual	1) Cracks: 30% line
	2) Disbonds: 15% line, Visual & NDI	2) Delaminations: 15% line, Visual NDI	2) Delaminations, disbonds <10% line, Visual		2) Delaminations: 10% line, Visual	2) Disbonds: 2% line	2) Delaminations: 20% line, Visual NDI	2) Delaminations; 0% line, Visual	2) Delaminations, disbonds: 10% line, Visual	2) Delaminations: 20% line, Visual	2) Delaminations: 20% line
	3) Impact: 80% line, Visual	3) Disbonds: 0% line, Coin tap	3) Impact: 90% line, Visual		3) Impact: 90% line, Visual	3) Wear; 5% line	3) Impact: 70% line, Visual	3) Impact: 50% line, Visual	3) Impact: 25% line, Visual	3) Disbonds: 10% line, Visual, NDI	3) Disbonds: 10% line
	4) Corrosion; 10% line, Visual	4) Impact: 90% line, Visual	4) Corrosion: <10% line, Visual		4) Corrosion: 10% line, Visual		4) Corrosion 30% line, Visual, NDI	4) Corrosion, 30% line, Visual, NDI	4) Corrosion, 5% line, Visual, NDI	4) Impact: 80% line, Visual	4) Impacts 90% line
	5) Erosion: 30% line, Visual	5) Corrosion; 10% line, Visual, NDI					5) Wear: 40% line, Visual	5) Wear: 0% line, Visual	5) Wear: 5% line, Visual	5) Corrosion: 20% line, Visual, some NDI	5) Corrosion 15% line
		6) Wear: 30% line, Visual					6) Lightning: 50% line, Visual		6) Lightning: 95% line, Visual	6) Lightning: 80% line, Visual	6) Wear 20% line
		7) Lightning: 90% line, Visual					7) Elongated holes: 20% line, Visual		7) Elongated holes: 20% line, Visual	7) Elongated holes: 1% line, Visual	7) Lightning: 25% line
		8) Elongated holes: 20% line, Visual									
What is the relative frequency of the following maintenance actions?											
- Negligible damage.	10%	10%	No response	3 △	No response	No response	25%	-	No response	No response	10%
- Permanent line station repair.	5%	-		2			10%	2%			Infrequent
- Permanent maintenance base repair using standard repair.	55%	25%		4			30%	90%			60%
- Permanent maintenance base repair requiring Engineering disposition.	25%	55%		1			20%	8%			30%
- Not repairable. Part replacement required.	5%	10%		5			15%	△			-

TABLE IV. - Continued

Questions	Airline Responses A										
	A	B	C	D	E	F	G	H	I	J	K
How often do the following situations occur?											
1 Temporary repairs at line stations followed by non-revenue ferry flight.	1-2 per year	15 per year	1 every 2 years	-	10-12 per year	-	10 per year	-	2-5 per year	5-6 per year	5 per year
2 Permanent repairs at line stations using personnel or equipment from maintenance base	4-6 per year	A	2 per year	-	10-12 per year	-	1 per year	-	2-5 per year	5-6 per year	2 per year
What percentage of permanent repairs are flush, aerodynamics repairs rather than external patches?	25%	80%	-	50-60%	70%	40%	10%	15%	5-15%	20%	25%
Where are flush repairs mandatory?	Engine inlet duct	Static port, wing L.E., passenger entry door area.	-	Leading edges, control surfaces, fairings, radome, high drag areas of wing, fuselage	Leading edges, fwd fuselage, engine inlets.	Fairings	Control surfaces. (sliding surfaces only), static port areas.	Aerodynamically critical areas only.	Leading edges	Leading edges	Fwd. fuselage, leading edges.
Under what circumstances and in what locations are external repairs permitted?	All other areas where flush repair not practical	Where accessibility limits flush repairs. Also in belly, cargo loading side.	Where complicated structures make flush repairs unfeasible.	Trailing edges, low drag areas of wing, fuselage. Where accessibility is problem.	Wing lower surface	Fuselage aft of wing, aft portion of wing surface.	All other areas.	All other areas.	All other areas.	All other areas.	All other non-critical aerodynamic areas.
Are on-aircraft repairs ever made on components which can be removed for repair, such as control surfaces?	Minor repairs on-aircraft, balance calculated. Parts removed for major repairs.	Nearly always removed and replaced before repair.	Generally removed.	Minor repairs made on-aircraft if balance data permits. Major damage repaired after removal.	Removed	Generally removed.	75% are removed for repair	Most repairs made on aircraft.	No response	Over 80% are removed when repaired during a maintenance base check.	Usually removed.
Indicate the relative percentage of damage due to:								747 707			
Impact	10% A	30%	20%	50%	15%	No response	1/3	35% 20%			80%
Corrosion	65%	50%	70%	25%	85%		1/3	60% 20%	No response	No response	10%
Fatigue	25%	20%	10%	25%			1/3	5% 60%			10%

TABLE IV. - Concluded

Questions	Airline Responses[1] A	B	C	D	E	F	G	H	I	J	K
Which of the following equipment are available at the maintenance base and line stations?											
Autoclave - Maint. base	Y	N	N	Y	N	N	Y	N	N	N	N
Line Station	N	N	N	N	N	N	N	N	N	N	N
Large Oven - Maint. base	Y	Y	Y	Y	N	N	Y	Y	N	Y	Y
Line Station	N	N	N	N	N	N	Y	N	N	N	N
Vacuum Pumps - Maint. base	Y	Y	Y	Y	Y	N	Y	Y	N	Y	Y
Line Station	N	N	N	Y [1]	N	N	Y	N	N	N	N
Heat Lamps - Maint. base Heater blankets	Y	Y	Y	Y	Y	Y	Y	Y	Y	Y	Y
Line Station	N	N	N	Y [1]	N	Y [1]	Y	N	N	N	N
Freezers - Maint. base	Y	Y	Y	Y	Y	Y	Y	Y	Y	Y	Y
Line Station	N	N	N	N	N	Y [1]	Y	N	N	N	N
Are maintenance people familiar and proficient with standard wet lay-up fiberglass or cold bonding repair techniques?	Y	Y	Y	Y	Y	Y	Y	Y	Y	Y	Y
With structural bonded repairs, vacuum or autoclave cured?	Y	Y [4]	N	Y	N	N	Y	N	N	N	N
Would you consider the use of portable repair kits for on-aircraft repairs at the maintenance base?	N	Y	Y	Y	Y	Y	N	N	Y	Y	Y
At line stations?	N	Y [2]	N	Y [2]	N	Y	N	N	Y	N	Y
What is the elapsed time available for bonded repairs during periodic maintenance "C" checks?	12 hours	4 Days	No response	16 Hours	12 Hours	48 Hours	24 Hours	12 Hours	24-48 Hours	5-14 Days	3 Days

NOTES:

[1] Participating airlines randomly coded by the letters A through K.

[2] For all responses, the remainder of the detections occur at the maintenance base.

[3] Ranking of frequency: 1=highest, 5 lowest

[4] This response assumed all parts could be repaired after replacement by a spare in the maintenance base using standard procedures.

[5] All repairs taking place at line stations are made by maintenance base personnel, and are considered maintenance base repairs.

[6] Based on L-1011 only

[7] Available to a limited degree

[8] Just beginning to develop capabilities

[9] For use by maintenance base personnel

TABLE V. - DEFECT CATEGORIZATION MATRIX

Impact ⚠

Damage Experience in Metallic Structure				Effect of Damage on Corresponding Composite Parts				
Component Type	Major Design Requirements of Components	Cause of Defect	Defect Type & Size ⚠	Estimated Type and Size of Damage in Composite ⚠	Estimated Strength of Damaged Composite		Potential for Growth of Defect	Maintenance Action Required
					Tension	Compression		
Wing Skins - Lower Skin	Tensile Strength, Shear Stiffness, Aerodynamic Pressure, Environmental Sealing, Fatigue Loading, Fuel containment, pressure	Tire Treads	Impact Damage: 7.6 x 15.2 cm. (3 x 6 in.) Indentation: 5.1 cm. (2 in.) deep	Delaminations Matrix Cracks: 12.7 x 20.3 cm. (5 x 8 in.)	40 - 60%	40 - 60%	Low	Structural Repairs
Wing Leading Edges -	Aerodynamic Smoothness, Pressure Loading, Shear Stiffness	Impact	Cracks: 22.9 x 30.5 cm. (9 x 12 in.) 5.1 x 12.7 cm. (2 x 5 in.) 2.54 to 12.7 cm. (1 to 5 in.)	Broken Fibers: Same as Metal	0 - 60% (for pressure loading)	0 - 60%	Low	Flush Repairs
Wing Trailing Edges - All Areas	Aerodynamic Smoothness, Stiffness	Impact	Cracks: 22.9 to 30 cm. (9 to 12 in.) Delaminations, Disbonds: 7.6 to 76.2 cm. (3 to 30 in.)	Broken Fibers: 22.9 to 30.5 cm. (9 to 12 in.) Delaminations, Matrix Cracks: 7.6 to 76.2 cm. (3 to 30 in.)	0 - 40% 40 - 100%	0 - 40% 40 - 60%	Low High	Structural Repairs
Panel Center		Tire Recap	2.54 to 17.8 cm. (1 to 7 in.)	7.6 to 22.9 cm. (3 to 9 in.)	40 - 60%	40 - 60%	Low	
Upper Inboard Area		Tire	40.6 x 40.6 cm. (16 x 16 in.) typ.	45.7 x 45.7 cm. (18 x 18 in.)	0 - 40%	0 - 40%	Low	

TABLE V. - Continued

Impact ⚠

Damage Experience in Metallic Structure				Effect of Damage on Corresponding Composite Parts				
Component Type	Major Design Requirements of Components	Cause of Defect	Defect Type & Size ⚠	Estimated Type and Size of Damage in Composite ⚠	Estimated Strength of Damaged Composite		Potential for Growth of Defect	Maintenance Action Required
					Tension	Compression		
Wing Control Surfaces - Honeycomb Areas	Stiffness, Smoothness, Weight and Balance to Prevent Flutter	Ground Equipment	Impact Damage: Size Not Given	Possible Delaminations, Matrix Cracks or Fiber Failure	0 - 60%	0 - 60 %	Low	Cut out and Replace Core and Patch Skins
		Hail	Impact Damage: Size Not Given					
All Honeycomb Areas		Impact	Delaminations, Disbonds: 7.6 to 15.2 cm. (3 to 6 in.) diam.	Delaminations, Disbonds: 12.7 to 20.3 cm. (5 to 8 in.) diam.	40 - 60%	40 - 60%	Low	Flush Patches Required on Nose Portions
Flaps		Impact	5.1 to 15.2 cm. (2 to 6 in.)	10.2 to 20.3 cm. (4 to 8 in.)	40 - 60%	40 - 60%	Low	
Panel Center		Tires	30.5 cm. (12 in.) typ.	35.6 cm. (14 in.) typ.	0 - 40%	0 - 40%	Low	
Wing Fairings -	Aerodynamic Smoothness	Impact	Cracks, Delaminations and Disbonds: 5.1 to 30.5 cm. (2 to 12 in.)	Broken Fibers, Delaminations, and Disbonds: 10.2 to 35.6 cm. (4 to 14 in.)	0 - 40%	0 - 60%	Low	Flush Patch
		Tire	Impact Damage: 22.9 x 61.0 cm. (9 x 24 in.)	Delamination and Matrix Cracks: 27.9 x 66.0 cm. (11 x 26 in.)	0 - 40%	0 - 40%	Low	

TABLE V. - Continued

Impact ⚠1

Damage Experience in Metallic Structure				Effect of Damage on Corresponding Composite Parts				
Component Type	Major Design Requirements of Components	Cause of Defect	Defect Type & Size ⚠2	Estimated Type and Size of Damage in Composite ⚠2	Estimated Strength of Damaged Composite		Potential for Growth of Defect	Maintenance Action Required
					Tension	Compression		
Horizontal Stabilizer - Lower Surface Skin	Torsional and Bending Stiffness with Strength Requirements Towards Root.	MLG Strut Door Lost in Flight	Cracks, Dents, Punctures: Size Not Available	Broken Fibers & Delaminations: Not Defined	-	-	-	Flush Patches Required on Nose Portions
Leading Edge	Balance on Moveable Surfaces ↓	Unknown	22.9 x 30.5 cm. (9 x 12 in.)	27.9 x 35.6 cm. (11 x 14 in.)	0 - 40%	0 - 60%	Low	
		Bird Strike	2.54 x 10.2 (1 to 4 in.)	7.6 to 15.2 cm. (3 to 6 in.)	0 - 40%	0 - 60%	Low	
Leading Edge Skin Panel Edges		Unknown	2.54 to 12.7 cm. (1 to 5 in.)	7.6 to 17.8 cm. (3 to 7 in.)	0 - 40%	0 - 60%	Low	
		Hail	2.54 to 20.3 cm. (1 to 8 in.)	7.6 to 25.4 cm. (3 to 10 in.)	0 - 40%	0 - 60%	Low	
Trailing Edges - Panel Edges and Center	Impact Resistance	Impact	2.54 to 25.4 cm. (1 to 10 in.)	7.6 to 30.5 cm. (3 to 12 in.)	0 - 40%	0 - 60%	Low	
Control Surface Edges	Aerodynamic Smoothness Balance ↓	Impact	2.54 to 50.8 cm. (1 to 20 in.)	7.6 to 55.9 cm. (3 to 22 in.)	0 - 40%	0 - 60%	Low	
Control Surface - Elevator Trailing Edge		Ground Equipment	5.1 x 12.7 cm. (2 x 5 in.)	10.2 x 17.8 cm. (4 x 7 in.)	0 - 40%	0 - 60%	Low	
Control Surface- Elevator Upper Skin		Ground Equipment	12.7 x 17.8 cm. (5 x 7 in.)	17.8 x 22.9 cm. (7 x 9 in.)	0 - 40%	0 - 60%	Low	
Fairings		Impact	7.6 x 30.5 cm. (3 x 12 in.)	12.7 x 35.6 cm. (5 x 14 in.)	0 - 40%	0 - 60%	Low	

TABLE V. - Continued

• Impact ⚠

Damage Experience in Metallic Structure				Effect of Damage on Corresponding Composite Parts				
Component Type	Major Design Requirements of Components	Cause of Defect	Defect Type & Size ⚠	Estimated Type and Size of Damage in Composite ⚠	Estimated Strength of Damaged Composite		Potential for Growth of Defect	Maintenance Action Required
					Tension	Compression		
Vertical Stabilizer - Skin Center	Torsional and Bending Stiffness with Strength Requirements Predominant for T-tail Configurations.	Impact	Cracks: 2.54 to 20.3 cm. (1 to 8 in.)	Broken Fibers: 7.6 to 25.4 cm. (3 to 10 in.)	0 - 40%	0 - 60%	Low	Flush Patches Required on Nose Portions
Leading Edge		Impact	2.54 to 20.3 cm. (1 to 8 in.)	7.6 to 25.4 cm. (3 to 10 in.)	0 - 40%	0 - 60%	Low	
Leading Edge		Bird Strike	2.54 to 10.2 cm. (1 to 4 in.)	7.6 to 15.2 cm. (3 to 6 in.)	0 - 40%	0 - 60%	Low	
Control Surface - Center Area Rudders	Balance on Moveable Surfaces	-	2.54 to 25.4 cm. (1 to 10 in.)	7.6 to 30.5 cm. (3 to 12 in.)	0 - 40%	0 - 60%	Low	
Fuselage Skins -	Fatigue (Cabin Pressure) Strength Around Doors and Towards Center Section ↓	Ground Equipment ↓	Impact Damage:	Possible Delaminations Matrix Cracks, or Fiber Failure:	-	-		Structural Repairs Around Doors
Exterior			10.2 x 30.5 cm. (4 x 12 in.)	15.2 to 35.6 cm. (6 to 14 in.)	0 - 40%	0 - 40%	Low	
Near Doors			5.1 to 61.0 cm. (2 to 24 in.)	10.2 cm. to 66.0 cm. (4 to 26 in.)	0 - 60%	0 - 60%	Low	
Below Cabin Floor			2.54 to 17.8 cm. (1 to 7 in.) - Occassionally up to 91.4 cm. (36 in.)	7.6 cm. to 22.9 cm. (3 to 9 in.)	0 - 60%	0 - 60%	Low	
RH Lower Areas, Cargo Service Areas			5.1 to 190.5 cm. (2 to 75 in.)	10.2 to 195.6 cm. (4 to 77 in.)	0 - 40%	0 - 60%	Low	

TABLE V. - Continued

Impact ⚠1

Damage Experience in Metallic Structure				Effect of Damage on Corresponding Composite Parts				
Component Type	Major Design Requirements of Components	Cause of Defect	Defect Type & Size ⚠2	Estimated Type and Size of Damage in Composite ⚠2	Estimated Strength of Damaged Composite		Potential For Growth of Defect	Maintenance Action Required
					Tension	Compression		
Fuselage Stringers -	Strength and Compressive Stability	Impact	Cracks, Impact Damage: 30.5 cm. (12 in.) dia.	Broken Fibers: 35.6 cm. (14 in.) dia.	0 - 40%	0 - 40%	Low	Structural Repair
			7.6 to 30.5 cm. (3 to 12 in.)	12.7 to 35.6 cm. (5 to 14 in.)	0 - 60%	0 - 60%	Low	
Fuselage Doors -	Strength and Sealing	Ground Handling	Impact Damage:	Delaminations, Matrix Cracks or Fiber Failure:				Structural Repair
Complete Area			5.1 to 15.2 cm. (2 to 6 in.)	10.2 to 20.3 cm. (4 to 8 in.)	0 - 60%	0 - 60%	Low	
Outer Frame			5.1 to 61.0 cm. (2 to 24 in.)	10.2 to 66.0 cm. (4 to 26 in.)	0 - 60%	0 - 60%	Low	
Floor Panels -	Point Loads on Surface, Crash Shear Loading		Impact Damage:	Delaminations, Matrix Cracks or Fiber Failure:				Nonstructural Repair
All Areas		Normal Service	30.5 cm. (12 in.) diam.	35.6 cm. (14 in.) diam.	0 - 40%	0 - 40%	Low	
			15.2 to 61.0 cm. (6 to 24 in.)	20.3 to 66.0 cm. (8 to 26 in.)	0 - 60%	0 - 60%	Low	
Galley and Lavatory Areas		Normal Service; Also Wear Effects	No Sizes Given	-	-	-	-	
Cargo Compartment		Ground Handling	25.4 x 30.5 cm. (10 x 12 in.)	30.5 x 35.6 cm. (12 x 14 in.)	0 - 40%	0 - 40%	Low	

TABLE V. - Continued

Impact (1)

Damage Experience in Metallic Structure				Effect of Damage on Corresponding Composite Parts				
Component Type	Major Design Requirements of Components	Cause of Defect	Defect Type & Size (2)	Estimated Type and Size of Damage in Composite (2)	Estimated Strength of Damaged Composite		Potential for Growth of Defect	Maintenance Action Required
					Tension	Compression		
Fuselage Fairings - Center	Aerodynamic Smoothness	Impact	Impact Damage, Cracks: 2.54 to 15.2 cm. (1 to 6 in.)	Delaminations, Matrix Cracks, or Fiber Failure: 7.6 to 20.3 cm. (3 to 8 in.)	0 - 60%	0 - 60%	Low	Flush Patch
Adjacent to Doors			15.2 to 61.0 cm. (6 to 24 in.)	20.3 to 66.0 cm. (8 to 26 in.)	0 - 40%	0 - 40%	Low	
Near Galley Service Doors		Ground Vehicle	2.54 x 15.2 cm. (1 x 6 in.)	7.6 x 20.3 cm. (3 x 8 in.)	0 - 60%	0 - 60%	Low	
Entire Area		Impact Damage	Delaminations, Disbonds 2.54 to 15.2 cm. (1 to 6 in.)	7.6 to 20.3 cm. (3 to 8 in.)	0 - 60%	0 - 60%	Low	
Radomes - Center	Aerodynamic Smoothness, and System Requirements	Impact:	Delaminations, Disbonds: 2.54 to 17.8 cm. (1 to 7 in.)		Not Applicable for Composites		Graphite/Epoxy	Flush Patch
		Hail, Bird Strike	2.54 to 17.8 cm. (1 to 7 in.)					
Entire Area			Impact Damage: 15.2 to 61.0 cm. (6 to 24 in.)					
Engine Cowling. Support Structure - Complete Area	Aerodynamic Smoothness on Inlet Areas, Sonic Fatigue	Impact	Impact Damage: 5.1 to 30.5 cm. (2 to 12 in.)	Delaminations, Matrix Cracks, or Fiber Failure: 10.2 to 35.6 cm. (4 to 14 in.)	0 - 60%	0 - 60%	Low	Flush Patches on Inlet Areas
Outer Skin		Ground Vehicle	35.6 cm (14 in.) Tear	40.6 cm. (16 in.) Tear	0 - 40%	0 - 40%	Low	
Center Engine Nose Cone Lip		Hangar Collision	91.4 cm (3 ft.)	91.4 cm. (3 ft.)	0 - 40%	0 - 40%	Low	

TABLE V. - Continued

Cracks Caused by Fatigue (1)

Damage Experience in Metallic Structure				Effect of Damage on Corresponding Composite Parts				
Component Type	Major Design Requirements of Components	Cause of Defect	Defect Size (2)	Estimated Type and Size of Damage in Composite (2)	Estimated Damaged Strength of Composite: Tension	Estimated Damaged Strength of Composite: Compression	Potential for Growth of Defect	Maintenance Action Required
Wing Skins — Lower Skin Spar Areas; and Rear Spar. Lower Skin Around Access Holes	Tensile Strength, Shear Stiffness, Aerodynamic Pressure, Environmental Sealing and Fatigue Loading	Fatigue	0.152 - 40.6 cm. (0.06 - 16 in.)					
Wing Stiffener Elements — Stringers, Radii	Strength and Compressive Stability	Fatigue	2.54 - 2.7 cm. (1 - 5 in.)					
Wing Leading Edge-Fixed Leading Edge Around Access Doors	Aerodynamic Smoothness, Pressure Loading; Shear Stiffness	Fatigue	5.1 cm. (2 in.) Typ.					
Wing Trailing Edges —	Aerodynamic Smoothness, Stiffness, Strength	Poor Bonding, Rigidity of Core						
Trailing Edge Member		Fatigue	2.54 - 12.7 cm. (1 - 5 in.)					
Lower Caps of Trailing Edge		Fatigue	Size not given					
Wing Control Surfaces — Flaps and slats, Spoiler Along Hinge Attach Fitting	Stiffness, Smoothness, Weight and Balance to Prevent Flutter	Fatigue Fretting	10.2 - 15.2 cm. (4 - 6 in.)					

Fatigue Cracks: The type of damage typical of fatigue cracks in metallic structures does not occur to the same degree in multidirectional fibrous composite materials. Fatigue cycling does not appear to be a significant initial cause of composite damage, and fatigue cycling does not result in significant propagation of damage.

TABLE V. - Continued

Cracks Caused by Fatigue ⚠1

Damage Experience in Metallic Structure				Effect of Damage on Corresponding Composite Parts				
Component Type	Major Design Requirements of Components	Cause of Defect	Defect Size ⚠2	Estimated Type and Size of Damage in Composite ⚠2	Estimated Strength of Damaged Composite		Potential for Growth of Defect	Maintenance Action Required
					Tension	Compression		
Wing Substructure - Flange Radii, Spars, Ribs, Spar Lower Chord.	Strength	Fatigue	3.8 - 15.2 cm. (1 1/2 - 6 in.)					
Wing Fairings -	Aerodynamic Smoothness	Fatigue Aerodynamic Vibration Loads	152.4 cm. (Up to 5 feet)					
Wing - Fuselage Joint - Drag Angle Upper Wing; Fuselage-to-Wing Center	Strength	Fatigue Resulting from Poor Design	2.54 - 20.3 cm. (1 - 8 in.)					
Horizontal Stabilizer Skins-Spar Skin Area	Torsional and Bending Stiffness and Strength	Fatigue	2.54 - 12.7 cm. (1 to 5 in.)					
Horizontal Stabilizer Stiffener Elements - Stringers Stiffeners	Strength and Stability	Fatigue	1.27 - 10.2 cm. (0.5 - 4 in.)					
Horizontal Stabilizer Trailing Edges - Inboard Closure Rib, Aft End	Strength	Fatigue	2.54 - 12.7 cm. (1 - 5 in.)					

Fatigue Cracks: The type of damage typical of fatigue cracks in metallic structures does not occur to the same degree in multidirectional fibrous composite materials. Fatigue cycling does not appear to be a significant initial cause of composite damage, and fatigue cycling does not result in significant propagation of damage.

TABLE V. - Continued

Cracks Caused by Fatigue (1)

Damage Experience in Metallic Structure				Effect of Damage on Corresponding Composite Parts				
Component Type	Major Design Requirements of Components	Cause of Defect	Defect Size (2)	Estimated Type and Size of Damage in Composite (2)	Estimated Strength of Damaged Composite		Potential for Growth of Defect	Maintenance Action Required
					Tension	Compression		
Horizontal Stabilizer Sub-Structure - Flange Radii, Spars	Strength	Fatigue Fatigue	3.8 - 12.7 cm. (1 1/2 - 5 in.)					
Vertical Stabilizer Skins - Entire Skin Area	Strength and Stiffness	Fatigue	(2.54 - 15.2 cm.) (1 - 6 in.)					
Vertical Stabilizer Stiffener Elements - Stiffeners	Strength and Stability	Fatigue	5.1 - 15.2 cm. (2 - 6 in.)					
Vertical Stabilizer - Leading Edges	Aerodynamic Smoothness	Fatigue	2.54 - 5.1 cm. (1 - 2 in.)					
Vertical Stabilizer - Trailing Edges	Impact Resistance	Fatigue	2.54 - 10.2 cm. (1 - 4 in.)					
Vertical Stabilizer Sub-Structure - Flange Radii	Strength and Stability	Fatigue	3.8 - 7.6 cm. (1 1/2 - 3 in.)					

Fatigue Cracks: The type of damage typical of fatigue cracks in metallic structures does not occur to the same degree in multidirectional fibrous composite materials. Fatigue cycling does not appear to be a significant initial cause of composite damage, and fatigue cycling does not result in significant propagation of damage.

TABLE V. - Continued

Cracks Caused by Fatigue [1]

Damage Experience in Metallic Structure				Effect of Damage on Corresponding Composite Parts				
Component Type	Major Design Requirements of Components	Cause of Defect	Defect Size [2]	Estimated Type and Size of Damage in Composite [2]	Estimated Strength of Damaged Composite		Potential for Growth of Defect	Maintenance Action Required
					Tension	Compression		
Vertical Stabilizer Sub-Structure (Cont) - Spars, Ribs, Doublers.	Strength Stability	Fatigue Fatigue	5.1 - 15.2 cm. (2 - 6 in.)					
Vertical Stabilizers Fairings - Trailing Edge, Top.	Aerodynamic Smoothness	Fatigue	10.2 - 30.5 cm. (4 - 12 in.)					
Vertical Stabilizer Fuselage Joint - Radii of Attach Angle.	Strength	Fatigue	5.1 - 15.2 cm. (2 - 6 in.)					
Vertical Stabilizer Hinge Actuator Joints - Fittings	Strength	Fatigue	5.1 - 15.2 cm. (2 - 6 in.)					
Fuselage Skins - Sides, Over-wing Area.	Fatigue (Cabin Pressure)	Fatigue	2.54 - 10.2 cm. (1 - 4 in.)					
Fuselage Frames - Flange Radii, Brace at Lower End.	Strength and Stability	Fatigue	3.8 - 10.2 cm. (1 1/2 - 4 in.)					

Fatigue Cracks: The type of damage typical of fatigue cracks in metallic structures does not occur to the same degree in multidirectional fibrous composite materials. Fatigue cycling does not appear to be a significant initial cause of composite damage, and fatigue cycling does not result in significant propagation of damage.

TABLE V. - Continued

Cracks Caused by Fatigue (1)

Damage Experience in Metallic Structure				Effect of Damage on Corresponding Composite Parts				
Component Type	Major Design Requirements of Components	Cause of Defect	Defect Size (2)	Estimated Type and Size of Damage in Composite (2)	Estimated Strength of Damaged Composite		Potential for Growth of Defect	Maintenance Action Required
					Tension	Compression		
Fuselage Stringers - Complete Area	Strength and Stability	Fatigue	5.1 - 10.2 cm. (2 - 4 in.)					
Fuselage Bulkheads - Complete Area	Pressure Loads	Fatigue	5.1 - 15.2 cm. (2 - 6 in.)					
Fuselage Doors - Flange Radii, Outer Frame, Center Area	Strength and Sealing	Fatigue	3.8 - 61.0 cm. (1 1/2 - 24 in.)					
Floor, Beams and Posts - Complete Area, Web, Beam Web	Strength and Stability	Fatigue	2.54 - 15.2 cm. (1 - 6 in.)					
Fuselage Fairings - Attach Pts. and Supports	Aerodynamic Smoothness	Airloads	Size Not Available					

Fatigue Cracks: The type of damage typical of fatigue cracks in metallic structures does not occur to the same degree in multidirectional fibrous composite materials. Fatigue cycling does not appear to be a significant initial cause of composite damage, and fatigue cycling does not result in significant propagation of damage.

TABLE V. - Continued

Cracks Caused by Fatigue (1)

Damage Experience in Metallic Structure				Effect of Damage on Corresponding Composite Parts				
Component Type	Major Design Requirements of Components	Cause of Defect	Defect Size (2)	Estimated Type and Size of Damage in Composite (2)	Estimated Strength of Damaged Composite		Potential for Growth of Defect	Maintenance Action Required
					Tension	Compression		
Engine Cowling Support Structure - Center of Panel, Back-up Structure	Aerodynamic Smoothness Inlet Areas, Sonic Fatigue	Heat Heat	25.8 cm^2-7430 cm^2 (4 in^2 - 8 $ft.^2$) 10.2 - 15.2 cm. (4 - 6 in.)					
Engine Cowling Support Structure - Complete Area, Nose Cowl Aft Bulkhead Stiffener	Aerodynamic Smoothness Inlet Areas, Sonic Fatigue	Fatigue	5.1 - 30.5 cm. (2 - 12 in.)					
Landing Gear - Main Landing Gear, Doors	Aerodynamic Pressure and Actuator Loading	Hydrogen Embrittlement, Fatigue	5.1 - 30.5 cm. (2 - 12 in.)					
Pylon - Skins		Wear	Sizes not given					
Skin and Stringers		Fatigue	5.1 - 30.5 cm. (2 - 12 in.)					
Wing Pylon Glove, Fairing		Fatigue	5.1 - 50.8 cm. (2 - 20 in.)					
Spar		Fatigue	1.27 - 5.1 cm. (1/2 - 2 in.)					
Lower Spar Web		Fatigue	3.8 - 7.6 cm. (1 1/2 - 3 in.)					
Aft Engine Mount Support Rib		Fatigue	2.54 - 20.3 cm. (1 - 8 in.)					

Fatigue Cracks: The type of damage typical of fatigue cracks in metallic structures does not occur to the same degree in multidirectional fibrous composite materials. Fatigue cycling does not appear to be a significant initial cause of composite damage, and fatigue cycling does not result in significant propagation of damage.

TABLE V. - Continued

Disbonds ⚠

Damage Experience in Metallic Structure				Effect of Damage on Corresponding Composite Parts				
Component Type	Major Design Requirements of Components	Cause of Defect	Defect Size ⚠	Estimated Type and Size of Damage in Composite ⚠	Estimated Strength of Composite Damaged: Tension	Estimated Strength of Composite Damaged: Compression	Potential for Growth of Defect	Maintenance Action Required
Wing Leading Edges—	Aerodynamic Smoothness, Pressure Loading, Sheer Stiffness	Fatigue	80% of Area					
Wing Trailing Edges	Aerodynamic Smoothness, Stiffness	Poor Bonding Fatigue	25.8 cm^2-2580 cm^2 (4 in^2 - 400 in^2) 2.54 - 32.3 cm. (1 - 5 in.)					
Wing Control Surfaces - All areas	Stiffness, Smoothness, Weight and Balance to Prevent Flutter	Poor Bonding	25.8 cm^2-2580 cm^2 (4 in^2 - 400 in^2)					
Trailing Edge Flaps		Poor Bonding	Variable					
Wing Fairings	Aerodynamic Smoothness	Aerodynamic Vibration Loads	Up to 3.65 cm. (12 ft.)					
Horizontal Stabilizer Stiffener Elements - Stringers	Strength and Stability	Fatigue	5.1 - 10.2 cm (2 - 4 in.)					
Horizontal Stabilizer Trailing Edges	Impact		5.1 - 15.2 cm (2 - 6 in.)					
Horizontal Stabilizer Control Surfaces - Trailing Edges	Impact	Poor Bonding	12.0 - 25.8 cm^2 (2 in^2 - 4 in^2)					

Disbonds: In general, disbonding of adhesive attachments which have occurred for metallic structure would be similar for graphite/epoxy composite structure since the point of failure is in the adhesive rather than the adherend. From the limited information available, the specific cause of the disbond cannot be determined. In most cases, the repair would be similar for either metallic or composite parts.

TABLE V. - Continued

Disbonds [1]

Damage Experience in Metallic Structure				Effect of Damage on Corresponding Composite Parts				
Component Type	Major Design Requirements of Components	Cause of Defect	Defect Size [2]	Estimated Type and Size of Damage in Composite [2]	Estimated Strength of Damaged Composite		Potential for Growth of Defect	Maintenance Action Required
					Tension	Compression		
Horizontal Stabilizer Fairings-Lower Face, Upper Trailing Edge Panel	Impact	Lightning Poor Bonding						
Vertical Stabilizer Fairings-Trailing Edge, Top	Aerodynamic Smoothness	Fatigue	10.2 - 30.5 cm. (4 - 12 in.)					
Floor Panels - Galley and Lavatory Areas, Upper Face	Point Loads on Surface, Crash Shear Loading	Normal Service Normal Service						
Fuselage Fairings - Adjacent to Door, Panel Center	Aerodynamic Smoothness	Poor Bonding	30.5 cm. (12 in.) Diam. 15.2 - 61.0 cm. (6 in. - 2 ft.) 25.8 - 7430 cm^2 (4 in^2 - 8 ft^2)					
Radomes - Entire Area, Nose	Transmission Efficiency, Impact, Aerodynamic Smoothness, Rain Erosion	Water Ingestion Moisture	15.2 - 61.0 cm. (6 in. - 2 ft.) 15.2 cm. (6 in.)					
Engine Cowling Support Structure - Center Landing Gear Doors	Aerodynamic Smoothness Inlet Area, Sonic Fatigue Aerodynamic Pressure and Actuator Loading	Heat	25.8 - 7430 cm^2 (4 in^2 - 8 ft^2) 5.1 - 30.5 cm. (2 - 12 in.)					
Pylon - Wing Pylon Trailing Edge Fairing	Aerodynamic Smoothness	Heat	90% (Area)					

Disbonds: In general, disbonding of adhesive attachments which have occurred for metallic structure would be similar for graphite/epoxy composite structure since the point of failure is in the adhesive rather than the adherend. From the limited information available, the specific cause of the disbond cannot be determined. In most cases, the repair would be similar for either metallic or composite parts.

TABLE V. - Continued

Miscellaneous Damage (1)

Damage Experience in Metallic Structure				Effect of Damage on Corresponding Composite Parts				
Component Type	Major Design Requirements of Components	Cause of Defect	Defect Size (2)	Estimated Type and Size of Damage in Composite (2)	Estimated Strength of Damaged Composite		Potential for Growth of Defect	Maintenance Action Required
					Tension	Compression		
Wing Fairings -	Aerodynamic Smoothness	Design Problems Wear; Fastener Hole Elongation						
Wing, Hinge and Actuator Joints -	Strength, Wear Resistance	Wear	61.0 cm. (2 ft.)					
Horizontal Stabilizer Leading Edges - Panel Edges, Nose	Balance on Moveable Surfaces	Wear	2.54 - 20.3 cm. (1 - 8 in.)					
Horizontal Stabilizer Trailing Edges	Impact Resistance	Lightning Cracks, Punctures	5.1 - 15.2 cm. (2 x 6 in.)					
Horizontal Stabilizer Fairings - Leading and Trailing Edge	Aerodynamic Smoothness	Wear						
Wing Control Surfaces - Honeycomb	Stiffness Smoothness, Balance to Prevent Flutter	Lightning	7.6 - 10.2 cm. (3 - 4 in. Dia.)					

Miscellaneous Damage:

Lightning - Specific lightning protection systems are used with graphite/epoxy composites. Damage may still occur, especially to surface plies, but damage to graphite/epoxy will not be as severe as to fiberglass/epoxy.

Fastener Hole Wear - Particularly for frequently removed and reinstalled fasteners, hole wear can occur in graphite/epoxy. Use of metal grommets in the holes prevents damage.

Surface Wear or Abrasion - This type of damage which occurs on exposed leading edge surfaces can be prevented by a sacrificial layer on graphite parts.

TABLE V. - Continued

Miscellaneous Damage ⚠1

Damage Experience in Metallic Structure				Effect of Damage on Corresponding Composite Parts				
Component Type	Major Design Requirements of Components	Cause of Defect	Defect Size ⚠2	Estimated Type and Size of Damage in Composite ⚠2	Estimated Strength of Damaged Composite		Potential for Growth of Defect	Maintenance Action Required
					Tension	Compression		
Horizontal Stabilizer Fuselage Joint -	Strength	Wear Elongated Holes						
Horizontal Stabilizer Hinge Actuator Joints - Hinge	Strength	Wear Cracks: Elongated Holes	61.0 cm. (2 ft. Typ.)					
Vertical Stabilizer Leading Edges - Nose	Aerodynamic Smoothness, Impact Resistance	Erosion Rain/Sand	2.54 - 20.3 cm. (1 x 8 in.)					
Vertical Stabilizer Fairings -	Aerodynamic Smoothness	Poor Design Elongated Fastener Holes						
Fuselage Doors -	Strength and Sealing	Wear						
Fuselage Fairings - Entire Area	Aerodynamic Smoothness	Fatigue Elongated Fastener Holes						
Radomes - Center Area	Transmission Efficiency, Aerodynamic Smoothness, Rain Erosion	Lightning	2.54 - 17.8 cm. (1 - 7 in.)					

Miscellaneous Damage:

Lightning - Specific lightning protection systems are used with graphite/epoxy composites. Damage may still occur, especially to surface plies, but damage to graphite/epoxy will not be as severe as to fiberglass/epoxy.

Fastener Hole Wear - Particularly for frequently removed and reinstalled fasteners, hole wear can occur in graphite/epoxy. Use of metal grommets in the holes prevents damage.

Surface Wear or Abrasion - This type of damage which occurs on exposed leading edge surfaces can be prevented by a sacrificial layer on graphite parts.

TABLE V. - Concluded

Miscellaneous Damage ⚠1

Damage Experience in Metallic Structure				Effect of Damage on Corresponding Composite Parts				
Component Type	Major Design Requirements of Components	Cause of Defect	Defect Size ⚠2	Estimated Type and Size of Damage in Composite ⚠2	Estimated Strength of Damaged Composite		Potential for Growth of Defect	Maintenance Action Required
					Tension	Compression		
Engine Cowling Support Structure -	Aerodynamic Smoothness in Inlet Area, Sonic Fatigue	Fatigue Elongated Fastener Holes Interference With Engine Components Wear						
Landing Gear - Trunnion and Struts	Strength	Elongated Fastener Holes	1.27 - 10.2 cm. (1/2 - 4 in.)					
Pylon - Access Door, Leading Edge Skins	Wear, Fatigue	Wind Wear Elongated Fastener Holes						
Wing Trailing Edges -	Impact Resistance	Lightning and Wear	7.6 - 76.2 cm. (3 - 30 in.)					

Miscellaneous Damage:

Lightning - Specific lightning protection systems are used with graphite/epoxy composites. Damage may still occur, especially to surface plies, but damage to graphite/epoxy will not be as severe as to fiberglass/epoxy.

Fastener Hole Wear - Particularly for frequently removed and reinstalled fasteners, hole wear can occur in graphite/epoxy. Use of metal grommets in the holes prevents damage.

Surface Wear or Abrasion - This type of damage which occurs on exposed leading edge surfaces can be prevented by a sacrificial layer on graphite parts.

NOTE: ⚠1 The Table is divided into four segments according to the general cause of defect: 1) Impact; 2) Cracks caused by fatigue; 3) Disbonds; 4) Miscellaneous damage. Corrosion damage has not been included as discussed.

⚠2 Damage types are underlined in this column, and refer to all items listed underneath until a different damage type is indicated.

TABLE VI. - STATIC TEST RESULTS OF REPAIR SPECIMENS
16 PLY FACED SANDWICH BEAMS (1)

Patch Description and Codes	Test	Test Temperature	Failure Load kN/m (lb/in.) (2)	Failure Strain μm/m	Average Joint Efficiency (3)	Failure Mode (1) (4)
Undamaged Control (Type C-16)	Tension	RT	1900 (10848) 2166 (12365) Avg. = 2033 (11607)	10981 12285 Avg. = 11633	—	Laminate failure
		82°C (180°F)	1899 (10841) 1811 (10338) Avg. = 1855 (10590)	11442 10889 Avg. = 11156	—	Laminate failure
	Compression	RT	2171 (12395) 2221 (12679) Avg. = 2196 (12537)	16918 17225 Avg. = 17072	—	Laminate failure
		82°C (180°F)	1900 (10848) 1833 (10468) Avg. = 1867 (10658)	13848 14455 Avg. = 14152	—	Laminate failure
	Fatigue	RT	1989 (11356) 1807 (10316) Avg. = 1898 (10836)	11080 9610 Avg. = 10345	—	Laminate failure
Cure-in-place flush graphite patch (vacuum cured, 350°F) (Type I)	Tension	82°C (180°F)	611 (3487)	3330	.327	Patch delamination
	Compression	82°C (180°F)	414 (2363) 413 (2357) Avg. = 413 (2360)	2166 2906 Avg. = 2536	.221	Patch delamination
Cure-in-place external graphite tape patch (vacuum cured, 350°F) (Type VI-T)	Tension	82°C (180°F)	1092 (6235) 1099 (6272) Avg. = 1095 (6254)	6312 6439 Avg. = 6376	.591	Patch delamination
	Compression	-54°C (-67°F)	970 (5538) 1144 (6531) Avg. = 1057 (6035)	5544 6557 Avg. = 6051	.481	Cohesive patch bond failure
		RT	1179 (6731)	7443	.631	Disbond and patch delamination
		82°C (180°F)	609 (3474) 483 (2759) Avg. = 546 (3117)	3790 2810 Avg. = 3200	.292	Disbond and patch delmaination
	Fatigue	RT	1375 (7851)	7264	.724	Patch delamination
Cure-in-place external graphite fabric patch (vacuum cured 350°F) (Type VI-F)	Tension	82°C (180°F)	754 (4303) 768 (4382) Avg. = 761 (4343)	4112 4285 Avg. = 4199	.410	Disbond extending from patch edge to filler
	Compression	82°C (180°F)	482 (2754) 597 (3400) Avg. = 539 (3077)	2865 3450 Avg. = 3158	.289	Disbond extending from patch edge to filler
	Fatigue	RT	921 (5256)	6397	.485	Delamination in ply of parent laminate adjacent to patch

TABLE VI. - Concluded

Patch Description and Codes	Test	Test Temperature	Failure Load kN/m (lb/in.) (2)	Failure Strain μm/m	Average Joint Efficiency (3)	Failure Mode (4)
Pre-cured bonded external graphite tape patch (bonded) with vacuum pressure, 350°F) (Type VII)	Tension	82°C (180°F)	608 (3471) 730 (4165) Avg. = 669 (3818)	3212 3918 Avg. = 3565	.360	Disbond from patch edge to filler
	Compression	-54°C (-67°F)	1318 (7524) 1193 (6813) Avg. = 1256 (7169)	8005 7242 Avg. = 7624	.572	Shear failure in patch layer adjacent to parent
		RT	1151 (6571) 1093 (6241) Avg. = 1122 (6406)	6861 7080 Avg. = 6971	.511	Disbond plus interlaminar failure in patch
		82°C (180°F)	665 (3795) 694 (3963) Avg. = 680 (3879)	4179 4365 Avg. = 4272	.364	Disbond plus interlaminar failure in patch
Pre-cured bonded external graphite tape patch (cold bonded with RT adhesives, contact pressure) (Type IX)	Compression	82°C (180°F)	124 (706) 159 (909) Avg. = 142 (808)	630 870 Avg. = 750	.076	Patch disbond
Wet lay up graphite fabric, patch using RT curing epoxy (cured under contact pressure) (Type X)	Compression	82°C (180°F)	117 (670) 122 (698) Avg. = 120 (684)	638 713 Avg. = 676	.064	Cohesive bond line failure between patch and laminate
External mechanically attached titanium patch (Type XI)	Tension	82°C (180°F)	426 (2429) 331 (1890) Avg. = 378 (2160)	2350 1937 Avg. = 2144	.204	Fasteners pulled through patch and laminate
	Compression	82°C (180°F)	351 (2002) 413 (2359) Avg. = 382 (2181)	1970 2451 Avg. = 2211	.205	Bearing failure in laminate
External mechanically attached aluminum patch (Type XII)	Tension	82°C (180°F)	587 (3350) 644 (3674) Avg. = 615 (3512)	3295 3715 Avg. = 3505	.332	Fasteners pulled through at one end of patch
	Compression	82°C (180°F)	585 (3337) 621 (3543) Avg. = 603 (3440)	3299 3567 Avg. = 3433	.323	1) Bearing failure in laminate 2) Stability failure of metal plate

NOTES:

(1) Parent laminate 16 ply $(\pm 45, 0, \pm 45_2, 0)_s$

(2) Values given are laminate loads.

(3) Required average failure load as a fraction of undamaged control average failure load.

(4) Complete failure descriptions are given in Appendix B

TABLE VII. - STATIC TEST RESULTS OF REPAIR SPECIMENS 50 PLY FACED SANDWICH BEAMS (1)

Patch Description and Codes	Test	Test Temperature	Failure Load kN/m (lb/in.) (2)	Failure Strain μm/m	Average Joint Efficiency (3)	Failure Mode (4)
Undamaged Control (Type C-50)	Tension	RT	3126 (17905) 2153 (12294) Avg. = 2645 (15100)	9860 6425 Avg. = 8143	—	Interlaminar failure of laminate near core at 0" ply, top 3 plies separated in one specimen.
		82°C (180°F)	1912 (10919) 3210 (18330) Avg. = 2561 (14625)	5420 9496 Avg. = 7458	—	1) Interlaminar failure with partial disbond 2) Fiber crushing through lam. thickness at one core splice. Top 3 plies separated at 90° ply.
	Compression	RT	2827 (16142) 3211 (18333) Avg. = 3019 (17238)	9463 11350 Avg. = 10407	—	Interlaminar shear failure in laminate
		82°C (180°F)	1939 (11071) 2810 (16044) Avg. = 2375 (13558)	6313 9597 Avg. = 7955	—	Combined interlaminar failure of plies near core, plus steel and composite disbonds
	Fatigue	RT	3366 (19217)	11152	—	Laminate failure
Cure-in-place flush graphite patch (vacuum cured at 350°F) (Type II)	Tension	82°C (180°F)	2043 (11664) 2211 (12623) Avg. = 2127 (12144)	4517 3405 Avg. = 3961	.830	Cohesive bond line failure propagated into delamination of patch at core end of scarf joint
	Compression	82°C (180°F)	1985 (11332) 1622 (9259) Avg. = 1803 (10296)	4955 4317 Avg. = 4636	.759	Same as tensile failure
Pre-cured bonded graphite flush patch, (bonded under vacuum pressure 350°F) (Type III)	Tension	82°C (180°F)	2252 (12859) 2163 (12349) Avg. = 2207 (12604)	6365 5379 Avg. = 6122	.862	Failed along scarfed bond line and propagated as delaminaion into parent laminate
	Compression	82°C (180°F)	2036 (11627) 2225 (12704) Avg. = 2131 (12166)	5840 7330 Avg. = 6585	.897	Interlaminar failure initiated at bond line in parent laminate
	Fatigue	RT	2396 (13677)	7702	.712	Adhesive failure in patch bond-line with ply fracture at end of scarf
Cure-in-place flush graphite patch (vacuum cured, 350°F) of partial through damage (Type IV)	Tension	82°C (180°F)	1787 (10203) 1816 (10366) Avg. = 1801 (10285)	4280 3230 Avg. = 3755	.703	Disbond of patch combined with parent laminate delamination
	Compression	82°C (180°F)	1543 (8810) 1530 (8736) Avg. = 1536 (8773)	3105 2227 Avg. = 2668	.647	Delamination failure in patch
	Fatigue	RT	1631 (9309)	5218	.484	Interlaminar tensile failure of parent laminate at maximum patch depth

TABLE VII. - Concluded

Patch Description and Codes	Test	Test Temperature	Failure Load kN/m (lb/in.) (2)	Failure Strain μm/m	Average Joint Efficiency (3)	Failure Mode (4)
Cure-in-place flush graphite patch (vacuum cured, 350°F) with precured bonded internal doubler (Type V)	Tension	82°C (180°F)	1818 (10377) 1110 (6335) Avg. = 1464 (8356)	5099 3193 Avg. = 4136	.571	1) Shear failure in bond line with fracture of cover plies at joint termination 2) Failure initiated at area of ply waviness in patch laminate, then propagated as interlaminar failure of patch
	Compression	82°C (180°F)	1879 (10725) 1393 (7951) Avg. = 1636 (9338)	6184 4376 Avg. = 5280	.689	1) Shear failure in bond line with fiber breakage and delamination in patch 2) Failure initiated at area of ply waviness in patch laminate, then propagated as interlaminar failure of patch
Precured bonded external graphite patch (vacuum cured 350°F) with supplemental fasteners (Type VIII)	Tension	82°C (180°F)	767 (4380) 596 (3405) Avg. = 682 (3892)	2135 1707 Avg. = 1921	.266	Failure initiated at bond line edge and propagated as interlaminar failure at patch
	Compression	82°C (180°F)	460 (2627) 453 (2584) Avg. = 456 (2606)	1622 1607 Avg. = 1615	.192	Bond line failure extending from edge to filler

(1) Parent laminate 50 ply (36% 0°, 56% ±45°, 8% 90°)

(2) Values given are laminate loads

(3) Repaired average failure load as a fraction of undamaged control average failure load

(4) Complete failure descriptions are given in Appendix B.

TABLE VIII. - STATIC TEST RESULTS OF TABBED COUPON SPECIMENS

Parent Laminate	Patch Description	Test	Test Temperature	Average Failure Load kN/m (lb/in)	Average Failure Strain μin/in	Repair Efficiencies	Failure Mode
16 ply $(\pm 45, 0, \pm 45_2, 0)_S$	Undamaged Control (C-U)	Tension	RT	6085 (34,750)	9,650	–	Fiber break and $\pm 45^0$ splitting
			82^0C (180^0F)	5848 (33,400)	9,175		
	Damaged, Unrepaired Control (C-D)	Tension	RT	2676 (15,280)	4,050	–	45^0 fiber splitting through hole
			82^0C (180^0F)	2758 (15,750)	4,065	–	
	Cure-in-place graphite flush patch (vacuum cured, 350^0F)(XIII) (1)	Tension	RT	3520 (20,100)	5,775	.578	Cohesive through scarf joint in area closest to tabs
			82^0C (180^0F)	3695 (21,100)	5,665	.632	
	Cure-in-place flush patch (vacuum cured 350^0F) (XIII A) (2)	Tension	RT	4955 (28,300)	8588	.814	Cohesive through scarf joint in area closest to tabs
	Pre-cured, bonded external graphite patch (cured under vacuum, 350^0F) (XIV)	Tension	RT	3187 (18,200)	4,705	.524	Corner patch delamination propagating into patch adhesive failure
			82^0C (180^0F)	4360 (24,900)	6,875	.746	

(1) Cured without use of bleeder

(2) Cured with addition of bleeder

TABLE IX. -- LAMINATE CHARACTERIZATION DATA

Panel No. (1)	Dimensions cm(in.) (2)	Specimen Type (3)	Density gg/c	Resin Content % by Wt.	Fiber Volume % (Calc.)	Voids % (Calc.)	Thickness Per Ply mm(mils)
1WG1428 (50 ply)	35.6x30.5 (14x12)	NDI standard	1.585	27.1	66.4	-0.36	0.132(5.2)
1WG1449 (50 ply)	139.7x66.0 (55x26)	Type C-50	1.574	29.2	63.3	0.35	0.137(5.4)
2WG1445 (50 ply)	81.3x35.6 (32x14)	Type II	1.582	27.9	64.8	0.30	0.132(5.2)
1WN1482 (50 ply)	81.3x35.6 (32x14)	Type III	1.591	25.6	67.2	0.60	0.127(5.0)
2WN1482 (50 ply)	81.3x35.6 (32x14)	Type III	1.587	26.9	66.0	0.36	0.127(5.0)
1WN1486 (50 ply)	139.7x35.6 (55x14)	Type IV	1.579	27.9	65.6	0.53	0.124(4.9)
1WG1445 (50 ply)	81.3x35.6 (32x14)	Type V	1.578	29.1	63.6	0.13	0.32(5.2)
1WN1469 (50 ply)	45.7x76.2 (18x30)	Type VIII	1.571	29.2	63.3	0.03	0.124(4.9)
1WN1470 (50 ply)	45.7x76.2 (18x30)	Type VIII	1.597	26.9	66.4	0.24	0.119(4.7)
1WN1488 (50 ply)	139.7x35.6 (55x14)	Spare A	1.582	27.9	64.8	0.31	0.127(5.0)
1WN1490 (50 ply)	139.7x35.6 (55x14)	Spare B	1.582	28.4	64.4	0.42	0.127(5.0)
1WN1504 (16 ply)	30.5x35.6 (12x14)	NDI standard	1.579	28.7	64.0	0.75	0.137(5.4)
1WN1510 (16 ply)	78.7x40.6 (31x16)	Type C-16	1.581	27.4	65.2	0.56	0.135(5.3)
2WN1510 (16 ply)	48.3x25.4 (19x10)	Type I	1.580	27.5	65.2	0.61	0.130(5.1)
1WX1539 (16 ply)	91.4x81.3 (36x32)	Type VI-T,IX, and X	1.576	28.6	64.0	0.45	0.130(5.1)
1WN1523 (16 ply)	91.4x50.8 (36x20)	Type VI-F, XI	1.575	28.4	64.1	0.58	0.130(5.1)
2WN1523 (16 ply)	91.4x71.1 (36x28)	Type VII, XII	1.581	27.7	65.0	0.48	0.135(5.3)
1WX1526 (16 ply)	127x96.5 (50x38)	Type C-U, and C-D	1.570	29.7	62.8	0.42	0.135(5.3)

TABLE IX. - Concluded

Panel No. (1)	Dimensions cm(in.) (2)	Specimen Type (3)	Density g/cc.	Resin Content % by Wt.	Fiber Volume % (Calc.)	% (Calc.)	Thickness Per Ply mm(mils)
1WX1528 (16 ply)	63.5x96.5 (25x38)	Type XIII	1.569	29.3	63.0	0.62	0.137(5.4)
2WX1539 (16 ply)	127.0x96.5 (50x38)	Type XIV	1.570	29.4	63.1	0.57	0.130(5.1)
1WX1531 (16 ply)	63.5x96.5 (25x38)	Spare	1.567	30.6	61.9	0.31	0.135(5.3)
1WN1520 (16 ply)	91.4x81.3 (36x32)	Spare	1.570	28.0	64.2	1.06	0.130(5.1)

(1) Four digit number is autoclave run number;
WG is Narmco 5208, Batch 1313;
WN is Narmco 5208, Batch 1353;
WX is Narmco 5208, Batch 1357.

(2) First dimension is 0^{o} direction.

(3) See Tables VI, VII, VIII for description of repairs by code number.

TABLE X. - LAMINATE CHARACTERIZATION DATA - 4 PLY PATCH LAMINATES

Laminate Identification	Resin Content % by Wt.	Specific Gravity	Fiber Volume (calc.) %	Voids (calc.) %
1 WZ 1549	27.8	1.588	65.2	0.03
2 WZ 1549	27.4	1.588	65.5	0.09
1 WZ 1550	27.0	1.583	65.7	0.59
2 WZ 1550	27.1	1.587	65.7	0.30
1 WX 1560	28.8	1.585	64.1	-0.14
2 WX 1560	28.8	1.584	64.2	-0.09
1 WZ 1560	27.6	1.584	64.5	0.27
2 WZ 1560	29.2	1.582	63.6	-0.12
1 WX 1561	30.2	1.583	62.9	-0.53
2 WX 1561	29.9	1.580	63.1	-0.23
3 WX 1561	28.9	1.581	63.9	0.08
4 WX 1561	30.5	1.568	62.0	0.31

TABLE XI. - PROCESS DEVELOPMENT PANEL FABRICATION PARAMETERS

Panel No.	Cure Cycle Parameters		Orientation During Cure	Bleed Plies
	Pressure	Dwell		
1	Vacuum	None	Horizontal	None
2	↓	↓	Vertical	↓
3	↓	↓	Horizontal	1 ply Style 120 glass cloth
4	↓	45 min @ 135°C (275F)	Horizontal	None
5	↓	↓	Vertical	↓
6	689.4 kPa (100 psi)	None	Horizontal	↓
7	↓	45 min @ 135°C (275F)	Horizontal	↓

TABLE XII. - CURE CYCLES FOR PROCESS DEVELOPMENT PANELS

Vacuum - No Dwell

1. Apply full vacuum
2. Heat to 177°C (350°F) at 1.1 - 3.3°C (2-6°F) /minute
3. Cure at 177°C ±5.5 (350°F ±10) for 60 minutes
4. Cool to 82.2°C (180°F) under full vacuum.

Vacuum - With Dwell

1. Apply full vacuum
2. Heat to 135°C ±2.8 (275°F ±5) at 1.1 - 2.2°C (2-4°F)/minute
3. Dwell at 135°C ±2.8 (275°F ±5) for 45 minutes [starting at 129.4°C (265°F)]
4. Heat to 179.4°C ±2.8 (355°F ±5) at 1.1 - 2.2°C (2-4°F)/minute
5. Cure at 179.4°C ±2.8 (355°F ±5) for 120 $^{+10}_{-0}$ minutes
6. Cool to 79.4°C (175°F) under vacuum.

689.4 kPa (100 psi) - No Dwell

1. Apply full vacuum and 586 kPa (95 psi) autoclave pressure
2. Heat to 177°C (350°F) at 1.1 - 3.3°C (2-6°F/minute)
3. Cure at 177°C ±5.5 (350°F ±10) for 60 minutes
4. Cool to 82.2°C (180°F) under pressure.

689.4 kPa (100 psi) - With Dwell

1. Apply full vacuum
2. Heat to 135°C ±2.8 (275°F ±5) at 1.1 - 2.2°C (2-4°F)/minute
3. Dwell at 135°C ±2.8 (275°F ±5) for 45 minutes [starting at 129.4°C (265°F)]
4. Apply 689.4 ±34.5 kPa (100 ±5 psi), venting vacuum at 138 kPa (20 psi)
5. Heat to 179.4 ±2.8°C (355 ±5°F) at 1.1 - 2.2°C (2-4°F)/minute
6. Cure at 179.4 ±2.8°C (355 ±5°F) for 120 $^{+10}_{-0}$ minutes
7. Cool to 79.4°C (175°F) under pressure.

TABLE XIII. - SUMMARY OF DATA ON PROCESS DEVELOPMENT PANELS

(1) Panel No.	Cure Cycle	Specific Gr.	Voids, Percent	Fiber Volume Percent	Resin Content, Percent	(2) Compression Strength MPa (ksi)	(3) Short Beam Shear Strength MPa (ksi)	Measured Thickness for 16 Plies, cm (in.)
1	Vacuum/No Dwell (Horizontal) (4)	-	-	-	-	-	-	-
2	Vacuum/No Dwell (Vertical (4)	-	-	-	-	-	-	-
3	Vacuum/No Dwell (Horizontal with 1 Bleeder Ply)	1.557	1.557	63.25	28.49	483.8(70.17)	35.96(5.215)	.213(.084)
4	Vacuum/With Dwell (Horizontal)	1.520	1.416	55.6	35.63	551.8(80.04)	41.78(6.06)	.246(.097)
5.	Vacuum/With Dwell (Vertical	1.521	1.423	55.8	35.46	567.4(82.3)	43.44(6.3)	.244(.096)
6.	689.4 kPa (100 psi)/No Dwell (Horizontal)	1.582	-0-	62.93	29.98	647.8(93.96)	61.50(8.92)	.221(.087)
7.	689.4 kPa (100 psi)/With Dwell (Horizontal)	1.549	-0-	56.81	35.44	668.0(96.88)	59.43(8.62)	.241(.095)
8.	Vacuum/No Dwell (Horizontal)	1.528	1.6	57.5	33.6	598.5(86.81)	47.71(6.92)	.244(.088)
9.	Vacuum/With Dwell (Horizontal)	1.549	1.23	60.9	30.8	628.2(91.11)	48.13(6.98)	.221(.087)

1. Prepreg for Panel No. 1-7 from Roll 6 Batch 7313, mfg, date 12/21/78, 34.5% resin content, 145.3 gm/m^2 fiber weight. Prepreg for Panel No. 8 and 9 from Roll 35, Batch 1356, 35% resin content, 142 gm/m^2 fiber weight.
2. Stresses based on nominal thicknesses of .015 cm (0.006 in.)/ply. Cured thicknesses varied from 0.013 to 0.015 centimeters (0.0052 to 0.0061 inches) per ply.
3. Panel orientation $[(\pm 45/0/90)_2]_S$
4. Panels delaminated during handling.

TABLE XIV. - REDUCED TEMPERATURE COUPON TEST RESULTS

Specimen No.	Cure Temp °C(°F)	Cycle Time	Stress at Failure MPa (ksi)	Percent of Strength for Normal Cure
Longitudinal Compression				
LC1-1	149(300)	1	434(62.9)	
LC2-1	↓	↓	454(65.8)	
Avg.	↓	↓	444(64.3)	76
LC1-2	149(300)	2	486(70.4)	
LC2-2	↓	↓	491(71.2)	
Avg.	↓	↓	488(70.8)	84
LC1-3	149(300)	3	571(82.7)	
LC2-3	↓	↓	502(72.7)	
Avg.	↓	↓	536(77.7)	92
LC1-4	177(350)	1	569(82.4)	
LC2-4	↓	↓	594(86.1)	
Avg.	↓	↓	581(84.2)	100
Longitudinal Tension				
LT1-1	149(300)	1	369(53.5)	
LT2-1	↓	↓	474(68.7)	
Avg.	↓	↓	422(61.1)	87
LT1-2	149(300)	2	561(81.3)	
LT2-2	↓	↓	515(74.6)	
Avg.	↓	↓	538(77.9)	111
LT1-3	149(300)	3	493(71.4)	
LT2-3	↓	↓	542(78.6)	
Avg.	↓	↓	517(75.0)	107
LT1-4	177(350)	1	464(67.3)	
LT2-4	↓	↓	503(72.9)	
Avg.	↓	↓	484(70.1)	100

TABLE XV. - REDUCED CURE TEMPERATURE PHYSICAL PROPERTIES

Cure Cycle	Resin Content %	Specific Gravity	Fiber Volume %	Void Content %
1 149°C(300°F) for 1 hour	28.0	1.55	63.7	1.55
2 149°C(300°F) for 2 hours	28.6	1.56	63.3	1.30
3 149°C(300°F) for 3 hours	31.8	1.54	59.8	1.11
4 177°C(350°F) for 1 hour	28.9	1.54	62.5	1.98

TABLE XVI. - GLASS TRANSITION TEMPERATURE (Tg) BY TMA AND DMA TESTS

Cure Conditions	TMA	DMA
1 hr @ 300°F	60°C	50-60°C sharp
2 hr @ 300°F	60°C	80°C sharp
3 hr @ 300°F	130°C	120-140°C broad
1 hr @ 350°F	175°C	150-180°C broad
1 hr @ 300°F		
3 hr @ 350°F PC	200°C (S)	
2 hr @ 300°F		
3 hr @ 350°F PC	200°C	
3 hr @ 300°F		
3 hr @ 350°F PC	205°C	
3 hr @ 300°F		
3 hr @ 300°F PC	175°C	140-160°C
3 hr @ 300°F		
6 hr @ 300°F PC	175°C	140-160°C
1 hr @ 350°F		190-220°C
3 hr @ 350°F PC	250°C	190-220°C

PC = post cure
S = softening
TMA = thermo-mechanical analysis
DMA = dynamic flexure

TABLE XVII. - FATIGUE LOADING SPECTRA - 50 PLY SPECIMENS
Definition of flight types and number of load cycles within each flight

Flight Type	Number of flights in one block of 4000 flights	Amplitude level No. and magnitude (S_a/S_m) I (1.60)	II (1.50)	III (1.30)	IV (1.15)	V (0.995)	VI (0.84)	VII (0.685)	VIII (0.53)	IX (0.375)	X (0.222)	Total number of cycles per flight
		Number of cycles per flight										
A	1	1	1	1	4	8	18	64	112	391	0	600
B	1		1	1	2	5	11	39	76	385	0	520
C	3			1	1	2	7	22	61	286	0	380
D	9				1	1	2	14	44	208	0	270
E	24					1	1	6	24	168	0	200
F	60						1	3	19	107	0	130
G	181							1	7	72	0	80
H	420								1	16	23	40
I	1 090									1	4	5
J	2 211										2	2
Total Number of cycles per block of 4000 flights		1	2	5	18	52	152	800	4 170	34 800	18 422	
Cumulative number of load cycles per block of 4000 flights.		1	3	8	26	78	230	1 030	5 200	40 000	58 422	

TABLE XVIII. - FATIGURE LOADING SPECTRA - 16 PLY SPECIMENS

% Reference Stress	360 Flight Cruise Spectrum* Cycles in A2 Block	Cycles in B2 Block	Cycles in G2 Block	Cycles in 36,000 Flights	360 Flight Climb and Descent Spectrum* Cycles A1 and A3 Block	Cycles in B1 and B3 Block	Cycles in C1 and C3 Block	Cycles in 36,000 Flights
100			1	4			3	24
90			2	8		1	1	40
78		1	1	20		3	4	128
67		4	6	88	1	7	5	424
56	3	3	5	308	7	10	13	1,544
44	19	19	22	1,912	47	49	51	9,496
33	96	99	99	9,660	232	230	233	46,344
22	240	240	240	24,000	820	820	820	164,000
11	240	240	240	24,000	240	240	240	48,000
Cycles/Block	598	606	616		1,347	1,360	1,370	
Blocks/Lifetime	80	16	4		160	32	8	
Cycles/Lifetime	47,840	9,696	2,464	60,000	215,520	43,520	10,960	270,000

TABLE XIX. - PHASE 3 TEST MATRIX

SPECIMEN TYPE	DESCRIPTION	NO. OF SPECIMENS		LOAD SENSE	TEST CONDITION
		REPAIRED	UNDAMAGED		
I	Hat-stiffened fin cover segment	1		Compression	Static room temperature, Wet
			1	Compression	
II	Hat-stiffened wing cover segment	1		Compression	
			1	Compression	
III	"T" section vertical fin spar segment	1		Tension	
			1	Tension	

TABLE XX. - PHASE 3 TEST RESULTS

SPECIMEN TYPE		FAILURE kN	LOAD (LBS)	FAILURE STRAIN (μm/m) GAGE NUMBER (FIGURES 26 THROUGH 28)				STRENGTH RESTORATION (PERCENT)
				1	2	3	4	
I	Control	-160.1	(-36,000)	-5272	-6125			
	Repair	-146.3	(-32,900)	-3838	-2050	-5058		91.4
II	Control	-398.5	(-89,600)	-4434	-4111			
	Repair	-314.9	(-70,800)	-2298	-1656	-3258		79.0
III	Control	+182.4	(+41,000)	+5215	+6415			
	Repair	+168.1	(+37,800)	+823	+2852	+790	+4358	92.2

TABLE XXI. - INCORPORATION OF PHASE 4 ACTIVITIES INTO ACVF GROUND TEST PLAN [1]

1. Strain and Deflection Response
2. Static Tests – Design Ultimate Load
3. Damage Tolerance Evaluation (with small area damage)
4. Fail Safe Evaluation
   a. Discrete Source Damage: impacting to obtain 12 by 4 in. delaminated area followed by burn-through with electric arc
   b. Application of two conditions of design limit loads
   c. Inspection of damage
5. Residual Strength Test
   a. Repair of discrete source damage using repairs selected from procedures evaluated in the Phase 2 coupon tests of this program
   b. Additional fatigue cycling for 1 lifetime. (This item is to be covered by Phase 4 of this program).
   c. Test to ultimate and failure

[1] Per the ACVF Ground Test Plan, LR 29583, January 1981, (reference 50)

TABLE XXII. - DAMAGE TOLERANCE EVALUATION FATIGUE SPECTRA

% Limit Load Cond 59 (1)	N	ΣN	Flight						
			1	36	360	1800	9000	18000	36000
15	166000	197020	4	22					
23	24860	31020		24	8	3			
31	4328	6160		4	3	1	2		
38	1279	1832		1	2	3	4	1	1
46	328	553			3	1	2		
54	134	225			1	1	3	1	
62	43	91				2		1	1
69	28	48				1	2		
77	9	20					2		1
81	3	11						1	1
85	3	8						1	1
88	3	5						1	1
92	1	2							1
100 & E.F. (2)(6%)	1	1							1
	Count		4	51	17	12	15	6	8
	Multiplier		36000	1000	100	20	4	2	1

(1) Loads defined in Table 5-2 of the Ground Test Plan (reference 4).

(2) Environmental factor applied to limit load only.

1. Report No.	2. Government Accession No.	3. Recipient's Catalog No.
NASA CR-159056		

4. Title and Subtitle	5. Report Date
REPAIR TECHNIQUES FOR GRAPHITE/EPOXY STRUCTURES FOR COMMERCIAL TRANSPORT APPLICATIONS	January 1983
	6. Performing Organization Code
7. Author(s)	8. Performing Organization Report No.
R. H. STONE	
	10. Work Unit No.
9. Performing Organization Name and Address	11. Contract or Grant No.
LOCKHEED-CALIFORNIA CO. P.O. Box 551 Burbank, California 91520	NAS 1-15269
	13. Type of Report and Period Covered
12. Sponsoring Agency Name and Address	
NATIONAL AERONAUTICS AND SPACE ADMINISTRATION WASHINGTON D.C. 20546	14. Sponsoring Agency Code

15. Supplementary Notes

FINAL REPORT FOR PHASES 1, 2, 3, AND 4 OF PROGRAM.
TECHNICAL MONITOR, J.W. DEATON, NASA-LANGLEY RESEARCH CENTER

16. Abstract

The program objective was development of repair concepts for graphite composite structures on commercial transports. Northrop assisted Lockheed as a major sub-contractor.

Phase 1 of the program consisted of surveys on composite defect sensitivity and airline damage experience and repair capabilities; and included preparation of a matrix categorizing typical in-service defects. The surveys indicated that flaw growth is not anticipated in most current composite applications, and that airlines require repairs adapted to facility, personnel, down-time and aerodynamic limitations.

Phase 2 consisted of screening repair concepts meeting these requirements, using 16 and 50 ply laminate specimens. Variables included flush and external patches, pre-cured and cure-in-place graphite patches bonded under vacuum, cold bonding, and bolted repairs. Results indicated that design strengths were restored by the vacuum hot bonded repairs.

Phase 3 consisted of repair of sub-element specimens - hat stiffened covers and an I-section spar cap. The covers were repaired with bonded and cure-in-place graphite patches; the spar was repaired with a bolted aluminum patch. Design strengths were restored in all cases.

Phase 4 consisted of a large-area bonded graphite repair of damage on the L-1011 vertical fin ground test article. The repair withstood testing of the part to ultimate and failure.

17. Key Words (Suggested by Author(s))	18. Distribution Statement
GRAPHITE COMPOSITES REPAIR DAMAGE TOLERANCES	

19. Security Classif. (of this report)	20. Security Classif. (of this page)	21. No. of Pages	22. Price
UNCLASSIFIED	UNCLASSIFIED		

For sale by the National Technical Information Service, Springfield, Virginia 22161